I

Programa de Doctorado en Neurociencias

.

Nutrient Sensing in the neuroendocrine control of sexual development: from phenotype characterization to transcriptomic profiling

.

Tesis Doctoral presentada por

Juan Carranza Valencia

Director/a de Tesis:

Dr. Javier Morante Oria

Instituto de Neurociencias

Universidad Miguel Hernández de Elche

- 2024 -

La presente Tesis Doctoral, titulada *"Nutrient Sensing in the neuroendocrine control of sexual development: from phenotype characterization to transcriptomic profiling."* se presenta bajo la modalidad de tesis por compendio de las siguientes publicaciones:

*Guirado, J., *Carranza-Valencia, J., & Morante, J. (2023). Mammalian puberty: a fly perspective. The FEBS journal, 290(2), 359–369. https://doi.org/10.1111/febs.16534

*equal contribution

Sant Joan d'Alacant, 30 de septiembre 2024

El Dr. D. Javier Morante Oria, director de la tesis doctoral titulada **"***Nutrient Sensing in the neuroendocrine control of sexual development: from phenotype characterization to transcriptomic profiling.***"**

INFORMA:

Que D. Juan Carranza Valencia ha realizado bajo mi supervisión el trabajo titulado **"***Nutrient Sensing in the neuroendocrine control of sexual development: from phenotype characterization to transcriptomic profiling.***"** conforme a los términos y condiciones definidos en su Plan de Investigación y de acuerdo al Código de Buenas Prácticas de la Universidad Miguel Hernández de Elche, cumpliendo los objetivos previstos de forma satisfactoria para su defensa pública como tesis doctoral.

Lo que firmo para los efectos oportunos, en Sant Joan d'Alacant, 11 de septiembre 2024

Director/a de la tesis
Dr. D. Javier Morante Oria.

Sant Joan d'Alacant, 30 de septiembre 2024

Dña. Cruz Morenilla Palao, Coordinadora del programa de Doctorado en Neurociencias del Instituto de Neurociencias de Alicante, centro mixto de la Universidad Miguel Hernández (UMH) y de la Agencia Estatal Consejo Superior de Investigaciones Científicas (CSIC),

INFORMA:

Que D. Juan Carranza Valencia ha realizado bajo la supervisión de nuestro Programa de Doctorado el trabajo titulado **"***Nutrient Sensing in the neuroendocrine control of sexual development: from phenotype characterization to transcriptomic profiling.***"** conforme a los términos y condiciones definidos en su Plan de Investigación y de acuerdo al Código de Buenas Prácticas de la Universidad Miguel Hernández de Elche, cumpliendo los objetivos previstos de forma satisfactoria para su defensa pública como tesis doctoral.

Lo que firmo para los efectos oportunos, en Sant Joan d'Alacant, 11 de septiembre 2024

Dra. Cruz Morenilla Palao

Coordinator of the PhD Programme in Neurosciences

Sant Joan d'Alacant, 30 de septiembre 2024

List of Abbreviations

5-HT7

5-Hydroxytryptamine Receptor 7

20E

20-hydroxyecdysone

AEL

After Egg Laying

AgRP

Agouti-Related Peptide

Alk

Anaplastic lymphoma kinase

apolpp

Apolipophorin

ARC

Arcuate Nucleus

AstA

Allatostatin A

AstAR1

Allatostatin A Receptor 1

ATG

Autophagy-Related Genes

BDSC

Bloomington Drosophila Stock Center

BMI

Body Mass Index

CART

Cocaine- and Amphetamine-Regulated Transcript

CC

Corpus Allatum

CDP

Cytidine Diphosphate

CMA

Chaperone-Mediated Autophagy

CPP

Central Precocious Puberty

Crz

Corazonin

DE

Differential Expression

DEGs

Differentially Expressed Genes

dib

Disembodied

DHT

Dihydrotestosterone

Dpp

Decapentaplegic Protein

EAAs

Excitatory Amino Acids

EGFR

Epidermal Growth Factor Receptor

eMI

Endosomal Microautophagy

ERK

Extracellular-Signal-Regulated Kinase

F1

First Filial Generation

Fatp2

Fatty Acid Transport Protein 2

FSH

Follicle-Stimulating Hormone

GI

Gastrointestinal

GnRH

Gonadotropin-Releasing Hormone

GSH

Glutathione

HDL

High-Density Lipoprotein

HPG

Hypothalamic-Pituitary-Gonad

IIS

Insulin/Insulin-like Growth Factor

Kiss1

Kisspeptin-1

Kiss1R

Kisspeptin 1 Receptor

L1

First Instar Larva

L2

Second Instar Larva

L3F

Third Instar Larva (Feeding Stage)

L3W

Third Instar Larva (Wandering Stage)

LD

Lipid Droplet

LH

Luteinizing hormone

LH

Lateral Hypothalamus

miRNAs

MicroRNAs

MKRN3

Makorin RING-finger Protein-3

mRNA

Messenger RNA

mTOR

Mechanistic Target of Rapamycin

NAA10

N-Alpha-Acetyltransferase 10

NAFLD

Nonalcoholic Fatty Liver Disease

NGS

Next Generation Sequencing

NMDAR

N-methyl-D-Aspartic acid Receptors

nobo

Noppera-bo

NPY

Neuropeptide Y

Octb3R

G Protein-Coupled Octopamine-b3 Receptor

PAS

Phagophore Assembly Site

PBS

Phosphate-Buffered Saline

PC

Phosphatidylcholine

PCA

Principal Component Analysis

PCOS

Polycystic Ovary Syndrome

PE

Phosphatidylethanolamine

PFA

Paraformaldehyde

PG

Prothoracic Gland

POMC

Pro-Opiomelanocortin

PPP

Peripheral Precocious Puberty

PTTH

Prothoracicotropic Hormone

PVH

Paraventricular nucleus

Pvr

PDGF/VEGF-related receptor

PYY

Peptide YY

RG

Ring Gland

sad

Shadow

SCN

Suprachiasmatic Nucleus

SE0$_{PG}$

Stomatogastric Serotoninergic PG Neurons

Sema1-a

Semaphorin1-a

shd

Shade

SLC18A3

Solute Carrier Family 18 Member A3

SLCs

Solute Carriers

SON

Supraoptic Nucleus

spo

Spook

SSHs

Sex Steroid Hormones

TGF-β

Transforming Growth Factor-β

Tkv

Thickveins

Upd2

Leptin-like Unpaired 2

VDRC

Vienna Drosophila Resource Center

VLDL

Very-Low-Density Lipoprotein

VMH

Ventromedial Hypothalamus

Table of Contents

Figures Index

Tables Index

Resumen

La adquisición de fertilidad es un hito crucial durante el desarrollo de los organismos con reproducción sexual. Numerosos estudios han avanzado en el análisis de los mecanismos subyacentes que desencadenan este evento. En general, existe una relación entre el estado nutricional del organismo y la correcta iniciación del proceso por parte de los centros de control neuroendocrino. Estos centros reguladores requieren una interpretación adecuada del estado nutricional, donde las reservas de energía en forma de lípidos y aminoácidos circulantes parecen ser importantes. En este trabajo, demostramos que el bloqueo de la detección tanto de lípidos (*Sema1a*) como de aminoácidos (*GlyT*) en células de la glándula protorácica (PG), el órgano neuroendocrino de *Drosophila melanogaster* responsable de la producción y secreción de la hormona esteroidea ecdisona, es suficiente para impedir la transición de juvenil a adulto, incluso en larvas bien alimentadas, que, como consecuencia, adquieren un fenotipo obeso. La autofagia parece desempeñar un papel esencial como mecanismo regulador en la conexión entre las dos vías metabólicas (metabolismo de lípidos y aminoácidos) y el inicio de la maduración sexual. La autofagia sistémica se activa en respuesta a la retirada de alimentos durante la transición larval de la fase de alimentación (L3F) a la fase errante (L3W), característica de esta etapa previa a la formación de la pupa. Así, en este estudio hemos probado que la reducción de la ingesta de glicina en la PG mediante el bloqueo del transportador *GlyT* sobre estimula anormalmente la autofagia local, escapando al control temporal de su activación. Como resultado, la grasa almacenada en forma de gotas lipídicas en la PG se degrada prematuramente, reduciendo la disponibilidad de colesterol. Como consecuencia de la interpretación de un estado nutricional fallido en términos de disponibilidad local de lípidos, no se produce el inicio de la maduración sexual y la producción de esteroides sexuales a partir del colesterol se ve afectada. La epistasis entre el transporte de lípidos (*Sema1a*) y aminoácidos (*GlyT*) en la PG no logra rescatar el fenotipo. Sin embargo, la movilización forzada de nutrientes mediante el ayuno en organismos deficientes en *GlyT* en la PG rescata el fenotipo tras la reactivación de la autofagia sistémica. En conjunto, estos resultados apoyan la idea de que la glicina desempeña un papel importante como regulador de la autofagia en la PG, y que esto puede ocurrir como consecuencia de su capacidad para modular el metabolismo de los lípidos localmente en los centros de control neuroendocrino.

Abstract

The acquisition of fertility is a critical developmental milestone in sexually reproducing organisms. A large number of studies have made progress in the analysis of the mechanisms underlying the triggering of this event. In general, there is a relationship between the nutritional state of the organism and the correct initiation of the process by the neuroendocrine control centers. These regulatory centers require a proper interpretation of the nutritional status, where energy reserves in the form of circulating lipids and amino acids seem to be important. Thus, we report here that the blockade of the detection of both lipids (Sema1a) and amino acids (GlyT) in cells of the prothoracic gland (PG), the neuroendocrine organelle of Drosophila melanogaster responsible for the production and secretion of the steroid hormone ecdysone, is sufficient to prevent the juvenile-to-adult transition, even in well-fed larvae, which consequently acquire an obese phenotype. Autophagy appears to play an essential role as a regulatory mechanism in the link between the two metabolic pathways (lipid and amino acid metabolism) and the onset of sexual maturation. Systemic autophagy is activated in response to food withdrawal during the larval transition from the feeding (L3F) to the wandering (L3W) phase, characteristic of this prepupal stage. Thus, in this study we have shown that reduction of glycine intake to PG by blockade of the GlyT transporter abnormally overstimulates local autophagy, thus escaping the temporal control of its activation. As a result, the fat stored as lipid droplets in the PG is prematurely degraded, reducing the availability of cholesterol. As a result of interpreting a failed nutritional state in terms of local lipid availability, the onset of sexual maturation does not occur and the production of sex steroids from cholesterol is impaired. Epistasis between lipid (Sema1a) and amino acid (GlyT) transport in the PG fails to rescue phenotype. However, forced mobilization of nutrients by starvation in organisms deficient in GlyT in the PG rescues the phenotype upon reactivation of systemic autophagy. Taken together, these results support the idea that glycine plays an important role as a regulator of autophagy in the PG, and that this may occur through its ability to modulate lipid metabolism locally in neuroendocrine control centers.

1. Introduction

1.1. Evolution and Sexual Selection

The discovery of the evolutionary process likely comprises the most important milestone of recent humanity. Evolution is the mechanism through which species change and adapt over time, giving rise to the diversity of life forms we see today. Hence, evolution is a fundamental process that explains the diversity of life on Earth.

1.1.1. The Evolutionary Process

Initially proposed by Charles Darwin in his seminal work "On the Origin of Species" in 1859, the concept of evolution describes how species change and adapt over time through natural selection. As main core of studies regarding the evolutionary process, Darwin observed that individuals of a species exhibit variations in their characteristics, and some of these variations confer advantages in survival and, more importantly, reproduction. Thus, those individuals with adaptive advantages are more likely to pass on their traits to the next generation, resulting in a gradual change in population characteristics over many generations.

1.1.2. Sexual Reproduction as a Main Force of Evolution

In this context, sexual reproduction plays a crucial role as the main driver of evolution. Unlike asexual reproduction, which produces offspring genetically identical to the parent, sexual reproduction mixes the genetic material of two individuals, adding an important genetic diversity to the genetic material of the offspring. This genetic variability is essential for evolution since it provides the material on which natural selection acts.

Consequently, sexual reproduction contributes to evolution in several ways. The combination of genetic material from two parents during sexual reproduction increases genetic variability within a population, providing a wide range of characteristics on which natural selection can act. During meiosis, the process of gamete formation, homologous chromosomes exchange segments of DNA in a process called recombination, generating new combinations of genes and increasing genetic diversity. Additionally, mutations that occur during sexual reproduction can introduce new genetic variants into the population. In addition to natural selection, sexual selection is an important evolutionary mechanism in sexual reproduction.

Darwin's concept of sexual selection highlights how certain traits, which might not necessarily aid survival, are favored because they enhance mate attraction and reproductive success.

The interaction between reproduction, genetic variability and selection is fundamental to understanding biological evolution, as expressed by Richard Dawkins in "The Selfish Gene" (1976): *"Natural selection is nothing more than the mechanism of selection of the genes that have succeeded in their own path to the future*". This view highlights the importance of reproduction as the vehicle through which genes are transmitted and compete to persist in future generations.

1.2. Acquisition of Reproductive Capacities

For the reproductive process to occur successfully, it is necessary for a given organism to previously acquire a series of very specific physiological capacities. These capacities will remain absent during their embryonic and juvenile development. In essence, an individual that belongs to a species with sexual reproduction, which could include many plant species, must be capable of producing a very specific cell type, gametes. Gametes are generated during meiosis from precursor cells that only exist in the reproductive organs. when it comes to animals, these reproductive organs are the gonads. Therefore, the gonads are very specialized organs in the production of this type of cell that will eventually allow sexual reproduction. However, this type of organ with such a specific function must have acquired its own maturity before being able to produce gametes and this is a finely regulated process. This point of maturity that the gonads must reach depends on a complex process of coordinated hormonal stimuli that will be detailed in later sections of this work.

Essentially, during the process of acquiring this physiological maturity of the gonads, the individual suffers a series of irreversible changes that clearly mark the transition from an organism without reproductive capabilities to an individual capable of generating offspring. In other words, this point marks the juvenile-to-adult transition.

1.2.1. Juvenile-to-Adult Transition. From Growth to Maturation

At first sight, during the life of an organism with sexual reproduction, two stages can be clearly differentiated. A juvenile stage of growth and an adult stage in which changes in physical size are little or absent. However, within the framework of sexual development, three distinct phases can be identified: the juvenile phase, the intermediate transition phase, known as puberty in humans, and the adult phase, characterized by achieved sexual maturity and full reproductive potential. In the juvenile stage, individuals primarily increase in size and cell number with minimal complexity and differentiation. This phase is characterized by volume gain and nutrient storage, predominantly through fat accumulation, which prepares the organism for the subsequent stages of development. Meanwhile, at the end of the intermediate transition stage, upon reaching the adult phase, growth in body size and nutrient storage ceases to give rise to a series of changes that occur both at the anatomical and physiological levels (Pangelinan et al., 2016, Vosberg et al., 2021, Natali et al., 2023). All these changes, which trigger the onset of sexual maturation and mark the entry into the adult phase, constitute the juvenile-to-adult transition process. In fact, the mechanisms underlying this process and its regulation are the core focus of this work.

In order to dissect the mechanisms that control this delicate transition process, we must pay special attention to the centers that trigger the beginning of this process, the neuroendocrine control centers. Furthermore, the regulation that these neuroendocrine centers of control perform is possible thanks to a group of molecules with a potent and selective action on its target tissues, steroid hormones. In fact, the strong influence that these hormones are able to exert on their target tissues largely explains the fine regulation needed regarding the moment in which this process is triggered.

In order to dissect the mechanisms controlling this delicate transition process, special attention must be given to the neuroendocrine control centers that initiate it. Furthermore, the regulation performed by these neuroendocrine centers is mediated by a group of molecules with potent and selective action on their target tissues: steroid hormones. The significant influence these hormones exert on their target tissues largely elucidates the critical importance of precise timing required to initiate this process, ensuring that target cells are in the appropriate state to undergo and respond correctly to these hormonal signals.

1.3. The Neuroendocrine System

Once eukaryotic organisms grow in size, complexity and acquire diverse functions throughout the phylogenetic scale, a communication system between the different organs capable of effectively coordinating external and internal stimuli, becomes necessary for the proper maintaining of a constant internal environment, the homeostasis balance.

The concept of the neuroendocrine system arises from the coordination that exists between the nervous and the endocrine systems (Harris, 1948, Harris, 1955). The nervous system generally allows the rapid and accurate transmission of information between distant regions of the body, normally within fractions of seconds. Conversely, hormone-mediated communication via its transport through the bloodstream is better suited for situations that require more widespread and longer lasting regulatory actions.

The neuroendocrine system is present in a large number of organs and tissues throughout the body and is made up of so-called neuroendocrine cells. In addition to the main neuroendocrine control centers, that will be treated in more detail in this section, specific populations of these neuroendocrine cells are located in organs such as the gastrointestinal (GI) tract, including the small intestine, rectum, stomach, colon and esophagus. They can be also found in the gallbladder, pancreas (islet cells), and thyroid (C cells). As well as the lungs, and airways (bronchi). This widespread distribution of neuroendocrine cells is known as the diffuse neuroendocrine system.

Essentially, neuroendocrine cells are nerve cells with exclusive qualities. Neuroendocrine cells have the ability to, not only integrate both electrical and hormonal stimuli, but also to produce and release hormones accordingly. In this way, neuroendocrine cells are capable of integrating afferent signals of diverse nature and responding to them with efferent hormonal outputs.

1.3.1. The Hypothalamic-Pituitary-Gonad Axis (HPG)

In mammals, the hypothalamic-pituitary-gonadal (HPG) axis acts as a neuroendocrine control complex orchestrating the onset and maintenance of sexual functionality (Figure 1). In response to certain environmental, hormonal and not yet fully described nutritional stimuli, Kisspeptin-releasing neurons fire on hypothalamic gonadotropin-releasing hormone (GnRH) neurons, causing the release of GnRH to the hypophyseal portal system. GnRH then binds to its receptors on the secretory cell of the adenohypophysis, the anterior pituitary (Oakley et al., 2009, Roa et al., 2011, Pinilla et al., 2012). This second component of the HPG axis, the anterior pituitary or adenohypophysis, releases the gonadotropins luteinizing hormone (LH) and follicle-stimulating hormone (FSH) into the blood stream. Gonadotropins, once delivered through the circulatory system to the gonads, promote cell maturation and differentiation which eventually leads to the production and release of sex steroids by mature gonadal tissues (Plant, 2015).

The regulation of the HPG axis involves complex feedback loops between its three main components to ensure the precise control of hormone levels needed for proper sexual development and reproductive function. High gonadal steroids (estrogens, progesterone and testosterone) levels activate negative feedback which inhibit the secretion of GnRH from the hypothalamus and the release of LH and FSH from the anterior pituitary thus preventing excessive hormone production (Tilbrook et al., 2001). In addition to steroid hormones, gonadal tissues can contribute to this negative feedback by releasing inhibin, a peptide hormone that specifically inhibits the secretion of FSH without affecting LH levels (Convissar et al., 2023). In males, this negative feedback loops are specially well localized with Sertoli cells producing inhibin to block FSH production by pituitary gland and Leydig cells producing testosterone to inhibit hypothalamic GnRH release (Jin et al., 2014). In females, despite the negative feedback during the menstrual cycle, with rising estrogen levels from developing follicles inhibiting hypothalamic GnRH release and FSH production by pituitary gland, there is also a switch to positive feedback. When estrogen levels reach a peak, a surge in GnRH takes place with the subsequent pituitary LH surge fostering ovulation and hence coordinating the reproductive cycle (Matt et al., 1998).
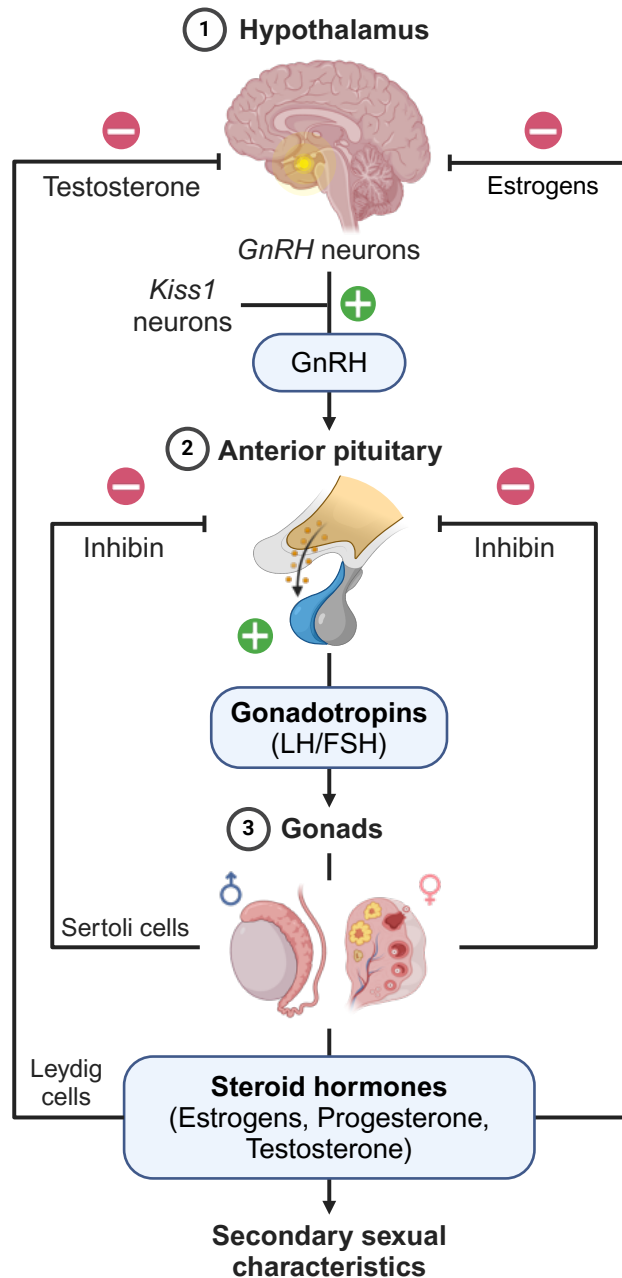
Figure 1. Schematic representation of Hypothalamic-Pituitary-Gonadal Axis. In the hypothalamus (1), GnRH neurons receive inputs from different sources, including Kiss1 neurons, to produce GnRH. Upon anterior pituitary stimulation by GnRH, gonadotropins luteinizing hormone (LH) and follicle-stimulating hormone (FSH) are release into the blood stream. Once gonadotropins are delivered to the gonads (3), steroid hormones are synthetized giving rise to secondary sexual characteristics on both the gonads and their target tissues. Regulatory negative feedbacks are shown where both steroid hormones themselves and inhibin participates over GnRH neurons and the anterior pituitary respectively.

1.3.2. Steroid Hormones

Once we have discussed the complex regulation process that occurs in the main neuroendocrine control centers that comprise the HPG axis, and how this finally triggers the production of sex hormones, we can address some details about the nature and structure of these sex steroid hormones (SSHs).

Sex hormones are crucial for reproductive function and secondary sexual characteristics. Among them, three major classes can be stablished: androgens, estrogens and progestogens. Androgens, the major male sex hormones, are represented mainly by Testosterone. Meanwhile, estrogens, mainly estradiol, together with progesterone, are the primary female sex hormones. Nevertheless, all of these hormones are synthesized in both females and males in different concentrations. Notably, testosterone can be aromatized to estradiol by the enzyme aromatase or reduced to the non-aromatizable androgen dihydrotestosterone (DHT) by 5α-reductase (Celotti et al., 1997, Goldman et al., 1974).

Unlike the peptide hormones that regulate the process at the level of the hypothalamus and pituitary, the SSHs released by the gonads are lipidic-derived hormones. All steroid hormones share a common chemical structure derived from cholesterol, a lipid that acts as their main precursor (Figure 2). Cholesterol has a structure of four fused hydrocarbon rings, and through a series of enzymatic reactions which include the elimination of side chains and the modification of hydrocarbon rings, it is converted into the different classes of steroid hormones (Singh et al., 2000, Payne et al., 2004, Nakamoto et al., 2010).

It is important to keep in mind that in both vertebrates and invertebrates, steroid hormones are of the same nature and are produced under essentially equivalent regulatory mechanisms (Moeller et al., 2013, Xie et al., 2024, Li et al., 2024, Golshan et al., 2024).
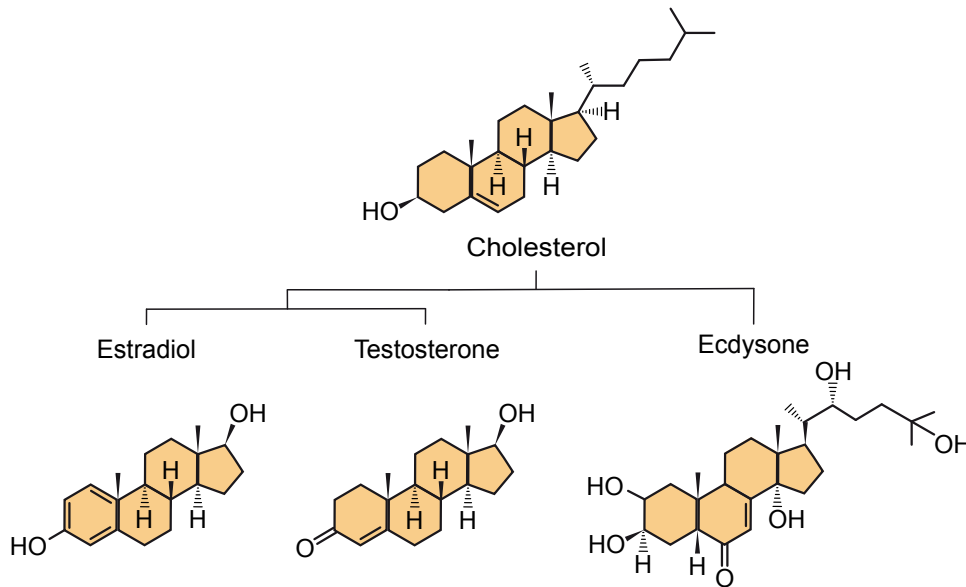
Figure 2. Chemical structure of cholesterol and its derived steroids. The four fused hydrocarbon rings structure of cholesterol (highlighted in orange) is shared among all steroid hormones. As an example of this, both mammals (estradiol, testosterone) and insects (ecdysone) main steroid hormones are shown.

1.4.   The Mammalian Onset of Sexual Maturation

In mammals, the onset of sexual maturation is known as puberty, the final phase of which in humans is known as adolescence, and which leads to the adult phase. Puberty is one of the most complex physiological processes that take place during the development of an organism, which can be noted in its fine and highly multifactorial regulation. According to this, many of the factors that intervene in the onset of puberty, especially when it comes to the integration of nutritional status with the activation of certain neuroendocrine circuits, remain to be important areas of research nowadays.

Puberty involves a large set of changes in the metabolism and physiology of the organism that experiences it and represents a point of no return for it. This is why the regulation of this process integrates a large number of initiating factors of different nature that ensure this transition to occurs in an optimal way. The investigation of these triggering factors for the onset of sexual maturation is crucial for comprehending the mechanisms underlying both typical and atypical pubertal development, as well as understanding the clinical implications of these dysregulations.

1.4.1. Triggering Factors in the Onset of Puberty

The onset of sexual maturation takes place under the influence of many triggering factors that must be well integrated to ensure not only success but also adequate timing.

Genetic inherited predisposition plays an important role in the timing of pubertal onset. Some variations in genes involved in signaling at the level of the HPG axis have an impact on the age of onset of puberty. Polymorphisms in the Kiss1 and GPR54 genes, which are critical for the proper activation of the gonadotropin-releasing hormone (GnRH) neurons, have been associated with the regulation of the timing of puberty onset (Ohtaki et al., 2001, Navarro et al., 2004). In addition, heterozygous mutations in makorin RING-finger protein-3 (MKRN3), a gene located in the Prader-Willi syndrome critical region, is known to cause precocious puberty in humans (Abreu et al., 2013).

Post-transcriptional modifications such those mediated by microRNAs (miRNAs) have been demonstrated to be implicated in numerous physiological processes, including pubertal onset (Messina et al., 2016). These miRNAs are short non-coding RNAs that binds to target messenger RNA (mRNA) to regulate their expression by degradation or inhibition of translation As said before in this section, MKRN3 has been gaining interest recently as putative pubertal repressor, as evidenced by the central precocious puberty caused by mutations in this gene in humans (Abreu et al., 2013). Hence, recent studies demonstrate that post-transcriptional modifications in the 3'UTR region of MKRN3 mediated by the miRNA, miR-30, operate as repressor of MKRN3 to control pubertal onset (Heras et al., 2019).

Epigenetic changes, such as DNA methylation and histone modifications, can also contribute to the timing of pubertal onset by regulating gene expression in response to environmental cues without changing the underlying DNA sequence. Some epigenetic regulation, for instance those that alters the methylation status of the GnRH gene promoter region, have been linked to the timing of puberty (Deshpande et al., 2023, Toro et al., 2018).

Besides the hormonal regulation from HPG axis itself, the high number of variables involved in regulating the onset of sexual maturation include a network of neurotransmitters and neuropeptides, including circulating levels of ghrelin, leptin, peptide YY (PYY), and neuropeptide (NPY) (Tarçin et al., 2024).

Additionally, melatonin, a hormone associated with circadian rhythms, has been implicated in the timing of puberty onset (Yang et al., 2021, Chen et al., 2022).

Importantly, external factors such as psychosocial stressors are another critical determinant of pubertal timing. Highly stressful situations in early life as well as childhood adverse experiences can lead to delayed or precocious pubertal onset depending on the moment, intensity and duration of the stress (Schlomer et al., 2022, Mendle et al., 2014).

Among the environmental factors that have an enormous influence on the timing of pubertal onset, nutritional status is undoubtedly the most determining. In fact, nutritional status remains the most studied factor in the context of the onset of sexual maturation (Anderson et al., 2024). It makes sense to think that the hypothalamus, which we have already highlighted as a main neuroendocrine control center, coordinates reproductive functions depending on the nutritional and metabolic status of an individual. Thus, we find different hypothalamic nuclei with very clear functions in this context (Tran et al., 2022). For instance, the Lateral hypothalamus (LH) is known as the "hunger center." Its stimulation enhances compulsive feeding behavior, while damage in this area can result in reduced food intake and weight loss (Stratford et al., 2013). The ventromedial hypothalamus (VMH) is traditionally considered the "satiety center" of the brain, it is involved in feeding behavior. Lesions in the VMH lead to hyperphagia and obesity, indicating its role in inhibiting feeding (Gaur et al., 2021). The arcuate nucleus (ARC) is involved in both energy balance and reproductive functions. ARC not only produces kisspeptins to stimulate GnRH neurons but also It produces several important neuropeptides for appetite regulation like NPY and Agouti-related peptide (AgRP) that stimulates appetite, while pro-opiomelanocortin (POMC) and cocaine- and amphetamine-regulated transcript (CART) suppress appetite (Lee et al., 2024). Regarding the nutritional state as a triggering factor for the initiation of sexual maturation, the hypothalamic nuclei are capable of integrating signals such as: nervous signals from the digestive tract that provide information about gastric filling (Filpa et al., 2016), chemical signals about the composition of minerals and blood glucose that provide information about satiety (Wasinski et al., 2020), signals from gastrointestinal hormones and those released by adipose tissue (Morano et al., 2022), and signals from the cerebral and somatosensory cortex that provide sensory information capable of modifying feeding behavior (Soria-Gómez et al., 2014).

1.4.2. Childhood Nutrition Impact on Pubertal Onset

Nutritional status, mainly in the form of body mass acquisition, accumulated fat and energy balance, plays a crucial role in triggering the onset of sexual maturation (Figure 3). This is especially notable when it comes to nutrition during childhood and pre-adolescence (Figure 3A). In fact, numerous studies support the idea that both overnutrition and malnutrition maintain a direct relationship with the timing of pubertal development (NCD Risk Factor Collaboration, 2017, Brix et al., 2020, Pereira et al., 2021, Soliman et al., 2022).

Overnutrition, usually leading to higher body mass index (BMI) and increased adiposity, has been strongly linked to precocious puberty (Figure 3B). High levels of adipose tissue increase leptin levels, this adipokine gives signals about nutritional sufficiency and the state of energy reserves to the hypothalamus, thus influencing the secretion of GnRH and consequently activating pubertal development (Chehab et al., 1997).

Undernutrition, chronic malnutrition or energy imbalance due to excessive training during childhood, can delay or even arrest pubertal development (Georgopoulos et al., 2010). Lack of energy intake or a low body fat reserve results in a drop in leptin levels which can inhibit GnRH secretion. This inhibition blocks the HPG axis, delaying the onset of puberty (Figure 3C). In addition, some conditions, such as anorexia nervosa or bulimia, are associated with delayed puberty that, in especially severe cases, comes to a complete halt in the onset of sexual maturation (Soliman et al., 2022). In line with this, the "critical weight hypothesis" proposes that a certain amount of body mass and volume must be acquired for the pubertal onset to take place (Frisch & Revelle, 1970).

However, sometimes the pubertal delay typical of malnutrition is not triggered by a lack of nutrition *per se*, but rather by defective signaling of body fat levels or even certain micronutrients in particular (Figure 3D). This is the known example of leptin mutants (Clément et al., 1998, Montague et al., 1997). In addition, other alterations, such as the one that affects the semaphorin signaling system, can result in defective development of hypothalamic circuits, leading to hypogonadotropic hypogonadism and delayed pubertal onset (Cariboni et al., 2015).

Despite in the field most studies on the timing of pubertal onset in relation to nutrition focus on the study of fat stores and their signaling to neuroendocrine control centers, other micronutrients, vitamins, solutes and small molecules collaborate in sensing of nutritional status, taking part of the metabolic regulation of sexual maturation (Wang et al., 2024, Liu, 2024, Kawade, 2012). However, the mechanisms by which these specific nutrients are coordinated together with fat sensing for a correct triggering of puberty still remain unknown.
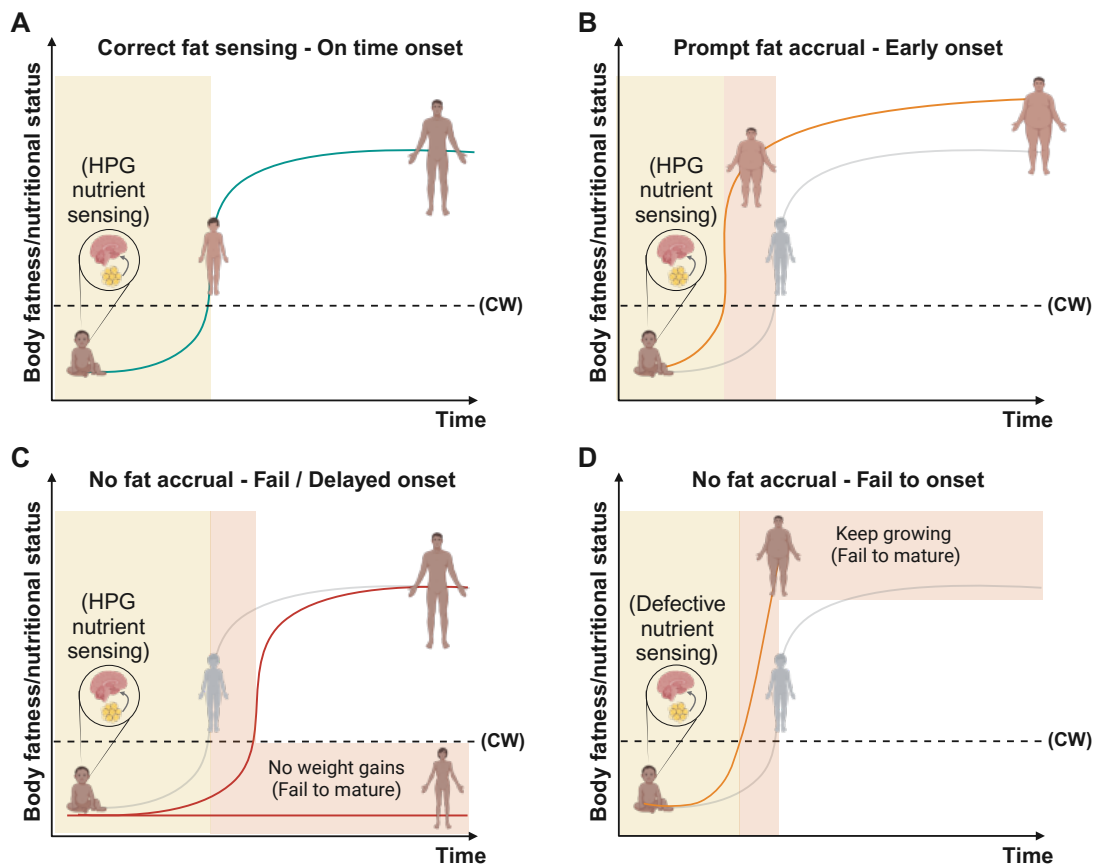
Figure 3. Growth curves in juvenile-to-adult transition. Four typical scenarios of pubertal onset timing are shown. A) On time pubertal onset takes place when levels of body fat and nutritional status allow to overcome the critical weight (CW). B) In childhood overnutrition condition, prompt fat accrual provokes early CW overcome leading to precocious puberty. C) In contrast, childhood undernutrition or severe starvation-like conditions corelate with either delayed or absent pubertal onset since CW is reached late or never respectively. D) In defective nutrient sensing conditions, juvenile individuals are not able to transition even though CW has been reached already. Figure adapted from Juarez-Carreño et al., 2021.

1.4.3. Implications of Precocious Puberty

Entering puberty at a time earlier than appropriate is known as precocious puberty or early puberty. Children who experience this condition develop early sexual characteristics. In the case of girls this is before the age of 8 and for boys before the age of 9 (Wei et al., 2017, Bradley et al., 2020). Within what we know as early puberty there are mainly two types: the central precocious puberty (CPP) is dependent on gonadotropins and is the most common type of early puberty. In CPP, there is an early release of gonadotropins from the HPG axis that triggers the entry into puberty out of time. On the other hand, peripheral precocious puberty (PPP), which is not dependent on gonadotropins and occurs due to the prompt release of androgens and estrogen from peripheral tissues (Marshall & Tanner, 1969, Marshall & Tanner, 1970, Tanner, 1981).

Obesity is one of the most significant public health challenges nowadays. Overweightness and obesity are well correlated with a number of syndromes and diseases that are more notable when it comes to childhood condition. This is especially dramatic due to the "pandemic-like" increasing of childhood obesity and overweightness worldwide and its long-term complications (de Onis et al., 2010, Majcher et al., 2021). Some major risks of precocious puberty include the core components of metabolic syndrome, type 2 diabetes and type 2 diabetes-related cardio-metabolic risks (Shah et al., 2022), adulthood obesity with coronary artery-related diseases (Fang et al., 2019), psycho-social complications like anxiety, depression and antisocial behavior during adolescence (Berembaum et al., 2015), premature bone maturation with early closure of the growth plates leading to shorter height (Lee, 2024), hormone-related conditions such as polycystic ovary syndrome (PCOS) in females and testicular abnormalities in males (Bremer, 2010), reproductive health, potentially leading to irregular menstrual cycles, subfertility, or infertility in adulthood (Ibitoye et al., 2017) and some types of cancer (Bodicoat et al., 2014) among other long-term complications (Kozioł-Kozakowska et al., 2023).

1.4.4. Implications of Delayed Puberty

Late puberty is defined as the absence of signs of pubertal development after age 13 in girls and age 14 in boys (Stanley & Misra, 2021). The delay in the age of onset of puberty is associated with a series of clinical risks that can also develop into long-term complications. Among others, some major risks of delayed puberty include musculoskeletal problems resulting from a lack of muscle and bone maturation that can lead to fractures due to low bone density (Palmert & Dunkel, 2012) and muscular dystrophy (McCarrison et al., 2024), cardiometabolic problems, which despite being more common in cases of precocious puberty, they also occur in cases of delayed puberty due to the effects on hormonal abnormal development (Zhang et al., 2024). In addition to this, children with late puberty may have a greater tendency to suffer affective symptoms such as depression and anxiety that can extend into adulthood. Particularly in men, delayed puberty is associated with an increased risk of continued depressive symptoms from adolescence to adulthood (Baker et al., 2019).

1.5. *Drosophila* as a Model Organism in Neuroendocrinology

Neuroendocrine processes are complicated processes in which usually the participation of several interactors located in different tissues and organs is desired. Traditional models and *in vitro* experiments for the analysis of the molecular components of neuroendocrine systems, often prevent the interaction with other physiological systems, which is crucial to understand their *in vivo* functions. The alternative to these classic approaches consists of the so called "genetic dissection". It consists of a non-invasive technique that involves the systematic generation of mutations or repression of individual genes, followed by an *in vivo* analysis of the phenotypic effects. This allows the alteration of a single protein or gene involved in the molecular pathway that is intended to be studied. This avoids the disruption of interactions that could be observed between other molecular components, giving a broader vision of how the manipulated gene affects the set of physiological systems of the organism in a given context. Of all the model organisms available in biomedical research, *Drosophila melanogaster* is the most suitable for this type of approaches. Not in vain has it been successfully used for more than 100 years in neuroscience research (Bellen et al., 2010).

Understanding the complicated processes on which the triggering of puberty is based, can be greatly benefited from the study of metamorphosis in a model organism such as *Drosophila melanogaster*. Metamorphosis, like puberty, involves an intricate hormonal and genetic signaling network that culminate in profound physiological changes leading to adulthood status acquisition. Both processes are characterized by the transformation of a juvenile organism into a sexually mature adult with reproductive potential, orchestrated from neuroendocrine control centers that regulate both growth, maturation and reproductive competencies.

Importantly, increasing accessibility to new transcriptomic approaches, linked to the extensive knowledge on genetic regulation in *Drosophila melanogaster*, make it an even more interesting model organism for neuroendocrinology research. Using such a small organism, allows its entire body to be processed, covering the whole set of its mRNAs. In this way, we can obtain an overview of the transcriptomic profile of the entire organism, thereby preserving the existing interactions between the different physiological systems and observing the effects between distant organs involved in a given process.

1.5.1. *Drosophila melanogaster* Life Cycle

One of the characteristics that make *Drosophila melanogaster* an ideal model organism for the study of neuroendocrine processes is the short period of time it requires to go through a complete life cycle. In the context of the regulatory processes involved in the onset of sexual maturation, it is interesting to have a number of individuals in which we can study the progression of the juvenile-to-adult transition in a synchronized manner.

The life cycle of *Drosophila* can be divided into four main stages that include the egg, larval instar, pupa and adult phases, which together cover a duration of 10 days at a constant temperature of 25ºC (Figure 4).

The egg phase begins the life cycle with the deposition of eggs by the female. These eggs, approximately 0.5 mm long, are usually deposited in decaying fruit (hence they are also known as "fruit fly") or other organic material.

The intermediate larval phase, which can be divided into three clearly differentiated stages, is in which the larvae mainly spend their time eating, gaining volume and weight, preparing themselves for metamorphosis.

The first one of the larval stages is known as First Instar (L1). This phase lasts around 24 hours after the egg hatches. At this stage the larvae are small and are dedicated almost exclusively to feeding on the fruit or organic substrate in which they were deposited as eggs almost immediately after hatching.

A second larval stage, known as Second Instar (L2), begins right after the molting that happens to divide the L1 and L2 larval instars. During the L2 stage, the larva undergoes significant growth, consuming large amounts of food. In fact, the larva molts another time, to accommodate its increasing size. This molting process marks the transition between instars. This instar takes around 24, depending on the temperature and food availability.

Following, the Third Instar (L3). This stage is lasting approximately 48-72 hours and is divided into two important phases according to the behavior that larvae exhibit: the Feeding phase (L3F) and the Wandering phase (L3W). The initial phase of this third phase, L3F, lasts around 24-36 hours and in it the larva eats voraciously, notably increasing its size and weight, reaching its maximum larval weight, which normally exceeds the weight of the pupa and of the adult. At the end of this phase, when enough weight gain allows it, the last larval phase, L3W, begins. In this phase, which lasts 12 to 24 hours, feeding behavior ceases and the larvae wander away from sources of food and hydration. It is a time of searching for a suitable place for the formation of the pupa. This phase marks a decisive point, signaling the change from the stages that make up the youth of the larva towards the beginning of its transition to the adult stage. This L3W phase is commonly used as a proxy for the study of the beginning of sexual maturation, since the change from feeding behavior to wandering behavior represents the declaration of readiness for metamorphosis.

The pupation phase begins once the larva has located a suitable site for pupation. The pupal phase lasts around 3-5 days, being the longest phase for obvious reasons; during this period, the larval structures undergo a series of modifications in which their juvenile characteristics are broken and replaced by their adult features through the process we know as metamorphosis. During this phase, the pupa will remain glued to the pupation location, protected by the pupal case that, among other things, prevents dehydration that could be fatal for larval tissues during these series of severe transformations.

Finally, the adult phase. This begins when the adult fly emerges from the pupal case in a process known as eclosion. Initially the adult is pale and soft in appearance, but it quickly acquires the darker colors that characterize it and that, in fact, give its name to the species ("*melanogaster*" comes from Greek and literally means dark belly) in addition to completing the development of chaetae and exoskeleton. Adults will reach sexual maturity within 8 to 12 hours after eclosion and can start mating shortly thereafter. Adult fruit flies typically live for 60 to 80 days, during which time females can lay hundreds of eggs, thus continuing the cycle.
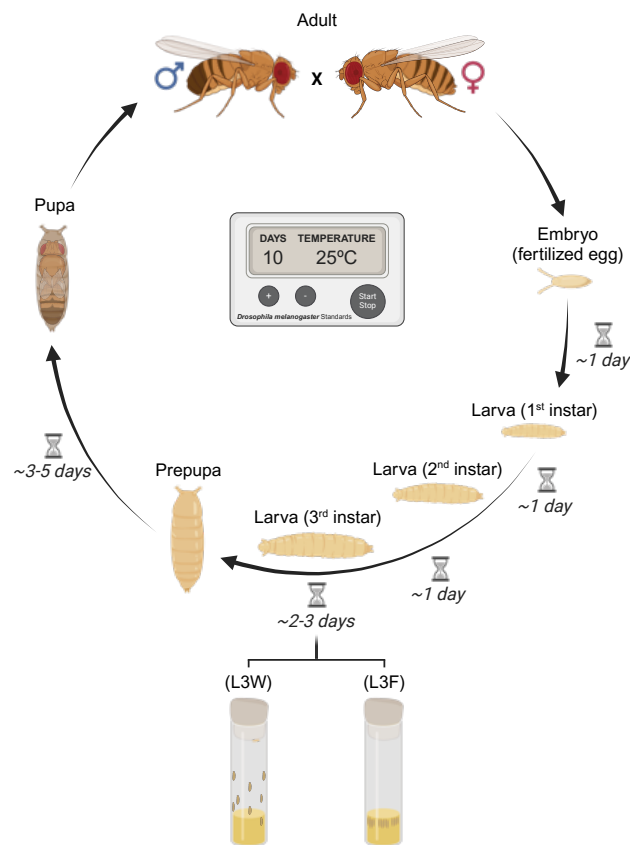
Figure 4. Drosophila melanogaster life cycle. Schematic view of "fruit fly" life cycle. Laid fertilized eggs take around 1 day to hatch to become first instar larva (L1). Around one more day is needed to reach the second instar larva (L2) after which third instar larva (L3) is reached within another 24 hours approximately. Between 2-3 days are required to transition from Feeding (L3F) to Wandering (L3W) larval stage. In a period of 3-5 days, prepupae are form leading to metamorphosis and eventual adult eclosion.

1.5.2. Metamorphosis as a System for Investigating the Pubertal Onset

In previous sections, we have commented on the importance of acquiring reproductive competences for sexually reproducing organisms. In essence, the mechanism that allows all sexually reproducing species to reproduce necessarily implies a non-return transition from a juvenile stage to an adult phase in which they obtain reproductive potential. Hence, the intermediate point between these two phases, the juvenile-to-adult transition, is of great interest to the scientific community. The coordination of this process from neuroendocrine control centers, its triggering factors and the nature of the hormones that intervene in its regulation, that is, its main components, preserve mechanisms that function in very similar ways in all these species (Barredo et al., 2021). Which means that the triggering of the juvenile-to-adult transition is an evolutionary conserved mechanism and that the processes we observe in mammalian puberty are, in most scenarios, parallel to those that take place in *Drosophila melanogaster* (Guirado et al., 2023). Therefore, details regarding these similarities between puberty and metamorphosis, that support the idea of using *Drosophila* metamorphosis as a system to investigate the onset of puberty, will be detailed below (Figure 5).

While, in the case of puberty in mammals, it is the HPG axis that is made up of the main neuroendocrine control centers, with hypothalamic GnRH neurons being the principal promoters of the activation of the process (Figure 5A), in the case of the *Drosophila melanogaster* larval brain, are a pair of prothoracicotropic hormone (PTTH)-releasing neurons located in each hemisphere that are considered primary promoters of the signal necessary for the production of steroid hormones (Figure 5B). In the case of insects this steroid hormone is ecdysone. These PTTH neurons secrete a neuropeptide that gives them their name, and which was initially discovered in the silkworm Bombyx mori (Kawakami et al., 1990). The neuropeptide PTTH is secreted into the glandular assembly responsible for most of the neuroendocrine regulation in *Drosophila*, the Ring Gland (RG), where we can distinguish three main components: The Corpus Cardiacum (CC), the Corpus Allatum (CA) and the Prothoracic Gland (PG), the latter being the target of PTTH neurons. It is in this portion of the RG, in the population of PG cells, where the Extracellular-Signal-Regulated Kinase (ERK) gene is activated as a consequence of the activation of the Ras/Raf/ERK signaling cascade and the Mitogen-Activated protein (MAP) kinase via its receptor tyrosine kinase, torso, to promote ecdysone synthesis and release hence regulating larval maturation (Rewitz et al., 2009).

It is at this time, about 12 hours before pupation, that the expression of the PTTH gene increases significantly. Genetic ablation of PTTH neurons extends the L3 larval stage and delays the time of pupariation by 4 or 5 days with a notable increase in adult body size (McBrayer et al., 2007).

Similar to the activation of kisspeptin signaling in mammals, recent studies have shown that the timing of PTTH secretion is regulated by the expression of several neuropeptides that are produced in different larval cell populations, such as the kisspeptin homolog Allatostatin A (AstA) (Deveci et al., 2019), the GnRH homolog Corazonin (Crz) (Imura et al., 2020), as well as the neurotransmitters acetylcholine and octopamine (Hao et al., 2021). Furthermore, AstA receptor 1 (AstAR1) is the insect homologue of Kiss1 receptor 1 (Kiss1R). In fact, its blockade in PTTH neurons causes a phenotype very similar to that of PTTH-null mutants, resulting in a delay in development and an abnormally increased pupal size (Shimell et al., 2018).

At this point, we know that the mechanisms that trigger the synthesis and release of steroid hormones in mammals are compartmentalized to take place in the gonads after the induction of the hormonal signals of LH and FSH from the pituitary gland once the axis via GnRH neurons is activated. Equivalently, in *Drosophila*, the Halloween genes are responsible for the synthesis and release of the steroid hormone ecdysone in the PG cells which, in a similar way to the process in mammals, are induced after receiving afferent signals from the PTTH neurons.

The Halloween genes are a group of genes in insects, including *Drosophila*, essential for the biosynthesis of ecdysteroids, which are the mammalian steroids homologous hormones critical for transition timing and development in insects. These genes include Spook (spo), Phantom (*phtm*), Disembodied (dib), Shadow (sad), Shade (shd) and Noppera-bo (nobo). Each gene encodes a specific enzyme that, as in the case of mammals, are involved in the conversion of cholesterol to the steroid hormone (Rewitz et al., 2006). In the case of *Drosophila*, this would be the ecdysone, the steroid precursor of the active hormone 20-hydroxyecdysone (20E).

Among the signals that are integrated at the level of the PG, functioning as the main neuroendocrine center of control, different types of inputs can be classified depending on their origin. Some signals are autocrine in nature, thus induced from the PG itself and do not involve the activity of PTTH neurons (Pan & O´Connor, 2021, Cruz et al., 2020).

Other signals are brain-derived (Hückesfeld et al., 2021, Shimada-Niwa et al., 2014) and others are non-brain-derived (Juarez-Carreño et al., 2021, Gibbens et al., 2011, Li et al., 2022) that come from distal organs that are capable of conveying nutritional status, environmental factors and other unknown inputs that directly modulate the activity of PG cells.

Autocrine signals that are integrated by PG cells include multiple receptor tyrosine kinases. For example, anaplastic lymphoma kinase (Alk), PDGF/VEGF-related receptor (Pvr), and epidermal growth factor receptor (EGFR) which together, in combination with the PTTH/torso axis, share the same signaling pathways that control triggering pupation through activation of the Ras/ERK pathway (Pan & O´Connor, 2021). However, although the activation of tyrosine kinase receptors is a predominant signal in PG, some studies suggest that activation by monoaminergic autocrine signaling through the G protein–coupled octopamine-b3 receptor (Octb3R) also plays a crucial role acting upstream of insulin/insulin-like growth factor (IIS) ligand family and Ras/ERK signaling (Ohhara et al., 2015). Furthermore, a second G protein-coupled receptor in the PG, 5-hydroxytryptamine receptor 7 (5-HT7), responds to conditions of nutrient scarcity by reducing signals from stomatogastric serotoninergic PG neurons ($SE0_{PG}$) reducing signaling from 5-HT towards PG cells reducing the release of ecdysone and thereby delaying development (Shimada-Niwa et al., 2014, Deliu et al., 2022).

The systemic non-brain-derived signals that are integrated into the PG coming directly from distal organs of the organism, cause these feedback circuits to be integrated in a manner homologous to the triggering factors in mammals that have already been discussed previously and thereby increasing the complexity of the system. Although, apparently, the genetic mechanisms that trigger the onset of sexual maturation in *Drosophila* are simpler than in mammals, this is not the case with the integration of these external signaling factors from distal organs. In fact, it is the integration of these mechanisms at the level of the PG that comprises the main focus of study of this work.

In a homologous manner to the regulatory mechanisms that occur in mammals, several diffusible signals coming from distal organs of *Drosophila* are capable of influencing the timing of the juvenile-to-adult transition upon reaching the PG. Under normal physiological conditions, the decapentaplegic protein (Dpp), a ligand for Transforming Growth Factor-β (TGF-β), is released from the imaginal discs into the hemolymph and its signaling via the activation of thickvenis (Tkv) receptor has been shown to be capable to negatively regulate ecdysone production (Setiawan et al., 2018).

Despite the number of peripheral signals that are known to be integrated in central neuroendocrine tissues, there are still many mechanisms that remain unclear both in mammals and *Drosophila*. For example, recent studies support the idea that communication between the fat body (the larval homologous to mammalian liver and adipose tissue) and the PG cells, is crucial to inform whether the total energy reserves are adequate to cover the eventual demands that will be required for a proper reproductive function, again maintaining a strong relationship with the mammalian processes such as those that involve leptin mutations (Clément et al., 1998, Montague et al., 1997).
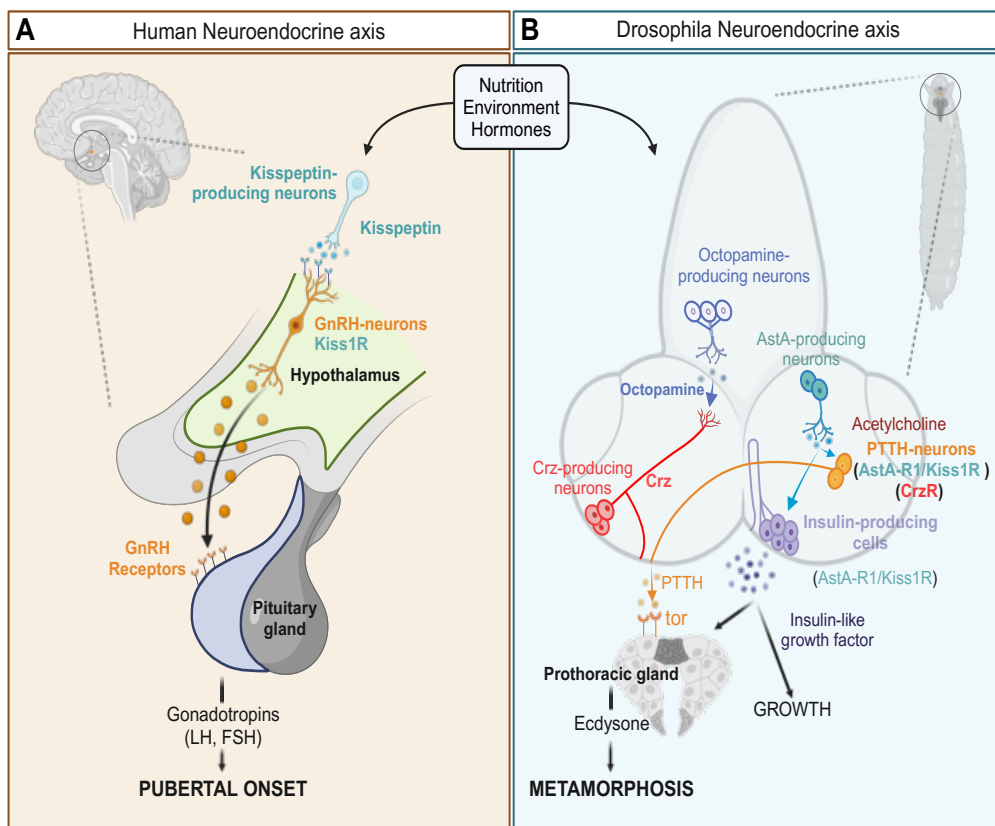
Figure 5. Human and Drosophila melanogaster neuroendocrine centers of control. Representative scheme of mammalian (A) and fruit fly (B) neuroendocrine centers of control and main pathways involved in the juvenile-to-adult transition are shown. Figure modified from Guirado et al., 2023.

1.6. Lipid Sensing in the Onset of Sexual Maturation

Lipid sensing is the most studied nutritional factor in the context of the metabolic status for both the triggering of sexual maturation (Nakamoto et al., 2010, Enya et al., 2014, Huang et al., 2020, Shi et al, 2022, Qi et al., 2022), and for reproductive performance itself (Samavat et al., 2014, Bianco & Josefson, 2019) in both mammals and insects.

1.6.1. Lipid Sensing and Puberty. The Mammalian Scenario

In mammals, under conditions of high nutritional intake, the pancreas and adipose tissue release insulin and adipokines (adipose cytokines), respectively, into the bloodstream. The interplay between these two is evident, as some adipokines are pro-inflammatory and can, in fact, promote insulin resistance (Kumar et al, 2020, Huang et al., 2020). The adipokine leptin plays a crucial role in the regulation of neuroendocrine circuits such as the one mainly mediated by Kiss1 and GnRH neurons (Ahn et al., 2012, Qiu et al., 2015). Studies in rodents with defects in leptin signaling, either due to mutations in the *ob* gene that encodes it (Zhang et al., 1994), or by ablation of its receptor (LepR) in AgRP GABAergic neurons of the hypothalamic ARC (Egan et al., 2017), have shown that such mutants have difficulties in determining nutritional status and fail to achieve proper activation of the HPG axis.

Hypothalamic function can be directly affected by high energy intake, regardless of circulating hormone levels. Numerous studies hold the idea that ceramides act as fatty acid sensors, influencing the hypothalamus to regulate eating behavior (Turpin-Nolan & Brüning, 2020, Cruciani-Guglielmacci et al., 2024). Experiments in obesity mouse models have shown a strong correlation between this condition and elevated ceramide levels in the paraventricular nucleus (PVH) of the hypothalamus. Furthermore, blocking ceramide synthesis in the PVH causes a delay in the activation of the HPG axis in overweight female rats (Heras et al, 2020). Importantly, when their presence is excessive, ceramides promote endoplasmic reticulum stress leading to cellular dysfunction (Contreras et al., 2014, González-García et al., 2018).

The number of pathways linking lipid sensing to the proper function of neuroendocrine circuits is currently increasing. Some studies point to slightly more complex pathways that involve epigenetic modifications derived from the nutritional condition of an individual

([Lomniczi er al., 2013](#)). In this context, the sirtuins, a family of conserved NAD$^+$-dependent deacetylases, are activated under high NAD$^+$, as a consequence of low cellular energy status, to modulate lipid metabolism, among other metabolic processes ([Nogueiras et al., 2012](#)). Experimental studies have demonstrated that the deacetylase SIRT1, acting as a "fuel-sensor" in Kiss1 neurons, is capable of acting on the promoter of the Kiss1 gene via interaction with the polycomb. In this way, during early childhood undernutrition, the levels of SIRT1 increase, thereby repressing the expression of Kiss1 with the consequent delay in the activation of the HGP axis ([Vázquez et al., 2018](#)).

1.6.2. Lipid Sensing and Metamorphosis. The Insects Scenario

In recent studies we have shown that the interaction between fat deposits and neuroendocrine cells is essential to trigger the onset of the juvenile-to-adult transition in *Drosophila*. Blocking the transport of lipids from the fat body to the neuroendocrine PG cells prevents the transition even when the critical weight has been exceeded. Larvae keep feeding without affecting the IIS signaling pathway and gaining weight until they die. This has been demonstrated through blocking both apolipophorin (*apolpp*), the major lipid transporter in *Drosophila*, in the larval fat body, or both Fatty acid transport protein2 (*Fatp2*), Semaphorin1a (*Sema1a*), and leptin-like unpaired 2 (*upd2*) directly in the PG. In addition, human Leptin transgene expression in *Sema1a* and *upd2* deficient individuals was enough to rescue the obese non-pupating phenotype ([Juarez-Carreño et al., 2021](#)).

Molting and metamorphosis are strictly regulated by ecdysteroids synthesized from dietary cholesterol in PG cells ([Gilbert et al., 2002](#)). Indeed, some studies in *Drosophila* raise the possibility that *nobo*, a glutathione S-Transferase member of the Halloween genes, is in charge of regulating the behavior of cholesterol in steroid biosynthesis through a mechanism that remains to be fully clarified ([Enya et al., 2014](#)). Furthermore, in situations in which a high production of steroid hormones is required, the levels of cholesterol available in the cytoplasm of the cells responsible for this hormonal synthesis must be adequate ([Pan & O´Connor, 2021](#)). Studies in *Drosophila* demonstrate that this cholesterol is made available to steroids production machinery in part thanks to an autophagy-mediated cholesterol trafficking mechanism ([Texada et al., 2019](#)). Since amino acid metabolism is a clear trigger of autophagy, as we will detail in next sections, the idea of autophagy as a point of confluence between lipid metabolism and amino acid sensing in the context of the onset of sexual maturation seems to be attractive.

1.7.   Solute Carriers in the Onset of Sexual Maturation

We have previously commented on the integration of triggering elements for the onset of sexual maturation in both mammals and *Drosophila*, as well as the similarities that both processes share. Most studies in this area of research focus their efforts on understanding the mechanisms that integrate the detection of peripheral fat from neuroendocrine control centers. In this context, it is important to make special mention of those nutritional factors that, without being lipid in nature, seem to be increasingly relevant among the set of triggering factors for the onset of sexual maturation. This is the case of the function of small solutes and micronutrients that could be necessary for a correct detection of, not only the energy reserves acquired in the juvenile phase, but also the ability to metabolize and mobilize these reserves, as well as to evaluate the availability of nutrients in a given external environment.

Solute carriers (SLCs) group of membrane transport proteins includes around 400 members organized into more than 50 families (Ceder & Fredriksson, 2022). This diverse group of transmembrane proteins allows the transport of different molecules and solutes across cell membranes by active, passive and combined transport in the form of symports. These transporters are essential for the maintenance of cellular homeostasis and signal transduction pathways, since many of them require agile and coordinated movements of small molecules and micronutrients between cells and tissues for a proper function. The role that SLCs play in the onset of sexual maturation is particularly significant if we take into account that they involve the transport of important molecules for cell function such as amino acids, glucose, vitamins, cations, anions and metals among many other small solutes that are essential for the regulation of the cell populations that compose the neuroendocrine centers of control in many species (Xia et al., 2021, Farenholtz et al., 2019, Sun et al., 2017).

Some recent studies show how certain SLCs are directly related to the regulation of the function of neuroendocrine centers by regulating the function of GnRH neurons. This has been recently reported in spatial transcriptomic studies of the hypothalamic ARC, in which four subclusters of neurons were detected based on their similar transcriptomic profiles. Examining in more detail, only one of the subclusters showed a robust and uniform expression of Kiss1 that, in fact, was isolated thanks to the expression of a single biomarker, the Solute carrier family 18 member A3 (SLC18A3) (Zhou et al., 2022).

1.7.1. Amino acid Sensing in Neuroendocrine Regulation

So far, some facts have been described about the importance of a correct homeostasis of small solutes and micronutrients for the for a proper function of the neuroendocrine control centers. If we add to this the extensive remodeling that their cell populations and tissues undergo during the juvenile-to-adult transition, it seems easy to think that amino acid transport must play an important role in the process. Hence, amino acids, as a basis for the construction of proteins, are essential not only for the cellular and tissue differentiation that takes place during the juvenile-to-adult transition, but also to ensure the correct functioning of the structures that are intended to provide reproductive potential (Wu et al., 2014, Gao H, 2020, Shao et al., 2023). Amino acids happen to be the most frequently substrate transported by proteins from the solute carriers (SLCs) family (Fredriksson et al., 2008). Essentially, cell differentiation involves the production of proteins that a given cell was not producing previously. Hence, not only the amount but also the balance between the different types of amino acids must be finely regulated during the process.

For more than thirty years, several studies have already described the importance of amino acid sensing by neuroendocrine centers of control to modulate the release of hormones and neuropeptides at a proper timing (Bourguignon et al., 1989, Terasawa & Fernandez, 2001). In this context, excitatory amino acids (EAAs) such as glutamate and aspartate, have been highlighted as essential components in the modulation of the anterior pituitary LH and FSH secretion upon GnRH neurons activation (Brann & Mahesh, 1994). For example, glutamate can act as a modulator of the activity of neuroendocrine circuits through the activation of N-methyl-D-aspartic acid receptors (NMDAR). This is the case in the GnRH neurons of the hypothalamus of mammals and in the neuroendocrine control centers of numerous species (Scacchi et al., 1998, Chiang et al., 2002, Vogeler et al., 2021). EAAs are found in high concentrations in the presynaptic boutons of several hypothalamic nuclei such as the ARC, the suprachiasmatic nucleus (SCN), the supraoptic nucleus (SON), the paraventricular nucleus (PVN), and the preoptic area (POA) (Brann & Mahesh, 1994). However, despite the role that EAAs play in neuroendocrine regulation, as in the case of NMDAR, they often require the presence of the obligatory co-agonist glycine to provide the necessary allosteric modulation. Both glutamate, through binding by guided diffusion in the N2A subunit, and glycine, through binding by unguided diffusion in the N1 subunit, are necessary for the NMDAR regulation of GnRH neurons activity (Yu & Lau, 2018).

1.7.2. Glycine Homeostasis in the Onset of Sexual Maturation

Glycine owes its name to the Greek word "glykis", meaning "sweet", after its discovery in 1820 from the acid hydrolysis of gelatin (Braconnot, 1820). Glycine is the only achiral amino acid and therefore lacks "levo"- (L-) or "dextro"- (D-) rotatory isomers. In addition, it is the smallest amino acid, with a molecular weight of 75.067 g/mol. Glycine is classified as non-essential amino acid since it can be synthesized internally from serine, choline, threonine and glyoxylate (Alves et al., 2019). However, in humans only 35% of the glycine available in the body comes from internal synthesis (Yu et al., 1985). Therefore, glycine is sometimes referred to as "partially essential" because, despite the capacity for internal synthesis, its dietary intake is essential for the correct maintenance of vital physiological processes. Among many other cellular functions, this is the case, for example, of collagen synthesis (Meléndez-Hevia et al., 2009).

Despite being an essential component of proteins, glycine is also involved in such a wide amalgam of physiological reactions and cellular processes that would be difficult to enumerate completely. Among many others, glycine is essential for protection against oxidative stress (Wang et al., 2014) and inflammatory processes (Zhang et al., 2020, Aguayo et al., 2023), synaptic function, for example in the mechanism for the transmission of itch and pain (Foster et al., 2015), regulation of gene expression (Luka, et al., 2002), type 2 diabetes (Gonzalez-Ortiz et al., 2001), some types of carcinomas (Martínez-Chantar et al., 2008) and of course in the fundamental context of this work, the onset of sexual maturation. Regarding this, we have already commented on the importance of the allosteric modulation of glycine in the N1 subunit of NMDARs (Yu & Lau, 2018). Old experimental evidence shows that high doses of glycine significantly elevated serum LH levels in female rats (Morishita et al., 1981) and that chlorpromazine and reserpine, considered to be ovulation-blocking agents, elevate the concentration of glycine in monkey hypothalamus, preventing ovulation only if applied before critical weight achievement (Singh & Malhotra, 1964), new studies demonstrate significant correlation between glycine metabolism and early puberty in children (Wang et al., 2023).

Due to the need for fine regulation of intracellular glycine homeostasis, there are selective transporters whose only function is the exclusive transport of Glycine. Membrane proteins such as the glycine transporter (GlyT), from the SLC6 family, are dedicated exclusively to the internalization of glycine. In the case of GlyT2, the most similar to the only GlyT isoform in *Drosophila*, this occurs through a stoichiometry of 3 Na+/Cl-/glycine (Roux & Supplisson, 2000).

1.8.   Glycine and Lipid Metabolism. Integrated Circuits

The influence of glycine on lipid metabolism is currently a field of increasing interest. For instance, glycine has been shown to have important therapeutic potential by modulating lipid metabolism in humans. Clinical evidence supports that plasma glycine levels are significantly low in patients with insulin resistance or type 2 diabetes (Floegel et al., 2013, Gar et al., 2018), acute myocardial infarction risk (Ding et al., 2015), aortic dissection (Wang et al., 2017), nonalcoholic fatty liver disease (NAFLD) and obesity (Gaggini et al., 2018). Essentially, the fact that numerous pathologies derived from defects in lipid metabolism relies on proper glycine homeostasis, suggests that both circuits are somehow integrated.

Besides clinical evidences, *in vivo* experimental studies with murine models have reported glycine as the most prominent lipid-lowering amino acid, mediating the inhibition of Very-Low-Density Lipoprotein (VLDL) cholesterol and triglyceride biosynthesis. In fact, glycine administration to apolipoprotein E-deficient (*apoE−/−*) mice, causes a decrease in serum triglycerides by enhancing the activity of the High-Density Lipoprotein (HDL)-associated enzyme paraoxonase 1 (Rom et al., 2017). Cell culture *in vitro* experiments has also demonstrated that glycine supplementation increases the mRNA levels of adiponectin and interleukin-10 (IL-10), two adipose-derived adipocytokines with anti-inflammatory effects, in 3T3-L1 adipocytes and facilitates lipid droplets formation (Chen et al., 2018).

Glycine and serine are crucial for lipid metabolism since they are key substrates of the Kennedy pathway for the biosynthesis of phospholipids (Kennedy & Lehninger, 1949, Kennedy & Weiss, 1956). Kennedy pathway is responsible for the synthesis of the most abundant phospholipids in cell membranes, phosphatidylcholine (PC) and phosphatidylethanolamine (PE) (Figure 6). Briefly, during this biosynthetic process, choline and ethanolamine are phosphorylated to form phosphocholine and phosphoethanolamine that will be eventually combined with cytidine diphosphate (CDP), resulting in CDP-choline and CDP-ethanolamine. Those intermediate molecules will be finally transformed in PC and PE, respectively (Déchamps et al., 2010, Meléndez-Hevia et al., 2009).

Autophagy, which will be treated with more detail in the next section, appears to have the potential to be an important integration point between pathways converging on glycine and lipid metabolism.
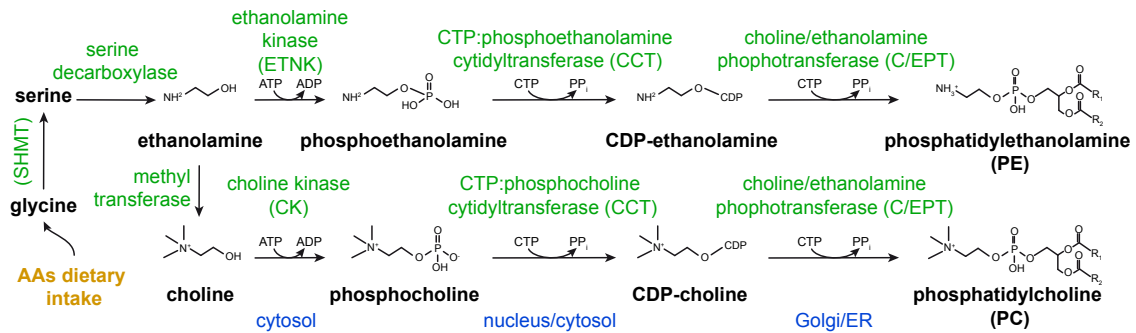
Figure 6. Phosphatidylethanolamine (PE) and phosphatidylcholine (PC) biosynthesis. Schematic representation of PE and PC biosynthesis from glycine and serine. Enzymes involved in the process are in green. SHMT refers to Serine Hydroxy-Methyl-Transferase enzyme that facilitates the conversion from glycine to serine. In blue, cellular compartments in which each reaction takes place.

1.9. Autophagy and its Implications

The term autophagy is derived from the Greek words for self (auto) and for eating (phagein), meaning "self-eating". It was first described by Christian de Duve in 1963 (Klionsky, 2008). Autophagy is a programmed cellular process that is active in almost all tissues of eukaryotic species (Kuma et al., 2017, Mathai et al., 2017, Khezri & Rusten, 2019, Gohel et al., 2020, Klionsky et al., 2021, Varga et al., 2022). Generally speaking, we can say that autophagy is the main cellular recycling process.

The processes that regulate autophagy are essential for the maintenance of homeostasis under physiological conditions and are usually more active during nutritional imbalance or starvation (Vainshtein et al., 2014). Furthermore, autophagy is crucial in the turnover of potentially damaging components, and prevention of infectious diseases (Mizushima, 2007) Thus, autophagy is critical in a wide range of physiological processes and a defective autophagic flux is related to numerous diseases in humans (Liu et al., 2018, Hwang et al., 2021, Feyder et al., 2021). In fact, autophagy seems to be a process linked to juvenile and developing structures. Some studies support that autophagic flux decrease during life, becoming very latent in old age, causing the accumulation of dysfunctional organelles and harmful proteins (Vainshtein et al., 2014) and promoting vascular senescence (Salazar et al., 2020).

The most generic mechanism of autophagy involves the engulfment of cytoplasmic material or microorganisms in double membrane vesicles, which subsequently fuse with a lysosome for its degradation to take place. However, in order to accurately describe the cellular mechanisms that occur during the autophagy recycling process, we must pay attention to the macromolecules or organelles on which such recycling is focused.

Hence, in the following section, both the types of autophagy and their main mechanisms are described, taking into account the classification they receive in mammals and *Drosophila*. Since the types of autophagy are very numerous and varied due to the high attention they are currently receiving, we will focus especially on the types of autophagy that are active in neuroendocrine control centers and that are potentially important regulators of them during the process of the onset of sexual maturation.

1.9.1. Types of Autophagy

Essentially, three main types of autophagy can be distinguished: macroautophagy, chaperone-mediated autophagy (CMA) and endosomal microautophagy (eMI). Despite their morphological differences, all of them conclude in the delivery of the target cargo to the lysosome for further degradation and recycling (Yang & Klionsky, 2010)

Macroautophagy is the most common type of autophagy (Figure 7A), so one can usually refer to it simply as autophagy. The process of macroautophagy begins with the formation of a double membrane structure, the phagophore, which later elongates to engulf the selected cargo for degradation in a complete vesicle called autophagosome. Subsequently, the autophagosomes fuse with the lysosomes, generating the autolysosome, where the cargo is finally degraded (Søreng et al., 2018). The main set of genes that regulate macroautophagy, the Autophagy-related genes (ATG), were discovered in yeast (Tsukada & Ohsumi, 1993). Currently more than 30 ATG genes are known, most of them highly evolutionarily conserved from mammals to *Drosophila*. In the case of non-selective bulk autophagy, the genes responsible for initiating the process are mainly those that form the Atg1 kinase complex (comprising of Atg1, Atg13, Atg17 and Atg101 in both *Drosophila* and mammals, Atg1 being the *Drosophila* homologue of the mammalian ULK1).

However, about 18 ATGs are mainly responsible for the processes of induction of autophagosome formation (with Atg101 and Atg1 kinase complex as a main player), vesicle nucleation and binding to the Phagophore Assembly Site (PAS), in which then Atg7, Atg16, Atg10 and Atg18 will attach to expand the phagophore, Atg5-Atg12 and Atg3, Atg7, Atg12 which are involved in vesicle expansion and finally SNARE-mediated fusion between the membrane of the autophagosome and the lysosome is controlled mainly by Rab GTPases. Thus, the engulfed autophagic cargo is released into the lysosomal lumen, where hydrolases and proteases facilitate final degradation and recycling of the given cargo molecules (Bhattacharjee et al., 2019). Macroautophagy can occur in a selective manner regarding the cargo they sequester for degradation. Thus, we find selective autophagy of mitochondria (mitophagy), selective autophagy of aggregated proteins (aggrephagy), of intracellular pathogens (xenophagy), of lipid droplets (lipophagy) and even of peroxisomes (pexophagy) (Gatica et al., 2018). Indeed, lipophagy is of special interest in the context of regulating the onset of sexual maturation in *Drosophila* (Pan et al., 2019). Let us remember that steroid hormones, protagonists in the maturation process, are synthesized from dietary cholesterol and hence this lipid must be present in the cytoplasm of the cells responsible for producing these hormones.

Regarding lipophagy and its contribution to neuroendocrine regulation centers, we will talk in the next section in which we will analyze in more detail the molecular factors and regulators of autophagy processes.

Additionally, we can comment some details regarding the type of autophagy mediated by chaperones, CMA. CMA is thought to depend on the level of LAMP-2A binding to proteins (Cuervo and Dice, 2000), a lysosomal-associated membrane protein currently identified only in mammals and birds. Based on that, CMA may not function in organisms such as *Drosophila* (Tekirdag and Cuervo, 2018). Therefore, this type of autophagy is the least relevant in the context of this work because its role is not excessively important, at least today, in the neuroendocrine processes that regulate the onset of sexual maturation in *Drosophila*. Briefly, CMA differs from macroautophagy in that autophagosomes are not produced. In contrast, the substrate proteins for degradation by CMA contain a pentapeptide motif that generally include the amino acids Lysine (K), Phenylalanine (F), Glutamic Acid (E), Arginine (R) and Glutamine (Q) (KFERQ), which is required for their targeting to the lysosome upon its delivery by the chaperone Hcs70 (Dice et al., 1990).

Lastly, the third type of autophagy, microautophagy or eMI (Figure 7B). This type of autophagy is the least studied at present, but importantly it serves as a link with macroautophagy and, in addition, happens to fill the existing gap regarding the absence of CMA in *Drosophila*.

Microautophagy can occur in a selective or non-selective manner. Non-selective eMI is responsible for the uptake of soluble cytosolic material by the formation of small tubular invaginations (Li et al., 2012). This process is mostly studied in yeast in which vacuoles are the primary lysosomal compartment (Kunzt et al., 2004).

Some studies in the past have emphasized in the cross-control of macro- and microautophagy. For instance, in the case of the absence of complete macroautophagic vesicles in t-SNARE mutants of microautophagy (Darsow et al., 1997). In the other hand, selective eMi refers to the specific degradation of substrates such as mitochondrial (micromitophagy), nuclear components (piecemeal microautophagy) and peroxisomes (micropexophagy) (Todde et al., 2009). Selective eMi also degrades proteins containing a pentapeptide- (KFERQ)-like motif, as in CMA (Kaushik and Cuervo, 2012). Thus, since CMA has not been identified in *Drosophila* due to the absence of the LAMP-2A, as commented before, *Drosophila* are believed to degrade pentapeptide- (KFERQ)-like motif-containing peptides via eMi (Figure 7C). Eventually, these substrates can either be degraded by the lysosome directly or by the fusion of late endosomes to the lysosome (Galluzzi et al., 2017).

In general terms, autophagy is currently of increasing interest when it comes to the mechanisms that regulate the trigger of the onset of sexual maturation. In the next sections we will detail some aspects of specific types of autophagy that seems to be crucial for a proper tempo in juvenile-to-adult transition, in both mammals, including humans, and insects, including *Drosophila.*
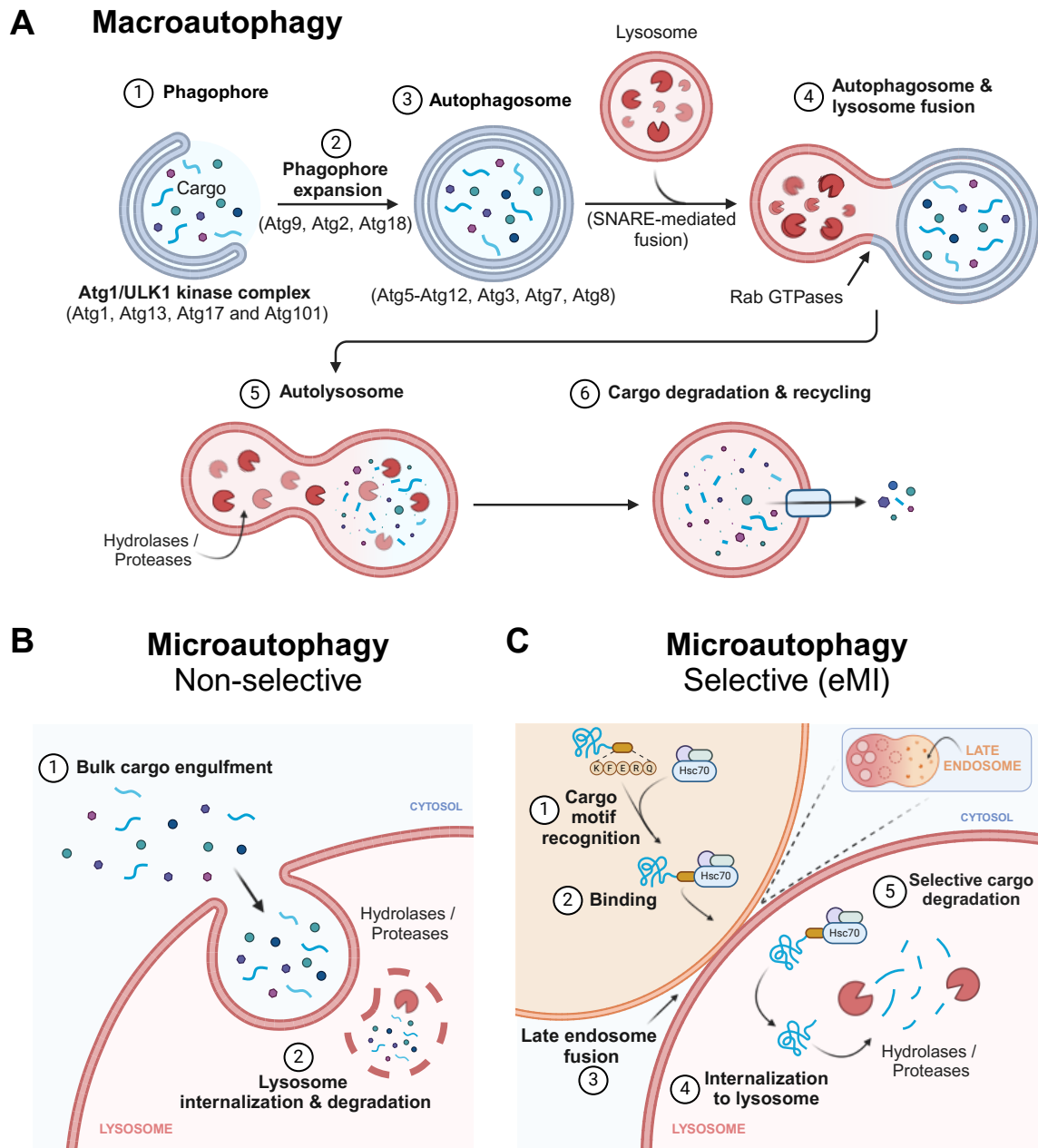
Figure 7. Macroautophagy and microautophagy in Drosophila melanogaster. A) Macroautophagy, also known as Autophagy, begins with the characteristic formation of a Phagophore (1). This double membrane vesicle gets extended (2) to engulf the either selected or bulk cargo within an Autophagosome (3). This will be fused to a lysosome (4) to give rise to the combined structure called Autolysosome (5), where cargo degradation and recycling (6) are going to take place. B) Microautophagy in a non-selective manner just implicate the engulfment of bulk cargo from the cytosol (1) for further lysosomal internalization and degradation (2). C) In selective endosomal Microautophagy (eMI), cargo KFERQ-motifs are recognized and attached to chaperone Hcs70 (1,2). After late endosome fusion to the lysosome (3), selected cargo is internalized (4) for degradation and recycling (5).

1.9.2. Triggering Factors of Autophagy

Autophagy is crucial for the regulation of many developmental processes, with nutritional status and cellular oxidative stress being the main modulatory factors. In this way, starvation is known to promote the initiation of autophagy pathways to increase availability of required nutrients as a source of energy and to build new proteins and membranes (Rabinowitz, & White, 2010). If we observe this phenomenon in more detail, we could say that there are several ways by which the activation of autophagic fluxes can be triggered. In fact, they differ depending on the metabolite or nutrient that is in short supply. In this way, we know that both a lack of blood glucose, insulin, or high levels of glucagon are clear triggers of autophagy through the starvation pathway, as well as a low protein intake (Park et al., 2023, Rabinowitz, & White, 2010, Yin et al., 2018).

The shortage of amino acids as a proxy of undernutrition is a clear activator of autophagy pathways through the classic Mechanistic Target of Rapamycin (mTOR) pathway (Cao et al., 2021), thus being one of the main mechanisms that triggers autophagy flux.

Additionally, glutathione is one of the main Thiol-containing compounds of eukaryotic cells. These compounds play a central role in many physiological reactions due to their capability to undergo redox cycles between reduced and oxidized status. Since oxidative stress is a clearly triggering factor for autophagy, it is important to take glutathione into account as a main activator of this pathway in the context of developmental processes (Sun et al., 2018).

Alternatively, autophagy can also be regulated through epigenetic modifications. This is the case, for example, of autophagy induced by cigarette smoking, which has been shown to promote and accelerate lung aging (Vij et al., 2018). Furthermore, we should take into account the regulation of autophagy through some miRNAs. For example, some studies suggest that Glycine decarboxylase induces autophagy and is downregulated by miRNA-30d-5p in some types of cancer (Zhuang et al., 2019).

1.9.3. Autophagy in Neuroendocrine Centers of Control

As we have already seen in previous sections, nutritional and metabolic status are key factors when it comes to precisely controlling the triggering of the onset of sexual maturation. Thus, neuroendocrine control centers are highly affected by lack or excess of nutrients. However, after the review that the introduction of this work entails, we can think that it is the consequences of this nutritional excess or deficiency, indirectly translated into the modulation of other metabolic processes, that ultimately end up being responsible of this fine regulation of the beginning of the juvenile-to-adult transition. In this regard, more and more studies place autophagy in neuroendocrine control centers as a crucial event in controlling the onset of sexual maturation in different species (Ommati et al., 2019, Texada et al., 2019, Tracy & Baehrecke, 2013), as well as in the reproductive function itself (Wang et al., 2022).

In humans, recent case report studies demonstrate that defects in the N-alpha-acetyltransferase 10 gene (NAA10), which plays and important role in cell growth, differentiation and autophagy, correlate with the diagnosis of NAA10-related syndrome (Ogden syndrome). Particularly, a girl aged 4 years and 3 months diagnosed with Ogden syndrome with p.Arg83Cys mutation in NAA10 gene, who had many characteristic features of the disorder, as well as precocious puberty (Wojciechowska et al., 2024).

Steroidogenic cells are only capable of storing small amounts of hormones. Therefore, when rapid hormone production becomes necessary, these cells depend on the mobilization of the steroid precursor cholesterol (Lavrynenko et al., 2015, Rewitz et al., 2013, Warren et al., 1988). Cholesterol reserves are stored in specialized organelles, the Lipid Droplets (LDs) (Danielsen et al., 2016). Although the mechanisms that allow cholesterol trafficking and mobilization are not fully described, some studies have shown that autophagosomes do, in fact, contain cholesterol, which reinforces the idea of autophagy as a determining factor in the promotion of the pathways that are regulated at the neuroendocrine level (Singh et al., 2009, Danielsen et al., 2016, Texada et al., 2019). Furthermore, lipophagy has been shown to selectively break down stored lipids by sequestering LDs (Cingolani and Czaja, 2016).

The mechanisms and molecular regulators of autophagy for the triggering of the onset of sexual maturation, remain a challenge for neuroendocrinology research. Comprehensive studies are necessary to reveal the coordination between autophagy pathways and the sensing of specific nutrients, such as amino acids and lipids, that takes place in the neuroendocrine circuits for the precise regulation of juvenile-to-adult transition. The research detailed in this thesis work aim to provide valuable insights into these processes in *Drosophila melanogaster*. These findings are anticipated to contribute to the broader understanding applicable to mammals, including humans.

2.   Objectives

The general objective of this doctoral thesis is to investigate the role that certain micronutrients, such as amino acids, play in combination with lipid metabolism to trigger the onset of sexual maturation. Therefore, we intend to analyze the mechanisms that allow the detection of these nutrients by neuroendocrine circuits during the juvenile-to-adult transition in *Drosophila melanogaster*.

To address it effectively, the general objective of this work was divided into the following partial objectives:

- *In vivo* RNA[i]-based screening of SLC transporters in the main *Drosophila* neuroendocrine cells, PG cells.

- Identify candidate SLCs whose expression in PG cells is necessary to trigger the juvenile-to-adult transition process.

- Phenotypic characterization resulting from the *in vivo* screening of SLCs, addressing key developmental, metabolic and cell biological consequences, both systemically and locally in PG cells.

- Analysis of the overall transcriptomic profile of candidate-transporter-ablated individuals by RNA-seq to identify expression patterns in comparison to controls at different developmental stages in whole larvae.

- To investigate the consequences of candidate SLCs ablation at the PG level by using single cell RNA-seq methodology.

- Propose a mechanism of action explaining the role of solutes transported by candidate SLCs in neuroendocrine triggering of juvenile-to-adult transition.

3. Materials and Methods

3.1. *Drosophila* Husbandry

The reference stock used for RNA[i] *in vivo* screenings (otherwise indicated) was *phtm^{22}-GAL4* (a gift from K. Rewitz). Other fly stocks used in this study were: *spo-GAL4.1.45* (BDSC #80578), *Aug21-GAL4* (BDSC #30137), *eyeless-GAL4* (a gift from M. Dominguez), *ppl-GAL4* (BDSC #58768), *UAS-Sema1a* (BDSC #65734), *UAS-Sema1a^{i}* (VDRC #4743), *UAS-TOR^{i}* (BDSC #33951), *UAS-TOR^{i}* (BDSC #34639), *UAS-S6K^{STDE}* (BDSC #6913), *UAS-S6K^{STDETE}* (BDSC #6914), *UAS-GstD1::*GFP (a gift from D. Bohmann), UAS-Leptin (Rajan and Perrimon, 2012; a gift from N. Perrimon), *UAS-GFP-mCherry-Atg8a* (BDSC #37749), *UAS-GFP-RpL10Ab* (BDSC #42681), *UAS-mCD8::GFP* (BDSC #5137), *UAS-Sec::GFP* (a gift from M. Gonzalez-Gaitan), *UAS-tdTomato-Sec61b* (BDSC #64747), *UAS-NMDAR1^{i}* (BDSC #41666) , *UAS-NMDAR1^{i}* (BDSC #41667), *UAS-NMDAR1^{i}* (BDSC #25941), *UAS-NMDAR1^{WT}* (BDSC #8275), *NMDA1$^{i\ (AP)}$* (VDRC #108378), *NMDAR2^{i}* (BDSC #40928), *NMDAR2^{i}* (BDSC #40846), *NMDAR2^{i}* (BDSC #26019), *UAS-GlyT-SAM2.0* (TRIP-OE GP08791, kindly generated by the TRiP; Transgenic RNAi project at Harvard Medical School), UAS-GlyT^{KO} (BDSC #82660), UAS-dCas9.P2 (BDSC #58985), UAS-dCas9.P2 (BDSC #58986), UAS-dCas9::VPR (BDSC #66561), UAS-dCas9::VPR (BDSC #66562), UAS-tdTomato-Sec61β (BDSC #64747), UAS-*Shmt^{i}* (BDSC #57739), oregon-R and w^{1118}.

When purchased, fly strains included in this work were obtained mainly from two well-known stocks facilities: The Vienna Drosophila Resource Center (VDRC), and Bloomington Drosophila Stock Center (BDSC).

The rest of the stocks used in this work are organized according to its *in vivo* screening group or category. Thus, strains used for solute carrier superfamily *in vivo* screening are listed in Table 1, strains used for autophagy and glutathione metabolism-related genes *in vivo* screening are listed in Table 2.

Flies were reared in standard "Iberian" fly food at 25ºC (otherwise indicated) on a 12 hours light/dark cycle. Standard "Iberian" fly food was made by mixing 15 L of water, 0,75 kg of wheat flour, 1 kg of brown sugar, 0.5 kg of yeast, 0.17 kg of agar, 130 ml of a 5% nipagin preservative solution in ethanol, and 130 ml of propionic acid.

3.2.   Solute Carrier Superfamily *in vivo* Screening by RNA[i]

The lists of fly strains used in this *in vivo* screening to evaluate RNA[i] transgenes belonging to SLCs Superfamily (Dietzl et al., 2007) are presented in Table 1 (highlighted in red, lines producing phenotype). Generally, about 10-15 *UAS-RNA[i]* males, the transgene carriers, were crossed with about 10-15 *phtm[22]-GAL4* virgin females and kept in standard Iberian fly food at 25ºC (otherwise indicated). The first filial generation (F1), resulting from the initial cross, was assessed to determine the presence of the specific phenotype of interest.

3.3.   Glycine Metabolism-Related Genes *in vivo* Screening by RNA[i]

The lists of lines used in this *in vivo* screening to evaluate RNA[i] transgenes related with Glycine metabolism pathways (Ni et al., 2011) are in Table 2. Generally, about 10-15 *UAS-RNA[i]* males, the transgene carriers, were crossed with about 10-15 *phtm[22]-GAL4* virgin females and kept in standard Iberian fly food at 25ºC (otherwise indicated). The first filial generation (F1), resulting from the initial cross, was assessed to determine the presence of the specific phenotype of interest.

3.4.   Autophagy and Glutathione-related Genes *in vivo* Screening by RNA[i]

The lists of lines used in this *in vivo* screening to evaluate RNA[i] transgenes related with Autophagy and glutathione pathways (Dietzl et al., 2007, Ni et al., 2011) are included in Table 3 (highlighted in red, lines producing phenotype). Generally, about 10-15 *UAS-RNA[i]* males, the transgene carriers, were crossed with about 10-15 *phtm[22]-GAL4* virgin females and kept in standard Iberian fly food at 25ºC (otherwise indicated). The first filial generation (F1), resulting from the initial cross, was assessed to determine the presence of the specific phenotype of interest.

3.5. Developmental Time Measurements

For proper synchronization of larvae developmental time and stage, about 20-30 females and 20-30 males were crossed in standard Drosophila vessels containing 5 ml of Drosophila standard "Iberian" food. After 24-48 hours, flies were transferred to 2 ml grape juice agar plates with yeast paste and left for 3 hours to allow egg deposition. Parental flies were removed, and laid eggs were incubated for 48 hours at 25ºC. Second-instar larvae were transferred into vessels containing 5 ml of Drosophila standard "Iberian" food (20 larvae per vessel) and reared at 25ºC. Pupae were examined at 8-hour intervals, with the time period 2-4 hours after the onset of egg laying serving as the baseline (referred to as time "0" or "after egg laying" (AEL)). This approach allowed for systematic observation and documentation of pupal development and associated changes at specific time points.

3.6. Larval Weight and Volume Measurements

To weigh larval flies, groups of 5 larvae at the required developmental stages were collected, totaling 30-45 larvae for each desired genotype. After being rinsed in cold 1 x Phosphate-buffered saline (PBS) buffer and dried with tissue paper, larvae weigh was measured using a digital precision scale.

For larval and pupal volume determination, 10 larvae and pupae of each genotype were collected and photographed with their dorsal side up. Subsequently, the length and width of the larvae and pupae were measured using ImageJ software (version 1.54b). The larval and pupal volume was then calculated using the following formula: $v = \left(\frac{4}{3}\right) \pi \cdot \left(\frac{L}{2}\right) \cdot \left(\frac{w}{2}\right)^2$, where "L" represents length and "w" represents weight.

3.7.   20-Hydroxyecdysone (20E) Treatment

About 40-50 previously synchronized second-instar larvae were transferred in groups of 10 to new vessels containing 5 ml of fresh "Iberian" standard food supplemented with 0.5 mg/mL of 20-hydroxyecdysone (20E) from an initial stock of 10 mg/mL (H5142, Sigma-Aldrich). Since 20E was diluted in ethanol, it was used as a vehicle control. Control genotype (*phtm>+*) was taken as a reference for pupation time. Once 120-144 hours AEL has been reached, pupae were collected and washed twice in cold 1 x PBS buffer and stored at -80ºC.

3.8.   Hemolymph Sample Preparation

At desired developmental stages, three replicates of 15 animals per group for each condition were rinsed and washed in cold 1 x PBS buffer. Larvae were placed in a manipulated 0.5 mL tube as previously described (Palomino-Schätzlein et al., 2022). Briefly, after tearing the larval cuticles carefully, larvae were collected in a 0.5 mL tube in which a cross-shaped cut has been made at the bottom with a No. 22 surgical blade. After that, the 0.5 mL tube (with the cross-shaped hole in the lower part) was fitted inside a 1.5 mL regular tube. Then, the tube tandems were gently centrifuged 3 times for 3 seconds each time at room temperature with open caps using a 5415 R centrifuge (Eppendorf). Finally, 10 µL of the supernatant were transferred to a new 1.5 mL tube and stored at -80ºC to avoid melanization if they were not to be used immediately.

3.9.   Glycine Measurements

Hemolymph samples from whole larvae at 72 and 120 hours AEL were collected as previously described ("Hemolymph sample preparation"). Free glycine levels were measured in both control (*phtm>+*) and knockdown (*phtm>GlyT^i*) animals at indicated time points. Samples and reagents were prepared for fluorometric-based Glycine Assay kit (Abcam, ab211100) according to manufacturer´s instructions. In a 96 well black plate with flat bottom (Thermo Scientific, 165305) fluorescence was measured at a wavelength of Ex/Em = 535/587 nm.

3.10. Ecdysteroid Measurements

Larvae were collected in groups of 20-40 animals according to its total weight. Since the sensitivity of the used commercially available 20-Hydroxyecdysone (20E) enzyme immunoassay kit (Bertin Pharma #A05120.96 wells) requires a minimum of 20 mg of starting material, about 20 larvae were enough in the case of 120h AEL individuals (both controls and knockdown), while about 40 larvae were required in the case of 96h AEL individuals (both controls and knockdown). Whole larvae were collected and preserved in methanol at -80ºC as described in (Koyama & Mirth, 2021). 20E titers were measured by Enzymatic immunoassay (EIA) in duplicate at room temperature following the instructions of the previously mentioned commercial kit. For a precoated 96-well Strip Plate, absorbance was measured at 410 nm on an Infinite M200 Pro Microplate Reader (Tecan, Männedorf, Switzerland) using Software I-control 1.6.

3.11. Immunohistochemistry on Larval Brain-RG Complexes and Fat Body.

Previously synchronized control (*phtm>+*) and knockdown (*phtm>GlyT^i*) animals at 72, 120 and 256 hours AEL were used for immunohistochemistry in groups of 10-20 larvae at indicated conditions. All tissues were dissected out in cold 1 x PBS buffer and fixed in 4% paraformaldehyde (PFA) for 20 minutes at 50 rpm in orbital shaker as we previously described (Palomino-Schätzlein et al., 2022). All larval brain-ring gland complexes and fat bodies were stained overnight at room temperature with the following primary antibodies: mouse anti-Dlg 4F3 (1/100, DSHB), mouse anti-nuclear pore complex proteins, MAB 4.14 (1/200, BioLegend), mouse anti-Fib 38F3 (1/500, Invitrogen) and rat anti-DE-Cad DCAD2 (1/50, DSHB). Secondary fluorophore conjugated antibodies (anti-mouse and anti-rat, Alexa FluorTM 488, 555 and 647) were purchased from Invitrogen and Jackson ImmunoResearch. When indicated, fat bodies were also incubated for 1 hour at 1:40 dilution of 1 x PBS with Alexa Fluor™ Plus 647 Phalloidin (ThermoFisher, A30107) at room temperature in orbital shaker at 50 rpm. Vectashield mounting medium with DAPI (H-1200, Vector Labs), was used for nuclear staining.

3.12. Super-Resolution Confocal Imaging of Larval Brains, Fat Bodies and Prothoracic Gland Cells

Once dissected tissues were prepared according to previous section ("3.11.Immunohistochemistry on larval brain-ring gland complexes and fat bodies"), stained brain-ring gland complexes and fat bodies were mounted in Vectashield mounting medium with DAPI (H-1200, Vector Labs), maintaining their 3D configuration (Palomino-Schätzlein et al., 2022). Super resolution images were obtained on a Zeiss LSM 880 confocal microscope with Airyscan, equipped with LD LCI plan-Apochromat 253 (NA 0.8 and WD 0.57 mm) and plan-Apochromat 633 (NA 1.4 Oil and WD 0.14 mm) immersion objectives with ZEN Black 2.3 software (Zeiss).

3.13. Prothoracic Gland Cell area and Nuclear to Cytoplasmic Ratio Quantification

Brain-ring gland complexes were dissected out in cold 1 x PBS buffer from both control (*phtm>+*) and knockdown (*phtm>GlyT^i*) animals at 72 and 120 hours AEL and fixed in 4% paraformaldehyde (PFA) for 20 minutes at 50 rpm in orbital shaker (Palomino-Schätzlein et al., 2022). Tissues were stained as described in previous section ("Immunohistochemistry on larval brain-ring gland complexes and fat bodies"). Super resolution images were obtained on a Zeiss LSM 880 confocal microscope with Airyscan, equipped with LD LCI plan-Apochromat 253 (NA 0.8 and WD 0.57 mm) and plan-Apochromat 633 (NA 1.4 Oil and WD 0.14 mm) immersion objectives with ZEN Black 2.3 software (Zeiss). ImageJ software was used to quantify cytoplasmic and nuclear area as well as segmentation and maximum projection acquisitions. Once nuclear and cytoplasmic areas were quantified, nuclear to cytoplasmic ratio (NC Ratio) was calculated by following the formula: $NC\ ratio = \frac{Area\ of\ the\ Nucleus}{Area\ of\ the\ Cytoplasm}$. For each condition, NC ratio values were presented as NC ratio value ± SEM of N replicates.

3.14. Neutral Lipid Staining and Quantification in Larval Brains and Fat Bodies

Dissected tissues underwent the protocol detailed in previous sections ("3.11.Immunohistochemistry on larval brain-ring gland complexes and fat bodies"). Larval brains and fat bodies were rinsed three times with cold 1 x PBS buffer prior to 40 minutes incubation at 1:500 dilution of 1 x PBS with 1 mg/ml Nile Red (Sigma-Aldrich) at 50 rpm in orbital shaker. Image acquisition utilized uniform scan settings across all conditions and time points, employing the equipment delineated in the previous section ("3.12.Super-resolution Confocal Imaging of Larval Brains, Fat Bodies, and Prothoracic Gland Cells"). Fluorescence quantification was executed using ImageJ software (version 1.54b) to evaluate the Nile Red signal intensity (555nm) within lipid droplets present in both brain and fat body tissues. Specifically, we measured mean fluorescence intensity within predetermined regions of interest (ROIs) thus facilitating the comparison of Nile Red distribution among lipid droplets across distinct tissue types.

3.15. Quantitative RT-PCR

To evaluate mRNA expression levels in both whole larvae or isolated ring gland tissue, total RNA was extracted from 5 larvae or 50 ring glands, respectively, at the desired developmental time points. For total mRNA isolation, RNeasy-Mini kit (Qiagen) was applied following the manufacturer's instructions. Briefly, tissue was homogenized with Tissuelyser LT (Qiagen) for 5 minutes at 50 rpm at room temperature to facilitate lysis before applying the standard RNA isolation protocol. To remove contaminating DNA, RNA was treated with RNase Free DNase Set (Qiagen). After total RNA quantification with NanoDrop One (Thermo Fisher Scientific), cDNA was synthesized with the SuperScript III First Strand Synthesis System for RT-PCR (Invitrogen) using random oligo-dT primers (Invitrogen). Quantitative real-time PCR was performed using SYBR Green PCR Master Mix (Applied Biosystems) with gene-specific primers, on an ABI7500 plate reader (Applied Biosystems). Normalization was performed against β-actin (otherwise indicated). Comparative qPCRs were performed in triplicate and relative mRNA expression was calculated using the ΔΔCt method. The primer sequences used for this study are provided in Table 4.

3.16. RNA-seq Sample Preparation and Total RNA Isolation

For whole larval transcriptomic profiling, both control (*phtm>+*) and knockdown (*phtm>GlyT^i*) animals were collected in groups of 3 larvae at 120 hours AEL. In the case of 72 hours AEL groups, where only control animals (*phtm>+*) were included, 6 larvae were collected for each group. At least 5 male and 5 female replicates were collected for each group of samples to ensure equal gender representation. All groups of larvae were rinsed twice in cold 1 x PBS before being dry collected in 2 ml tubes (Eppendorf). RNA isolation was carried out as described in previous section ("Quantitative RT-PCR") with the same procedure and reagents. After total mRNA concentration was quantified with NanoDrop One (Thermo Fisher Scientific), further quality control was carried out for an aliquot of 1 µl from the initial RNA isolation with the Agilent Bioanalyzer 2100 system to ensure RNA integrity prior to sample shipping in dry ice.

3.17. RNA-seq Library Construction and Sequencing

Library preparation for whole-transcriptome sequencing with Illumina technology (Illumina, Inc., San Diego, CA, USA) was implemented externally at the genomics core facilities of CNAG-CRG (Centro Nacional de Análisis Genómico, Barcelona, Spain). In brief, upon receipt of the samples at CNAG-CRG, a secondary local quality control assessment was performed using the Agilent Bioanalyzer 2100 system to verify RNA integrity post-shipment. RNA-seq libraries were constructed using the TruSeq® Stranded Total RNA kit (Illumina) for a reverse-strand 2x150bp (base pair) paired-end design, following the manufacturer's instructions. Ribo-Zero ribosomal RNA reduction chemistry was applied in order to reduce ribosomal RNA contamination. The constructed libraries were sequenced together on an Illumina NovaSeq 6000 platform in 2 x 150 bp (base pair) paired-end mode. A minimum depth of 100 million reads was generated from each library. Raw sequencing files were then received in Fastq format through the server of CNAG-CRG accompanied by their MD5 checksum.

3.18. Bioinformatic Analysis of RNA-Seq Data

After decrypting the MD5 checksum to verify the integrity of the downloaded Fastq sequences from the sequencing facility server, the raw sequencing data underwent quality checks using the FastQC program (FastQC v0.12.1). A reference genome for Drosophila melanogaster (BDGP6.32) was generated using the STAR package (STAR 2.7.9a). Subsequently, the raw sequencing reads were aligned and mapped to the mentioned reference genome using the STAR aligner algorithm from the same STAR package (STAR 2.7.9a). The annotation file in Gene Transfer Format (GTF) provided was the "Drosophila_melanogaster.BDGP6.32.109". Total expression quantification was performed at the exon level using the FeatureCounts function from the Subread package (Subread v2.0.1). Thus, producing a count matrix capturing the expression levels of each gene among samples. Genome building, mapping-aligning and feature quantification steps were executed via Linux command-line tools, ensuring accurate read placement and quantification. Differential gene expression analysis (DE Analysis) was carried out in R version 4.3.1 (2023-06-16) for a platform x86_64-apple-darwin20 (64-bit) running under macOS Sonoma 14.1.2. DE Analysis was performed using the negative binomial distribution (Generalized Linear Model algorithm) implemented by the DESeq2 package (DESeq2 v1.40.2). Among other considerations, genes with a significant adjusted P-value (< 0.05) were considered to be differentially expressed. Functional Gene Ontology enrichment analysis (GO Enrichment Analysis) was implemented using the Pangea website and resources from Harvard Medical School (2023 version) to gain insights into biological processes and molecular functions associated with differentially expressed genes. Otherwise indicated, GGplot2 (ggplot2_3.4.4) was the package used to visualize RNA-seq results. In order to calculate the Transcripts per Million (TPM) values, the main algorithms of GenomicRanges (GenomicRanges_1.52.1) and GenomicFeatures (GenomicFeatures_1.52.2) packages were applied. Briefly, effective length of each gene in Kilobases (Kb) was calculated thanks to GTF file prior to obtaining the normalized average effective length. TPM values were presented as $\mathrm{Log}_2(TPM + 1)$ to avoid any undefined zero value logarithm ($\mathrm{Log}_2 0$).

3.19. Statistical Analysis

For the majority of the statistical analyzes in this work, unless otherwise specifically indicated, ANOVA Analysis of Variance was implemented to compare the means of three or more groups to detect any significant difference among them when applied to parametric variables, while the Kruskal-Wallis test was employed for non-parametric variables to assess equivalent comparisons. Student's t-test and Mann-Whitney U test were applied for pairwise comparisons between two groups and for significance determination in parametric and non-parametric variables, respectively. The results are presented as mean values along with standard error of the mean (SEM). Data analysis was conducted using GraphPad Prism (version 9; GraphPad Software, San Diego, CA, USA) and R (version 4.3.1). Correlation analyses were conducted using Pearson and Spearman tests; The Pearson test is employed to assess the correlation between two continuous variables that follow a normal distribution, while the Spearman test is utilized to evaluate the correlation between two variables that may lack a normal distribution or have a non-linear relationship.

3.20. Software and algorithms

Even though mentioned throughout the material and methods sections, all main software tools, algorithms and packages used for this work are listed in Table 5.

4.   Tables

Table 1. RNA[i] lines included in Solute Carrier superfamily *in vivo* screening

Gene name (symbol)	VDRC ID	FlyBase N.º	FlyBase Gene Group
Excitatory Amino Acid Transporter 1 (Eaat1)	v109401	KK100187	SLC1: GLUTAMATE/NEUTRAL AMINO ACID TRANSPORTERS
Excitatory Amino Acid Transporter 1 (Eaat1)	v330103	SH330103	SLC1: GLUTAMATE/NEUTRAL AMINO ACID TRANSPORTERS
Excitatory Amino Acid Transporter 2 (Eaat2)	v104371	KK107989	SLC1: GLUTAMATE/NEUTRAL AMINO ACID TRANSPORTERS
Uncharacterized Protein (CG1213)	v6488	GD1677	SLC2: HEXOSE SUGAR TRANSPORTERS
Uncharacterized Protein (CG1213)	v6487	GD1677	SLC2: HEXOSE SUGAR TRANSPORTERS
Uncharacterized Protein (CG14605)	v105310	KK110488	SLC2: HEXOSE SUGAR TRANSPORTERS
Uncharacterized Protein (CG14605)	v5776	GD2841	SLC2: HEXOSE SUGAR TRANSPORTERS
Uncharacterized Protein (CG14606)	v100903	KK106185	SLC2: HEXOSE SUGAR TRANSPORTERS
Uncharacterized Protein (CG14606)	v7523	GD2840	SLC2: HEXOSE SUGAR TRANSPORTERS
Uncharacterized Protein (CG15406)	v45887	GD860	SLC2: HEXOSE SUGAR TRANSPORTERS
Uncharacterized Protein (CG15406)	v105077	KK113373	SLC2: HEXOSE SUGAR TRANSPORTERS
Uncharacterized Protein (CG15408)	v43817	GD865	SLC2: HEXOSE SUGAR TRANSPORTERS
Uncharacterized Protein (CG15408)	v43816	GD865	SLC2: HEXOSE SUGAR TRANSPORTERS
Uncharacterized Protein (CG31100)	v42630	GD2869	SLC2: HEXOSE SUGAR TRANSPORTERS
Uncharacterized Protein (CG31100)	v42627	GD2869	SLC2: HEXOSE SUGAR TRANSPORTERS
Uncharacterized Protein (CG3285)	v52669	GD864	SLC2: HEXOSE SUGAR TRANSPORTERS
Uncharacterized Protein (CG3285)	v51060	GD864	SLC2: HEXOSE SUGAR TRANSPORTERS
Uncharacterized Protein (CG33281)	v7273	GD863	SLC2: HEXOSE SUGAR TRANSPORTERS
Uncharacterized Protein (CG33281)	v7274	GD863	SLC2: HEXOSE SUGAR TRANSPORTERS
Uncharacterized Protein (CG33282)	v100325	KK105921	SLC2: HEXOSE SUGAR TRANSPORTERS
Uncharacterized Protein (CG33282)	v46454	GD16042	SLC2: HEXOSE SUGAR TRANSPORTERS
Uncharacterized Protein (CG4607)	v5450	GD3268	SLC2: HEXOSE SUGAR TRANSPORTERS
Uncharacterized Protein (CG4607)	v107219	KK104152	SLC2: HEXOSE SUGAR TRANSPORTERS
Uncharacterized Protein (CG6484)	v109481	KK106784	SLC2: HEXOSE SUGAR TRANSPORTERS
Uncharacterized Protein (CG6484)	v4954	GD2054	SLC2: HEXOSE SUGAR TRANSPORTERS
Uncharacterized Protein (CG7882)	v8101	GD3480	SLC2: HEXOSE SUGAR TRANSPORTERS
Uncharacterized Protein (CG7882)	v109918	KK109827	SLC2: HEXOSE SUGAR TRANSPORTERS
Uncharacterized Protein (CG8249)	v50885	GD17266	SLC2: HEXOSE SUGAR TRANSPORTERS
Uncharacterized Protein (CG8249)	v106077	KK106127	SLC2: HEXOSE SUGAR TRANSPORTERS
Uncharacterized Protein (CG8837)	v44217	GD862	SLC2: HEXOSE SUGAR TRANSPORTERS
Uncharacterized Protein (CG8837)	v100670	KK106661	SLC2: HEXOSE SUGAR TRANSPORTERS
Glucose Transporter 1 (Glut1)	v13326	GD4552	SLC2: HEXOSE SUGAR TRANSPORTERS
Glucose Transporter 1 (Glut1)	v13328	GD4552	SLC2: HEXOSE SUGAR TRANSPORTERS
Glucose Transporter 1 (Glut1)	v47179	GD16461	SLC2: HEXOSE SUGAR TRANSPORTERS
Glucose Transporter 1 (Glut1)	v47178	GD16461	SLC2: HEXOSE SUGAR TRANSPORTERS
Glucose Transporter 1 (Glut1)	v101365	KK108683	SLC2: HEXOSE SUGAR TRANSPORTERS
Glucose Transporter Type 3 (Glut3)	v100253	KK107267	SLC2: HEXOSE SUGAR TRANSPORTERS
Glucose Transporter Type 3 (Glut3)	v13302	GD3029	SLC2: HEXOSE SUGAR TRANSPORTERS
Nebulosa (Nebu)*	v8359	GD2444	SLC2: HEXOSE SUGAR TRANSPORTERS

Pippin (Pippin)	v10598	GD4548	SLC2: HEXOSE SUGAR TRANSPORTERS
Sugar Transporter 1 (Sut1)	v104983	KK112749	SLC2: HEXOSE SUGAR TRANSPORTERS
Sugar Transporter 1 (Sut1)	v9950	GD1864	SLC2: HEXOSE SUGAR TRANSPORTERS
Sugar Transporter 1 (Sut1)	v9951	GD1864	SLC2: HEXOSE SUGAR TRANSPORTERS
Sugar Transporter 2 (Sut2)	v28207	GD12395	SLC2: HEXOSE SUGAR TRANSPORTERS
Sugar Transporter 2 (Sut2)	v28206	GD12395	SLC2: HEXOSE SUGAR TRANSPORTERS
Sugar Transporter 2 (Sut2)	v102028	KK110424	SLC2: HEXOSE SUGAR TRANSPORTERS
Sugar Transporter 3 (Sut3)	v4009	GD1865	SLC2: HEXOSE SUGAR TRANSPORTERS
Sugar Transporter 4 (Sut4)	v44935	GD3494	SLC2: HEXOSE SUGAR TRANSPORTERS
Sugar Transporter 4 (Sut4)	v44934	GD3494	SLC2: HEXOSE SUGAR TRANSPORTERS
Trehalose Transporter 1-1 (Tret1-1)	v8126	GD3500	SLC2: HEXOSE SUGAR TRANSPORTERS
Trehalose Transporter 1-1 (Tret1-1)	v103045	KK111741	SLC2: HEXOSE SUGAR TRANSPORTERS
Trehalose Transporter 1-1 (Tret1-1)	v52360	GD17787	SLC2: HEXOSE SUGAR TRANSPORTERS
Trehalose Transporter 1-1 (Tret1-1)	v52361	GD17787	SLC2: HEXOSE SUGAR TRANSPORTERS
Trehalose Transporter 1-2 (Tret1-2)	v49889	GD17847	SLC2: HEXOSE SUGAR TRANSPORTERS
Trehalose Transporter 1-2 (Tret1-2)	v40980	GD3501	SLC2: HEXOSE SUGAR TRANSPORTERS
Cd98 Heavy Chain (Cd98hc)	v108365	KK104374	SLC3: HETEROMERIC AMINO ACID TRANSPORTERS
Cd98 Heavy Chain (Cd98hc)	v42622	GD2852	SLC3: HETEROMERIC AMINO ACID TRANSPORTERS
Anion Exchanger 2 (Ae2)	v109594	KK100095	SLC4: BICARBONATE TRANSPORTERS
Anion Exchanger 2 (Ae2)	v39492	GD2397	SLC4: BICARBONATE TRANSPORTERS
Na^{+}-Driven Anion Exchanger 1 (Ndae1)	v102707	KK112232	SLC4: BICARBONATE TRANSPORTERS
Na^{+}-Driven Anion Exchanger 1 (Ndae1)	v107948	KK100362	SLC4: BICARBONATE TRANSPORTERS
Na^{+}-Driven Anion Exchanger 1 (Ndae1)	v3664	GD967	SLC4: BICARBONATE TRANSPORTERS
Uncharacterized Protein (CG10444)	v107008	KK101545	SLC5: SODIUM/GLUCOSE TRANSPORTERS
Uncharacterized Protein (CG10444)	v4722	GD2104	SLC5: SODIUM/GLUCOSE TRANSPORTERS
Uncharacterized Protein (CG2187)	v101065	KK106763	SLC5: SODIUM/GLUCOSE TRANSPORTERS
Uncharacterized Protein (CG2187)	v7576	GD575	SLC5: SODIUM/GLUCOSE TRANSPORTERS
Uncharacterized Protein (CG31262)	v106408	KK111744	SLC5: SODIUM/GLUCOSE TRANSPORTERS
Uncharacterized Protein (CG31262)	v52605	GD12397	SLC5: SODIUM/GLUCOSE TRANSPORTERS
Uncharacterized Protein (CG31668)	v104093	KK103908	SLC5: SODIUM/GLUCOSE TRANSPORTERS
Uncharacterized Protein (CG31668)	v2548	GD823	SLC5: SODIUM/GLUCOSE TRANSPORTERS
Uncharacterized Protein (CG32669)	v102859	KK105555	SLC5: SODIUM/GLUCOSE TRANSPORTERS
Uncharacterized Protein (CG32669)	v47916	GD15931	SLC5: SODIUM/GLUCOSE TRANSPORTERS
Uncharacterized Protein (CG33124)	v105570	KK105791	SLC5: SODIUM/GLUCOSE TRANSPORTERS
Uncharacterized Protein (CG33124)	v2552	GD824	SLC5: SODIUM/GLUCOSE TRANSPORTERS
Uncharacterized Protein (CG5687)	v330241	SH330241	SLC5: SODIUM/GLUCOSE TRANSPORTERS
Uncharacterized Protein (CG5687)	v33262	GD2255	SLC5: SODIUM/GLUCOSE TRANSPORTERS
Brother Of Rumpel (Bumpel)	v13769	GD3636	SLC5: SODIUM/GLUCOSE TRANSPORTERS
Choline Transporter (Cht)	v30302	GD3648	SLC5: SODIUM/GLUCOSE TRANSPORTERS
Choline Transporter (Cht)	v101485	KK109385	SLC5: SODIUM/GLUCOSE TRANSPORTERS

Kin Of Rumpel (Kumpel)	v107662	KK112702	SLC5: SODIUM/GLUCOSE TRANSPORTERS
Kin Of Rumpel (Kumpel)	v107975	KK112047	SLC5: SODIUM/GLUCOSE TRANSPORTERS
Kin Of Rumpel (Kumpel)	v108499	KK112312	SLC5: SODIUM/GLUCOSE TRANSPORTERS
Kin Of Rumpel (Kumpel)	v103285	KK112777	SLC5: SODIUM/GLUCOSE TRANSPORTERS
Kin Of Rumpel (Kumpel)	v107896	KK104911	SLC5: SODIUM/GLUCOSE TRANSPORTERS
Rumpel (Rumpel)	v43922	GD3270	SLC5: SODIUM/GLUCOSE TRANSPORTERS
Rumpel (Rumpel)	v107361	KK106220	SLC5: SODIUM/GLUCOSE TRANSPORTERS
Salty Dog (Salt)	v28349	GD12732	SLC5: SODIUM/GLUCOSE TRANSPORTERS
Salty Dog (Salt)	v108782	KK113232	SLC5: SODIUM/GLUCOSE TRANSPORTERS
Sodium-Dependent Multivitamin Transporter (Smvt)	v40650	GD12439	SLC5: SODIUM/GLUCOSE TRANSPORTERS
Sodium-Dependent Multivitamin Transporter (Smvt)	v102662	KK105033	SLC5: SODIUM/GLUCOSE TRANSPORTERS
Sodium/Solute Co-Transporter-Like 5a11 (Slc5a11)	v104177	KK107159	SLC5: SODIUM/GLUCOSE TRANSPORTERS
Sodium/Solute Co-Transporter-Like 5a11 (Slc5a11)	v48984	GD17030	SLC5: SODIUM/GLUCOSE TRANSPORTERS
Sodium/Solute Co-Transporter-Like 5a11 (Slc5a11)	v3424	GD394	SLC5: SODIUM/GLUCOSE TRANSPORTERS
Uncharacterized Protein (CG10804)	v30225	GD3218	SLC6: NA+/CL- NEUROTRANSMITTER TRANSPORTERS
Uncharacterized Protein (CG10804)	v100400	KK104172	SLC6: NA+/CL- NEUROTRANSMITTER TRANSPORTERS
Uncharacterized Protein (CG10804)	v30226	GD3218	SLC6: NA+/CL- NEUROTRANSMITTER TRANSPORTERS
Uncharacterized Protein (CG13793)	v50167	GD16550	SLC6: NA+/CL- NEUROTRANSMITTER TRANSPORTERS
Uncharacterized Protein (CG13793)	v3668	GD973	SLC6: NA+/CL- NEUROTRANSMITTER TRANSPORTERS
Uncharacterized Protein (CG13793)	v3669	GD973	SLC6: NA+/CL- NEUROTRANSMITTER TRANSPORTERS
Uncharacterized Protein (CG13794)	v49068	GD17136	SLC6: NA+/CL- NEUROTRANSMITTER TRANSPORTERS
Uncharacterized Protein (CG13794)	v102583	KK112071	SLC6: NA+/CL- NEUROTRANSMITTER TRANSPORTERS
Uncharacterized Protein (CG13795)	v102250	KK111253	SLC6: NA+/CL- NEUROTRANSMITTER TRANSPORTERS
Uncharacterized Protein (CG13795)	v49156	GD17355	SLC6: NA+/CL- NEUROTRANSMITTER TRANSPORTERS
Uncharacterized Protein (CG13796)	v45895	GD976	SLC6: NA+/CL- NEUROTRANSMITTER TRANSPORTERS
Uncharacterized Protein (CG13796)	v102516	KK111872	SLC6: NA+/CL- NEUROTRANSMITTER TRANSPORTERS
Uncharacterized Protein (CG15279)	v330043	SH330043	SLC6: NA+/CL- NEUROTRANSMITTER TRANSPORTERS
Uncharacterized Protein (CG15279)	v108759	KK110894	SLC6: NA+/CL- NEUROTRANSMITTER TRANSPORTERS
Uncharacterized Protein (CG1698)	v101947	KK110310	SLC6: NA+/CL- NEUROTRANSMITTER TRANSPORTERS
Uncharacterized Protein (CG33296)	v50499	GD17468	SLC6: NA+/CL- NEUROTRANSMITTER TRANSPORTERS
Uncharacterized Protein (CG43066)	v101768	KK109457	SLC6: NA+/CL- NEUROTRANSMITTER TRANSPORTERS
Uncharacterized Protein (CG43066)	v37183	GD2069	SLC6: NA+/CL- NEUROTRANSMITTER TRANSPORTERS
Uncharacterized Protein (CG4476)	v46846	GD16940	SLC6: NA+/CL- NEUROTRANSMITTER TRANSPORTERS
Uncharacterized Protein (CG4476)	v109677	KK103062	SLC6: NA+/CL- NEUROTRANSMITTER TRANSPORTERS
Uncharacterized Protein (CG8850)	v104098	KK103989	SLC6: NA+/CL- NEUROTRANSMITTER TRANSPORTERS
Bedraggled (Bdg)	v110054	KK105846	SLC6: NA+/CL- NEUROTRANSMITTER TRANSPORTERS
Bedraggled (Bdg)	v44375	GD2018	SLC6: NA+/CL- NEUROTRANSMITTER TRANSPORTERS
Bloated Tubules (Blot)	v101083	KK106850	SLC6: NA+/CL- NEUROTRANSMITTER TRANSPORTERS
Bloated Tubules (Blot)	v5296	GD2690	SLC6: NA+/CL- NEUROTRANSMITTER TRANSPORTERS
Dopamine Transporter (Dat)	v106961	KK100046	SLC6: NA+/CL- NEUROTRANSMITTER TRANSPORTERS

Dopamine Transporter (Dat)	v12082	GD2034	SLC6: NA+/CL- NEUROTRANSMITTER TRANSPORTERS
Gaba Transporter (Gat)	v106638	KK107895	SLC6: NA+/CL- NEUROTRANSMITTER TRANSPORTERS
Glycine Transporter (Glyt)	v8222	GD3564	SLC6: NA+/CL- NEUROTRANSMITTER TRANSPORTERS
Glycine Transporter (Glyt)	v330127	SH330127	SLC6: NA+/CL- NEUROTRANSMITTER TRANSPORTERS
Inebriated (Ine)	v330044	SH330044	SLC6: NA+/CL- NEUROTRANSMITTER TRANSPORTERS
Lithium-Inducible Slc6 Transporter (List)	v109791	KK107024	SLC6: NA+/CL- NEUROTRANSMITTER TRANSPORTERS
Lithium-Inducible Slc6 Transporter (List)	v44909	GD2072	SLC6: NA+/CL- NEUROTRANSMITTER TRANSPORTERS
Neurotransmitter Transporter-Like (Ntl)	v102776	KK112412	SLC6: NA+/CL- NEUROTRANSMITTER TRANSPORTERS
Neurotransmitter Transporter-Like (Ntl)	v3666	GD972	SLC6: NA+/CL- NEUROTRANSMITTER TRANSPORTERS
Nutrient Amino Acid Transporter 1 (Naat1)	v50064	GD17302	SLC6: NA+/CL- NEUROTRANSMITTER TRANSPORTERS
Nutrient Amino Acid Transporter 1 (Naat1)	v106027	KK112890	SLC6: NA+/CL- NEUROTRANSMITTER TRANSPORTERS
Serotonin Transporter (Sert)	v11346	GD3824	SLC6: NA+/CL- NEUROTRANSMITTER TRANSPORTERS
Serotonin Transporter (Sert)	v100584	KK108310	SLC6: NA+/CL- NEUROTRANSMITTER TRANSPORTERS
Uncharacterized Protein (CG12531)	v6203	GD3456	SLC7: AMINO ACID TRANSPORTERS
Uncharacterized Protein (CG12531)	v105771	KK109373	SLC7: AMINO ACID TRANSPORTERS
Uncharacterized Protein (CG13248)	v330028	SH330028	SLC7: AMINO ACID TRANSPORTERS
Uncharacterized Protein (CG13248)	v102635	KK103406	SLC7: AMINO ACID TRANSPORTERS
Uncharacterized Protein (CG5535)	v107030	KK100907	SLC7: AMINO ACID TRANSPORTERS
Uncharacterized Protein (CG5535)	v42583	GD2703	SLC7: AMINO ACID TRANSPORTERS
Uncharacterized Protein (CG7255)	v107802	KK110010	SLC7: AMINO ACID TRANSPORTERS
Uncharacterized Protein (CG7255)	v8373	GD2469	SLC7: AMINO ACID TRANSPORTERS
Slimfast (Slif)	v45588	GD12619	SLC7: AMINO ACID TRANSPORTERS
Slimfast (Slif)	v26786	GD12619	SLC7: AMINO ACID TRANSPORTERS
Slimfast (Slif)	v45587	GD12619	SLC7: AMINO ACID TRANSPORTERS
Slimfast (Slif)	v45590	GD12619	SLC7: AMINO ACID TRANSPORTERS
Slimfast (Slif)	v45589	GD12619	SLC7: AMINO ACID TRANSPORTERS
Slimfast (Slif)	v110425	KK101643	SLC7: AMINO ACID TRANSPORTERS
Torn And Diminished Rhabdomeres (Tadr)	v330472	SH330472	SLC7: AMINO ACID TRANSPORTERS
Uncharacterized Protein (CG1607)	v14925	GD4651	SLC7: AMINO ACID TRANSPORTERS
Uncharacterized Protein (CG1607)	v105677	KK107364	SLC7: AMINO ACID TRANSPORTERS
Uncharacterized Protein (CG1607)	v13793	GD4651	SLC7: AMINO ACID TRANSPORTERS
Genderblind (Gb)	v1262	GD315	SLC7: AMINO ACID TRANSPORTERS
Genderblind (Gb)	v1261	GD315	SLC7: AMINO ACID TRANSPORTERS
Juvenile Hormone Inducible-21 (Jhi-21)	v108509	KK112996	SLC7: AMINO ACID TRANSPORTERS
Juvenile Hormone Inducible-21 (Jhi-21)	v45190	GD3466	SLC7: AMINO ACID TRANSPORTERS
Juvenile Hormone Inducible-21 (Jhi-21)	v45193	GD3466	SLC7: AMINO ACID TRANSPORTERS
Juvenile Hormone Inducible-21 (Jhi-21)	v45192	GD3466	SLC7: AMINO ACID TRANSPORTERS
Juvenile Hormone Inducible-21 (Jhi-21)	v45191	GD3466	SLC7: AMINO ACID TRANSPORTERS
Minidiscs (Mnd)	v42485	GD453	SLC7: AMINO ACID TRANSPORTERS
Minidiscs (Mnd)	v110217	KK102686	SLC7: AMINO ACID TRANSPORTERS

Sobremesa (Sbm)	v108867	KK101306	SLC7: AMINO ACID TRANSPORTERS
Sobremesa (Sbm)	v45178	GD3355	SLC7: AMINO ACID TRANSPORTERS
Sobremesa (Sbm)	v45180	GD3355	SLC7: AMINO ACID TRANSPORTERS
Uncharacterized Protein (CG14744)	v40828	GD1878	SLC8: SODIUM/CALCIUM EXCHANGERS
Uncharacterized Protein (CG14744)	v108697	KK105635	SLC8: SODIUM/CALCIUM EXCHANGERS
Na/Ca-Exchange Protein (Calx)	v104789	KK109144	SLC8: SODIUM/CALCIUM EXCHANGERS
Na/Ca-Exchange Protein (Calx)	v42661	GD3094	SLC8: SODIUM/CALCIUM EXCHANGERS
Na/Ca-Exchange Protein (Calx)	v42660	GD3094	SLC8: SODIUM/CALCIUM EXCHANGERS
Na+/H+ Hydrogen Antiporter 1 (Nha1)	v110016	KK109202	SLC9: SODIUM/PROTON EXCHANGERS
Na+/H+ Hydrogen Antiporter 1 (Nha1)	v33149	GD961	SLC9: SODIUM/PROTON EXCHANGERS
Na+/H+ Hydrogen Exchanger 1 (Nhe1)	v110205	KK102521	SLC9: SODIUM/PROTON EXCHANGERS
Na+/H+ Hydrogen Exchanger 1 (Nhe1)	v7245	GD775	SLC9: SODIUM/PROTON EXCHANGERS
Na+/H+ Hydrogen Exchanger 2 (Nhe2)	v106053	KK102518	SLC9: SODIUM/PROTON EXCHANGERS
Na+/H+ Hydrogen Exchanger 2 (Nhe2)	v330363	SH330363	SLC9: SODIUM/PROTON EXCHANGERS
Na+/H+ Hydrogen Exchanger 3 (Nhe3)	v330286	SH330286	SLC9: SODIUM/PROTON EXCHANGERS
Na+/H+ Hydrogen Exchanger 3 (Nhe3)	v100742	KK108326	SLC9: SODIUM/PROTON EXCHANGERS
Malvolio (Mvl)	v44000	GD3095	SLC11: PROTON-COUPLED METAL ION TRANSPORTERS
Malvolio (Mvl)	v109434	KK108406	SLC11: PROTON-COUPLED METAL ION TRANSPORTERS
Uncharacterized Protein (CG10413)	v103780	KK102660	SLC12: CATION-COUPLED CHLORIDE TRANSPORTERS
Uncharacterized Protein (CG10413)	v3882	GD1761	SLC12: CATION-COUPLED CHLORIDE TRANSPORTERS
Uncharacterized Protein (CG10413)	v3883	GD1761	SLC12: CATION-COUPLED CHLORIDE TRANSPORTERS
Uncharacterized Protein (CG12773)	v9899	GD3189	SLC12: CATION-COUPLED CHLORIDE TRANSPORTERS
Uncharacterized Protein (CG12773)	v108667	KK102472	SLC12: CATION-COUPLED CHLORIDE TRANSPORTERS
Kazachoc (Kcc)	v10278	GD3565	SLC12: CATION-COUPLED CHLORIDE TRANSPORTERS
Kazachoc (Kcc)	v101742	KK107965	SLC12: CATION-COUPLED CHLORIDE TRANSPORTERS
Sodium Chloride Cotransporter 69 (Ncc69)	v106499	KK108763	SLC12: CATION-COUPLED CHLORIDE TRANSPORTERS
Sodium Chloride Cotransporter 69 (Ncc69)	v30000	GD14863	SLC12: CATION-COUPLED CHLORIDE TRANSPORTERS
Sodium Chloride Cotransporter 69 (Ncc69)	v30001	GD14863	SLC12: CATION-COUPLED CHLORIDE TRANSPORTERS
Sodium Potassium Chloride Cotransporter (Nkcc)	v8552	GD3622	SLC12: CATION-COUPLED CHLORIDE TRANSPORTERS
Sodium Potassium Chloride Cotransporter (Nkcc)	v105911	KK106175	SLC12: CATION-COUPLED CHLORIDE TRANSPORTERS
Sodium Potassium Chloride Cotransporter (Nkcc)	v8551	GD3622	SLC12: CATION-COUPLED CHLORIDE TRANSPORTERS
I'm Not Dead Yet (Indy)	v9982	GD2712	SLC13: DICARBOXYLATE/CITRATE TRANSPORTERS
I'm Not Dead Yet (Indy)	v9981	GD2712	SLC13: DICARBOXYLATE/CITRATE TRANSPORTERS
Yin (Yin)	v7028	GD3221	SLC15: PEPTIDE TRANSPORTERS
Yin (Yin)	v104181	KK109637	SLC15: PEPTIDE TRANSPORTERS
Uncharacterized Protein (CG10019)	v7292	GD877	SLC16: MONOCARBOXYLATE TRANSPORTERS
Uncharacterized Protein (CG10019)	v7291	GD877	SLC16: MONOCARBOXYLATE TRANSPORTERS
Uncharacterized Protein (CG13907)	v330032	SH330032	SLC16: MONOCARBOXYLATE TRANSPORTERS
Uncharacterized Protein (CG13907)	v107339	KK110059	SLC16: MONOCARBOXYLATE TRANSPORTERS
Uncharacterized Protein (CG8028)	v102317	KK109927	SLC16: MONOCARBOXYLATE TRANSPORTERS

Uncharacterized Protein (CG8028)	v9163	GD3445	SLC16: MONOCARBOXYLATE TRANSPORTERS
Uncharacterized Protein (CG8389)	v107639	KK105290	SLC16: MONOCARBOXYLATE TRANSPORTERS
Uncharacterized Protein (CG8389)	v8976	GD2022	SLC16: MONOCARBOXYLATE TRANSPORTERS
Uncharacterized Protein (CG8468)	v6453	GD1648	SLC16: MONOCARBOXYLATE TRANSPORTERS
Uncharacterized Protein (CG8468)	v6452	GD1648	SLC16: MONOCARBOXYLATE TRANSPORTERS
Chaski (Chk)	v37139	GD1829	SLC16: MONOCARBOXYLATE TRANSPORTERS
Chaski (Chk)	v37141	GD1829	SLC16: MONOCARBOXYLATE TRANSPORTERS
Hermes (Hrm)	v7314	GD1807	SLC16: MONOCARBOXYLATE TRANSPORTERS
Karmoisin (Kar)	v330377	SH330377	SLC16: MONOCARBOXYLATE TRANSPORTERS
Karmoisin (Kar)	v105429	KK101781	SLC16: MONOCARBOXYLATE TRANSPORTERS
Monocarboxylate Transporter 1 (Mct1)	v106773	KK108618	SLC16: MONOCARBOXYLATE TRANSPORTERS
Outsiders (Out)	v108364	KK104187	SLC16: MONOCARBOXYLATE TRANSPORTERS
Outsiders (Out)	v51157	GD3448	SLC16: MONOCARBOXYLATE TRANSPORTERS
Silnoon (Sln)	v109464	KK104306	SLC16: MONOCARBOXYLATE TRANSPORTERS
Silnoon (Sln)	v4609	GD1940	SLC16: MONOCARBOXYLATE TRANSPORTERS
Silnoon (Sln)	v4607	GD1940	SLC16: MONOCARBOXYLATE TRANSPORTERS
Tarag (Targ)	v101290	KK105659	SLC16: MONOCARBOXYLATE TRANSPORTERS
Tarag (Targ)	v39545	GD1995	SLC16: MONOCARBOXYLATE TRANSPORTERS
Uncharacterized Protein (CG12490)	v51115	GD17730	SLC17: ORGANIC ANION TRANSPORTERS
Uncharacterized Protein (CG12490)	v1706	GD433	SLC17: ORGANIC ANION TRANSPORTERS
Uncharacterized Protein (CG15096)	v39462	GD2078	SLC17: ORGANIC ANION TRANSPORTERS
Uncharacterized Protein (CG15096)	v103956	KK103186	SLC17: ORGANIC ANION TRANSPORTERS
Uncharacterized Protein (CG18788)	v42469	GD401	SLC17: ORGANIC ANION TRANSPORTERS
Uncharacterized Protein (CG18788)	v101610	KK105194	SLC17: ORGANIC ANION TRANSPORTERS
Uncharacterized Protein (CG2003)	v330210	SH330210	SLC17: ORGANIC ANION TRANSPORTERS
Uncharacterized Protein (CG2003)	v6872	GD3147	SLC17: ORGANIC ANION TRANSPORTERS
Uncharacterized Protein (CG30265)	v106618	KK106781	SLC17: ORGANIC ANION TRANSPORTERS
Uncharacterized Protein (CG30265)	v3513	GD2162	SLC17: ORGANIC ANION TRANSPORTERS
Uncharacterized Protein (CG3036)	v108500	KK112317	SLC17: ORGANIC ANION TRANSPORTERS
Uncharacterized Protein (CG3036)	v42754	GD895	SLC17: ORGANIC ANION TRANSPORTERS
Uncharacterized Protein (CG3036)	v42755	GD895	SLC17: ORGANIC ANION TRANSPORTERS
Uncharacterized Protein (CG3649)	v104762	KK105225	SLC17: ORGANIC ANION TRANSPORTERS
Uncharacterized Protein (CG3649)	v3517	GD2164	SLC17: ORGANIC ANION TRANSPORTERS
Uncharacterized Protein (CG6978)	v7041	GD3227	SLC17: ORGANIC ANION TRANSPORTERS
Uncharacterized Protein (CG7881)	v105576	KK105812	SLC17: ORGANIC ANION TRANSPORTERS
Uncharacterized Protein (CG7881)	v9942	GD1811	SLC17: ORGANIC ANION TRANSPORTERS
Uncharacterized Protein (CG9254)	v13409	GD1128	SLC17: ORGANIC ANION TRANSPORTERS
Uncharacterized Protein (CG9254)	v13407	GD1128	SLC17: ORGANIC ANION TRANSPORTERS
Uncharacterized Protein (CG9825)	v105868	KK104373	SLC17: ORGANIC ANION TRANSPORTERS
Uncharacterized Protein (CG9825)	v1712	GD434	SLC17: ORGANIC ANION TRANSPORTERS

Uncharacterized Protein (CG9826)	v6630	GD2163	SLC17: ORGANIC ANION TRANSPORTERS
Uncharacterized Protein (CG9826)	v101880	KK110114	SLC17: ORGANIC ANION TRANSPORTERS
Uncharacterized Protein (CG9864)	v44423	GD3556	SLC17: ORGANIC ANION TRANSPORTERS
Uncharacterized Protein (CG9864)	v103970	KK103499	SLC17: ORGANIC ANION TRANSPORTERS
Dietary And Metabolic Glutamate Transporter (Dmglut)	v6938	GD1094	SLC17: ORGANIC ANION TRANSPORTERS
Dietary And Metabolic Glutamate Transporter (Dmglut)	v100034	KK103047	SLC17: ORGANIC ANION TRANSPORTERS
Major Facilitator Superfamily Transporter 1 (Mfs1)	v105475	KK107259	SLC17: ORGANIC ANION TRANSPORTERS
Major Facilitator Superfamily Transporter 1 (Mfs1)	v3509	GD2161	SLC17: ORGANIC ANION TRANSPORTERS
Major Facilitator Superfamily Transporter 10 (Mfs10)	v108045	KK106680	SLC17: ORGANIC ANION TRANSPORTERS
Major Facilitator Superfamily Transporter 10 (Mfs10)	v11078	GD3340	SLC17: ORGANIC ANION TRANSPORTERS
Major Facilitator Superfamily Transporter 12 (Mfs12)	v7945	GD1858	SLC17: ORGANIC ANION TRANSPORTERS
Major Facilitator Superfamily Transporter 12 (Mfs12)	v7944	GD1858	SLC17: ORGANIC ANION TRANSPORTERS
Major Facilitator Superfamily Transporter 14 (Mfs14)	v11117	GD1653	SLC17: ORGANIC ANION TRANSPORTERS
Major Facilitator Superfamily Transporter 15 (Mfs15)	v5002	GD2077	SLC17: ORGANIC ANION TRANSPORTERS
Major Facilitator Superfamily Transporter 15 (Mfs15)	v106207	KK103229	SLC17: ORGANIC ANION TRANSPORTERS
Major Facilitator Superfamily Transporter 18 (Mfs18)	v7303	GD886	SLC17: ORGANIC ANION TRANSPORTERS
Major Facilitator Superfamily Transporter 18 (Mfs18)	v110554	KK109132	SLC17: ORGANIC ANION TRANSPORTERS
Major Facilitator Superfamily Transporter 3 (Mfs3)	v107656	KK110254	SLC17: ORGANIC ANION TRANSPORTERS
Major Facilitator Superfamily Transporter 3 (Mfs3)	v330237	SH330237	SLC17: ORGANIC ANION TRANSPORTERS
Major Facilitator Superfamily Transporter 9 (Mfs9)	v104145	KK105221	SLC17: ORGANIC ANION TRANSPORTERS
Major Facilitator Superfamily Transporter 9 (Mfs9)	v330461	SH330461	SLC17: ORGANIC ANION TRANSPORTERS
Na+-Dependent Inorganic Phosphate Cotransporter (Napi-T)	v48951	GD16902	SLC17: ORGANIC ANION TRANSPORTERS
Na+-Dependent Inorganic Phosphate Cotransporter (Napi-T)	v106729	KK106711	SLC17: ORGANIC ANION TRANSPORTERS
Picot (Picot)	v101082	KK106848	SLC17: ORGANIC ANION TRANSPORTERS
Picot (Picot)	v6455	GD1651	SLC17: ORGANIC ANION TRANSPORTERS
Vesicular Glutamate Transporter (Vglut)	v104324	KK107498	SLC17: ORGANIC ANION TRANSPORTERS
Vesicular Glutamate Transporter (Vglut)	v2574	GD834	SLC17: ORGANIC ANION TRANSPORTERS
Portabella (Prt)	v104763	KK105279	SLC18: VESICULAR NEUROTRANSMITTER TRANSPORTERS
Portabella (Prt)	v9535	GD557	SLC18: VESICULAR NEUROTRANSMITTER TRANSPORTERS
Vesicular Acetylcholine Transporter (Vacht)	v330317	SH330317	SLC18: VESICULAR NEUROTRANSMITTER TRANSPORTERS
Vesicular Acetylcholine Transporter (Vacht)	v40918	GD3054	SLC18: VESICULAR NEUROTRANSMITTER TRANSPORTERS
Vesicular Monoamine Transporter (Vmat)	v4856	GD1982	SLC18: VESICULAR NEUROTRANSMITTER TRANSPORTERS
Vesicular Monoamine Transporter (Vmat)	v104072	KK112993	SLC18: VESICULAR NEUROTRANSMITTER TRANSPORTERS
Uncharacterized Protein (CG17036)	v100656	KK106227	SLC19: VITAMIN TRANSPORTERS
Uncharacterized Protein (CG17036)	v2869	GD1105	SLC19: VITAMIN TRANSPORTERS
Na+-Dependent Inorganic Phosphate Cotransporter (Napi-Iii)	v107624	KK100734	SLC20: SODIUM/PHOSPHATE CO-TRANSPORTERS
Na+-Dependent Inorganic Phosphate Cotransporter (Napi-Iii)	v49973	GD16853	SLC20: SODIUM/PHOSPHATE CO-TRANSPORTERS
Na+-Dependent Inorganic Phosphate Cotransporter (Napi-Iii)	v49971	GD16853	SLC20: SODIUM/PHOSPHATE CO-TRANSPORTERS
Organic Anion Transporting Polypeptide 26f (Oatp26f)	v2650	GD955	SLC21: ORGANIC ANION TRANSPORTING POLYPEPTIDES
Organic Anion Transporting Polypeptide 26f (Oatp26f)	v109633	KK101764	SLC21: ORGANIC ANION TRANSPORTING POLYPEPTIDES

Organic Anion Transporting Polypeptide 30b (Oatp30b)	v110237	KK100887	SLC21: ORGANIC ANION TRANSPORTING POLYPEPTIDES
Organic Anion Transporting Polypeptide 30b (Oatp30b)	v22983	GD12775	SLC21: ORGANIC ANION TRANSPORTING POLYPEPTIDES
Organic Anion Transporting Polypeptide 33ea (Oatp33ea)	v105560	KK104771	SLC21: ORGANIC ANION TRANSPORTING POLYPEPTIDES
Organic Anion Transporting Polypeptide 33ea (Oatp33ea)	v45896	GD1102	SLC21: ORGANIC ANION TRANSPORTING POLYPEPTIDES
Organic Anion Transporting Polypeptide 33eb (Oatp33eb)	v42805	GD1104	SLC21: ORGANIC ANION TRANSPORTING POLYPEPTIDES
Organic Anion Transporting Polypeptide 33eb (Oatp33eb)	v100431	KK104304	SLC21: ORGANIC ANION TRANSPORTING POLYPEPTIDES
Organic Anion Transporting Polypeptide 58da (Oatp58da)	v6623	GD2149	SLC21: ORGANIC ANION TRANSPORTING POLYPEPTIDES
Organic Anion Transporting Polypeptide 58da (Oatp58da)	v106377	KK110605	SLC21: ORGANIC ANION TRANSPORTING POLYPEPTIDES
Organic Anion Transporting Polypeptide 58db (Oatp58db)	v100348	KK106007	SLC21: ORGANIC ANION TRANSPORTING POLYPEPTIDES
Organic Anion Transporting Polypeptide 58db (Oatp58db)	v330225	SH330225	SLC21: ORGANIC ANION TRANSPORTING POLYPEPTIDES
Organic Anion Transporting Polypeptide 58dc (Oatp58dc)	v39470	GD2151	SLC21: ORGANIC ANION TRANSPORTING POLYPEPTIDES
Organic Anion Transporting Polypeptide 58dc (Oatp58dc)	v39469	GD2151	SLC21: ORGANIC ANION TRANSPORTING POLYPEPTIDES
Organic Anion Transporting Polypeptide 74d (Oatp74d)	v37295	GD2693	SLC21: ORGANIC ANION TRANSPORTING POLYPEPTIDES
Uncharacterized Protein (CG10486)	v5045	GD2324	SLC22: ORGANIC IONS TRANSPORTERS
Uncharacterized Protein (CG10486)	v107903	KK105599	SLC22: ORGANIC IONS TRANSPORTERS
Uncharacterized Protein (CG14855)	v40906	GD2986	SLC22: ORGANIC IONS TRANSPORTERS
Uncharacterized Protein (CG14856)	v101004	KK106567	SLC22: ORGANIC IONS TRANSPORTERS
Uncharacterized Protein (CG14856)	v5875	GD2987	SLC22: ORGANIC IONS TRANSPORTERS
Uncharacterized Protein (CG16727)	v33363	GD3066	SLC22: ORGANIC IONS TRANSPORTERS
Uncharacterized Protein (CG16727)	v100852	KK103742	SLC22: ORGANIC IONS TRANSPORTERS
Uncharacterized Protein (CG17751)	v50914	GD17388	SLC22: ORGANIC IONS TRANSPORTERS
Uncharacterized Protein (CG17751)	v50469	GD17388	SLC22: ORGANIC IONS TRANSPORTERS
Uncharacterized Protein (CG17752)	v50273	GD16859	SLC22: ORGANIC IONS TRANSPORTERS
Uncharacterized Protein (CG17752)	v106787	KK110261	SLC22: ORGANIC IONS TRANSPORTERS
Uncharacterized Protein (CG3168)	v48011	GD3258	SLC22: ORGANIC IONS TRANSPORTERS
Uncharacterized Protein (CG3168)	v48010	GD3258	SLC22: ORGANIC IONS TRANSPORTERS
Uncharacterized Protein (CG42269)	v100344	KK105997	SLC22: ORGANIC IONS TRANSPORTERS
Uncharacterized Protein (CG42269)	v5054	GD2328	SLC22: ORGANIC IONS TRANSPORTERS
Uncharacterized Protein (CG42269)	v101600	KK104118	SLC22: ORGANIC IONS TRANSPORTERS
Uncharacterized Protein (CG4630)	v101254	KK104040	SLC22: ORGANIC IONS TRANSPORTERS
Uncharacterized Protein (CG5592)	v110489	KK103933	SLC22: ORGANIC IONS TRANSPORTERS
Uncharacterized Protein (CG6006)	v11641	GD3644	SLC22: ORGANIC IONS TRANSPORTERS
Uncharacterized Protein (CG6006)	v106513	KK111485	SLC22: ORGANIC IONS TRANSPORTERS
Uncharacterized Protein (CG6126)	v7326	GD1821	SLC22: ORGANIC IONS TRANSPORTERS
Uncharacterized Protein (CG6231)	v105194	KK112511	SLC22: ORGANIC IONS TRANSPORTERS
Uncharacterized Protein (CG6231)	v42655	GD3067	SLC22: ORGANIC IONS TRANSPORTERS
Uncharacterized Protein (CG6356)	v23013	GD12814	SLC22: ORGANIC IONS TRANSPORTERS
Uncharacterized Protein (CG6356)	v101866	KK110028	SLC22: ORGANIC IONS TRANSPORTERS
Uncharacterized Protein (CG7084)	v102270	KK111309	SLC22: ORGANIC IONS TRANSPORTERS
Uncharacterized Protein (CG7084)	v35677	GD3109	SLC22: ORGANIC IONS TRANSPORTERS

Uncharacterized Protein (CG7084)	v12163	GD3109	SLC22: ORGANIC IONS TRANSPORTERS
Uncharacterized Protein (CG7084)	v12162	GD3109	SLC22: ORGANIC IONS TRANSPORTERS
Uncharacterized Protein (CG7333)	v101790	KK109643	SLC22: ORGANIC IONS TRANSPORTERS
Uncharacterized Protein (CG7333)	v8617	GD3672	SLC22: ORGANIC IONS TRANSPORTERS
Uncharacterized Protein (CG7342)	v48002	GD3065	SLC22: ORGANIC IONS TRANSPORTERS
Uncharacterized Protein (CG7342)	v48001	GD3065	SLC22: ORGANIC IONS TRANSPORTERS
Uncharacterized Protein (CG7458)	v12299	GD2774	SLC22: ORGANIC IONS TRANSPORTERS
Uncharacterized Protein (CG7458)	v12298	GD2774	SLC22: ORGANIC IONS TRANSPORTERS
Uncharacterized Protein (CG7458)	v108770	KK111470	SLC22: ORGANIC IONS TRANSPORTERS
Uncharacterized Protein (CG8654)	v100112	KK103694	SLC22: ORGANIC IONS TRANSPORTERS
Uncharacterized Protein (CG8654)	v4715	GD2099	SLC22: ORGANIC IONS TRANSPORTERS
Uncharacterized Protein (CG8654)	v20102	GD2099	SLC22: ORGANIC IONS TRANSPORTERS
Uncharacterized Protein (CG8925)	v101128	KK106998	SLC22: ORGANIC IONS TRANSPORTERS
Uncharacterized Protein (CG8925)	v37461	GD3645	SLC22: ORGANIC IONS TRANSPORTERS
Beta-Alanine Transporter (Balat)	v4667	GD1967	SLC22: ORGANIC IONS TRANSPORTERS
Beta-Alanine Transporter (Balat)	v108223	KK103020	SLC22: ORGANIC IONS TRANSPORTERS
Carcinine Transporter (Cart)	v101145	KK104029	SLC22: ORGANIC IONS TRANSPORTERS
Carcinine Transporter (Cart)	v9321	GD1791	SLC22: ORGANIC IONS TRANSPORTERS
Organic Cation Transporter (Orct)	v47133	GD16316	SLC22: ORGANIC IONS TRANSPORTERS
Organic Cation Transporter (Orct)	v52658	GD16316	SLC22: ORGANIC IONS TRANSPORTERS
Organic Cation Transporter (Orct)	v6782	GD226	SLC22: ORGANIC IONS TRANSPORTERS
Organic Cation Transporter 2 (Orct2)	v1176	GD225	SLC22: ORGANIC IONS TRANSPORTERS
Organic Cation Transporter 2 (Orct2)	v1177	GD225	SLC22: ORGANIC IONS TRANSPORTERS
Organic Cation Transporter 2 (Orct2)	v48870	GD16460	SLC22: ORGANIC IONS TRANSPORTERS
Organic Cation Transporter 2 (Orct2)	v106681	KK102141	SLC22: ORGANIC IONS TRANSPORTERS
Slc22a Family Member (Slc22a)	v106555	KK112539	SLC22: ORGANIC IONS TRANSPORTERS
Slc22a Family Member (Slc22a)	v8450	GD2773	SLC22: ORGANIC IONS TRANSPORTERS
Nckx30c (Nckx30c)	v51459	GD1040	SLC24: POTASSIUM-DEPENDENT Na+/Cl- EXCHANGERS
Nckx30c (Nckx30c)	v51877	GD1040	SLC24: POTASSIUM-DEPENDENT Na+/Cl- EXCHANGERS
Zydeco (Zyd)	v40988	GD3723	SLC24: POTASSIUM-DEPENDENT Na+/Cl- EXCHANGERS
Zydeco (Zyd)	v40987	GD3723	SLC24: POTASSIUM-DEPENDENT Na+/Cl- EXCHANGERS
Uncharacterized Protein (CG1628)	v47475	GD8885	SLC25: MITOCHONDRIAL TRANSPORTERS
Uncharacterized Protein (CG1628)	v19267	GD8885	SLC25: MITOCHONDRIAL TRANSPORTERS
Uncharacterized Protein (CG1628)	v19268	GD8885	SLC25: MITOCHONDRIAL TRANSPORTERS
Uncharacterized Protein (CG1628)	v109588	KK108506	SLC25: MITOCHONDRIAL TRANSPORTERS
Uncharacterized Protein (CG18324)	v105401	KK100953	SLC25: MITOCHONDRIAL TRANSPORTERS
Uncharacterized Protein (CG18324)	v33234	GD1989	SLC25: MITOCHONDRIAL TRANSPORTERS
Uncharacterized Protein (CG18327)	v100920	KK106230	SLC25: MITOCHONDRIAL TRANSPORTERS
Uncharacterized Protein (CG18418)	v102109	KK110768	SLC25: MITOCHONDRIAL TRANSPORTERS
Uncharacterized Protein (CG18418)	v9009	GD2311	SLC25: MITOCHONDRIAL TRANSPORTERS

Uncharacterized Protein (CG18418)	v9008	GD2311	SLC25: MITOCHONDRIAL TRANSPORTERS
Uncharacterized Protein (CG1907)	v1341	GD360	SLC25: MITOCHONDRIAL TRANSPORTERS
Uncharacterized Protein (CG1907)	v103359	KK100238	SLC25: MITOCHONDRIAL TRANSPORTERS
Uncharacterized Protein (CG1907)	v1342	GD360	SLC25: MITOCHONDRIAL TRANSPORTERS
Uncharacterized Protein (CG2616)	v11052	GD2849	SLC25: MITOCHONDRIAL TRANSPORTERS
Uncharacterized Protein (CG2616)	v102630	KK103354	SLC25: MITOCHONDRIAL TRANSPORTERS
Uncharacterized Protein (CG4743)	v9487	GD276	SLC25: MITOCHONDRIAL TRANSPORTERS
Uncharacterized Protein (CG4743)	v103950	KK102952	SLC25: MITOCHONDRIAL TRANSPORTERS
Uncharacterized Protein (CG4995)	v106173	KK101024	SLC25: MITOCHONDRIAL TRANSPORTERS
Uncharacterized Protein (CG5254)	v45164	GD3172	SLC25: MITOCHONDRIAL TRANSPORTERS
Uncharacterized Protein (CG5254)	v45163	GD3172	SLC25: MITOCHONDRIAL TRANSPORTERS
Uncharacterized Protein (CG5646)	v4402	GD328	SLC25: MITOCHONDRIAL TRANSPORTERS
Uncharacterized Protein (CG5805)	v35592	GD12806	SLC25: MITOCHONDRIAL TRANSPORTERS
Uncharacterized Protein (CG5805)	v104015	KK107805	SLC25: MITOCHONDRIAL TRANSPORTERS
Uncharacterized Protein (CG7514)	v37233	GD2310	SLC25: MITOCHONDRIAL TRANSPORTERS
Uncharacterized Protein (CG7514)	v103023	KK113131	SLC25: MITOCHONDRIAL TRANSPORTERS
Uncharacterized Protein (CG7943)	v28632	GD13199	SLC25: MITOCHONDRIAL TRANSPORTERS
Uncharacterized Protein (CG8026)	v105681	KK108392	SLC25: MITOCHONDRIAL TRANSPORTERS
Uncharacterized Protein (CG8026)	v4165	GD1894	SLC25: MITOCHONDRIAL TRANSPORTERS
Uncharacterized Protein (CG8026)	v4163	GD1894	SLC25: MITOCHONDRIAL TRANSPORTERS
Uncharacterized Protein (CG8323)	v4861	GD1987	SLC25: MITOCHONDRIAL TRANSPORTERS
Uncharacterized Protein (CG9582)	v100256	KK107278	SLC25: MITOCHONDRIAL TRANSPORTERS
Uncharacterized Protein (CG9582)	v2845	GD1027	SLC25: MITOCHONDRIAL TRANSPORTERS
Uncharacterized Protein (CG9582)	v2846	GD1027	SLC25: MITOCHONDRIAL TRANSPORTERS
Adenine Nucleotide Translocase 2 (Ant2)	v45177	GD3303	SLC25: MITOCHONDRIAL TRANSPORTERS
Adenine Nucleotide Translocase 2 (Ant2)	v45176	GD3303	SLC25: MITOCHONDRIAL TRANSPORTERS
Adenine Nucleotide Translocase 2 (Ant2)	v102533	KK111914	SLC25: MITOCHONDRIAL TRANSPORTERS
Aralar1 (Aralar1)	v330528	SH330528	SLC25: MITOCHONDRIAL TRANSPORTERS
Congested-Like Trachea (Colt)	v106089	KK107449	SLC25: MITOCHONDRIAL TRANSPORTERS
Congested-Like Trachea (Colt)	v47964	GD841	SLC25: MITOCHONDRIAL TRANSPORTERS
Congested-Like Trachea (Colt)	v47965	GD841	SLC25: MITOCHONDRIAL TRANSPORTERS
Dephosphocoenzyme A Carrier (Dpcoac)	v101378	KK109328	SLC25: MITOCHONDRIAL TRANSPORTERS
Dicarboxylate Carrier 1 (Dic1)	v5864	GD2971	SLC25: MITOCHONDRIAL TRANSPORTERS
Dicarboxylate Carrier 1 (Dic1)	v103757	KK102461	SLC25: MITOCHONDRIAL TRANSPORTERS
Dicarboxylate Carrier 2 (Dic2)	v104152	KK105452	SLC25: MITOCHONDRIAL TRANSPORTERS
Dicarboxylate Carrier 3 (Dic3)	v100255	KK107274	SLC25: MITOCHONDRIAL TRANSPORTERS
Dicarboxylate Carrier 3 (Dic3)	v36497	GD14764	SLC25: MITOCHONDRIAL TRANSPORTERS
Dicarboxylate Carrier 4 (Dic4)	v8416	GD2711	SLC25: MITOCHONDRIAL TRANSPORTERS
Glutamate Carrier 1 (Gc1)	v106319	KK109028	SLC25: MITOCHONDRIAL TRANSPORTERS
Glutamate Carrier 2 (Gc2)	v109013	KK110811	SLC25: MITOCHONDRIAL TRANSPORTERS

Glutamate Carrier 2 (Gc2)	v42649	GD2932	SLC25: MITOCHONDRIAL TRANSPORTERS
Mitochondrial Magnesium Exporter 1 (Mme1)	v100372	KK106089	SLC25: MITOCHONDRIAL TRANSPORTERS
Mitochondrial Magnesium Exporter 1 (Mme1)	v2734	GD964	SLC25: MITOCHONDRIAL TRANSPORTERS
Mitochondrial Phosphate Carrier Protein 1 (Mpcp1)	v44297	GD2105	SLC25: MITOCHONDRIAL TRANSPORTERS
Mitochondrial Phosphate Carrier Protein 1 (Mpcp1)	v101848	KK109958	SLC25: MITOCHONDRIAL TRANSPORTERS
Mitochondrial Phosphate Carrier Protein 2 (Mpcp2)	v8366	GD2457	SLC25: MITOCHONDRIAL TRANSPORTERS
Mitochondrial Phosphate Carrier Protein 2 (Mpcp2)	v101316	KK107535	SLC25: MITOCHONDRIAL TRANSPORTERS
Mitoferrin (Mfrn)	v12342	GD336	SLC25: MITOCHONDRIAL TRANSPORTERS
Mitoferrin (Mfrn)	v100597	KK108379	SLC25: MITOCHONDRIAL TRANSPORTERS
Peroxisomal Membrane Protein 34 (Pmp34)	v108323	KK105713	SLC25: MITOCHONDRIAL TRANSPORTERS
Peroxisomal Membrane Protein 34 (Pmp34)	v7491	GD2302	SLC25: MITOCHONDRIAL TRANSPORTERS
Replication In Mitochondria 2 (Rim2)	v44203	GD807	SLC25: MITOCHONDRIAL TRANSPORTERS
Replication In Mitochondria 2 (Rim2)	v100807	KK108751	SLC25: MITOCHONDRIAL TRANSPORTERS
Scheggia (Sea)	v109169	KK116001	SLC25: MITOCHONDRIAL TRANSPORTERS
Shawn (Shawn)	v109948	KK114811	SLC25: MITOCHONDRIAL TRANSPORTERS
Short Calcium-Binding Mitochondrial Carrier (Scamc)	v108078	KK100089	SLC25: MITOCHONDRIAL TRANSPORTERS
Short Calcium-Binding Mitochondrial Carrier (Scamc)	v29439	GD14864	SLC25: MITOCHONDRIAL TRANSPORTERS
Stress-Sensitive B (Sesb)	v104576	KK108773	SLC25: MITOCHONDRIAL TRANSPORTERS
Stress-Sensitive B (Sesb)	v52457	GD16160	SLC25: MITOCHONDRIAL TRANSPORTERS
Stress-Sensitive B (Sesb)	v11968	GD4655	SLC25: MITOCHONDRIAL TRANSPORTERS
Stress-Sensitive B (Sesb)	v48582	GD16160	SLC25: MITOCHONDRIAL TRANSPORTERS
Stress-Sensitive B (Sesb)	v48581	GD16160	SLC25: MITOCHONDRIAL TRANSPORTERS
Thiamine Pyrophosphate Carrier Protein 1 (Tpc1)	v6005	GD2905	SLC25: MITOCHONDRIAL TRANSPORTERS
Thiamine Pyrophosphate Carrier Protein 2 (Tpc2)	v7417	GD2220	SLC25: MITOCHONDRIAL TRANSPORTERS
Thiamine Pyrophosphate Carrier Protein 2 (Tpc2)	v107215	KK104062	SLC25: MITOCHONDRIAL TRANSPORTERS
Uncoupling Protein 4a (Ucp4a)	v6162	GD3419	SLC25: MITOCHONDRIAL TRANSPORTERS
Uncoupling Protein 4a (Ucp4a)	v102571	KK112027	SLC25: MITOCHONDRIAL TRANSPORTERS
Uncoupling Protein 4b (Ucp4b)	v33130	GD9562	SLC25: MITOCHONDRIAL TRANSPORTERS
Uncoupling Protein 4b (Ucp4b)	v33128	GD9562	SLC25: MITOCHONDRIAL TRANSPORTERS
Uncoupling Protein 4c (Ucp4c)	v100064	KK103259	SLC25: MITOCHONDRIAL TRANSPORTERS
Uncoupling Protein 4c (Ucp4c)	v2647	GD933	SLC25: MITOCHONDRIAL TRANSPORTERS
Uncharacterized Protein (CG5002)	v100600	KK108414	SLC26: ANION EXCHANGERS
Uncharacterized Protein (CG5002)	v10058	GD2060	SLC26: ANION EXCHANGERS
Uncharacterized Protein (CG5404)	v100953	KK106341	SLC26: ANION EXCHANGERS
Uncharacterized Protein (CG5404)	v40907	GD3006	SLC26: ANION EXCHANGERS
Uncharacterized Protein (CG6125)	v45090	GD3001	SLC26: ANION EXCHANGERS
Uncharacterized Protein (CG6125)	v107894	KK104795	SLC26: ANION EXCHANGERS
Uncharacterized Protein (CG6928)	v5229	GD2434	SLC26: ANION EXCHANGERS
Uncharacterized Protein (CG6928)	v106739	KK106942	SLC26: ANION EXCHANGERS
Uncharacterized Protein (CG7912)	v1377	GD376	SLC26: ANION EXCHANGERS

Uncharacterized Protein (CG7912)	v1378	GD376	SLC26: ANION EXCHANGERS
Uncharacterized Protein (CG9702)	v6859	GD3131	SLC26: ANION EXCHANGERS
Uncharacterized Protein (CG9702)	v6860	GD3131	SLC26: ANION EXCHANGERS
Uncharacterized Protein (CG9717)	v42670	GD3132	SLC26: ANION EXCHANGERS
Uncharacterized Protein (CG9717)	v42669	GD3132	SLC26: ANION EXCHANGERS
Epidermal Stripes And Patches (Esp)	v9797	GD251	SLC26: ANION EXCHANGERS
Epidermal Stripes And Patches (Esp)	v9795	GD251	SLC26: ANION EXCHANGERS
Prestin (Prestin)	v5341	GD2707	SLC26: ANION EXCHANGERS
Fatty Acid Transport Protein 2 (Fatp2)	v50234	GD16599	SLC27: FATTY ACID TRANSPORTERS
Fatty Acid Transport Protein 2 (Fatp2)	v3528	GD2170	SLC27: FATTY ACID TRANSPORTERS
Fatty Acid Transport Protein 2 (Fatp2)	v50235	GD16599	SLC27: FATTY ACID TRANSPORTERS
Fatty Acid Transport Protein 2 (Fatp2)	v106140	KK102884	SLC27: FATTY ACID TRANSPORTERS
Fatty Acid Transport Protein 3 (Fatp3)	v3621	GD2203	SLC27: FATTY ACID TRANSPORTERS
Concentrative Nucleoside Transporter 1 (Cnt1)	v7374	GD1888	SLC28: CONCENTRATIVE NUCLEOSIDE CO-TRANSPORTERS
Concentrative Nucleoside Transporter 1 (Cnt1)	v106218	KK105246	SLC28: CONCENTRATIVE NUCLEOSIDE CO-TRANSPORTERS
Concentrative Nucleoside Transporter 2 (Cnt2)	v105828	KK100597	SLC28: CONCENTRATIVE NUCLEOSIDE CO-TRANSPORTERS
Concentrative Nucleoside Transporter 2 (Cnt2)	v37161	GD1887	SLC28: CONCENTRATIVE NUCLEOSIDE CO-TRANSPORTERS
Equilibrative Nucleoside Transporter 1 (Ent1)	v49328	GD783	SLC29: EQUILIBRATIVE NUCLEOSIDE TRANSPORTERS
Equilibrative Nucleoside Transporter 1 (Ent1)	v109885	KK101972	SLC29: EQUILIBRATIVE NUCLEOSIDE TRANSPORTERS
Equilibrative Nucleoside Transporter 2 (Ent2)	v7618	GD953	SLC29: EQUILIBRATIVE NUCLEOSIDE TRANSPORTERS
Equilibrative Nucleoside Transporter 2 (Ent2)	v100464	KK104419	SLC29: EQUILIBRATIVE NUCLEOSIDE TRANSPORTERS
Equilibrative Nucleoside Transporter 3 (Ent3)	v47537	GD2445	SLC29: EQUILIBRATIVE NUCLEOSIDE TRANSPORTERS
Equilibrative Nucleoside Transporter 3 (Ent3)	v47536	GD2445	SLC29: EQUILIBRATIVE NUCLEOSIDE TRANSPORTERS
Zinc Transporter 33d (Znt33d)	v7688	GD1098	SLC30: ZINC TRANSPORTERS
Zinc Transporter 33d (Znt33d)	v103398	KK100432	SLC30: ZINC TRANSPORTERS
Zinc Transporter 35c (Znt35c)	v3836	GD1730	SLC30: ZINC TRANSPORTERS
Zinc Transporter 35c (Znt35c)	v103263	KK112697	SLC30: ZINC TRANSPORTERS
Zinc Transporter 41f (Znt41f)	v107931	KK111282	SLC30: ZINC TRANSPORTERS
Zinc Transporter 41f (Znt41f)	v13311	GD4522	SLC30: ZINC TRANSPORTERS
Zinc Transporter 49b (Znt49b)	v108929	KK101094	SLC30: ZINC TRANSPORTERS
Zinc Transporter 49b (Znt49b)	v4654	GD1962	SLC30: ZINC TRANSPORTERS
Zinc Transporter 63c (Znt63c)	v7461	GD2276	SLC30: ZINC TRANSPORTERS
Zinc Transporter 63c (Znt63c)	v105145	KK102261	SLC30: ZINC TRANSPORTERS
Zinc Transporter 77c (Znt77c)	v5390	GD2749	SLC30: ZINC TRANSPORTERS
Zinc Transporter 86d (Znt86d)	v107388	KK101698	SLC30: ZINC TRANSPORTERS
Copper Transporter 1a (Ctr1a)	v46757	GD16726	SLC31: COPPER TRANSPORTERS
Copper Transporter 1b (Ctr1b)	v5805	GD2859	SLC31: COPPER TRANSPORTERS
Copper Transporter 1b (Ctr1b)	v5804	GD2859	SLC31: COPPER TRANSPORTERS
Copper Transporter 1c (Ctr1c)	v102136	KK110883	SLC31: COPPER TRANSPORTERS
Copper Transporter 1c (Ctr1c)	v10263	GD3136	SLC31: COPPER TRANSPORTERS

Vesicular Gaba Transporter (Vgat)	v103586	KK101500	SLC32: VESICULAR GABA TRANSPORTERS
Vesicular Gaba Transporter (Vgat)	v45916	GD1990	SLC32: VESICULAR GABA TRANSPORTERS
Vesicular Gaba Transporter (Vgat)	v45917	GD1990	SLC32: VESICULAR GABA TRANSPORTERS
Uncharacterized Protein (CG9706)	v49347	GD4617	SLC33 ACETYL-COA TRANSPORTERS
Uncharacterized Protein (CG9706)	v100567	KK108219	SLC33 ACETYL-COA TRANSPORTERS
Uncharacterized Protein (CG9706)	v49346	GD4617	SLC33 ACETYL-COA TRANSPORTERS
Uncharacterized Protein (CG14511)	v4427	GD349	SLC35: NUCLEOTIDE SUGAR TRANSPORTERS
Uncharacterized Protein (CG14511)	v107875	KK104618	SLC35: NUCLEOTIDE SUGAR TRANSPORTERS
Uncharacterized Protein (CG14971)	v39479	GD2279	SLC35: NUCLEOTIDE SUGAR TRANSPORTERS
Uncharacterized Protein (CG14971)	v108955	KK102388	SLC35: NUCLEOTIDE SUGAR TRANSPORTERS
Er Gdp-Fucose Transporter (Efr)	v30238	GD3254	SLC35: NUCLEOTIDE SUGAR TRANSPORTERS
Er Gdp-Fucose Transporter (Efr)	v30240	GD3254	SLC35: NUCLEOTIDE SUGAR TRANSPORTERS
Fringe Connection (Frc)	v21469	GD10475	SLC35: NUCLEOTIDE SUGAR TRANSPORTERS
Fringe Connection (Frc)	v47542	GD2691	SLC35: NUCLEOTIDE SUGAR TRANSPORTERS
Fringe Connection (Frc)	v47543	GD2691	SLC35: NUCLEOTIDE SUGAR TRANSPORTERS
Fringe Connection (Frc)	v5302	GD2691	SLC35: NUCLEOTIDE SUGAR TRANSPORTERS
Fringe Connection (Frc)	v21468	GD10475	SLC35: NUCLEOTIDE SUGAR TRANSPORTERS
Fringe Connection (Frc)	v107816	KK102002	SLC35: NUCLEOTIDE SUGAR TRANSPORTERS
Medial Glomeruli (Meigo)	v6800	GD3097	SLC35: NUCLEOTIDE SUGAR TRANSPORTERS
Medial Glomeruli (Meigo)	v103753	KK102431	SLC35: NUCLEOTIDE SUGAR TRANSPORTERS
Neuronally Altered Carbohydrate (Nac)	v105410	KK101122	SLC35: NUCLEOTIDE SUGAR TRANSPORTERS
Neuronally Altered Carbohydrate (Nac)	v42623	GD2857	SLC35: NUCLEOTIDE SUGAR TRANSPORTERS
Senju (Senju)	v110668	KK100688	SLC35: NUCLEOTIDE SUGAR TRANSPORTERS
Senju (Senju)	v13399	GD902	SLC35: NUCLEOTIDE SUGAR TRANSPORTERS
Slalom (Sll)	v12149	GD3032	SLC35: NUCLEOTIDE SUGAR TRANSPORTERS
Slalom (Sll)	v12148	GD3032	SLC35: NUCLEOTIDE SUGAR TRANSPORTERS
Udp-Galactose Transporter (Ugalt)	v100803	KK108744	SLC35: NUCLEOTIDE SUGAR TRANSPORTERS
Udp-Galactose Transporter (Ugalt)	v10149	GD3211	SLC35: NUCLEOTIDE SUGAR TRANSPORTERS
Uncharacterized Protein (CG1139)	v102363	KK111566	SLC36: PROTON-COUPLED AMINO ACID TRANSPORTERS
Uncharacterized Protein (CG1139)	v8907	GD3830	SLC36: PROTON-COUPLED AMINO ACID TRANSPORTERS
Uncharacterized Protein (CG13384)	v44246	GD1007	SLC36: PROTON-COUPLED AMINO ACID TRANSPORTERS
Uncharacterized Protein (CG13384)	v106698	KK102447	SLC36: PROTON-COUPLED AMINO ACID TRANSPORTERS
Uncharacterized Protein (CG16700)	v110058	KK105945	SLC36: PROTON-COUPLED AMINO ACID TRANSPORTERS
Uncharacterized Protein (CG16700)	v45188	GD3405	SLC36: PROTON-COUPLED AMINO ACID TRANSPORTERS
Uncharacterized Protein (CG32079)	v39496	GD2409	SLC36: PROTON-COUPLED AMINO ACID TRANSPORTERS
Uncharacterized Protein (CG32079)	v104454	KK107121	SLC36: PROTON-COUPLED AMINO ACID TRANSPORTERS
Uncharacterized Protein (CG32081)	v107023	KK105324	SLC36: PROTON-COUPLED AMINO ACID TRANSPORTERS
Uncharacterized Protein (CG32081)	v5209	GD2410	SLC36: PROTON-COUPLED AMINO ACID TRANSPORTERS
Uncharacterized Protein (CG4991)	v108419	KK109628	SLC36: PROTON-COUPLED AMINO ACID TRANSPORTERS
Uncharacterized Protein (CG4991)	v30263	GD3406	SLC36: PROTON-COUPLED AMINO ACID TRANSPORTERS

Uncharacterized Protein (CG4991)	v30264	GD3406	SLC36: PROTON-COUPLED AMINO ACID TRANSPORTERS
Uncharacterized Protein (CG7888)	v37264	GD2411	SLC36: PROTON-COUPLED AMINO ACID TRANSPORTERS
Uncharacterized Protein (CG7888)	v37263	GD2411	SLC36: PROTON-COUPLED AMINO ACID TRANSPORTERS
Uncharacterized Protein (CG8785)	v4651	GD1961	SLC36: PROTON-COUPLED AMINO ACID TRANSPORTERS
Uncharacterized Protein (CG8785)	v4650	GD1961	SLC36: PROTON-COUPLED AMINO ACID TRANSPORTERS
Pathetic (Path)	v44536	GD2391	SLC36: PROTON-COUPLED AMINO ACID TRANSPORTERS
Pathetic (Path)	v44537	GD2391	SLC36: PROTON-COUPLED AMINO ACID TRANSPORTERS
Polyphemus (Polyph)	v107119	KK112469	SLC36: PROTON-COUPLED AMINO ACID TRANSPORTERS
Polyphemus (Polyph)	v6762	GD421	SLC36: PROTON-COUPLED AMINO ACID TRANSPORTERS
Major Facilitator Superfamily Transporter 16 (Mfs16)	v6589	GD2124	SLC37: PHOSPHOSUGAR/PHOSPHATE EXCHANGERS
Major Facilitator Superfamily Transporter 16 (Mfs16)	v6591	GD2124	SLC37: PHOSPHOSUGAR/PHOSPHATE EXCHANGERS
Major Facilitator Superfamily Transporter 16 (Mfs16)	v108635	KK102318	SLC37: PHOSPHOSUGAR/PHOSPHATE EXCHANGERS
Uncharacterized Protein (CG13743)	v110773	KK107968	SLC38: Na+-COUPLED AMINO ACID TRANSPORTERS
Uncharacterized Protein (CG13743)	v40974	GD3488	SLC38: Na+-COUPLED AMINO ACID TRANSPORTERS
Uncharacterized Protein (CG30394)	v3470	GD2127	SLC38: Na+-COUPLED AMINO ACID TRANSPORTERS
Uncharacterized Protein (CG30394)	v330312	SH330312	SLC38: Na+-COUPLED AMINO ACID TRANSPORTERS
Catecholamines Up (Catsup)	v7183	GD1635	SLC39: ZINC ION TRANSPORTERS
Catecholamines Up (Catsup)	v100095	KK103630	SLC39: ZINC ION TRANSPORTERS
Fear-Of-Intimacy (Foi)	v330251	SH330251	SLC39: ZINC ION TRANSPORTERS
Fear-Of-Intimacy (Foi)	v10102	GD2367	SLC39: ZINC ION TRANSPORTERS
Zinc/Iron Regulated Transporter Protein 102b (Zip102b)	v51083	GD3683	SLC39: ZINC ION TRANSPORTERS
Zinc/Iron Regulated Transporter Protein 102b (Zip102b)	v51084	GD3683	SLC39: ZINC ION TRANSPORTERS
Zinc/Iron Regulated Transporter Protein 42c.1 (Zip42c.1)	v3987	GD1830	SLC39: ZINC ION TRANSPORTERS
Zinc/Iron Regulated Transporter Protein 42c.1 (Zip42c.1)	v3986	GD1830	SLC39: ZINC ION TRANSPORTERS
Zinc/Iron Regulated Transporter Protein 42c.1 (Zip42c.1)	v107309	KK108319	SLC39: ZINC ION TRANSPORTERS
Zinc/Iron Regulated Transporter Protein 42c.2 (Zip42c.2)	v110047	KK104365	SLC39: ZINC ION TRANSPORTERS
Zinc/Iron Regulated Transporter Protein 42c.2 (Zip42c.2)	v7338	GD1831	SLC39: ZINC ION TRANSPORTERS
Zinc/Iron Regulated Transporter Protein 42c.2 (Zip42c.2)	v7339	GD1831	SLC39: ZINC ION TRANSPORTERS
Zinc/Iron Regulated Transporter Protein 48c (Zip48c)	v105650	KK101374	SLC39: ZINC ION TRANSPORTERS
Zinc/Iron Regulated Transporter Protein 48c (Zip48c)	v330401	SH330401	SLC39: ZINC ION TRANSPORTERS
Zinc/Iron Regulated Transporter Protein 71b (Zip71b)	v101031	KK106638	SLC39: ZINC ION TRANSPORTERS
Zinc/Iron Regulated Transporter Protein 71b (Zip71b)	v44539	GD2461	SLC39: ZINC ION TRANSPORTERS
Zinc/Iron Regulated Transporter Protein 71b (Zip71b)	v44538	GD2461	SLC39: ZINC ION TRANSPORTERS
Zinc/Iron Regulated Transporter Protein 88e (Zip88e)	v49329	GD2997	SLC39: ZINC ION TRANSPORTERS
Zinc/Iron Regulated Transporter Protein 88e (Zip88e)	v106785	KK110168	SLC39: ZINC ION TRANSPORTERS
Zinc/Iron Regulated Transporter Protein 89b (Zip89b)	v37357	GD3013	SLC39: ZINC ION TRANSPORTERS
Zinc/Iron Regulated Transporter Protein 89b (Zip89b)	v37358	GD3013	SLC39: ZINC ION TRANSPORTERS
Zinc/Iron Regulated Transporter Protein 99c (Zip99c)	v1362	GD370	SLC39: ZINC ION TRANSPORTERS
Zinc/Iron Regulated Transporter Protein 99c (Zip99c)	v1364	GD370	SLC39: ZINC ION TRANSPORTERS
Uncharacterized Protein (CG33181)	v103142	KK107703	SLC41: MAGNESIUM ION TRANSPORTERS

Uncharacterized Protein (CG33181)	v47868	GD16951	SLC41: MAGNESIUM ION TRANSPORTERS
Choline Transporter-Like 1 (Ctl1)	v12242	GD3579	SLC44 CHOLINE TRANSPORTER-LIKE FAMILY
Choline Transporter-Like 1 (Ctl1)	v13480	GD3579	SLC44 CHOLINE TRANSPORTER-LIKE FAMILY
Choline Transporter-Like 1 (Ctl1)	v39695	GD3579	SLC44 CHOLINE TRANSPORTER-LIKE FAMILY
Choline Transporter-Like 1 (Ctl1)	v103764	KK102528	SLC44 CHOLINE TRANSPORTER-LIKE FAMILY
Choline Transporter-Like 2 (Ctl2)	v106968	KK100290	SLC44 CHOLINE TRANSPORTER-LIKE FAMILY
Choline Transporter-Like 2 (Ctl2)	v22867	GD12636	SLC44 CHOLINE TRANSPORTER-LIKE FAMILY
Solute Carrier Family 45 Member 1 (Slc45-1)	v5172	GD2383	SLC45: SUCROSE TRANSPORTERS
Solute Carrier Family 45 Member 1 (Slc45-1)	v5174	GD2383	SLC45: SUCROSE TRANSPORTERS
Solute Carrier Family 45 Member 1 (Slc45-1)	v105439	KK102699	SLC45: SUCROSE TRANSPORTERS
Uncharacterized Protein (CG15553)	v6866	GD3138	SLC46 FOLATE TRANSPORTER-LIKE FAMILY
Uncharacterized Protein (CG15553)	v104514	KK109617	SLC46 FOLATE TRANSPORTER-LIKE FAMILY
Uncharacterized Protein (CG30344)	v106870	KK110555	SLC46 FOLATE TRANSPORTER-LIKE FAMILY
Uncharacterized Protein (CG30344)	v7378	GD1890	SLC46 FOLATE TRANSPORTER-LIKE FAMILY
Uncharacterized Protein (CG30344)	v7379	GD1890	SLC46 FOLATE TRANSPORTER-LIKE FAMILY
Uncharacterized Protein (CG30345)	v103652	KK107768	SLC46 FOLATE TRANSPORTER-LIKE FAMILY
Uncharacterized Protein (CG30345)	v42868	GD1891	SLC46 FOLATE TRANSPORTER-LIKE FAMILY
Saliva (Slv)	v104666	KK101522	SLC50: SUGAR TRANSPORTERS

Table 2. RNA[i] lines included in Glycine metabolism-related *in vivo* screening

Gene name (symbol)	Annotation CG	BDSC Nº.	FlyBase Gene Group
Alanine-glyoxylate transaminase (CG11241)	CG11241	58188	TRANSAMINASES
Alanine-glyoxylate (Agxt)	CG3926	80408	TRANSAMINASES
bb in a boxcar (bbc)	CG6016	57704	PHOSPHATE GROUP PHOSPHOTRANSFERASES
Betaine-homocysteine S-methyltransferase (Bhmt)	CG10623	43986	UNCLASSIFIED METHYLTRANSFERASES
Cystathionine gamma-lyase (Cth)	CG5345	36766	CARBON-SULFUR LYASES
Cystathionine gamma-lyase (Cyh)	CG5345	41876	CARBON-SULFUR LYASES
Cystathionine β-synthase (Cbs)	CG1753	41877	OTHER NITROGENOUS GROUP OXIDOREDUCTASES
Cystathionine β-synthase (Cbs)	CG1753	36767	OTHER NITROGENOUS GROUP OXIDOREDUCTASES
D-amino acid oxidase 2 (Daao2)	CG11236	57486	CH-NH2 OXIDOREDUCTASES
Formyltetrahydrofolate dehydrogenase (CG8665)	CG8665	62266	CH-NH OXIDOREDUCTASES
Glutathione synthetase 2 (Gss2)	CG32495	55150	ACID-AMINO ACID LIGASES
Glycine N-methyltransferase (Gnmt)	CG6188	53282	UNCLASSIFIED METHYLTRANSFERASES
Glycine N-methyltransferase (Gnmt)	CG6188	43148	UNCLASSIFIED METHYLTRANSFERASES
L-allo-threonine aldolase (CG10184)	CG10184	65079	ALDEHYDE-LYASES
Methionyl-tRNA formyltransferase (CG1750)	CG1750	62267	HYDROXYMETHYL-/FORMYL- RELATED TRANSFERASES
Methylenetetrahydrofolate reductase (CG7560)	CG7560	64993	CH-NH OXIDOREDUCTASES
Pugilist (pug)	CG4067	62268	UNCLASSIFIED CARBON-NITROGEN LIGASES
Pugilist (pug)	CG4067	53332	UNCLASSIFIED CARBON-NITROGEN LIGASES
S-adenosylmethionine Synthetase (Sam-S)	CG2674	53291	UNCLASSIFIED ALKYL OR ARYL TRANSFERASES
Sarcosine dehydrogenase (Sardh)	CG6385	42950	UNCLASSIFIED CH-NH OXIDOREDUCTASES
Thymidylate synthase (Ts)	CG3181	29415	UNCLASSIFIED METHYLTRANSFERASES

Table 3. RNA[i] lines for Autophagy & Glutathione metabolism-related *in vivo* screening

Gene name (symbol)	Annotation CG	BDSC Nº.	FlyBase Gene Group
Autophagy-related 1 (Atg1)	CG10967	26731	ATG1 PROTEIN KINASE COMPLEX
Autophagy-related 1 (Atg1)	CG10967	35177	ATG1 PROTEIN KINASE COMPLEX
Autophagy-related 1 (Atg1)	CG10967	44034	ATG1 PROTEIN KINASE COMPLEX
Autophagy-related 1 (Atg1)	CG10967	80434	ATG1 PROTEIN KINASE COMPLEX
Autophagy-related 2 (Atg 2)	CG1241	27706	AUTOPHAGY-RELATED GENES
Autophagy-related 2 (Atg 2)	CG1241	34719	AUTOPHAGY-RELATED GENES
Autophagy-related 3 (Atg3)	CG6877	34359	ATG8 TRANSFERASES
Autophagy-related 4a (Atg 4a)	CG4428	28367	ATG8 PROTEASES
Autophagy-related 4a (Atg 4a)	CG4428	35740	ATG8 PROTEASES
Autophagy-related 4a (Atg 4a)	CG4428	44421	ATG8 PROTEASES
Autophagy-related 4b (Atg4b)	CG6194	56046	ATG8 PROTEASES
Autophagy-related 5 (Atg 5)	CG1643	27551	ATG12-ATG5-ATG16 COMPLEX
Autophagy-related 5 (Atg 5)	CG1643	34899	ATG12-ATG5-ATG16 COMPLEX
Autophagy-related 6 (Atg 6)	CG5429	28060	AUTOPHAGY-SPECIFIC PHOSPHATIDYLINOSITOL 3-KINASE
Autophagy-related 6 (Atg 6)	CG5429	35741	AUTOPHAGY-SPECIFIC PHOSPHATIDYLINOSITOL 3-KINASE
Autophagy-related 7 (Atg 7)	CG5489	27707	ATG8/12 ACTIVATING ENZYMES
Autophagy-related 7 (Atg 7)	CG5489	34369	ATG8/12 ACTIVATING ENZYMES
Autophagy-related 7 (Atg 7)	CG5489	28989	ATG8/12 ACTIVATING ENZYMES
Autophagy-related 8a (Atg 8a)	CG32672	34340	ATG8 PROTEINS
Autophagy-related 8a (Atg 8a)	CG32672	80428	ATG8 PROTEINS
Autophagy-related 8a (Atg 8a)	CG32672	82955	ATG8 PROTEINS
Autophagy-related 9 (Atg9)	CG3615	28055	AUTOPHAGY-RELATED GENES
Autophagy-related 10 (Atg10)	CG12821	40859	ATG12 TRANSFERASES
Autophagy-related 12 (Atg12)	CG10861	27552	ATG12-ATG5-ATG16 COMPLEX
Autophagy-related 12 (Atg12)	CG10861	34675	ATG12-ATG5-ATG16 COMPLEX
Autophagy-related 13 (Atg13)	CG7331	40861	ATG1 PROTEIN KINASE COMPLEX
Autophagy-related 14 (Atg14)	CG11877	40858	AUTOPHAGY-SPECIFIC PHOSPHATIDYLINOSITOL 3-KINASE
Autophagy-related 14 (Atg14)	CG11877	55398	AUTOPHAGY-SPECIFIC PHOSPHATIDYLINOSITOL 3-KINASE
Autophagy-related 16 (Atg16)	CG31033	34358	ATG12-ATG5-ATG16 COMPLEX
Autophagy-related 17 (Atg17)	CG1347	36918	ATG1 PROTEIN KINASE COMPLEX
Autophagy-related 17 (Atg17)	CG1347	28061	AUTOPHAGY-RELATED GENES
Autophagy-related 18a (Atg 18a)	CG7986	34714	AUTOPHAGY-RELATED GENES
Autophagy-related 18a (Atg 18a)	CG7986	80430	AUTOPHAGY-RELATED GENES
Autophagy-related 18a (Atg 18a)	CG7986	80440	AUTOPHAGY-RELATED GENES
Autophagy-related 18a (Atg 18a)	CG7986	82954	AUTOPHAGY-RELATED GENES
Autophagy-related 18b (Atg18b)	CG8678	34715	AUTOPHAGY-RELATED GENES
Autophagy-related 101 (Atg101)	CG7053	34360	ATG1 PROTEIN KINASE COMPLEX
AMP-activated protein kinase α subunit (AMPKα)	CG3051	32371	CALCIUM/CALMODULIN-DEPENDENT PROTEIN KINASES
Phosphatidylinositol 3-kinase 59F (Pi3K59F)	CG5373	33384	PHOSPHATIDYLINOSITOL 3-KINASE COMPLEX
Phosphatidylinositol 3-kinase 59F (Pi3K59F)	CG5373	36056	PHOSPHATIDYLINOSITOL 3-KINASE COMPLEX
Phosphatidylinositol 3-kinase 59F (Pi3K59F)	CG5373	64011	PHOSPHATIDYLINOSITOL 3-KINASE COMPLEX
Synaptosomal-associated protein 29kDa (Snap 29)	CG11173	25862	Qbc-SNAREs

Synaptosomal-associated protein 29kDa (Snap 29)	CG11173	51893	Qbc-SNAREs
Syntaxin 17 (Syx17)	CG7452	25896	Qbc-SNAREs
Vacuolar H+-ATPase 55kD subunit (Vha55)	CG17369	40884	VACUOLAR ATPASE V1 DOMAIN NON-CATALYTIC SUBUNITS
Vacuolar protein sorting 15 (Vps 15)	CG9746	34092	PHOSPHATIDYLINOSITOL 3-KINASE COMPLEX
Vacuolar protein sorting 15 (Vps 15)	CG9746	35209	PHOSPHATIDYLINOSITOL 3-KINASE COMPLEX
Vacuolar protein sorting 15 (Vps 15)	CG9746	57011	PHOSPHATIDYLINOSITOL 3-KINASE COMPLEX
Vesicle-associated membrane protein 7 (Vamp 7)	CG1599	38300	R-SNAREs
Vesicle-associated membrane protein 7 (Vamp 7)	CG1599	43543	R-SNAREs

(Expresses wild type transcript under UAS control)

Gene name (symbol)	Annotation CG	BDSC Nº.	FlyBase Gene Group
Autophagy-related 1 (Atg1)	CG10967	51655	ATG1 PROTEIN KINASE COMPLEX
Autophagy-related 1 (Atg1)	CG10967	51654	ATG1 PROTEIN KINASE COMPLEX

(Expresses HA-tagged transcript under UAS control)

Gene name (symbol)	Annotation CG	BDSC Nº.	FlyBase Gene Group
Autophagy-related 1 (Atg1-HA)	CG10967	93405	ATG1 PROTEIN KINASE COMPLEX

(For expression of sgRNA by a Cas9-based transcriptional activator)

Gene name (symbol)	Annotation CG	BDSC Nº.	FlyBase Gene Group
Autophagy-related 16 (Atg16-TOE)	CG31033	78149	ATG12-ATG5-ATG16 COMPLEX
Sirtuin 4 (Sirt4-TOE)	CG3187	78741	SIRTUIN LYSINE DEACETYLASES-ADP-RIBOSYLTRANSFERASES

(Expresses full-length transcript tagged at the N-terminal end with three copies of FLAG under UAS control)

Gene name (symbol)	Annotation CG	BDSC Nº.	FlyBase Gene Group
Autophagy-related 17 (Atg17-FLAG)	CG1347	91226	ATG1 PROTEIN KINASE COMPLEX

(Glutathione metabolism-related genes)

Gene name (symbol)	Annotation CG	VDRC ID	FlyBase Gene Group
Glutathione S transferase D2 (GstD2)	CG4181	115817 - KK109123	CYTOSOLIC GLUTATHIONE S-TRANSFERASES/ PEROXIDASES
Glutathione S transferase D6 (GstD6)	CG4423	105805 - KK112104	CYTOSOLIC GLUTATHIONE S-TRANSFERASES
Glutathione S transferase D9 (GstD9)	CG10091	103798 - KK113031	CYTOSOLIC GLUTATHIONE S-TRANSFERASES
Glutathione S transferase D10 (GstD10)	CG18548	102760 - KK112359	CYTOSOLIC GLUTATHIONE S-TRANSFERASES

Table 4. List of oligonucleotides sequences for qPCR assays

Gene symbol	Forward Sequence (5'-3')	Reverse Sequence (5'-3')
Atg1	5'-GTCAGCCTGGTCATGGAGTAT-3'	5'-CGTCCCCTTGACACTCAGAT-3'
Atg2	5'-GGAGTGCATGAAGCAGGTTG-3'	5'-GAACTTCTCCAACCCAATCAGG-3'
Atg3	5'-CCAAGACAAAACCCTACCTACC-3'	5'-GCCGACGTATTCCATCTGCT-3'
Atg5	5'-GCCGAACACCAGGATGGAG-3'	5'-AGCAGATCGTATAGGACACCAAT-3'
Atg7	5'-CTACACGGCCTACAACAGTCC-3'	5'-GGCTGTCATCGATGTTCATTT-3'
Atg8a	5'-TTCATTGCAATCATGAAGTTCC-3'	5'-GGGAGCCTTCTCGACGAT-3'
Atg8b	5'-CATCCGCAAGCGTATCAATCT-3'	5'-CGATGTCGGTGGGATCACA-3'
Atg9	5'-TTCAACATTGACTTCATCTTGTTTC-3'	5'-CTGCCAATTGTTCTGGAAGG-3'
Atg12	5'-GCAGAGACACCAGAATCCCAG-3'	5'-GTGGCGTTCAGAAGGATACAAA-3'
β-actin	5'-CCAACCGCGAGAAGATGA-3'	5'-CCAGAGGCGTACAGGGATAG-3'
E75B	5'-CAACAGCAACAACACCCAGA-3'	5'-CAGATCGGCACATGGCTTT-3'
EcR	5'-GCAAGGGGTTCTTTCGACG-3'	5'-CGGCCAGGCACTTTTTCAG-3'
GlyT	5'-CTTCCGTGGCAGAATTGC-3'	5'--CCTGAGCGTACGAGAAGCA-3'
InR	5'-GCTGTCAAGCAAGCAGTGAA-3'	5'-TCTTTTTACCCGTCGTCTCC-3'
Jhamt	5'-ATTCGCATCGACCATGCAGT-3'	5'-GAAGTCCATGAGCACGTTACC-3'
phtm	5'-TAAAGGCCTTGGGCATGA-3'	5'-TTTGCCTCAGTATCGAAAAGC-3'
Ppl	5'-ATTCACCTGACAAGCCTTCTAGC-3'	5'-AGCTGGAGATGCCTACTATGG-3'
Thor/4E-BP	5'-GAAGGTTGTCATCTCGGATCC 3'	5'-ATGAAAGCCCGCTCGTAG-3'

Table 5. List of software tools and algorithms

Software	Version	Purpose
GraphPad	version 9.5.1	Statistical analysis and graphing software
IGV	version 2.16.0	Software for visualizing and analyzing genomic data
Illustrator	version 27.0	Graphic design software for creating vector graphics and illustrations
ImageJ	version 2.9.0	Image processing and analysis software used in scientific research
Keynote	version 13.2	Presentation software developed by Apple
Microsoft® Excel	version 16.78	Spreadsheet software for data organization, analysis, and visualization
Microsoft® Power Point	version 16.78	Presentation software for creating slideshows
Microsoft® Word	version 16.78	Word processing and document creation
Pages	version 13.2	Word processing and document layout software developed by Apple
Photoshop	version 27.0	Image editing and graphic design software
Python	version 3.12	General-purpose programming language
R studio	version 4.3.1	Programming language and environment for statistical computing and graphics
Terminal	version 2.14	Command-line interface (CLI) application for shell or command interpreter
Visual studio code	version: 1.81.1	Integrated development environment (IDE) for software development

Package/algorithm	Version	Purpose
AnnotationDbi	version 1.62.2	Annotation and querying of genomic data
apeglm	version 1.22.1	Adaptive shrinkage of log-fold changes
Biobase	version 2.60.0	Basic functions for bioinformatics data
BiocGenerics	version 0.46.0	Generic functions for Bioconductor
BiocManager	version 1.30.22	Management of Bioconductor packages
ComplexHeatmap	version 2.16.0	Creation of complex heatmaps for visualization of high-dimensional data
CorLevelPlot	version 0.99.0	Correlation matrix visualization
dendextend	version 1.17.1	Extending functionality for dendrogram objects
DESeq2	version 1.40.2	Differential expression analysis of RNA-seq data
dplyr	version 1.1.4	Data manipulation and transformation
dynamicTreeCut	version 1.63	Dynamic tree cutting algorithm for hierarchical clustering
GenomeInfoDb	version 1.36.4	Manipulation of genome annotation data
GenomicFeatures	version 1.52.2	Extraction and manipulation of genomic features
GenomicRanges	version 1.52.1	Representation and manipulation of genomic ranges
ggdendro	version 0.1.23	Extension for ggplot2 to create dendrograms
Ggplot2	version 3.4.4	Data visualization with grammar of graphics
ggplotify	version 0.1.2	Extension for ggplot2 graphics
ggrepel	version 0.9.4	Extension for ggplot2 to avoid overlapping text labels
ggVennDiagram	version 1.2.3	Venn diagrams with ggplot2
gridExtra	version 2.3	Extension package for grid graphics system
IRanges	version 2.34.1	Infrastructure for manipulating ranges of integers
kableExtra	version 1.4.0	Creation of complex tables in Markdown and HTML
knitr	version 1.45	Dynamic report generation with R
org.Dm.eg.db	version 3.17.0	Annotation package for Drosophila melanogaster
plotly	version 4.10.3	Creation of interactive and dynamic visualizations.
readxl	version 1.4.3	Reading Excel files into R
S4Vectors	version 0.38.2	Fundamental data structures for genomic data
stringr	version 1.5.1	String manipulation functions
tibble	version 3.2.1	Data frame extension with modern features
tidyr	version 1.3.0	Data manipulation with tidy data principles
tidyverse	version 2.0.0	Collection of packages for data manipulation and visualization
WGCNA	version 1.72-1	Weighted correlation network analysis for gene expression data

Table 6. List of candidates from first round of SLCs *in vivo* RNA[i] screening

Gene name (symbol)	Annotation CG	VDRC Nº.	FlyBase Gene Group
Adenine Nucleotide Translocase 2 (Ant2)	CG1683	v45177	SLC25: MITOCHONDRIAL TRANSPORTERS
Adenine Nucleotide Translocase 2 (Ant2)	CG1683	v45176	SLC25: MITOCHONDRIAL TRANSPORTERS
Chaski (Chk)	CG3409	v37139	SLC16: MONOCARBOXYLATE TRANSPORTERS
Dicarboxylate Carrier 4 (Dic4)	CG18363	v8416	SLC25: MITOCHONDRIAL TRANSPORTERS
Fatty Acid Transport Protein 2 (Fatp2)	CG44252	v3528	SLC27: FATTY ACID TRANSPORTERS
Fear-Of-Intimacy (Foi)	CG6817	v10102	SLC39: ZINC ION TRANSPORTERS
Glycine Transporter (Glyt)	CG5549	v330127	SLC6: NA+/CL- NEUROTRANSMITTER TRANSPORTERS
Mitochondrial Phosphate Carrier Protein 2 (Mpcp2)	CG4994	v8366	SLC25: MITOCHONDRIAL TRANSPORTERS
Mitochondrial Phosphate Carrier Protein 2 (Mpcp2)	CG4994	v101316	SLC25: MITOCHONDRIAL TRANSPORTERS
Organic Anion Transporting Polypeptide 33ea (Oatp33ea)	CG5427	v45896	SLC21: ORGANIC ANION TRANSPORTING POLYPEPTIDES
Organic Cation Transporter (Orct)	CG6331	v6782	SLC22: ORGANIC IONS TRANSPORTERS
Pippin (Pippin)	CG4797	v10598	SLC2: HEXOSE SUGAR TRANSPORTERS
Sodium-Dependent Multivitamin Transporter (Smvt)	CG2191	v40650	SLC5: Na+/GLUCOSE CO-TRANSPORTER TRANSPORTERS
Sodium-Dependent Multivitamin Transporter (Smvt)	CG2191	v102662	SLC5: Na+/GLUCOSE CO-TRANSPORTER TRANSPORTERS
Stress-Sensitive B (Sesb)	CG16944	v104576	SLC25: MITOCHONDRIAL TRANSPORTERS
Stress-Sensitive B (Sesb)	CG16944	v11968	SLC25: MITOCHONDRIAL TRANSPORTERS
Stress-Sensitive B (Sesb)	CG16944	v48582	SLC25: MITOCHONDRIAL TRANSPORTERS
Stress-Sensitive B (Sesb)	CG16944	v48581	SLC25: MITOCHONDRIAL TRANSPORTERS
Uncharacterized Protein (CG10486)	CG10486	v5045	SLC22: ORGANIC IONS TRANSPORTERS
Uncharacterized Protein (CG10804)	CG10804	v30226	SLC6: NA+/CL- NEUROTRANSMITTER TRANSPORTERS
Uncharacterized Protein (CG13743)	CG13743	v110773	SLC38: Na+-COUPLED AMINO ACID TRANSPORTERS
Uncharacterized Protein (CG14856)	CG14856	v5875	SLC22: ORGANIC IONS TRANSPORTERS
Uncharacterized Protein (CG3168)	CG3168	v48011	SLC22: ORGANIC IONS TRANSPORTERS
Uncharacterized Protein (CG3168)	CG3168	v48010	SLC22: ORGANIC IONS TRANSPORTERS
Uncharacterized Protein (CG6006)	CG6006	v106513	SLC22: ORGANIC IONS TRANSPORTERS
Uncharacterized Protein (CG6231)	CG6231	v42655	SLC22: ORGANIC IONS TRANSPORTERS
Uncharacterized Protein (CG6356)	CG6356	v101866	SLC22: ORGANIC IONS TRANSPORTERS
Uncharacterized Protein (CG7084)	CG7084	v35677	SLC22: ORGANIC IONS TRANSPORTERS
Uncharacterized Protein (CG7084)	CG7084	v12163	SLC22: ORGANIC IONS TRANSPORTERS
Uncharacterized Protein (CG9864)	CG9864	v103970	SLC17: ORGANIC ANION TRANSPORTERS
Uncoupling Protein 4b (Ucp4b)	CG18340	v33128	SLC25: MITOCHONDRIAL TRANSPORTERS
Zinc Transporter 86d (Znt86d)	CG6672	v107388	SLC30: ZINC TRANSPORTERS

Table 7. Last set of candidates from SLCs *in vivo* RNA[i] screening and human orthologs

Gene name (symbol)	Annotation CG	SLC Family ID	Human Ortholog gene name (symbol)
Glycine Transporter (GlyT)	CG5549	SLC6	Glycine transporter 2 (GlyT)
Uncharacterized Protein (CG10804)	CG10804	SLC6	Inactive sodium-dependent neutral amino acid transporter (B0AT3)
Organic Cation Transporter (Orct)	CG6331	SLC22	Organic cationic transporter-like 3 (OCTL3)
Uncharacterized Protein (CG3168)	CG3168	SLC22	Synaptic vesicle glycoprotein 2B (SV2B)
Uncharacterized Protein (CG3168)	CG3168	SLC22	Synaptic vesicle glycoprotein 2B (SV2B)
Adenine Nucleotide Translocase 2 (Ant2)	CG1683	SLC25	ADP/ATP carrier protein 3 (AAC3)
Adenine Nucleotide Translocase 2 (Ant2)	CG1683	SLC25	ADP/ATP carrier protein 3 (AAC3)
Dicarboxylate Carrier 4 (Dic4)	CG18363	SLC25	Mitochondrial dicarboxylate carrier (DIC)
Mitochondrial Phosphate Carrier Protein 2 (Mpcp2)	CG4994	SLC25	Phosphate carrier protein, mitochondrial (PiC)
Mitochondrial Phosphate Carrier Protein 2 (Mpcp2)	CG4994	SLC25	Phosphate carrier protein, mitochondrial (PiC)
Stress-Sensitive B (Sesb)	CG16944	SLC25	Adenine nucleotide translocator 1 (ANT1)
Stress-Sensitive B (Sesb)	CG16944	SLC25	Adenine nucleotide translocator 1 (ANT1)
Stress-Sensitive B (Sesb)	CG16944	SLC25	Adenine nucleotide translocator 1 (ANT1)
Stress-Sensitive B (Sesb)	CG16944	SLC25	Adenine nucleotide translocator 1 (ANT1)
Fatty Acid Transport Protein 2 (Fatp2)	CG44252	SLC27	Fatty acid transport protein 4 (FATP4)
Zinc Transporter 86d (Znt86d)	CG6672	SLC30	Zinc transporter 7 (ZnT-7)
Uncharacterized Protein (CG13743)	CG13743	SLC38	Putative sodium-coupled neutral amino acid transporter 11 (AVT2)
Fear-Of-Intimacy (Foi)	CG6817	SLC39	Zinc transporter protein 10 (ZIP10)

5.   Results

5.1. In vivo RNA[i] Screening of Solute Carriers Superfamily Identifies New Candidates Linking Sexual Development and Micronutrient Supply

Prior studies have investigated the involvement of lipid transporters and lipid sensing in steroid hormone signaling and the initiation of sexual maturation (Ahmed et al., 2009, Rosenfield et al., 2009, Juarez-Carreño et al., 2021, Anderson et al., 2024). Meanwhile, the function of other small molecules such as vitamins, sugar, organic cations and anions, metals, and amino acids among other micronutrients, required for a complete comprehension of the mechanisms underlying the acquisition of sexual capacities in multicellular organisms, remains unclear. In order to comprehend how micronutrients and small molecules influence the function of endocrine steroidogenic cells and the initiation of sexual maturation in *Drosophila melanogaster*, which may have implications for other animals including mammals, we conducted an extensive RNA[i]-based *in vivo* screening. This screening aims to focus on the primary cell type responsible for neuroendocrine regulation within the Ring Gland (RG); the Prothoracic Gland (PG) cells. To tackle this issue, we utilized the *Drosophila* RNA[i] library (Dietzl et al., 2007, Ni et al., 2011) to reduce the expression of available SLCs genes.

The list of 287 evaluated genes in this study (Table 1) comprises 578 RNA[i] transgenic lines that represents most of the solute membrane transporters found in PG cells. The UAS-GAL4 genetic system (Brand & Perrimon, 1993) was applied to evaluate the effect of those RNA[i] transgenic lines in a tissue-specific manner. Generally, about 10-15 UAS-RNA[i] males, the transgene carriers, were crossed with 10-15 *phtm*[22]-GAL4 virgin females and kept at 25ºC in standard "Iberian" fly food.

The most common GAL4 driver for targeting PG cells is the gene "*Phantom*" (*phtm*), one of the so-called Halloween genes. The Halloween genes, particularly "*Spook*" (*spo*) and *phtm* play vital roles in Ecdysteroid biosynthesis (Niwa et al., 2004, Warren et al., 2004). In *Drosophila*, the temporal and spatial expression of these genes has been analyzed in early-to-late larval stages and adults, showing a correlation between circulating Ecdysteroid levels and *spo* and *phtm* expression profiles (Rewitz et al., 2006). Thus, using the gene *phtm* as a GAL4 driver ensures precise tissue specificity for expressing each RNA[i] transgene in PG cells.

Once the parameters of this *in vivo* screening have been established, the first filial generation (F1), resulting from the initial cross, was assessed to determine whether a given RNA[i] transgene has an effect over the function of endocrine steroidogenic cells based on the outcoming phenotype. To determine what we would consider a phenotype of phenotype of interest, we proposed the following main criteria: i) the F1 larvae should neither undergo metamorphosis nor exhibit a wandering behavior, so the absence of pupariation would be the main feature for the fulfillment of these criteria; ii) the F1 larvae should not be able to control body size; iii) the F1 larvae should exhibit a sustained feeding behavior.

A representative image of what would be considered a phenotype of interest can be seen in Image 1. Following these initial criteria, we identified the first set of 24 candidate genes outlined in Table 6. Subsequently, genes lacking a known ortholog for *Homo sapiens* were excluded from further analysis to facilitate an eventual translational approach. Therefore, we end up having a list of 12 main candidates for which we conducted further phenotypical analysis. The lists of 12 candidates and their human ortholog genes are included in Table 7.

A schematic overview of both the main neuroendocrine tissue of study and GAL4-UAS system utilized for screening are presented in Figure 8A. Primary steps of the screening process including the initial number of genes assessed and the final selected candidate are represented in Figure 8B. The main candidate of study, which would be the nucleus of this work, is the RNA[i] line SH330127 from the VDRC fly stock center, targeting RNA interference for the transcription product of *Drosophila melanogaster* Glycine Transporter (*GlyT*) gene.
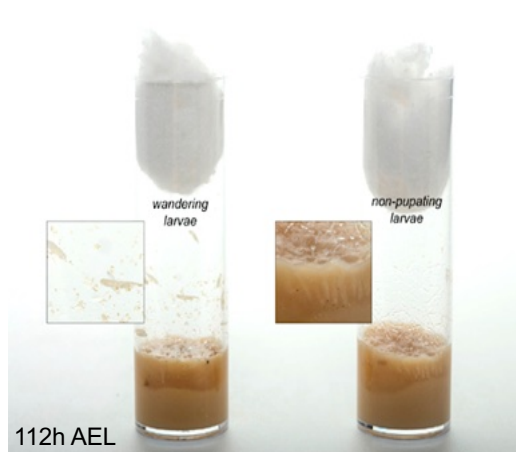
Image 1. Representative image of larval phenotype of interest. On the left, control larvae advance in development to the wandering stage (L3W). On the right, third instar larvae that maintain feeding behavior (L3F) and are unable to exit the food. Zoom of both described situations are shown for left and right insets respectively. Images were taken at 112 hours after egg laying (AEL).
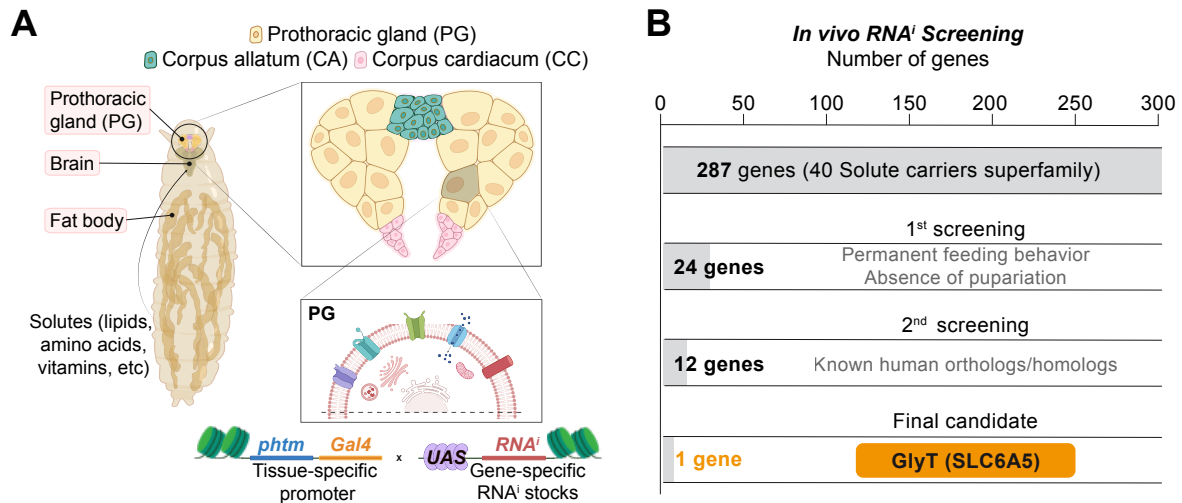
Figure 8. Schematic representation of in vivo RNAi screening. Overview of Drosophila melanogaster larva, main neuroendocrine tissues of study and major steps for in vivo RNAi screening procedure. A) Drawing of a Drosophila melanogaster third instar larva in which the fat body is represented occupying the interior of the larva as well as the main nutritional signals that come from this tissue. In the anterior part of the larva, the Ring gland is noted. Additionally, a zoom in on the Ring gland tissue shows the three main cell populations in this gland: Corpus Allatum (CA), Corpora Cardiaca (CC) and Prothoracic Gland (PG). For the latter, the PG presents in zoom the scheme of use of the UAS-GAL4 genetic system used for this screening with Phantom (*phtm*) as the driver gene. B) Two major rounds of screening are represented with 24 and 12 candidate genes, respectively, towards the selection of the final candidate, Glycine Transporter (SH330127).

The following details elaborate on the supplementary criteria and phenotype assays employed to further narrow down the list of 12 candidates highlighted in Table 7, leading to the ultimate selection of *GlyT* as a main candidate to study. Additionally, it provides insights into the exclusion of certain candidates based on their inherent characteristics and established functionalities.

Since the first two initial screening conditions were based on the inability of F1 to pupate, and on F1 larvae maintaining a permanent L3F feeding behavior, we wanted to be able to exclude phenotypes that were showing just a developmental delay or larval death due to exhaustion or medium contamination, for a better categorization of a strict developmental arrest situation.

To test this issue, serial vial transfers were performed. F1 larvae from primary crosses at around 200h AEL were relocated from the original vial to fresh vials containing standard "Iberian" food, where the larvae should continue feeding permanently without exiting the food and thus increasing in body size and weight. This, in turn, would lead to obese phenotype as a result of a total developmental arrest in which they would never turn off their active feeding behavior thus never leaving the food (Image 1). This first phenotypical review ruled out all RNA[i] lines for the initial candidates Adenine Nucleotide Translocase 2 (Ant2), Dicarboxylate Carrier 4 (Dic4), Organic Cation Transporter (Orct), Zinc Transporter 86d (Znt86d), and Uncharacterized Protein (CG10804).

Furthermore, we wanted to ensure that the phenotype penetrance of selected candidates was close to a 100% to make sure that each of the tested genes comprises, in fact, an essential component for the proper functioning of neuroendocrine circuits over the onset of sexual maturation. To address this, a series of sequential crosses were systematically conducted just to note phenotypical consistencies. As a result of these series of extra assessments, several candidates were excluded from further consideration due to inconsistencies in their phenotypical profiles. Specifically, Fear-Of-Intimacy (Foi), Mitochondrial Phosphate Carrier Protein 2 (Mpcp2), which predominantly governs mitochondrial transport, Uncharacterized Protein (CG13743), Uncharacterized Protein (CG3168), and Stress-Sensitive B (SesB), were among those disregarded.

In alignment with the main aim of our screening process, which emphasizes the role of small molecules and micronutrients, the decision was made to exclude Fatty Acid Transport Protein 2 (Fatp2) given its known association with lipid transport pathways, even though it came out with a phenotype of interest in both this screening and previous ones made in the laboratory.

After all these extra requirements and phenotypical assessments, we end up selecting our main SLC candidate, GlyT (SLC6A5) due to its 100% of phenotype penetrance and consistency in L3 active feeding behavior.

The phenotype of GlyT ablated individuals in PG cells, as well as further local and systemic characterizations, will be detailed in next sections.

5.2. Glycine Transporter Ablation in PG Cells is Specific and Provokes Juvenile-to-Adult Transition Impairment

Upon reaching this stage and guided by the aforementioned criteria, the Glycine Transporter (GlyT) has emerged as the most promising candidate requiring thorough scrutiny and meticulous phenotype characterization. It is important to highlight that the RNA[i] line SH330127 from the VDRC fly stock center, targeting RNA interference for the transcription product of *Drosophila melanogaster* Glycine Transporter (*GlyT*) gene, has been selected as the primary subject of investigation for this thesis project (Figure 9).

The comparisons (N>50 crosses) of *phtm>GlyT[i]* and control *phtm>* individuals throughout their whole juvenile-to-adult transition are shown by time lapse photographs in Figure 9A-B. To confirm that the observed effect of *phtm>GlyT[i]* was purely associated with the GlyT interfering line (SH330127), we crossed again GlyT[i] substituting the PG phtmGAL4 driver for *spook*, another PG specific driver gene, using the same UAS-GAL4 system, obtaining the same phenotype as in the case from *phtm>GlyT[i]* individuals (Figure 9C.I). Similarly, other drivers were used to rule out similar off-target effect in other tissues: eyeless (*ey*) for imaginal eye disc (Figure 9C.II) and *Aug21* for CA (Figure 9C.III), obtaining a control-like phenotype. Likewise, thanks to the guides for Cas9-directed expression of GlyT (TRiP; Transgenic RNAi project at Harvard Medical School) we proved that the reestablishment of GlyT expression in the PG cells was sufficient to return the expression of GlyT and thereby to rescue the phenotype caused by *phtm>GlyT[i]* (Figure 9C.IV). Additionally, blocking GlyT expression with a second construct, GlyT[-KO], mimics the phenotype of *phtm>GlyT[i]* phenotype (Figure 9C.V).

Importantly, we aimed to conduct a direct local approach to prove the effective reduction of GlyT expression in PG cells provoked by *phtm>GlyT[i]*. First of all, since *phtm* is barely express in brain compared to PG cell population within the ring gland (RG), and because RG is a complicated tissue to isolate given its nature and size, we wanted to prove that we were actually able to specifically isolate RGs from L3 individuals. To facilitate accurate isolation of RG tissue, we took advantage again of phtmGAL4 driver linked to the *mCD8::GFP* marker (Figure 9D). By doing so, we have proved almost absent mRNA levels of *phtm* in brain relative to RG samples by qPCR (Figure 9E). Then, a significant reduction of *GlyT* mRNA levels in RG was confirmed in *phtm>GlyT[i]* relative to control *phtm>* RG samples (Figure 9F), demonstrating both precise RG-isolation protocol (Palomino-Schätzlein et al., 2022) and a proper RNA[i] performance of the line SH330127 for targeted GlyT ablation.
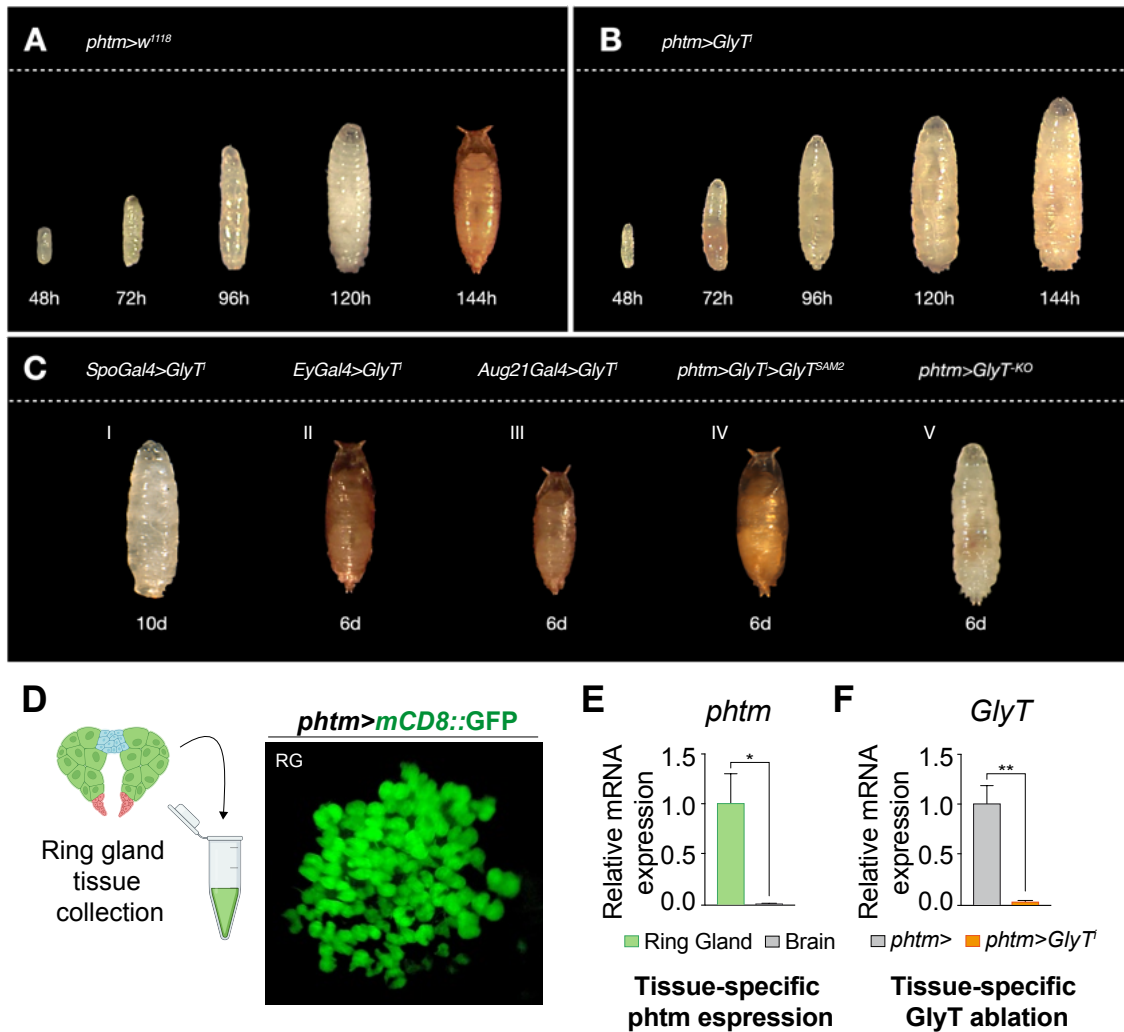
Figure 9. Phenotypic, genetic and transcriptomic checks of expression and specificity for *phtm>GlyT^i* individuals and their controls. A) Larval and pupa images showing the whole juvenile-to-adult transition phenotype of control *phtm>white*[1118] individuals from 48 to 144 hours after egg laying (AEL). B) Larval images showing the whole juvenile-to-adult transition phenotype of *phtm>GlyT^i* individuals from 48 to 144 hours after egg laying (AEL). C) Additional alternative drivers; spo(I), ey(II) and Aug21(III). And rescue of the phenotype by overexpression of GlyT(IV) and phenotype replication by GlyT ablation (V), from left to right respectively. Representative larvae are shown (n=10). D) Schematic presentation and real view of mCD8::GFP positive ring glands of control individuals. E) qPCR for *phtm* expression showing an almost absent expression of *phtm* in brain sample relative to ring gland tissue. F) qPCR for *GlyT* expression showing an effective reduction in expression of *GlyT* in *phtm>GlyT^i* ring gland tissues relative to control ring gland samples. All data are presented as mean ± standard error of the mean (SEM), *p ≤ 0.05, **p ≤ 0.01.

5.3. Glycine Transporter Ablation in PG Cells Prevents Ecdysone Secretion and Signaling

Ecdysone is synthesized and secreted primarily by the PG cells and is known to act as a master regulator of developmental transitions such as molting and metamorphosis. The dynamic regulation of ecdysone levels is characterized by distinct peaks of hormone secretion that coincide with key developmental transitions and life cycle stages (Figure 4) , including larval molting, pupation, and adult hatching (Fraenkel, G. 1935, Riddiford et al., 2010).

The transition towards metamorphosis and sexual maturation is intricately intertwined with nutritional availability. Hence, once 'critical weight' threshold (CW; Nijhout and Williams, 1974) is surpassed, a subtle release of the steroid prohormone ecdysone from the PG cells is triggered. This is commonly referred to as the 'commitment' pulse (Berreur et al., 1979). As a consequence, and approximately two days later, another surge of ecdysone occurs, acting as the catalyst for pivotal behavioral changes such as cessation of feeding, initiation of wandering behavior, and transition into the pupal stage (Fletcher & Thummel 1995, Yamanaka et al., 2013).

Thus, upon confirming that our individuals fail to pupate in any case, we aimed to prove that the observed phenotype was exclusively due to an effect associated with poor PG function. To address this, we conducted a classic experiment in the field in which animals are supplemented in the diet with the active form of the hormone ecdysone (20E), right before the commitment peak, to mimic the 20E peak that is schematically represented in left condition (phtm>) of Figure 10A. As we were expecting, 20E treatment managed to rescue the wild type-pupating phenotype in *phtm>GlyT^i* non-pupating larvae, so demonstrating active functional sensitivity to the circulant hormone by major target tissues at a systemic level (Figure 10B).

Additionally, we wanted to demonstrate that *phtm>GlyT^i* larvae fail to produce and release ecdysone from PG cells by measuring titers of the active hormone, 20E, using an whole-larvae enzymatic immunoassay (ELISA). Consistently, we observed that the peak of 20E typically found in control animals at 96 and 120 hours AEL, was virtually absent in *phtm>GlyT^i* at indicated time points (Figure 10C).

In the described scenario, in which the hormone ecdysone is not being released anymore in *phtm>GlyT^i* larvae, its peripheral target tissues should not be able to receive neither respond to any endogenous signal. For further evaluation of ecdysone peripheral signals in *phtm>GlyT^i* animals, we analyzed its systemic responses by measuring the mRNA expression levels of ecdysone signaling pathway main components; its receptor (EcR) and its main effector (E75), through whole larval qPCR at 120 hours AEL. Hence, demonstrating that the expression of E75 effector remain absent, as well as that of its principal receptor EcR in *phtm>GlyT^i* animals, relative to control *phtm>* individuals ([Figure 10](#)D).
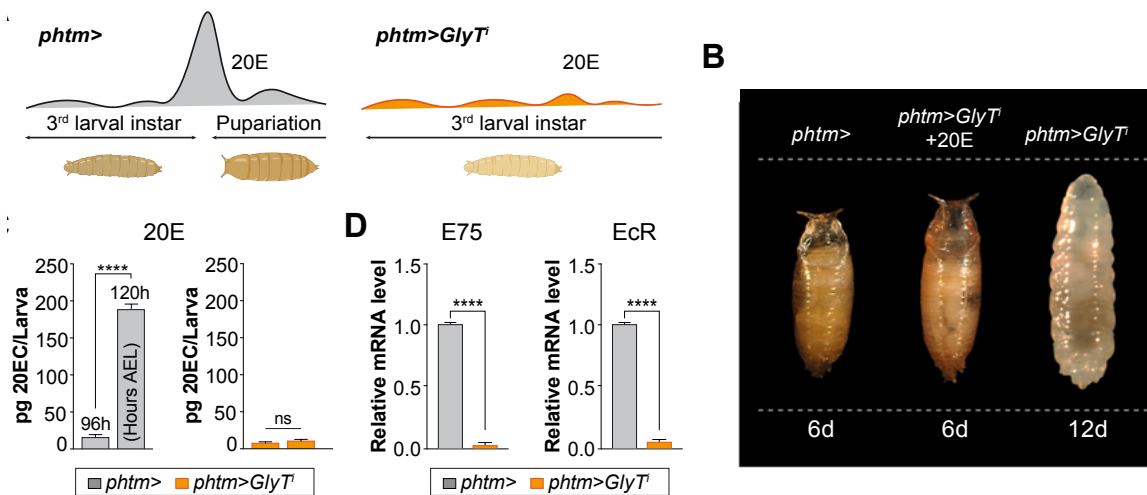
Figure 10. Ecdysteroid levels and signaling in control and PG GlyT ablated animals. A) Schematic overview of 20E peak, typically observed at third larval instar, causing pupariation initiation in control but absent in *phtm>GlyT^i* animals. B) Additional peak of 20E by dietary supplementation rescues the *phtm>GlyT^i* phenotype. C) Measurement of systemic 20E by ELISA assay in control and *phtm>GlyT^i* at 96 and 120 hours AEL. D) mRNA relative quantification of main effector (left) and receptor (right) of ecdysone signaling pathway in control and *phtm>GlyT^i* at 120 hours AEL. All data are presented as mean ± standard error of the mean (SEM), ****p < 0.0001, ns for non-significant. Representative larvae are shown (n=10).

5.4. Glycine Transporter Ablation Disrupts Active Secretion Pathways in PG Cells

From previous work, the fact that ecdysone secretion relies on an active transport mechanism, which entails the formation of exocytosis transport vesicles in PG cells, is well stablished (Yamanaka et al., 2015). Without this crucial active transport of ecdysone, even if synthetized, the hormone would remain trapped within PG cells in vesicles. Hence, its most visible actions as a pupariation promoter at the end of L3 larvae, will be prevent likely leading to developmental arrest at this instar.

For a better evaluation of the PG cells fitness in *phtm>GlyT*^{i} individuals, we conducted super-resolution imaging of brain-RG complexes, to be able to visually focus on the integrity of PG secretory pathways, using a secreted GFP protein construct (SecGFP; Entchev et al., 2000) in both *phtm>GlyT*^{i} and control individuals.

In *phtm>* control subjects, the SecGFP signal effectively co-localizes with the cell membrane (Figure 11A, left panel), in line with our understanding of the process at the developmental stage under assessment (120 hours AEL). At this juncture, PG cells actively release ecdysone into the hemolymph upon triggering of the 'commitment' pulse (Berreur et al., 1979). Notably, the cortical distribution of vesicles in control PG cells (Figure 11A, left panel insets) indicates the robust activity of secretory pathways, consistent with prior knowledge. In contrast, PG cells from in *phtm>GlyT*^{i} individuals exhibit cytoplasmic SecGFP positive vesicle accumulation, suggesting a deficiency in active transport processes (Figure 11A, right panel insets). Consequently, we demonstrated that PG cells in in *phtm>GlyT*^{i} individuals fail to secrete ecdysone, corroborated by cytoplasmic GFP quantification (Figure 11B) and in line with the absence of enzymatic detection of its active form in peripheral tissues by ELISA (Figure 10C).

A reliable proxy for cellular maturation according to transcriptional activity is the measurement of the nuclear-to-cytoplasmic ratio (N:C ratio), particularly in oncology and hematology, disciplines in which this parameter is currently taken into account clinically for diagnosis and monitoring diseases (Zhang et al., 2024, Gupta et al., 2024, Lee et al., 2024). As can be seen in PG cell images of *phtm>GlyT*^{i} (Figure 11A, right panel and Figure 11C, right panel), nuclei assume a horseshoe shape and their physical boundaries can be challenging to interpret. This condition and its potential causes will be further discussed later in the discussion section.

Thus, given the mentioned nuclei particularities of PG cells in *phtm>GlyT^i* individuals, it became highly recommended for N:C ratio measuring, to properly label nuclear boundaries of PG cells, in order to avoid misleading measurements in nuclear size quantifications. Since the nuclear envelope is mostly cover by nucleoporins, we took advantage of the MAB-414 primary antibody, which specifically labels nuclear pore complex proteins, to accurately define nuclear membrane limits (Figure 11C). Consequently, precise measurements of cell (Figure 11D left), and nuclear size (not shown) were obtained, allowing reliable calculation of N:C ratios in both *phtm>GlyT^i* and control samples (Figure 11D right). After those quantifications, and due to the PG cell size reduction in *phtm>GlyT^i* (Figure 11D left), we have proved a significant increase in the N:C ratio of *phtm>GlyT^i* PG cells when compared to *phtm>* control images at the same time point (Figure 11D right). Finally, the theoretical progression linking the N:C ratio to the maturation level of a given cell, is depicted in the scheme of Figure 11E.
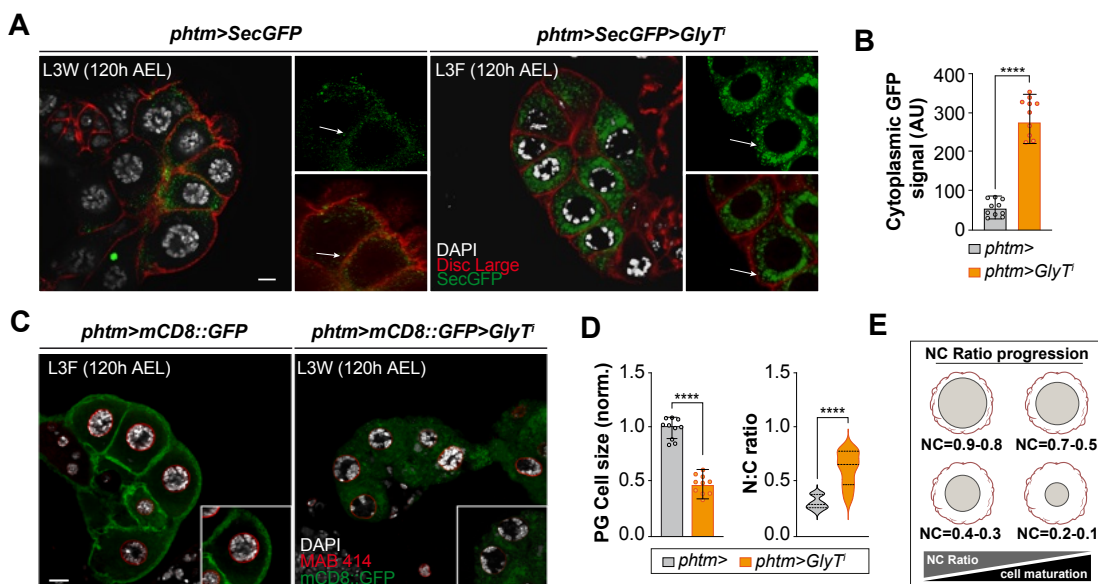
Figure 11. Secretion pathways imaging and nuclear to cytoplasmic ratio in GlyT ablated PG cells. A) Imaging of *phtm>GlyT^i* and control animals PG cells with SecGFP construction at 120 hours AEL. B) Cytoplasmic GFP signal quantification of *phtm>GlyT^i* and controls PG cells at same conditions of A. C) Imaging of *phtm>GlyT^i* and control animals PG cells with mCD8::GFP marker and MAB-414 nuclear labeling at 120 hours AEL. D) PG cell size quantification and N:C ratio for both *phtm>GlyT^i* and control animals at same conditions of C. E) Schematic representation of inverse progression for N:C ratio against cell maturation. Measures in arbitrary units (AU). All data are presented as mean ± standard error of the mean (SEM), ****p ≤ 0.0001. Scale bars = 10µm.

5.5.   Defective Nutrient Sensing in GlyT-Ablated non-pupating Individuals Leads to Obese Phenotype

So far, during the characterization of the phenotype of *phtm>GlyT^i* individuals, we observed a clear disruption in the endocrine system as a result of reduced glycine transporter expression in the PG cells. This impairment in the functionality of neuroendocrine control centers hinders the animals from progressing throughout the normal stages of development ([Figure 9](#)A-B). As a consequence, *phtm>GlyT^i* individuals are unable to achieve juvenile-to-adult transition. This developmental arrest, which is hormonally dependent, occurs during the final stage of larval development, the third larval instar (L3). Specifically, the feeding phase (L3F), extends until death without progressing to the subsequent wandering stage (L3W), which would lead to the abandonment of food and hydration sources and ultimately the formation of the pupa. Notably, the primary criteria established for *in vivo* RNA^i screening of the SLC superfamily seems to be strictly met in the case of *phtm>GlyT^i* individuals.

Furthermore, we can confidently infer that *phtm>GlyT^i* larvae are either unable to detect their nutritional status, or incapable of responding appropriately to it. In other words, these individuals fail to integrate nutritional signals with the functioning of the neuroendocrine axis. Therefore, even though having surpassed their critical weight, this is insufficient to trigger neither the onset of the wandering phase nor metamorphosis.

Considering precise measurements of the body condition of these individuals, we observed that, as a consequence of the arrest in L3F, *phtm>GlyT^i* larvae exhibit a notable obese phenotype characterized by significant weight gain ([Figure 12](#)A-B) and larval volume increase ([Figure 12](#)C) relative to control individuals. In both cases, body weight and volume experiment an increasing trend but, even after 10 days (240 hours AEL), *phtm>GlyT^i* animals still show a clear feeding behavior and so keep growing. Meanwhile, control subjects stop gaining body weight and volume since they transition to the L3W instar at around 112 hours AEL abandoning the food to find a pupation location.

Moreover, we wanted to assess the condition of fat body (FB) tissue, the primary organ for lipid storage and a crucial center for metabolic regulation, that shares many functionalities with mammalian liver. It is important to note that any genetic manipulation was made in FB. Thus, any observable effect will be a consequence of distal GlyT ablation in PG cells.

Nile Red staining, a compound that binds to lipids for their labeling and visualization, allowed us to demonstrate a significant increase in the red signal of lipid droplets in the FB of *phtm>GlyT^i* individuals, due to excessive lipid accumulation within lipid droplets (Figure 12D). Additionally, both the Nile Red signal (Figure 12E, left plot) and the size of lipid droplets (Figure 12E, right plot) increase significantly in *phtm>GlyT^i* animals when compared to their controls.
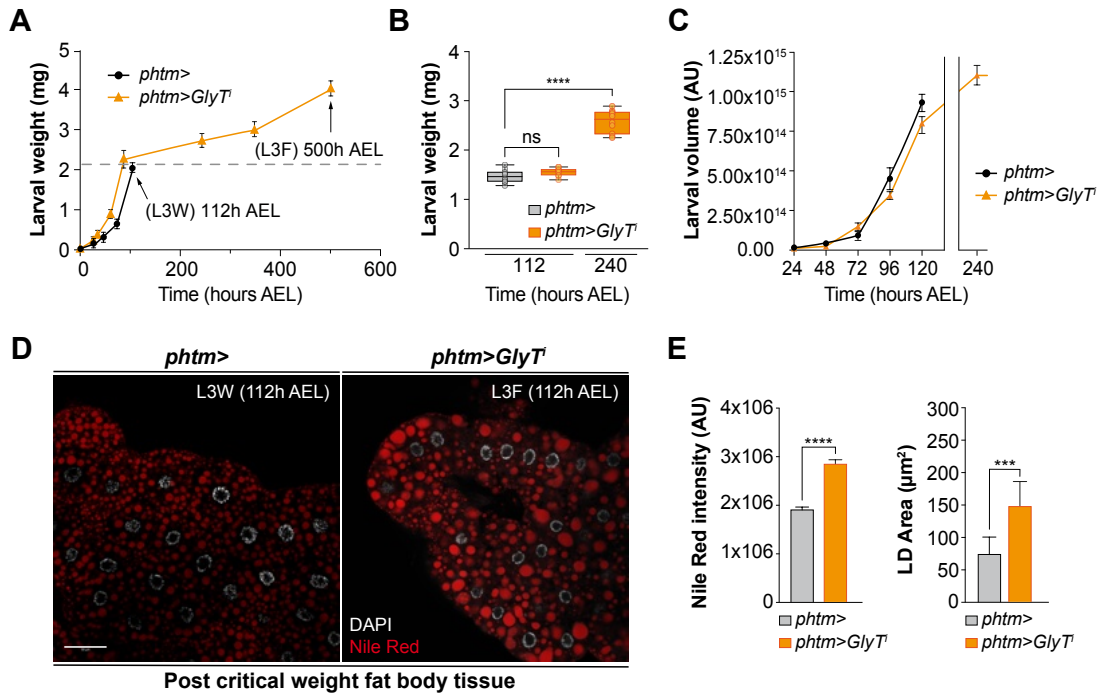
Figure 12. Body weight, larval volume and fat body measurements. A) Larval weight measurements in *phtm>* (control) and *phtm>GlyT^i* individuals from 24 to 112 hours AEL and from 24 to 500 hours AEL, respectively. B) Statistical comparison of larval weight at 112 hours AEL in controls and 112 to 240 hours AEL in *phtm>GlyT^i* C) Larval volume measurements from 20 to 112 hours AEL in controls and from 24 to 240 hours AEL in *phtm>GlyT^i*. D) Fat body post-critical weight imaging at 112 hours AEL in both control and *phtm>GlyT^i* individuals. E) Lipid droplets Nile red intensity (left plot) and area (right panel) quantifications in both control and *phtm>GlyT^i* individuals. Measures are in milligrams (mg), arbitrary units (AU) and square microns (μm^2). All data are presented as mean ± standard error of the mean (SEM), ****$p \leq 0.0001$, ***$p \leq 0.001$, ns for non-significant. Scale bars = 50μm.

5.6. Transcriptomic Profiling of 120h PG-GlyT Ablated Animals Reveals Common Patterns with pre-CW 72h Controls

In addition to the large genetic manipulation toolbox available in *Drosophila melanogaster*, a significant advantage of using this model organism in neuroendocrinology research is the possibility to conduct next-generation sequencing (NGS) studies on the entire organism. Due to their size and nearly homogeneous texture, larvae can be fully sequenced, preserving the complete mRNA sets that articulate inter-organ interaction mechanisms. This allows for obtaining a comprehensive transcriptomic profile, which is particularly useful for analyzing the distal effects of single-gene manipulation in a specific tissue or cell population. Furthermore, we can evaluate the transcriptional dynamics that the presence or absence of circulating hormones cause throughout the juvenile organism without the potential bias of isolating the consequences in a single organ or tissue.

Since hormones can affect numerous tissues of the organism at the same time, as well as to modulate important behavioral changes, we wanted to conduct whole larva RNA-seq studies to evaluate both the dynamics in the transcriptomic profiles during the juvenile-to-adult transition in controls, as well as the systemic consequences of an absent or aberrant transition in individuals in which GlyT has been ablated only in the neuroendocrine PG cell population. Hence, the three conditions included in this first study were: i) control individuals prior to reaching the CW (*phtm*> 72 hours AEL) representing the strict juvenile stage, ii) control individuals after reaching the CW, in which the behavioral decision to activate L3W behavior has already been made and the neuroendocrine circuits are fully activated (*phtm*> 120 hours AEL) and iii) the GlyT ablated individuals, in which the developmental progression should take place exclusively without the presence of the glycine transporter (*phtm*>*GlyT^i* 120 hours AEL) in this transition-directing tissue (PG cells).

The initial results of the principal component analysis (PCA) reveal a clear trend in which the *phtm*>*GlyT^i* samples cluster closely with the *phtm*> 72h juvenile control samples, despite being individuals at 120 hours of development (Figure 13A). *A priori*, this suggests a juvenile-like state in the transcriptomic profiles of *phtm*>*GlyT^i*, which appears to be of interest.

However, to assess the robustness of our data, we first wanted to compare the control groups at the indicated time points (72 and 120 hours AEL) to corroborate that the dynamics previously described in the literature regarding the changes occurring during the juvenile-adult transition in *Drosophila* were accurately represented in our analyses (Gilbert et al., 2002), Warren et al., 2004, Niwa et al., 2004, Singh et al., 2009, Texada et al., 2019, Pan et al., 2019). According to this, the transcriptomic profiles of 72h and 120h control samples followed a proper clustering in the heatmap representation, displaying classical patterns of a proper transition and hormonal activation (Figure 13B). For instance, we observe upregulation of ecdysone pathway-related genes such as *sad*, *spo*, *phtm*, and *EcR* in *phtm*>120h samples compared to their *phtm*>72h controls. In addition to the overexpression of these *Halloween genes*, and consistent with what was previously described (Texada et al., 2019), in the 120h control condition we find genes characteristic of a starvation situation, typical of the L3W condition where nutritional resources are abandoned. Among other functions, the autophagy pathway is responsible for mobilizing the nutrients necessary for pupal construction once an appropriate spot has been located during the larval wandering phase. Accordingly, we observe a significant upregulation of some characteristic genes of this pathway (*Atgs*) in the *phtm*>120h condition (Figure 13B, in black letters). In contrast, in the *phtm*>72h juvenile control condition, what we see is a clear upregulation of the glutathione metabolism pathway, as a consequence of the high active feeding, which is natural characteristic of 72h larval instar behavior (Figure 13B, in blue letters).

Normalization in transcripts per million (TPM) allows us to visualize and compare the total expression levels for a gene between conditions. By including *phtm*>*GlyT^i* condition to the comparisons between controls already described, we can see how the dynamics during the control transition from 72h to 120h in the panel described in Figure 13B are not seen in the case of *phtm*>*GlyT^i* (Figure 13C), which profiles remain to be more similar to a juvenile stage in accordance with the PCA (Figure 13A). In this way, both the expression of characteristic genes of the ecdysone pathway, as well as those involved in autophagy and glutathione metabolism, are similar between juvenile control organisms at 72h and *phtm*>*GlyT^i* organisms at 120h, suggesting again a clear arrest in development despite their age and size. Representation of the differential expression (DE) profiles of this triple comparison in the Heatmap (Figure 13D), and the Fold change DE representation of *phtm*>*GlyT^i* compared to the control *phtm*>120h by MA plot (Figure 13E), showed also a clear trend of *phtm*>*GlyT^i* 120h to follow the patterns of control *phtm*>72h samples.

Moreover, in the unsupervised clustering dendrogram for the three conditions included in Heatmap (Figure 13D) it is notable how, again, *phtm>*72h and *phtm>GlyT^i* 120h samples cluster together despite their substantial age diferences. However, in addition to the Halloween genes, and the autophagy and glutathione metabolism pathways, some genes responsible for lipid binding and beta oxidation of fatty acids (Mcad, Acox3, Acox57D-p, SREBP, AcsI), seem to be upregulated in *phtm>GlyT^i* (Figure 13E), in line with what was detailed previously (Figure 12). Also, genes responsible for the glycine cleavage system (Gclc, AMT, Dld) (Kikuchi et al., 2008) were upregulated in *phtm>GlyT^i* at 120h when compared to control *phtm>*120h (Figure 13E). This suggest that this system, firstly described in 1961 by Sagers & Gunsalus, is being activated in order to maintain glycine homeostasis under chronic obese and feeding conditions. Importantly, despite the levels of free glycine quantifications were higher in *phtm>GlyT^i* at 72h when compared to control *phtm>*72h due to the high nutrient intake, there were no significant differences when quantified at 120h in both control and *phtm>GlyT^i* (not shown).

To evaluate the metabolic pathways affected at a systemic level by *GlyT* ablation in PG cells, we did a gene ontology enrichment analysis for biological processes (GO:BP) (Figure 13F). For the group of differentially expressed genes (DEGs) upregulated in *phtm>GlyT^i* with respect to *phtm>*120h we found enriched terms for lipid and glutathione metabolism pathways, suggesting a situation of nutrient abundance in line with its permanent feeding condition. This is in sharp contrast to the enrichment of starvation response pathways (Figure 13F, left panel). Meanwhile, for the group of DEGs upregulated in *phtm>*120h with respect to *phtm>GlyT^i*, we found enriched terms that we expected, related to the triggering of metamorphosis, hormonal response, autophagy and sex differentiation (Figure 13F, right panel).

Finally, we used a Gstd1-GFP marker to visually evaluate the status of this enzyme responsible for glutathione metabolism in fat body tissue. The GstD1-GFP signal is significantly higher in *phtm>GlyT^i* than in its control phtm120h (Figure 13G). The possible implications of glutathione in the metabolic link between glycine availability and autophagy flux activation will be treated in the discussion section.
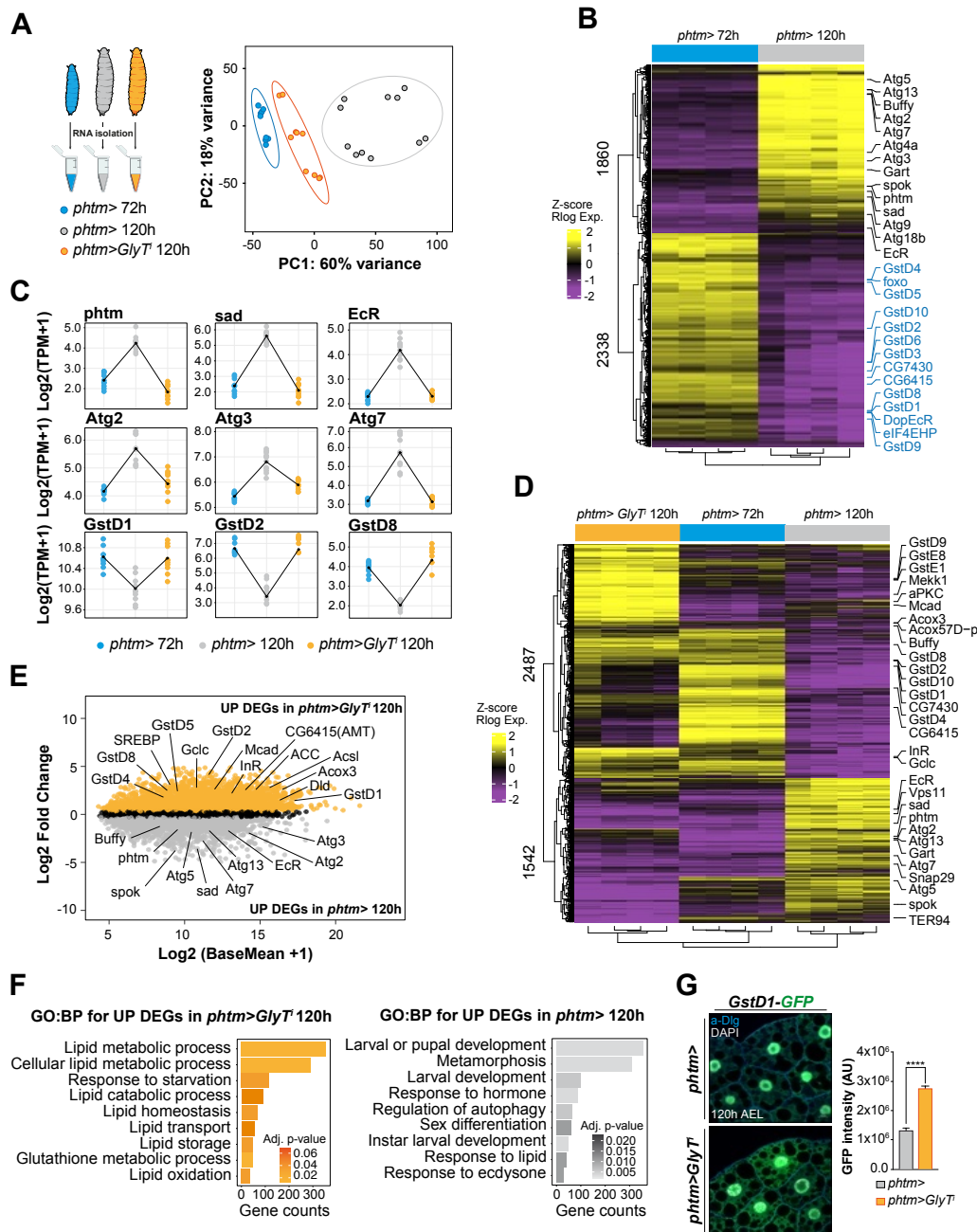
Figure 13. RNA-seq profiling of *phtm>GlyT^i* at 120h and controls *phtm>* at 72 and 120h. A) Scheme of sample collection for RNA-seq study and Principal component analysis (PCA). B) Heatmap of DE analysis in controls. C) TPM normalized plots in *phtm>*72h, *phtm>*120h and *phtm>GlyT^i* 120h. D-E) Heatmap and MA plot of DE analysis in *phtm>*72h, *phtm>*120h and *phtm>GlyT^i* 120h. F) Gene ontology enrichment analysis for biological processes terms in upregulated DEGs in *phtm>GlyT^i* and *phtm>*120h, respectively. G) Imaging of fat body in *phtm>GlyT^i* and *phtm>*120h and its GFP intensity quantification. Data are presented as mean ± standard error of the mean (SEM), ****p ≤ 0.0001.

5.7. Transcriptomic Profiling of 120h PG-Sema1a and PG-GlyT Ablated Animals Reveals Common Patterns with pre-CW Controls

As we have established throughout this study, the main aim for us was to evaluate the effect of other non-lipid nutrients on the mechanisms that trigger the onset of sexual maturation. Taking advantage of the fact that in the laboratory we have already well characterized the effect of Sema1a ablation in PG cells (Juarez-Carreño et al., 2021), we decided to include samples for this condition in the whole larvae RNA-seq studies for a deeper comprehension of what distinguishes them.

Principal component analysis (PCA) reveals a clear trend for both *phtm>Sema1a^i* and *phtm>GlyT^i* samples to cluster closely with the *phtm>* 72h juvenile control samples, despite being individuals at 120 hours of development (Figure 14A). In fact, *phtm>Sema1a^i* samples seems to cluster even closer to *phtm>* 72h than *phtm>GlyT^i*.

DE analysis proves *phtm>Sema1a^i* samples to exhibit similar transcriptomic profiles to *phtm>GlyT^i* when compared to both control *phtm>*72 and *phtm>*120h (Figure 14B-C). For instance, *phtm>Sema1a^i* shares most sets of modulated genes with *phtm>GlyT^i* when compared to *phtm>*120h in DE fold change MA plot (Figure 14B). Thus, the Halloween genes, autophagy and glutathione pathways remain to be metabolic branches affected in both *phtm>Sema1a^i* and *phtm>GlyT^i* samples which are closer to the transcriptomic profiles of *phtm>*72h samples while being a factor that distinguish them from *phtm>*120h samples (Figure 14C). Note that, as in the dendrogram of Heatmap from Figure 13C, in Heatmap for all samples including *phtm>Sema1a^i* (Figure 14C), also the unsupervised clustering shows a dendrogram which cluster together all three non-pupating samples; *phtm>*72h, *phtm>Sema1a^i* and *phtm>GlyT^i*.

Gene ontology analysis reveals some GO:BP terms regarding lipid homeostasis and glutathione metabolism in *phtm>Sema1a^i* upregulated DEGs (Figure 14D, top panel), while metamorphosis, sex differentiation and autophagy remain to be enriched in *phtm>*120h upregulated DEGs (Figure 14D, bottom panel).

The normalized expression in TPM values of some core genes for the three metabolic branches: Ecdysone pathway (*phtm, sad, EcR*), autophagy (*Atg2, Atg3, Atg7*), and glutathione metabolism (*GstD1, GstD6, GstD10*), remain to exhibit a common trend in *phtm>*72h, *phtm>Sema1a^i* and *phtm>GlyT^i* (Figure 14E).
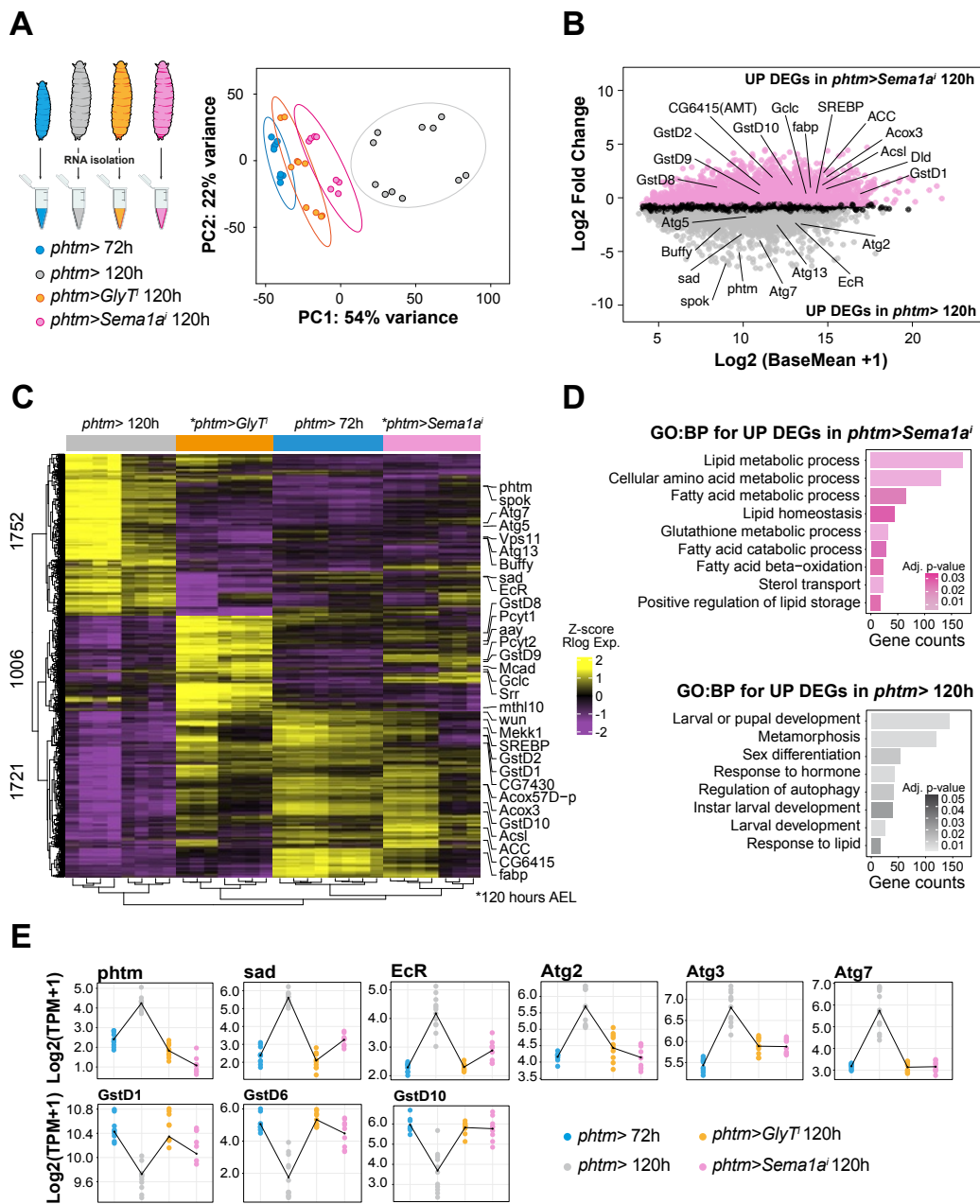
Figure 14. RNA-seq profiling of *phtm>Sema1a^i* and *phtm>GlyT^i* at 120h, and controls *phtm>* at 72 and 120h. A) Scheme of sample collection for RNA-seq study and Principal component analysis (PCA) for all conditions included. B-C) Heatmap and MA plot of DE analysis in *phtm>*72h, *phtm>*120h, *phtm>Sema1a^i* and *phtm>GlyT^i* 120h. D) Gene ontology enrichment analysis for biological processes terms in upregulated DEGs for *phtm>Sema1a^i* and *phtm>*120h, respectively. E) TPM normalized plots in *phtm>*72h, *phtm>*120h and *phtm>GlyT^i, phtm>Sema1a^i* at 120h.

5.8. Glycine Transporter Ablation Disrupts Lipid Storage Locally in PG Cells in Contrast with a Systemic Obese Phenotype

So far, It seems that at a systemic level both *phtm>Sema1a^i* and *phtm>GlyT^i* are very similar in their transcriptomic profiles to the 72h control individuals and to each other. However, epistasis approaches between them, either by gain or loss of function for Sema1a or GlyT, fails to rescue the non-pupating phenotype in both scenarios (Figure 15A, I-III).

Additionally, transgenic expression of human leptin in PG cells fails to rescue the phenotype caused by *phtm>GlyT^i* (Figure 15A, IV), while in *phtm>Sema1a^i* we have previously demonstrated that it is sufficient to rescue the phenotype (Figure 15A, V, from Juarez-Carreño et al., 2021). This suggests that, despite sharing similar patterns at the systemic level, the mechanisms by which GlyT and Sema1a participate in PG cells to modulate the onset of juvenile-to-adult transition must somehow differ. Therefore, we wanted to conduct local experiments to understand the hidden differences between the phenotypes of *phtm>Sema1a^i* and *phtm>GlyT^i* in PG cells.

Since Sema1a is involved in lipid signaling, but the mechanism underlying the effects of GlyT in PG cells are not so clear yet, we wanted to evaluate the state of lipid storage in the PG cells of *phtm>Sema1a^i* and *phtm>GlyT^i* conditions compared to *phtm>*120h.

Thus, by staining ring gland tissues with Nile Red, we demonstrated that, indeed, local lipid reserves are adequate in control individuals *phtm>*120h and *phtm>Sema1a^i*, but significantly scarce in PG cells of *phtm>GlyT^i* individuals (Figure 15B). Furthermore, the number of positive Nile Red puncta per cell (Figure 15C), the intensity of the Nile Red signal (Figure 15D) and the lipid droplets area (Figure 15E) showed a significant reduction in *phtm>GlyT^i* when compared to *phtm>Sema1a^i* and control *phtm>*120h individuals.
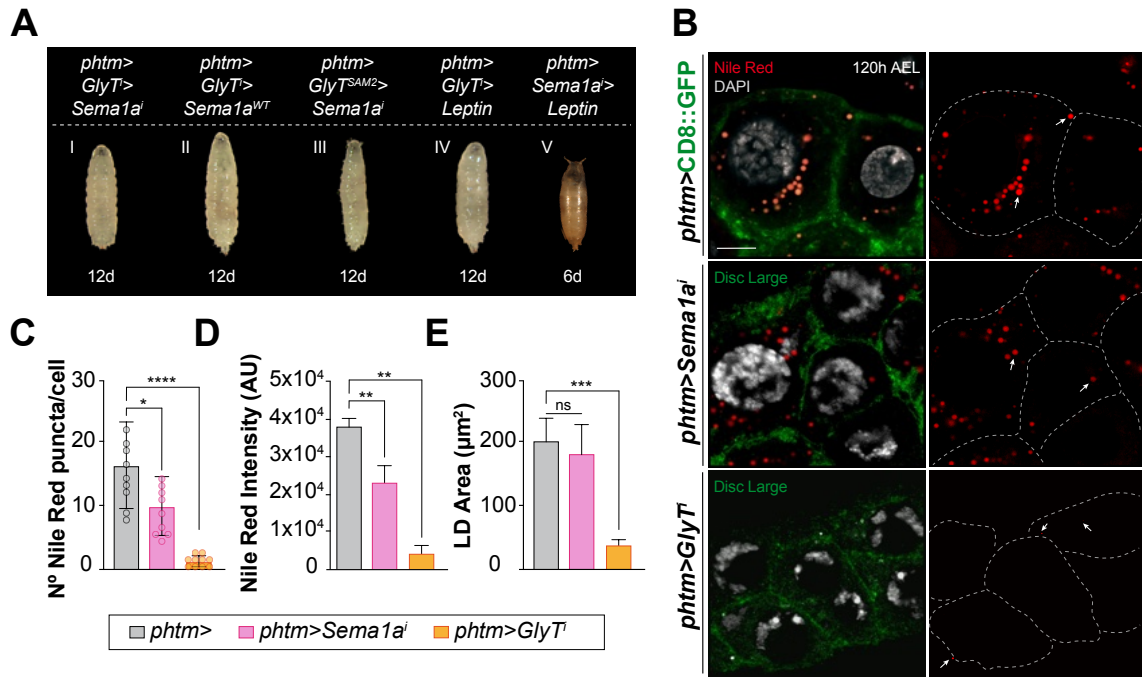
Figure 15. GlyT-Sema1a epistasis and local lipid storage evaluation in PG cells.
A) Images of combinatory epistasis in GlyT Sema1a PG ablated individuals and human leptin expression. Double depletion of GlyT and Sema1a by corresponding RNA[i] lines (I), Sema1a gain of function in GlyT reduced background (II), GlyT gain of function in Sema1a reduced background (III), human leptin expression in GlyT reduced background (IV) and human leptin expression in Sema1a reduced background (IV). B) Imaging of Nile Red staining in PG cells from *phtm>*120h, *phtm>Sema1a[i]* and *phtm>GlyT[i]*. Scale bar = 5μm. C) Number of Nile Red positive puncta per cell. D) Nile Red intensity quantifications in arbitrary units (AU). E) Lipid droplets area measurements in square microns (μm^2). Data are presented as mean ± standard error of the mean (SEM), ****$p \leq 0.0001$, ***$p \leq 0.001$, **$p \leq 0.01$, *$p \leq 0.05$, ns for non-significant.

5.9. Autophagy is Upregulated in PG Cells but Downregulated Systemically in Non-Pupating *phtm>GlyT^i*

So far, local PG lipid storage seems to be significantly affected in *phtm>GlyT^i* when compared to *phtm>Sema1a^i* and control individuals (Figure 15B). Additionally, it is also the case for cytoplasmic volume measurements (Figure 11C-D). In line with this, we performed some local PG evaluations of autophagic fluxes status to determine whether local lipid droplets selective autophagy could be the aspect that distinguishes *phtm>GlyT^i* from *phtm>Sema1a^i* and control *phtm*>120h PG local phenotypes (proposed scheme Figure 16A).

Local PG autophagy evaluation with mCherry-GFP-Atg8a construct, demonstrated a significant increase of autophagic vesicles in contrast with *phtm>Sema1a^i* and *phtm*>120h PG tissues (Figure 16B-C). Meanwhile, forced activation of starvation-induced autophagy at a systemic level (Figure 16D) foster *phtm>GlyT^i* larvae to initiate wandering with consequent pupariation thus rescuing the non-pupating phenotype (Figure 16E, I).

Genetic ablation of autophagy pathway (Atgs) core genes in PG cells demonstrated to be leading to *phtm>GlyT^i* -like phenotypes; loss of function by Atg101 RNA^i line in PG cells exhibit similar phenotype to non-pupating *phtm>GlyT^i* larvae. This was true either when Atg101 was reduced alone with phtmGal4 driver (Figure 16E, II) or in a *phtm>GlyT^i* background (Figure 16E, III), which was also the case for Atg2 (Figure 16E, IV). Additionally, other core Atg genes evaluated by *in vivo* RNA^i -based screening in PG cells, came out with similar phenotypes to non-pupating *phtm>GlyT^i* larvae (orange labeled Atgs in Figure 16A,). In line with the mentioned works from Texada and colleagues, Atg1 gain of function was sufficient to trigger precocious wandering behavior either alone or in a GlyT reduced background leading to tiny larvae that suffer premature death due to dehydration in absence of pupal case formation (Figure 16E, V-VI).

Moreover, reduction of nutrient sensor mTOR in PG cells also provokes *phtm>GlyT^i* -like phenotype (Figure 16E, VII). Nevertheless, mTOR activation by S6K kinase gain of function in a *phtm>GlyT^i* background, failed to rescue the non-pupating phenotype (Figure 16E, VIII-IX), suggesting GlyT is acting independently of canonical mTOR-amino acid-mediated autophagy.
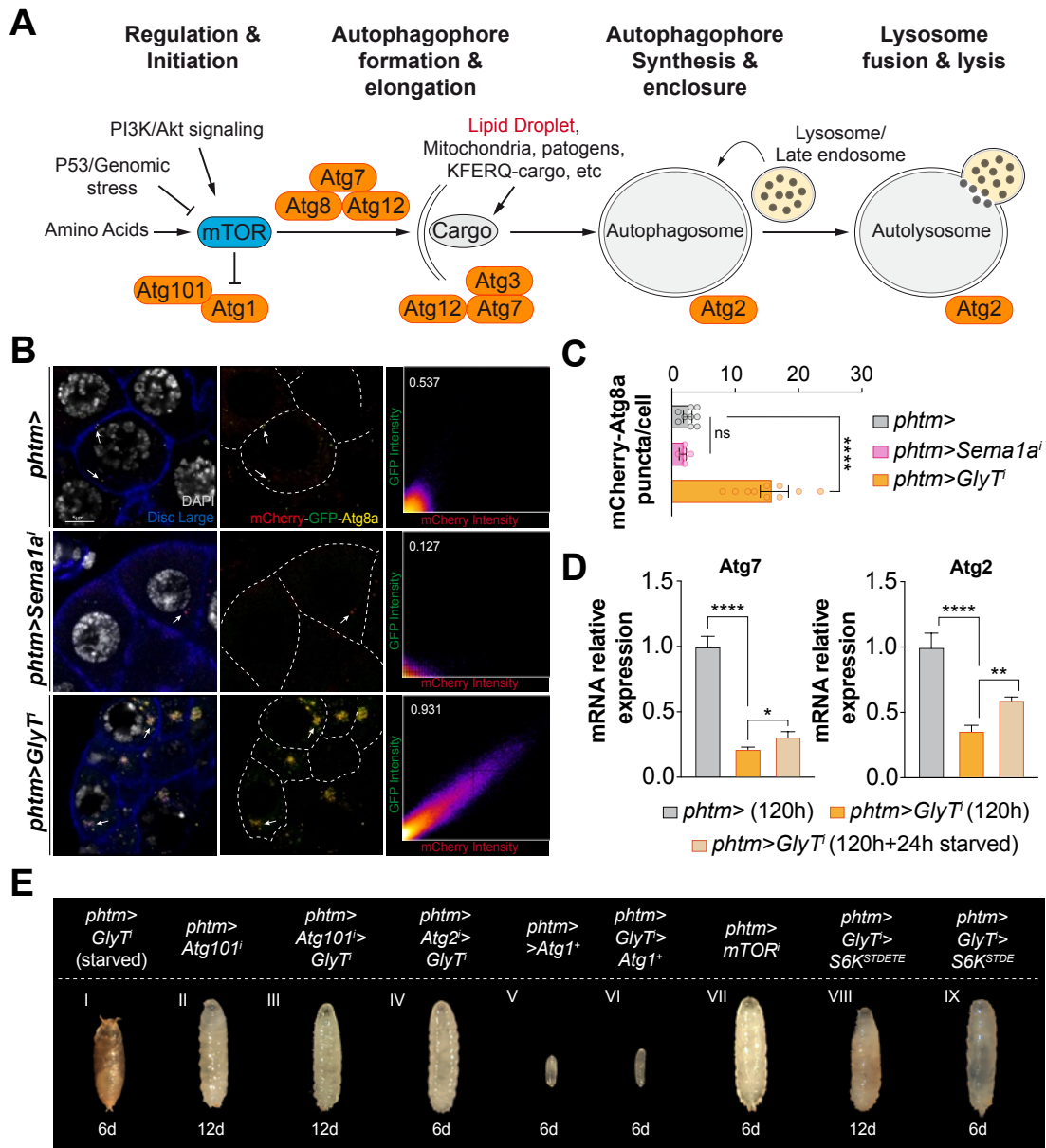
Figure 16. Autophagic PG fluxes evaluation and related genes *in vivo* RNA[i] screening. A) Scheme of main autophagy pathway steps and core genes. In orange, Atgs with *phtm>GlyT[i]*-like phenotypes. B) Larvae photographs resulting from crosses of autophagy and mTOR-related genes (I-VIII) and pupae resulting from *phtm>GlyT[i]* starvation (IX). C) Imaging of *phtm>*120h, *phtm>Sema1a[i]* and *phtm>GlyT[i]* PG tissue with mCherry-GFP-Atg8a marker and its mCherry-GFP colocalization quantifications (right panels) along with their corresponding Pearson correlation coefficients. Scale = 5μm. D) Autophagic vesicles quantifications in mCherry-Atg8a puncta per cell for *phtm>*120h, *phtm>Sema1a[i]* and *phtm>GlyT[i]* images. E) Systemic whole larvae mRNA relative expression of Atg7 (left plot) and Atg2 (right plot) in *phtm>*120h, *phtm>GlyT[i]* and starved (24h) *phtm>GlyT[i]* individuals. Data presented as mean ± standard error of the mean (SEM), ****p ≤ 0.0001, **p ≤ 0.01, *p ≤ 0.05, ns for non-significant.

6. Discussion

Traditionally, studies that aim to dissect the mechanisms underlying the triggering of the onset of sexual maturation has mainly focused on their interaction with lipid metabolism (Nakamoto et al., 2010, Enya et al., 2014, Qi et al., 2022). Especially, in the interpretation that the neuroendocrine control centers are capable of carrying out through their sensing, which has been one of the main research lines in our laboratory (Juarez-Carreño et al., 2021). However, these studies have not completely described the mechanisms involved. In this study, we aim to provide a new approach in which we evaluate how other metabolites, and specifically glycine, participates in the mechanism at the level of PG neuroendocrine cells. With this, we intend to give a more comprehensive view to such an important question for the biology of sexual species, involving different branches of metabolism as well as the short- and long-term effects on organisms that suffer alterations in those pathways.

In this study we have identified the glycine transporter GlyT as a promising gene for the regulation of the mechanisms that trigger steroid production in *Drosophila melanogaster* by the neuroendocrine axis. While in insects the glycine transporter lacks alternative isoforms, in mammals there are two isoforms of this transporter. GlyT1, predominantly located in astrocytes and to a lesser extent in neurons, is involved in the uptake of glycine into the synapse, especially in areas such as the cerebral cortex and hippocampus (Borowsky et al., 1993). GlyT2 is mainly found in inhibitory neurons of the spinal cord and brainstem, where it is essential for glycine reuptake at inhibitory synapses, facilitating vesicular glycine reloading and ensuring efficient inhibitory neurotransmission (Borowsky et al., 1993). GlyT2 is the closest in sequence and functionality to the unique GlyT variant in *Drosophila* (FB2024_03, released June 25, 2024, https://flybase.org/reports/FBgn0034911.htm#orthologs). This is something to take into account regarding eventual translational approaches that could be drawn from this work, since our results would be closer to the function of GlyT2 if we intend to translate the given data to mammals and humans.

Among the lines tested in the SLC *in vivo* RNA[i] screening, we used both traditional lines based on inverted repeats of 400 to 600 bp (Dietzl et al., 2007), and some more recent ones based on small hairpin RNAs (shRNA) containing 21-nucleotide target sequences inserted into a miRNA scaffold. These shRNA constructs are proved to be effective in reducing gene expression in *Drosophila*. Furthermore, its shorter length reduces the likelihood of off-target effects compared to longer inverted repetitions (Ni et al., 2011).

Probably due to the nature of utilized constructs, the GD3564 line included in the screening, did not result in GlyT reduced expression in PG cells, while the SH330127 stock was effective in doing so, reason why this was the line primarily used in this study.

Although our target tissue for *GlyT* silencing is the PG with the phtmGal4 driver, in order to verify the effective reduction of *GlyT* by the SH330127 line, we resorted to the analysis of its expression in Ring Gland tissue (Figure 9D-F). We must keep in mind that isolating RG tissues is a technical challenge itself due to their size and location between the two optic lobes of the larval brain. Exclusively isolating the PGs from whole RGs would imply their isolation by cell dispersion and some attempts to do this in the laboratory using FACS shorting were ineffective in terms of recovered number of cells and cell death ratios. Therefore, taking into account that the major cell population of the RG is the PG (Figure 8A), we assume that the quantification of GlyT expression in RG dissected tissues would be representative to prove the correct activity of the SH330127 line for reducing *GlyT* expression in PG cells.

In *Drosophila* steroidogenic PG cells, we have proved that GlyT reduction is enough to avoid steroids to be produced and released (Figure 10). In line with these results, we observed that, in the case of *phtm>GlyT^i^*, the basal expression levels of EcR remained slightly active even after reaching 120h AEL, hence keeping a mild level of expression that did not increase in absence of positive feedback from its ligand signaling ecdysone (Figure 10D). This contrasts with the results obtained from control individuals, in which levels of EcR are significantly overexpressed at same time point. Meanwhile, the expression levels of a major effector of the pathway, E75, remained completely blocked in *phtm>GlyT^i^* individuals, with virtually non-existent expression due to the lack of hormonal signaling by 20E in comparison to *phtm>*120h control animals.

As a consequence of the lack of development in PG cells upon reduced GlyT expression, these cells suffer an alteration in their N:C ratio caused by the reduction of their cytoplasmic volume (Figure 11C-D). As indicated in the scheme of Figure 11E, the lack of cellular maturation is highly correlated with an increase in the N:C ratio (Balachandra et al., 2022). Indeed, this factor is used in clinical oncology and hematology to assess cell malignancy (Zhang et al., 2024, Gupta et al., 2024, Lee et al., 2024). Hence, cells like erythrocytes, leukocytes, and megakaryocytes start with a high N:C ratio, which decreases significantly as they mature (Fraser et al., 2007). Briefly, we could say that the more a cell progresses in its maturation line, the transcriptional activity increases, thereby increasing the cytoplasmic volume and in this way, reducing its N:C ratio, while

a cell that is still immature or with difficulties when carrying out a proper differentiation of cellular functions, will maintain a higher N:C ratio due to the lack of gain in activity and therefore volume of its cytoplasm.

When we have commented on the effect on the nuclei that we see in PG cell images of *phtm>GlyT^i*, in which nuclei assume a horseshoe shape and their physical boundaries can be challenging to interpret (Figure 11A, right panel and Figure 11C, right panel), We mean that, for some unknown reason, the signal density for DAPI in these nuclei is reduced in some regions, giving rise to a horseshoe shape. This is probably due to a displacement of the nucleolus or an uncontrolled increase its size. On the other hand, we must take into account that the proteins of the nuclear pore complex that form the basket that controls nucleus-cytoplasm transport, are composed of proteins that depend on the concentration of glycine to a large extent. In line with this, the phenylalanine-glycine tails that make up "the net" of this basket (similar to a basketball basket) require the adequate presence of glycine for their correct formation. In this sense, blocking some proteins of the nuclear pore complex (Nups) gives a phenotype very similar to that obtained after blocking *GlyT* in PG cells (not shown). Furthermore, blocking Nups such as Nup214 not only results in a similar phenotype to the one caused by *phtm>GlyT^i*, but also provokes a similar appearance of the nucleus, being larger than usual and exhibiting a horseshoe shape as well.

We have demonstrated that even in well-fed animals, deficiencies in one single amino acid, such as glycine, is sufficient to prevent developmental progression. In line with this, lipid signal supplementation by expression of the human leptin gene in PG cells, which we have proved already to rescue the phenotype caused by *Sema1a* ablation by restoring the activation of neuroendocrine axis (Juarez-Carreño et al., 2021), is not able to reestablish the phenotype caused by *GlyT* reduced expression (Figure 15A, IV). Suggesting that *GlyT* is part of a mechanism that senses nutritional status through a lipid-independent pathway. In fact, epistasis with gain of function of *Sema1a* in *phtm>GlyT^i* background (Figure 15A, II), the opposite approach by overexpression of *GlyT* in *phtm>Sema1a^i* background (Figure 15A, III) or the silencing of both (Figure 15A, I), result in the same non-pupating phenotype. However, numerous studies demonstrate the ability of glycine to collaborate in the correct maintenance of lipid metabolism and hemostasis (Wang et al., 2017, Gaggini et al., 2018, Chen et al., 2018, Kennedy & Lehninger, 1949, Kennedy & Weiss, 1956).

Ghrelin signal, another important nutritional proxy for neuroendocrine tissues, is thought to act via SIRT1 to signal energy status in the mammalian hypothalamus (Nogueiras et al., 2012, Vázquez et al., 2018). In our RNA-seq data, SIRT1 appears upregulated in *phtm>GlyT^i* organisms when compared to *phtm>72h*. Generally speaking, in *phtm>72h* it is expectable that SIRT1 levels are low since they are feeding organisms that do not need to activate energy deficit signaling pathways. However, when we compared the levels of SIRT1 between *phtm>GlyT^i* and *phtm>120* we did not find significant differences, in both SIRT1 was equally elevated compared to *phtm>72h*. In this way, the data suggest a situation consistent with the GO:PG analyzes carried out (Figure 13) This would explain why we found elevated SIRT1 in *phtm>GlyT^i*, manifesting a situation of deficient nutritional sensing that foster them to activate response pathways to starvation such as the one mediated by SIRT1, which we only expected to be found in the controls at 120h since these have indeed abandoned food and activated with them the starvation pathways typical of a wandering behavior situation in L3W.

Contrary to the starvation response situation shown by *phtm>GlyT^i* individuals at 120h, some genes responsible for lipid binding and beta oxidation of fatty acids (*Mcad, Acox3, Acox57D-p*) appear upregulated in *phtm>GlyT^i*, in line with what was previously detailed in Figure 12. This suggests that, despite the poor nutritional sensing condition that keeps them in chronic feeding although with an active response to starvation, the pathways responsible for breaking down and metabolizing excess peripheral fat remain active (Figure 13E- F).

From our data, autophagy in PG cells facilitated by *GlyT* seems to be a promising hypothesis to explain our proposed mechanism. The shortage of amino acids and specifically of some specific amino acids, have been described as clear triggers of autophagy in certain cells. This is why we include starvation activation due to amino acids deficiency and its link with cellular oxidative stress as main modulators. While the shortage of amino acids is a clear activator of autophagic fluxes through the classic Mechanistic Target of Rapamycin (mTOR) pathway (Cao et al., 2021), simply the lack of glycine, due to defects in some of its transporters, has been described as an important promoter of autophagy in recent studies (Johnson & Cuellar, 2023). Importantly, our results demonstrate that there is no dependence of the *GlyT*-mediated mechanism on the canonical mTOR pathway (Figure 16E, VII-IX).

Related studies support that it is ecdysone and the onset of metamorphosis that causes autophagy at a systemic level by initiating wandering (Pan et al., 2019, Texada et al., 2019). However, we can mimic this situation with an inverse approach in which we indicate starvation-induced autophagy at a systemic level by starvation and this is sufficient to rescue the non-pupating phenotype (Figure 16E, I). This suggests that nutrient reserves must be mobilized in some way or another to trigger the onset of the juvenile-to-adult transition. In our results, a situation of clear opposition between the metabolic state of PG and metabolism at the systemic level is revealed. Thus, while in systemic there is no activation of autophagy due to chronic feeding (Figure 13), in PG we find abnormally high autophagy (Figure 16A-C) that is even compromising lipid reserves (Figure 15B-E), suggesting a situation, also supported by our data, in which the synthesis of steroids from these lipid storage in form of lipid droplets is also affected (Figure 10 and Figure 11). The situation that we observe in PG cells as a result of the specific blockade of *GlyT*, on the one hand shows the clear effect that the ablation of *GlyT* has on a neuroendocrine tissue such as the PG, and on the other hand proposes *GlyT* as an important element in the regulation of short- and long-term systemic metabolism orchestrated directly from the PG.

An interesting way to explain the relationship between *GlyT*-mediated intracellular glycine concentrations in neuroendocrine cells and the triggering of autophagy in our model, is the effect that glycine causes on intracellular glutathione homeostasis (Kumar et al., 2022). Glutathione has been shown to regulate the behavior of lipid droplets in *Drosophila* to allow ecdysteroid biosynthesis in PG cells (Enya et al., 2014). Moreover, glycine is essential for the synthesis of glutathione (GSH), the main antioxidant agent in eukaryotic cells (Desideri et al., 2012). Since we know that oxidative stress is a clearly triggering factor for autophagy, it is important to take glutathione into account as a main activator of this pathway in the context of developmental processes (Sun et al., 2018). Glutathione is one of the main Thiol-containing compounds of eukaryotic cells. These compounds play a central role in many physiological reactions due to their capability to undergo redox cycles between reduced and oxidized status. Cellular response to stress often involves changes in thiol content that are crucial in reactions aimed at protecting cellular component from oxidative insults (Wu et al., 2021). Hence, the dual activation mechanism of autophagy promoted by the scarcity of specific amino acids such as glycine, and its indirect action on the redox state of the cell is interesting for this work.

Moreover, autophagy plays a key role in the regulation of cell size by balancing the synthesis and degradation of cellular components. Under conditions of stress or lack of nutrients, autophagy is activated, promoting the degradation of organelles and proteins, which can induce a reduction in cell size. For example, inactivation of the protein phosphatidylinositol 5-phosphate 4-kinase (*PIP4K*) in *Drosophila* causes an elevation of *PI3P*, which activates autophagy and reduces cell size, an effect that can be reversed by decreasing the expression of Atg8a, a key regulator of autophagosome maturation (Ghosh et al., 2023). Furthermore, the protein vimentin, through *mTORC1* signaling, has been found to regulate cell size and suppress autophagy in the absence of growth factors, suggesting a link between the cytoskeleton and the regulation of autophagy and cell growth (Mohanasundaram et al., 2022). On the other hand, a proper balance of autophagy is crucial for maintaining normal cell size, as both its deficiency and excess can interfere with cell growth, as observed in studies with mutants of the unc-51 and bec-1 genes in C. elegans (Vellai et al., 2008).

Overall, the complexity involved in triggering the onset of sexual maturation, as well as the number of interactions that take place in their neuroendocrine centers of control during this delicate combinatory process, reflects the importance of these nutritional sensing mechanisms that ensure both reproductive success and appropriate environment for the development of future offspring.

Although there are numerous research groups joining efforts to increase knowledge about these processes, there is still much to contribute to the field. Therefore, we hope that the humble contribution that this thesis work represents, will provide some evidences in this regard. Nevertheless, we foresee that the presented results obtained in *Drosophila melanogaster* will, eventually, may be interesting not only to scientific general knowledge, but also for a better understanding of this crucial biological question in higher organisms such as mammals, including humans.

7. Conclusions

1. The glycine transporter GlyT is a crucial component in the mechanism that allows nutrient sensing in neuroendocrine control centers to trigger the onset of sexual maturation.

2. Ablation of GlyT in neuroendocrine cells arrest development by inhibiting both hormone synthesis and its release by active secretion pathways in PG cells.

3. The reduction in GlyT expression leads to immaturity in the PG, resulting in a significant decrease in cytoplasmic volume within its cells.

4. Chronic feeding behavior upon GlyT ablation in PG cells triggers an obese phenotype that results in larval weight and volume gains, in addition to a disorganization of lipid reserves due to excess in Fat body tissue.

5. Both local ablation of AA-sensing (GlyT) and lipid-sensing (Sema1a) in PG cells causes systemic effects that maintain their transcriptomic profile similar to that of a juvenile organism.

6. Abnormally elevated autophagy fluxes in PG cells upon GlyT ablation cause excessive degradation of lipid droplets that deplete cholesterol reserves, thus preventing the synthesis of steroidal hormones, leading to developmental arrest in L3F.

8.   Conclusiones

1. El transportador de glicina GlyT es un componente crucial en el mecanismo que permite la detección de nutrientes en los centros de control neuroendocrinos para desencadenar el inicio de la maduración sexual.

2. La ablación de GlyT en células neuroendocrinas detiene el desarrollo al inhibir tanto la síntesis hormonal como su liberación a través de las vías de secreción activa en las células PG.

3. La reducción en la expresión de GlyT causa una falta de madurez en las células PG, cuyo síntoma es una disminución en el volumen citoplasmático.

4. El comportamiento alimentario crónico tras la ablación de GlyT en las células PG desencadena un fenotipo obeso que resulta en un aumento de peso y volumen larval, además de una desorganización de las reservas lipídicas debido al exceso en el cuerpo graso.

5. Tanto la ablación local del sensado de aminoácidos (GlyT) como del sensado de lípidos (Sema1a) en las células PG causa efectos sistémicos que mantienen sus perfiles transcriptómicos similares a los de un organismo juvenil.

6. Los flujos de autofagia anormalmente elevados en las células PG tras la ablación de GlyT provocan una degradación excesiva de las gotas lipídicas, lo que agota las reservas de colesterol y, por lo tanto, impide la síntesis de hormonas esteroides, conduciendo al arresto del desarrollo en L3F.

9. References

Abreu, A. P., Dauber, A., Macedo, D. B., Noel, S. D., Brito, V. N., Gill, J. C., Cukier, P., Thompson, I. R., Navarro, V. M., Gagliardi, P. C., Rodrigues, T., Kochi, C., Longui, C. A., Beckers, D., de Zegher, F., Montenegro, L. R., Mendonca, B. B., Carroll, R. S., Hirschhorn, J. N., Latronico, A. C., Kaiser, U. B. (2013). Central precocious puberty caused by mutations in the imprinted gene MKRN3. The New England journal of medicine, 368(26), 2467–2475. https://doi.org/10.1056/NEJMoa1302160

Aguayo-Cerón, K. A., Sánchez-Muñoz, F., Gutierrez-Rojas, R. A., Acevedo-Villavicencio, L. N., Flores-Zarate, A. V., Huang, F., Giacoman-Martinez, A., Villafaña, S., & Romero-Nava, R. (2023). Glycine: The Smallest Anti-Inflammatory Micronutrient. International journal of molecular sciences, 24(14), 11236. https://doi.org/10.3390/ijms241411236

Ahmed, M. L., Ong, K. K., & Dunger, D. B. (2009). Childhood obesity and the timing of puberty. Trends in endocrinology and metabolism: TEM, 20(5), 237–242. https://doi.org/10.1016/j.tem.2009.02.004

Ahn, S. Y., Yang, S. W., Lee, H. J., Byun, J. S., Om, J. Y., & Shin, C. H. (2012). Excess of leptin inhibits hypothalamic KiSS-1 expression in pubertal mice. Korean journal of pediatrics, 55(9), 337–343. https://doi.org/10.3345/kjp.2012.55.9.337

Alves, A., Bassot, A., Bulteau, A. L., Pirola, L., & Morio, B. (2019). Glycine Metabolism and Its Alterations in Obesity and Metabolic Diseases. Nutrients, 11(6), 1356. https://doi.org/10.3390/nu11061356

Anderson, G. M., Hill, J. W., Kaiser, U. B., Navarro, V. M., Ong, K. K., Perry, J. R. B., Prevot, V., Tena-Sempere, M., & Elias, C. F. (2024). Metabolic control of puberty: 60 years in the footsteps of Kennedy and Mitra's seminal work. Nature reviews. Endocrinology, 20(2), 111–123. https://doi.org/10.1038/s41574-023-00919-z

Anderson, G. M., Hill, J. W., Kaiser, U. B., Navarro, V. M., Ong, K. K., Perry, J. R. B., Prevot, V., Tena-Sempere, M., & Elias, C. F. (2024). Metabolic control of puberty: 60 years in the footsteps of Kennedy and Mitra's seminal work. Nature reviews. Endocrinology, 20(2), 111–123. https://doi.org/10.1038/s41574-023-00919-z

Baker, J. H., Higgins Neyland, M. K., Thornton, L. M., Runfola, C. D., Larsson, H., Lichtenstein, P., & Bulik, C. (2019). Body dissatisfaction in adolescent boys. Developmental psychology, 55(7), 1566–1578. https://doi.org/10.1037/dev0000724

Balachandra, S., Sarkar, S., & Amodeo, A. A. (2022). The Nuclear-to-Cytoplasmic Ratio: Coupling DNA Content to Cell Size, Cell Cycle, and Biosynthetic Capacity. Annual review of genetics, 56, 165–185. https://doi.org/10.1146/annurev-genet-080320-030537

Barredo, C. G., Gil-Marti, B., Deveci, D., Romero, N. M., & Martin, F. A. (2021). Timing the Juvenile-Adult Neurohormonal Transition: Functions and Evolution. Frontiers in endocrinology, 11, 602285. https://doi.org/10.3389/fendo.2020.602285

Bellen, H. J., Tong, C., & Tsuda, H. (2010). 100 years of Drosophila research and its impact on vertebrate neuroscience: a history lesson for the future. Nature reviews. Neuroscience, 11(7), 514–522. https://doi.org/10.1038/nrn2839

Berenbaum, S. A., Beltz, A. M., & Corley, R. (2015). The importance of puberty for adolescent development: conceptualization and measurement. Advances in child development and behavior, 48, 53–92. https://doi.org/10.1016/bs.acdb.2014.11.002

Berreur, P., Porcheron, P., Berreur-Bonnenfant, J., & Simpson, P. (1979). Ecdysteroid levels and pupariation in Drosophila melanogaster. *Journal of Experimental Zoology*, *210*(2), 347-352.

Bhattacharjee, A., Szabó, Á., Csizmadia, T., Laczkó-Dobos, H., & Juhász, G. (2019). Understanding the importance of autophagy in human diseases using *Drosophila*. Journal of genetics and genomics = Yi chuan xue bao, 46(4), 157–169. https://doi.org/10.1016/j.jgg.2019.03.007

Bianco, M. E., & Josefson, J. L. (2019). Hyperglycemia During Pregnancy and Long-Term Offspring Outcomes. Current diabetes reports, 19(12), 143. https://doi.org/10.1007/s11892-019-1267-6

Bodicoat, D. H., Schoemaker, M. J., Jones, M. E., McFadden, E., Griffin, J., Ashworth, A., & Swerdlow, A. J. (2014). Timing of pubertal stages and breast cancer risk: the Breakthrough Generations Study. Breast cancer research: BCR, 16(1), R18. https://doi.org/10.1186/bcr3613

Borowsky, B., Mezey, E., & Hoffman, B. J. (1993). Two glycine transporter variants with distinct localization in the CNS and peripheral tissues are encoded by a common gene. Neuron, 10(5), 851–863. https://doi.org/10.1016/0896-6273(93)90201-2

Bourguignon, J. P., Gérard, A., & Franchimont, P. (1989). Direct activation of gonadotropin-releasing hormone secretion through different receptors to neuroexcitatory amino acids. Neuroendocrinology, 49(4), 402–408. https://doi.org/10.1159/000125145

Braconnot, H. (1820). Sur la conversion des matières animales en nouvelles substances par le moyen de l'acide sulfurique [On the conversion of animal materials into new substances by means of sulfuric acid]. Annales de Chimie et de Physique, 2nd series, 13, 113–125. (see p. 114).

Bradley, S. H., Lawrence, N., Steele, C., & Mohamed, Z. (2020). Precocious puberty. BMJ (Clinical research ed.), 368, l6597. https://doi.org/10.1136/bmj.l6597

Brand, A. H., & Perrimon, N. (1993). Targeted gene expression as a means of altering cell fates and generating dominant phenotypes. Development (Cambridge, England), 118(2), 401–415. https://doi.org/10.1242/dev.118.2.401

Brann, D. W., & Mahesh, V. B. (1994). Excitatory amino acids: function and significance in reproduction and neuroendocrine regulation. Frontiers in neuroendocrinology, 15(1), 3–49. https://doi.org/10.1006/frne.1994.1002

Bremer A. A. (2010). Polycystic ovary syndrome in the pediatric population. Metabolic syndrome and related disorders, 8(5), 375–394. https://doi.org/10.1089/met.2010.0039

Brix, N., Ernst, A., Lauridsen, L. L. B., Parner, E. T., Arah, O. A., Olsen, J., Henriksen, T. B., & Ramlau-Hansena, C. H. (2020). Childhood overweight and obesity and timing of puberty in boys and girls: cohort and sibling-matched analyses. International journal of epidemiology, 49(3), 834–844. https://doi.org/10.1093/ije/dyaa056

Cao, W., Li, J., Yang, K., & Cao, D. (2021). An overview of autophagy: Mechanism, regulation and research progress. Bulletin du cancer, 108(3), 304–322. https://doi.org/10.1016/j.bulcan.2020.11.004

Cariboni, A., André, V., Chauvet, S., Cassatella, D., Davidson, K., Caramello, A., Fantin, A., Bouloux, P., Mann, F., & Ruhrberg, C. (2015). Dysfunctional SEMA3E signaling underlies gonadotropin-releasing hormone neuron deficiency in Kallmann syndrome. The Journal of clinical investigation, 125(6), 2413–2428. https://doi.org/10.1172/JCI78448

Ceder, M. M., & Fredriksson, R. (2022). A phylogenetic analysis between humans and D. melanogaster: A repertoire of solute carriers in humans and flies. Gene, 809, 146033. https://doi.org/10.1016/j.gene.2021.146033

Celotti, F., Negri-Cesi, P., & Poletti, A. (1997). Steroid metabolism in the mammalian brain: 5alpha-reduction and aromatization. Brain research bulletin, 44(4), 365–375. https://doi.org/10.1016/s0361-9230(97)00216-5

Chehab, F. F., Mounzih, K., Lu, R., & Lim, M. E. (1997). Early onset of reproductive function in normal female mice treated with leptin. Science (New York, N.Y.), 275(5296), 88–90. https://doi.org/10.1126/science.275.5296.88

Chen, J., Ma, X., Yang, Y., Dai, Z., Wu, Z., & Wu, G. (2018). Glycine enhances expression of adiponectin and IL-10 in 3T3-L1 adipocytes without affecting adipogenesis and lipolysis. Amino acids, 50(5), 629–640. https://doi.org/10.1007/s00726-018-2537-3

Chen, Z., Si, L., Shu, W., Zhang, X., Wei, C., Wei, M., Cheng, L., Chen, Z., Qiao, Y., & Yang, S. (2022). Exogenous Melatonin Regulates Puberty and the Hypothalamic GnRH-GnIH System in Female Mice. Brain sciences, 12(11), 1550. https://doi.org/10.3390/brainsci12111550

Chiang, A. S., Lin, W. Y., Liu, H. P., Pszczolkowski, M. A., Fu, T. F., Chiu, S. L., & Holbrook, G. L. (2002). Insect NMDA receptors mediate juvenile hormone biosynthesis. Proceedings of the National Academy of Sciences of the United States of America, 99(1), 37–42. https://doi.org/10.1073/pnas.012318899

Cingolani, F., & Czaja, M. J. (2016). Regulation and Functions of Autophagic Lipolysis. Trends in endocrinology and metabolism: TEM, 27(10), 696–705. https://doi.org/10.1016/j.tem.2016.06.003

Clément, K., Vaisse, C., Lahlou, N., Cabrol, S., Pelloux, V., Cassuto, D., Gourmelen, M., Dina, C., Chambaz, J., Lacorte, J. M., Basdevant, A., Bougnères, P., Lebouc, Y., Froguel, P., & Guy-Grand, B. (1998). A mutation in the human leptin receptor gene causes obesity and pituitary dysfunction. Nature, 392(6674), 398–401. https://doi.org/10.1038/32911

Contreras, C., González-García, I., Martínez-Sánchez, N., Seoane-Collazo, P., Jacas, J., Morgan, D. A., Serra, D., Gallego, R., Gonzalez, F., Casals, N., Nogueiras, R., Rahmouni, K., Diéguez, C., & López, M. (2014). Central ceramide-induced hypothalamic lipotoxicity and ER stress regulate energy balance. Cell reports, 9(1), 366–377. https://doi.org/10.1016/j.celrep.2014.08.057

Convissar, S., Bennett-Toomey, J., & Stocco, C. (2023). Insulin-like growth factor 1 enhances follicle-stimulating hormone-induced phosphorylation of GATA4 in rat granulosa cells. Molecular and cellular endocrinology, 559, 111807. https://doi.org/10.1016/j.mce.2022.111807

Cruciani-Guglielmacci, C., Le Stunff, H., & Magnan, C. (2024). Brain lipid sensing and the neural control of energy balance. Biochimie, 223, 159–165. https://doi.org/10.1016/j.biochi.2024.05.020

Cruz, J., Martín, D., & Franch-Marro, X. (2020). Egfr Signaling Is a Major Regulator of Ecdysone Biosynthesis in the *Drosophila* Prothoracic Gland. Current biology: CB, 30(8), 1547–1554.e4. https://doi.org/10.1016/j.cub.2020.01.092

Cuervo, A. M., & Dice, J. F. (2000). Age-related decline in chaperone-mediated autophagy. The Journal of biological chemistry, 275(40), 31505–31513. https://doi.org/10.1074/jbc.M002102200

Danielsen, E. T., Moeller, M. E., Yamanaka, N., Ou, Q., Laursen, J. M., Soenderholm, C., Zhuo, R., Phelps, B., Tang, K., Zeng, J., Kondo, S., Nielsen, C. H., Harvald, E. B., Faergeman, N. J., Haley, M. J., O'Connor, K. A., King-Jones, K., O'Connor, M. B., & Rewitz, K. F. (2016). A *Drosophila* Genome-Wide Screen Identifies Regulators of Steroid Hormone Production and Developmental Timing. Developmental cell, 37(6), 558–570. https://doi.org/10.1016/j.devcel.2016.05.015

Darsow, T., Rieder, S. E., & Emr, S. D. (1997). A multispecificity syntaxin homologue, Vam3p, essential for autophagic and biosynthetic protein transport to the vacuole. The Journal of cell biology, 138(3), 517–529. https://doi.org/10.1083/jcb.138.3.517

de Onis, M., Blössner, M., & Borghi, E. (2010). Global prevalence and trends of overweight and obesity among preschool children. The American journal of clinical nutrition, 92(5), 1257–1264. https://doi.org/10.3945/ajcn.2010.29786

Déchamps, S., Wengelnik, K., Berry-Sterkers, L., Cerdan, R., Vial, H. J., & Gannoun-Zaki, L. (2010). The Kennedy phospholipid biosynthesis pathways are refractory to genetic disruption in Plasmodium berghei and therefore appear essential in blood stages. Molecular and biochemical parasitology, 173(2), 69–80. https://doi.org/10.1016/j.molbiopara.2010.05.006

Deliu, L. P., Turingan, M., Jadir, D., Lee, B., Ghosh, A., & Grewal, S. S. (2022). Serotonergic neuron ribosomal proteins regulate the neuroendocrine control of *Drosophila* development. PLoS genetics, 18(9), e1010371. https://doi.org/10.1371/journal.pgen.1010371

Deshpande, S. S. S., Bera, P., Khambata, K., & Balasinor, N. H. (2023). Paternal obesity induces epigenetic aberrations and gene expression changes in placenta and fetus. Molecular reproduction and development, 90(2), 109–126. https://doi.org/10.1002/mrd.23660

Desideri, E., Filomeni, G., & Ciriolo, M. R. (2012). Glutathione participates in the modulation of starvation-induced autophagy in carcinoma cells. Autophagy, 8(12), 1769–1781. https://doi.org/10.4161/auto.22037

Deveci, D., Martin, F. A., Leopold, P., & Romero, N. M. (2019). AstA Signaling Functions as an Evolutionary Conserved Mechanism Timing Juvenile to Adult Transition. Current biology: CB, 29(5), 813–822.e4. https://doi.org/10.1016/j.cub.2019.01.053

Dice J. F. (1990). Peptide sequences that target cytosolic proteins for lysosomal proteolysis. Trends in biochemical sciences, 15(8), 305–309. https://doi.org/10.1016/0968-0004(90)90019-8

Dietzl, G., Chen, D., Schnorrer, F., Su, K. C., Barinova, Y., Fellner, M., Gasser, B., Kinsey, K., Oppel, S., Scheiblauer, S., Couto, A., Marra, V., Keleman, K., & Dickson, B. J. (2007). A genome-wide transgenic RNAi library for conditional gene inactivation in Drosophila. Nature, 448(7150), 151–156. https://doi.org/10.1038/nature05954

Ding, Y., Svingen, G. F., Pedersen, E. R., Gregory, J. F., Ueland, P. M., Tell, G. S., & Nygård, O. K. (2015). Plasma Glycine and Risk of Acute Myocardial Infarction in Patients With Suspected Stable Angina Pectoris. Journal of the American Heart Association, 5(1), e002621. https://doi.org/10.1161/JAHA.115.002621

Egan, O. K., Inglis, M. A., & Anderson, G. M. (2017). Leptin Signaling in AgRP Neurons Modulates Puberty Onset and Adult Fertility in Mice. The Journal of neuroscience : the official journal of the Society for Neuroscience, 37(14), 3875–3886. https://doi.org/10.1523/JNEUROSCI.3138-16.2017

Entchev, E. V., Schwabedissen, A., & González-Gaitán, M. (2000). Gradient formation of the TGF-beta homolog Dpp. Cell, 103(6), 981–991. https://doi.org/10.1016/s0092-8674(00)00200-2

Enya, S., Ameku, T., Igarashi, F., Iga, M., Kataoka, H., Shinoda, T., & Niwa, R. (2014). A Halloween gene noppera-bo encodes a glutathione S-transferase essential for ecdysteroid biosynthesis via regulating the behaviour of cholesterol in Drosophila. Scientific reports, 4, 6586. https://doi.org/10.1038/srep06586

Fang, X., Zuo, J., Zhou, J., Cai, J., Chen, C., Xiang, E., Li, H., Cheng, X., & Chen, P. (2019). Childhood obesity leads to adult type 2 diabetes and coronary artery diseases: A 2-sample mendelian randomization study. Medicine, 98(32), e16825. https://doi.org/10.1097/MD.0000000000016825

Farenholtz, J., Artelt, N., Blumenthal, A., Endlich, K., Kroemer, H. K., Endlich, N., & von Bohlen Und Halbach, O. (2019). Expression of Slc35f1 in the murine brain. Cell and tissue research, 377(2), 167–176. https://doi.org/10.1007/s00441-019-03008-8

Feyder, M., Plewnia, C., Lieberman, O. J., Spigolon, G., Piccin, A., Urbina, L., Dehay, B., Li, Q., Nilsson, P., Altun, M., Santini, E., Sulzer, D., Bezard, E., Borgkvist, A., & Fisone, G. (2021). Involvement of Autophagy in Levodopa-Induced Dyskinesia. Movement disorders : official journal of the Movement Disorder Society, 36(5), 1137–1146. https://doi.org/10.1002/mds.28480

Filpa, V., Moro, E., Protasoni, M., Crema, F., Frigo, G., & Giaroni, C. (2016). Role of glutamatergic neurotransmission in the enteric nervous system and brain-gut axis in health and disease. Neuropharmacology, 111, 14–33. https://doi.org/10.1016/j.neuropharm.2016.08.024

Fletcher, J. C., & Thummel, C. S. (1995). The Drosophila E74 gene is required for the proper stage- and tissue-specific transcription of ecdysone-regulated genes at the onset of metamorphosis. *Development (Cambridge, England)*, *121*(5), 1411–1421. https://doi.org/10.1242/dev.121.5.1411

Floegel, A., Stefan, N., Yu, Z., Mühlenbruch, K., Drogan, D., Joost, H. G., Fritsche, A., Häring, H. U., Hrabě de Angelis, M., Peters, A., Roden, M., Prehn, C., Wang-Sattler, R., Illig, T., Schulze, M. B., Adamski, J., Boeing, H., & Pischon, T. (2013). Identification of serum metabolites associated with risk of type 2 diabetes using a targeted metabolomic approach. Diabetes, 62(2), 639–648. https://doi.org/10.2337/db12-0495

Foster, E., Wildner, H., Tudeau, L., Haueter, S., Ralvenius, W. T., Jegen, M., Johannssen, H., Hösli, L., Haenraets, K., Ghanem, A., et al. (2015). Targeted ablation, silencing, and activation establish glycinergic dorsal horn neurons as key components of a spinal gate for pain and itch. Neuron, 85(6), 1289–1304. https://doi.org/10.1016/j.neuron.2015.02.028

Fraenkel, G. (1935). A hormone causing pupation in the blowfly Calliphora erythrocephala. *Proceedings of the Royal Society of London. Series B-Biological Sciences*, *118*(807), 1-12.

Fraser, S. T., Isern, J., & Baron, M. H. (2007). Maturation and enucleation of primitive erythroblasts during mouse embryogenesis is accompanied by changes in cell-surface antigen expression. Blood, 109(1), 343–352. https://doi.org/10.1182/blood-2006-03-006569

Fredriksson, R., Nordström, K. J., Stephansson, O., Hägglund, M. G., & Schiöth, H. B. (2008). The solute carrier (SLC) complements of the human genome: phylogenetic classification reveals four major families. FEBS letters, 582(27), 3811–3816. https://doi.org/10.1016/j.febslet.2008.10.016

Frisch, R. E., & Revelle, R. (1970). Height and weight at menarche and a hypothesis of critical body weights and adolescent events. Science (New York, N.Y.), 169(3943), 397–399. https://doi.org/10.1126/science.169.3943.397

Gaggini, M., Carli, F., Rosso, C., Buzzigoli, E., Marietti, M., Della Latta, V., Ciociaro, D., Abate, M. L., Gambino, R., Cassader, M., Bugianesi, E., & Gastaldelli, A. (2018). Altered amino acid concentrations in NAFLD: Impact of obesity and insulin resistance. Hepatology (Baltimore, Md.), 67(1), 145–158. https://doi.org/10.1002/hep.29465

Galluzzi, L., Baehrecke, E. H., Ballabio, A., Boya, P., Bravo-San Pedro, J. M., Cecconi, F., Choi, A. M., Chu, C. T., Codogno, P., Colombo, M. I., Cuervo, A. M., Debnath, J., Deretic, V., Dikic, I., Eskelinen, E. L., Fimia, G. M., Fulda, S., Gewirtz, D. A., Green, D. R., Hansen, M., … Kroemer, G. (2017). Molecular definitions of autophagy and related processes. The EMBO journal, 36(13), 1811–1836. https://doi.org/10.15252/embj.201796697

Gao H. (2020). Amino Acids in Reproductive Nutrition and Health. Advances in experimental medicine and biology, 1265, 111–131. https://doi.org/10.1007/978-3-030-45328-2_7

Gar, C., Rottenkolber, M., Prehn, C., Adamski, J., Seissler, J., & Lechner, A. (2018). Serum and plasma amino acids as markers of prediabetes, insulin resistance, and incident diabetes. Critical reviews in clinical laboratory sciences, 55(1), 21–32. https://doi.org/10.1080/10408363.2017.1414143

Gatica, D., Lahiri, V., & Klionsky, D. J. (2018). Cargo recognition and degradation by selective autophagy. Nature cell biology, 20(3), 233–242. https://doi.org/10.1038/s41556-018-0037-z

Gaur, A., Pal, G. K., & Pal, P. (2021). Role of Ventromedial Hypothalamus in Sucrose-Induced Obesity on Metabolic Parameters. Annals of neurosciences, 28(1-2), 39–46. https://doi.org/10.1177/09727531211005738

Georgopoulos, N. A., Roupas, N. D., Theodoropoulou, A., Tsekouras, A., Vagenakis, A. G., & Markou, K. B. (2010). The influence of intensive physical training on growth and pubertal development in athletes. Annals of the New York Academy of Sciences, 1205, 39–44. https://doi.org/10.1111/j.1749-6632.2010.05677.x

Ghosh, A., Venugopal, A., Shinde, D., Sharma, S., Krishnan, M., Mathre, S., Krishnan, H., Saha, S., & Raghu, P. (2023). PI3P-dependent regulation of cell size and autophagy by phosphatidylinositol 5-phosphate 4-kinase. Life science alliance, 6(9), e202301920. https://doi.org/10.26508/lsa.202301920

Gibbens, Y. Y., Warren, J. T., Gilbert, L. I., & O'Connor, M. B. (2011). Neuroendocrine regulation of *Drosophila* metamorphosis requires TGFbeta/Activin signaling. Development (Cambridge, England), 138(13), 2693–2703. https://doi.org/10.1242/dev.063412

Gilbert, L. I., Rybczynski, R., & Warren, J. T. (2002). Control and biochemical nature of the ecdysteroidogenic pathway. Annual review of entomology, 47, 883–916. https://doi.org/10.1146/annurev.ento.47.091201.145302

Gohel, R., Kournoutis, A., Petridi, S., & Nezis, I. P. (2020). Molecular mechanisms of selective autophagy in *Drosophila*. International review of cell and molecular biology, 354, 63–105. https://doi.org/10.1016/bs.ircmb.2019.08.003

Goldman, A. S., & Klingele, D. A. (1974). Persistent postpubertal elevation of activity of steroid 5alpha-reductase in the adrenal of rat pseudohermaphrodites and correction by large doses of testosterone or DHT. Endocrinology, 94(5), 1232–1240. https://doi.org/10.1210/endo-94-5-1232

Golshan, M., Alavi, S. M. H., Hatef, A., Kazori, N., Socha, M., Milla, S., Sokołowska-Mikołajczyk, M., Unniappan, S., Butts, I. A. E., & Linhart, O. (2024). Impact of absolute food deprivation on the reproductive system in male goldfish exposed to sex steroids. Journal of comparative physiology. B, Biochemical, systemic, and environmental physiology, 10.1007/s00360-024-01570-4. Advance online publication. https://doi.org/10.1007/s00360-024-01570-4

González-García, I., Contreras, C., Estévez-Salguero, Á., Ruíz-Pino, F., Colsh, B., Pensado, I., Liñares-Pose, L., Rial-Pensado, E., Martínez de Morentin, P. B., Fernø, J., Diéguez, C., Nogueiras, R., Le Stunff, H., Magnan, C., Tena-Sempere, M., & López, M. (2018). Estradiol Regulates Energy Balance by Ameliorating Hypothalamic Ceramide-Induced ER Stress. Cell reports, 25(2), 413–423.e5. https://doi.org/10.1016/j.celrep.2018.09.038

Gonzalez-Ortiz, M., Medina-Santillan, R., Martinez-Abundis, E., & von Drateln, C. R. (2001). Effect of glycine on insulin secretion and action in healthy first-degree relatives of type 2 diabetes mellitus patients. *Hormone and Metabolic Research, 33*(6), 358–360. https://doi.org/10.1055/s-2001-15421

Guirado, J., Carranza-Valencia, J., & Morante, J. (2023). Mammalian puberty: a fly perspective. The FEBS journal, 290(2), 359–369. https://doi.org/10.1111/febs.16534

Gupta, P., Siraj, F., Shankar, K. B., Rawat, M., Mankotia, D. S., Yadav, V., & Dagar, A. (2024). Clinical and histopathological spectrum of cranial small round cell tumors: An experience from a tertiary care center. *Journal of cancer research and therapeutics*, *20*(1), 238–242. https://doi.org/10.4103/jcrt.jcrt_383_22

Hao, S., Gestrich, J. Y., Zhang, X., Xu, M., Wang, X., Liu, L., & Wei, H. (2021). Neurotransmitters Affect Larval Development by Regulating the Activity of Prothoracicotropic Hormone-Releasing Neurons in *Drosophila melanogaster*. Frontiers in neuroscience, 15, 653858. https://doi.org/10.3389/fnins.2021.653858

Harris G. W. (1948). Neural control of the pituitary gland. Physiological reviews, 28(2), 139–179. https://doi.org/10.1152/physrev.1948.28.2.139

Harris G. W. (1955). The function of the pituitary stalk. Bulletin of the Johns Hopkins Hospital, 97(5), 358–375.

Heras, V., Castellano, J. M., Fernandois, D., Velasco, I., Rodríguez-Vazquez, E., Roa, J., Vazquez, M. J., Ruiz-Pino, F., Rubio, M., Pineda, R., Torres, E., Avendaño, M. S., Paredes, A., Pinilla, L., Belsham, D., Diéguez, C., Gaytán, F., Casals, N., López, M., & Tena-Sempere, M. (2020). Central Ceramide Signaling Mediates Obesity-Induced Precocious Puberty. Cell metabolism, 32(6), 951–966.e8. https://doi.org/10.1016/j.cmet.2020.10.001

Heras, V., Sangiao-Alvarellos, S., Manfredi-Lozano, M., Sanchez-Tapia, M. J., Ruiz-Pino, F., Roa, J., Lara-Chica, M., Morrugares-Carmona, R., Jouy, N., Abreu, A. P., Prevot, V., Belsham, D., Vazquez, M. J., Calzado, M. A., Pinilla, L., Gaytan, F., Latronico, A. C., Kaiser, U. B., Castellano, J. M., & Tena-Sempere, M. (2019). Hypothalamic miR-30 regulates puberty onset via repression of the puberty-suppressing factor, Mkrn3. PLoS biology, 17(11), e3000532. https://doi.org/10.1371/journal.pbio.3000532

Huang, A., Reinehr, T., & Roth, C. L. (2020). Connections Between Obesity and Puberty: Invited by Manuel Tena-Sempere, Cordoba. Current opinion in endocrine and metabolic research, 14, 160–168. https://doi.org/10.1016/j.coemr.2020.08.004

Hückesfeld, S., Schlegel, P., Miroschnikow, A., Schoofs, A., Zinke, I., Haubrich, A. N., Schneider-Mizell, C. M., Truman, J. W., Fetter, R. D., Cardona, A., & Pankratz, M. J. (2021). Unveiling the sensory and interneuronal pathways of the neuroendocrine connectome in *Drosophila*. eLife, 10, e65745. https://doi.org/10.7554/eLife.65745

Hwang, H. Y., Shim, J. S., Kim, D., & Kwon, H. J. (2021). Antidepressant drug sertraline modulates AMPK-MTOR signaling-mediated autophagy via targeting mitochondrial VDAC1 protein. Autophagy, 17(10), 2783–2799. https://doi.org/10.1080/15548627.2020.1841953

Ibitoye, M., Choi, C., Tai, H., Lee, G., & Sommer, M. (2017). Early menarche: A systematic review of its effect on sexual and reproductive health in low- and middle-income countries. PloS one, 12(6), e0178884. https://doi.org/10.1371/journal.pone.0178884

Imura, E., Shimada-Niwa, Y., Nishimura, T., Hückesfeld, S., Schlegel, P., Ohhara, Y., Kondo, S., Tanimoto, H., Cardona, A., Pankratz, M. J., & Niwa, R. (2020). The Corazonin-PTTH Neuronal Axis Controls Systemic Body Growth by Regulating Basal Ecdysteroid Biosynthesis in *Drosophila melanogaster*. Current biology: CB, 30(11), 2156–2165.e5. https://doi.org/10.1016/j.cub.2020.03.050

Jin, J. M., & Yang, W. X. (2014). Molecular regulation of hypothalamus-pituitary-gonads axis in males. Gene, 551(1), 15–25. https://doi.org/10.1016/j.gene.2014.08.048

Johnson, A. A., & Cuellar, T. L. (2023). Glycine and aging: Evidence and mechanisms. Ageing research reviews, 87, 101922. https://doi.org/10.1016/j.arr.2023.101922

Juarez-Carreño, S., Vallejo, D. M., Carranza-Valencia, J., Palomino-Schätzlein, M., Ramon-Cañellas, P., Santoro, R., de Hartog, E., Ferres-Marco, D., Romero, A., Peterson, H. P., Ballesta-Illan, E., Pineda-Lucena, A., Dominguez, M., & Morante, J. (2021). Body-fat sensor triggers ribosome maturation in the steroidogenic gland to initiate sexual maturation in *Drosophila*. Cell reports, 37(2), 109830. https://doi.org/10.1016/j.celrep.2021.109830

Kaushik, S., & Cuervo, A. M. (2012). Chaperone-mediated autophagy: a unique way to enter the lysosome world. Trends in cell biology, 22(8), 407–417. https://doi.org/10.1016/j.tcb.2012.05.006

Kawade R. (2012). Zinc status and its association with the health of adolescents: a review of studies in India. Global health action, 5, 7353. https://doi.org/10.3402/gha.v5i0.7353

Kawakami, A., Kataoka, H., Oka, T., Mizoguchi, A., Kimura-Kawakami, M., Adachi, T., Iwami, M., Nagasawa, H., Suzuki, A., & Ishizaki, H. (1990). Molecular cloning of the Bombyx mori prothoracicotropic hormone. Science (New York, N.Y.), 247(4948), 1333–1335. https://doi.org/10.1126/science.2315701

Kennedy, E. P., & Lehninger, A. L. (1949). Oxidation of fatty acids and tricarboxylic acid cycle intermediates by isolated rat liver mitochondria. The Journal of biological chemistry, 179(2), 957–972.

Kennedy, E. P., & Weiss, S. B. (1956). The function of cytidine coenzymes in the biosynthesis of phospholipides. The Journal of biological chemistry, 222(1), 193–214.

Khezri, R., & Rusten, T. E. (2019). Autophagy and Tumorigenesis in *Drosophila*. Advances in experimental medicine and biology, 1167, 113–127. https://doi.org/10.1007/978-3-030-23629-8_7

Kikuchi, G., Motokawa, Y., Yoshida, T., & Hiraga, K. (2008). Glycine cleavage system: reaction mechanism, physiological significance, and hyperglycinemia. Proceedings of the Japan Academy. Series B, Physical and biological sciences, 84(7), 246–263. https://doi.org/10.2183/pjab.84.246

Klionsky D. J. (2008). Autophagy revisited: a conversation with Christian de Duve. *Autophagy*, *4*(6), 740–743. https://doi.org/10.4161/auto.6398

Klionsky, D. J., Petroni, G., Amaravadi, R. K., Baehrecke, E. H., Ballabio, A., Boya, P., Bravo-San Pedro, J. M., Cadwell, K., Cecconi, F., Choi, A. M. K., Choi, M. E., Chu, C. T., Codogno, P., Colombo, M. I., Cuervo, A. M., Deretic, V., Dikic, I., Elazar, Z., Eskelinen, E. L., Fimia, G. M., … Pietrocola, F. (2021). Autophagy in major human diseases. The EMBO journal, 40(19), e108863. https://doi.org/10.15252/embj.2021108863

Koyama, T., & Mirth, C. K. (2021). Ecdysone Quantification from Whole Body Samples of Drosophila melanogaster Larvae. Bio-protocol, 11(3), e3915. https://doi.org/10.21769/BioProtoc.3915

Kozioł-Kozakowska, A., Januś, D., Stępniewska, A., Szczudlik, E., Stochel-Gaudyn, A., & Wójcik, M. (2023). Beyond the Metabolic Syndrome: Non-Obvious Complications of Obesity in Children. Children (Basel, Switzerland), 10(12), 1905. https://doi.org/10.3390/children10121905

Kuma, A., Komatsu, M., & Mizushima, N. (2017). Autophagy-monitoring and autophagy-deficient mice. Autophagy, 13(10), 1619–1628. https://doi.org/10.1080/15548627.2017.1343770

Kumar, P., Osahon, O. W., & Sekhar, R. V. (2022). GlyNAC (Glycine and N-Acetylcysteine) Supplementation in Mice Increases Length of Life by Correcting Glutathione Deficiency, Oxidative Stress, Mitochondrial Dysfunction, Abnormalities in Mitophagy and Nutrient Sensing, and Genomic Damage. Nutrients, 14(5), 1114. https://doi.org/10.3390/nu14051114

Kumar, R., Mal, K., Razaq, M. K., Magsi, M., Memon, M. K., Memon, S., Afroz, M. N., Siddiqui, H. F., & Rizwan, A. (2020). Association of Leptin With Obesity and Insulin Resistance. Cureus, 12(12), e12178. https://doi.org/10.7759/cureus.12178

Kunz, J. B., Schwarz, H., & Mayer, A. (2004). Determination of four sequential stages during microautophagy in vitro. The Journal of biological chemistry, 279(11), 9987–9996. https://doi.org/10.1074/jbc.M307905200

Lavrynenko, O., Rodenfels, J., Carvalho, M., Dye, N. A., Lafont, R., Eaton, S., & Shevchenko, A. (2015). The ecdysteroidome of *Drosophila*: influence of diet and development. Development (Cambridge, England), 142(21), 3758–3768. https://doi.org/10.1242/dev.124982

Lee P. A. (2024). Short Adult Height After Rapid-tempo Puberty: When is it too Late to Treat. Journal of clinical research in pediatric endocrinology, 16(2), 235–242. https://doi.org/10.4274/jcrpe.galenos.2024.2024-1-13

Lee, J., Lee, K. J., Hwang, D. W., & Hong, S. M. (2024). Malignant potential of neuroendocrine microtumor of the pancreas harboring high-grade transformation: lesson learned from a patient with von Hippel-Lindau syndrome. *Journal of pathology and translational medicine*, *58*(2), 91–97. https://doi.org/10.4132/jptm.2024.02.13

Lee, J., Song, Y., Kim, Y. A., Kim, I., Cha, J., Lee, S. W., Ko, Y., Kim, C. S., Kim, S., & Lee, S. (2024). Characterization of a new selective glucocorticoid receptor modulator with anorexigenic activity. Scientific reports, 14(1), 7844. https://doi.org/10.1038/s41598-024-58546-1

Li, W. H., Li, Z. Q., Bu, M. D., Li, J. Z., & Chen, L. B. (2024). Metabolomic-based analysis reveals bile acid-mediated ovarian failure induced by low temperature in zebrafish. Zoological research, 45(4), 791–804. https://doi.org/10.24272/j.issn.2095-8137.2023.369

Li, W. W., Li, J., & Bao, J. K. (2012). Microautophagy: lesser-known self-eating. Cellular and molecular life sciences : CMLS, 69(7), 1125–1136. https://doi.org/10.1007/s00018-011-0865-5

Li, Z., Qian, W., Song, W., Zhao, T., Yang, Y., Wang, W., Wei, L., Zhao, D., Li, Y., Perrimon, N., Xia, Q., & Cheng, D. (2022). A salivary gland-secreted peptide regulates insect systemic growth. Cell reports, 38(8), 110397. https://doi.org/10.1016/j.celrep.2022.110397

Liu Z. (2024). Association between 25-hydroxyvitamin D concentrations and pubertal timing: 6-14-year-old children and adolescents in the NHANES 2015-2016. Frontiers in endocrinology, 15, 1394347. https://doi.org/10.3389/fendo.2024.1394347

Liu, J., Liu, W., Lu, Y., Tian, H., Duan, C., Lu, L., Gao, G., Wu, X., Wang, X., & Yang, H. (2018). Piperlongumine restores the balance of autophagy and apoptosis by increasing BCL2 phosphorylation in rotenone-induced Parkinson disease models. Autophagy, 14(5), 845–861. https://doi.org/10.1080/15548627.2017.1390636

Lomniczi, A., Loche, A., Castellano, J. M., Ronnekleiv, O. K., Bosch, M., Kaidar, G., Knoll, J. G., Wright, H., Pfeifer, G. P., & Ojeda, S. R. (2013). Epigenetic control of female puberty. Nature neuroscience, 16(3), 281–289. https://doi.org/10.1038/nn.3319

Luka, Z., Cerone, R., Phillips, J. A., Mudd, H. S., & Wagner, C. (2002). Mutations in human glycine N-methyltransferase give insights into its role in methionine metabolism. Human Genetics, 110(1), 68–74. https://doi.org/10.1007/s00439-001-0648-4

Majcher, A., Czerwonogrodzka-Senczyna, A., Kądziela, K., Rumińska, M., & Pyrżak, B. (2021). Development of obesity from childhood to adolescents. Rozwój otyłości od dzieciństwa do wieku młodzieńczego. Pediatric endocrinology, diabetes, and metabolism, 27(2), 70–75. https://doi.org/10.5114/pedm.2021.105297

Marshall, W. A., & Tanner, J. M. (1969). Variations in pattern of pubertal changes in girls. Archives of disease in childhood, 44(235), 291–303. https://doi.org/10.1136/adc.44.235.291

Marshall, W. A., & Tanner, J. M. (1970). Variations in the pattern of pubertal changes in boys. Archives of disease in childhood, 45(239), 13–23. https://doi.org/10.1136/adc.45.239.13

Martínez-Chantar, M. L., Vázquez-Chantada, M., Ariz, U., Martínez, N., Varela, M., Luka, Z., Capdevila, A., Rodríguez, J., Aransay, A. M., Matthiesen, R., et al. (2008). Loss of the glycine N-methyltransferase gene leads to steatosis and hepatocellular carcinoma in mice. Hepatology, 47(4), 1191–1199. https://doi.org/10.1002/hep.22159

Mathai, B. J., Meijer, A. H., & Simonsen, A. (2017). Studying Autophagy in Zebrafish. Cells, 6(3), 21. https://doi.org/10.3390/cells6030021

Matt, D. W., Kauma, S. W., Pincus, S. M., Veldhuis, J. D., & Evans, W. S. (1998). Characteristics of luteinizing hormone secretion in younger versus older premenopausal women. American journal of obstetrics and gynecology, 178(3), 504–510. https://doi.org/10.1016/s0002-9378(98)70429-6

McBrayer, Z., Ono, H., Shimell, M., Parvy, J. P., Beckstead, R. B., Warren, J. T., Thummel, C. S., Dauphin-Villemant, C., Gilbert, L. I., & O'Connor, M. B. (2007). Prothoracicotropic hormone regulates developmental timing and body size in *Drosophila*. Developmental cell, 13(6), 857–871. https://doi.org/10.1016/j.devcel.2007.11.003

McCarrison, S., Denker, M., Dunne, J., Horrocks, I., McNeilly, J., Joseph, S., & Wong, S. C. (2024). Frequency of Delayed Puberty in Boys with Contemporary Management of Duchenne Muscular Dystrophy. Journal of clinical research in pediatric endocrinology, 10.4274/jcrpe.galenos.2024.2024-2-18. Advance online publication. https://doi.org/10.4274/jcrpe.galenos.2024.2024-2-18

Meléndez-Hevia, E., De Paz-Lugo, P., Cornish-Bowden, A., & Cárdenas, M. L. (2009). A weak link in metabolism: the metabolic capacity for glycine biosynthesis does not satisfy the need for collagen synthesis. Journal of biosciences, 34(6), 853–872. https://doi.org/10.1007/s12038-009-0100-9

Mendle, J., Leve, L. D., Van Ryzin, M., & Natsuaki, M. N. (2014). Linking Childhood Maltreatment with Girls' Internalizing Symptoms: Early Puberty as a Tipping Point. Journal of research on adolescence: the official journal of the Society for Research on Adolescence, 24(4), 689–702. https://doi.org/10.1111/jora.12075

Messina, A., Langlet, F., Chachlaki, K., Roa, J., Rasika, S., Jouy, N., Gallet, S., Gaytan, F., Parkash, J., Tena-Sempere, M., Giacobini, P., & Prevot, V. (2016). A microRNA switch regulates the rise in hypothalamic GnRH production before puberty. Nature neuroscience, 19(6), 835–844. https://doi.org/10.1038/nn.4298

Mizushima N. (2007). Autophagy: process and function. Genes & development, 21(22), 2861–2873. https://doi.org/10.1101/gad.1599207

Moeller, M. E., Danielsen, E. T., Herder, R., O'Connor, M. B., & Rewitz, K. F. (2013). Dynamic feedback circuits function as a switch for shaping a maturation-inducing steroid pulse in *Drosophila*. Development (Cambridge, England), 140(23), 4730–4739. https://doi.org/10.1242/dev.099739

Mohanasundaram, P., Coelho-Rato, L. S., Modi, M. K., Urbanska, M., Lautenschläger, F., Cheng, F., & Eriksson, J. E. (2022). Cytoskeletal vimentin regulates cell size and autophagy through mTORC1 signaling. PLoS biology, 20(9), e3001737. https://doi.org/10.1371/journal.pbio.3001737

Montague, C. T., Farooqi, I. S., Whitehead, J. P., Soos, M. A., Rau, H., Wareham, N. J., Sewter, C. P., Digby, J. E., Mohammed, S. N., Hurst, J. A., Cheetham, C. H., Earley, A. R., Barnett, A. H., Prins, J. B., & O'Rahilly, S. (1997). Congenital leptin deficiency is associated with severe early-onset obesity in humans. Nature, 387(6636), 903–908. https://doi.org/10.1038/43185

Morano, R., Yates, E., Barnes, R., Wohleb, E. S., & Perez-Tilve, D. (2022). Influence of Nutritional Status and Leptin Action on Agrp and Pomc Co-Expression in Hypothalamic Melanocortin System Neurons. Neuroendocrinology, 112(3), 287–297. https://doi.org/10.1159/000516834

Morishita, H., Hashimoto, T., Kishi, K., Nakago, K., Mitani, H., Tomioka, M., Kuroiwa, S., & Miyauchi, Y. (1981). Effects of glycine on serum gonadotropins and estradiol and on concentrations of free amino acids in the middle hypothalamus in female rats. Gynecologic and obstetric investigation, 12(4), 187–196. https://doi.org/10.1159/000299602

Nakamoto, M., Fukasawa, M., Orii, S., Shimamori, K., Maeda, T., Suzuki, A., Matsuda, M., Kobayashi, T., Nagahama, Y., & Shibata, N. (2010). Cloning and expression of medaka cholesterol side chain cleavage cytochrome P450 during gonadal development. Development, growth & differentiation, 52(4), 385–395. https://doi.org/10.1111/j.1440-169X.2010.01178.x

Natali, A. L., Reddy, V., & Bordoni, B. (2023). Neuroanatomy, Corticospinal Cord Tract. In StatPearls. StatPearls Publishing.

Navarro, V. M., Castellano, J. M., Fernández-Fernández, R., Barreiro, M. L., Roa, J., Sanchez-Criado, J. E., Aguilar, E., Dieguez, C., Pinilla, L., & Tena-Sempere, M. (2004). Developmental and hormonally regulated messenger ribonucleic acid expression of KiSS-1 and its putative receptor, GPR54, in rat hypothalamus and potent luteinizing hormone-releasing activity of KiSS-1 peptide. Endocrinology, 145(10), 4565–4574. https://doi.org/10.1210/en.2004-0413

NCD Risk Factor Collaboration (NCD-RisC) (2017). Worldwide trends in body-mass index, underweight, overweight, and obesity from 1975 to 2016: a pooled analysis of 2416 population-based measurement studies in 128·9 million children, adolescents, and adults. Lancet (London, England), 390(10113), 2627–2642. https://doi.org/10.1016/S0140-6736(17)32129-3

Ni, J. Q., Zhou, R., Czech, B., Liu, L. P., Holderbaum, L., Yang-Zhou, D., Shim, H. S., Tao, R., Handler, D., Karpowicz, P., Binari, R., Booker, M., Brennecke, J., Perkins, L. A., Hannon, G. J., & Perrimon, N. (2011). A genome-scale shRNA resource for transgenic RNAi in Drosophila. Nature methods, 8(5), 405–407. https://doi.org/10.1038/nmeth.1592

Nijhout, H. F., & Williams, C. M. (1974). Control of moulting and metamorphosis in the tobacco hornworm, Manduca sexta (L.): growth of the last-instar larva and the decision to pupate. The Journal of experimental biology, 61(2), 481–491. https://doi.org/10.1242/jeb.61.2.481

Niwa, R., Matsuda, T., Yoshiyama, T., Namiki, T., Mita, K., Fujimoto, Y., & Kataoka, H. (2004). CYP306A1, a cytochrome P450 enzyme, is essential for ecdysteroid biosynthesis in the prothoracic glands of Bombyx and Drosophila. The Journal of biological chemistry, 279(34), 35942–35949. https://doi.org/10.1074/jbc.M404514200

Nogueiras, R., Habegger, K. M., Chaudhary, N., Finan, B., Banks, A. S., Dietrich, M. O., Horvath, T. L., Sinclair, D. A., Pfluger, P. T., & Tschöp, M. H. (2012). Sirtuin 1 and sirtuin 3: physiological modulators of metabolism. Physiological reviews, 92(3), 1479–1514. https://doi.org/10.1152/physrev.00022.2011

Oakley, A. E., Clifton, D. K., & Steiner, R. A. (2009). Kisspeptin signaling in the brain. Endocrine reviews, 30(6), 713–743. https://doi.org/10.1210/er.2009-0005

Ohhara, Y., Shimada-Niwa, Y., Niwa, R., Kayashima, Y., Hayashi, Y., Akagi, K., Ueda, H., Yamakawa-Kobayashi, K., & Kobayashi, S. (2015). Autocrine regulation of ecdysone synthesis by β3-octopamine receptor in the prothoracic gland is essential for *Drosophila* metamorphosis. Proceedings of the National Academy of Sciences of the United States of America, 112(5), 1452–1457. https://doi.org/10.1073/pnas.1414966112

Ohtaki, T., Shintani, Y., Honda, S., Matsumoto, H., Hori, A., Kanehashi, K., Terao, Y., Kumano, S., Takatsu, Y., Masuda, Y., Ishibashi, Y., Watanabe, T., Asada, M., Yamada, T., Suenaga, M., Kitada, C., Usuki, S., Kurokawa, T., Onda, H., Nishimura, O., … Fujino, M. (2001). Metastasis suppressor gene KiSS-1 encodes peptide ligand of a G-protein-coupled receptor. Nature, 411(6837), 613–617. https://doi.org/10.1038/35079135

Ommati, M. M., Heidari, R., Manthari, R. K., Tikka Chiranjeevi, S., Niu, R., Sun, Z., Sabouri, S., Zamiri, M. J., Zaker, L., Yuan, J., Wang, J., Zhang, J., & Wang, J. (2019). Paternal exposure to arsenic resulted in oxidative stress, autophagy, and mitochondrial impairments in the HPG axis of pubertal male offspring. Chemosphere, 236, 124325. https://doi.org/10.1016/j.chemosphere.2019.07.056

Palmert, M. R., & Dunkel, L. (2012). Clinical practice. Delayed puberty. The New England journal of medicine, 366(5), 443–453. https://doi.org/10.1056/NEJMcp1109290

Palomino-Schätzlein, M., Carranza-Valencia, J., Guirado, J., Juarez-Carreño, S., & Morante, J. (2022). A toolbox to study metabolic status of *Drosophila melanogaster* larvae. *STAR protocols*, 3(1), 101195. https://doi.org/10.1016/j.xpro.2022.101195

Pan, X., & O'Connor, M. B. (2021). Coordination among multiple receptor tyrosine kinase signals controls *Drosophila* developmental timing and body size. Cell reports, 36(9), 109644. https://doi.org/10.1016/j.celrep.2021.109644

Pan, X., Neufeld, T. P., & O'Connor, M. B. (2019). A Tissue- and Temporal-Specific Autophagic Switch Controls *Drosophila* Pre-metamorphic Nutritional Checkpoints. Current biology : CB, 29(17), 2840–2851.e4. https://doi.org/10.1016/j.cub.2019.07.027

Pangelinan, M. M., Leonard, G., Perron, M., Pike, G. B., Richer, L., Veillette, S., Pausova, Z., & Paus, T. (2016). Puberty and testosterone shape the corticospinal tract during male adolescence. Brain structure & function, 221(2), 1083–1094. https://doi.org/10.1007/s00429-014-0956-9

Park, J. M., Lee, D. H., & Kim, D. H. (2023). Redefining the role of AMPK in autophagy and the energy stress response. Nature communications, 14(1), 2994. https://doi.org/10.1038/s41467-023-38401-z

Payne, A. H., & Hales, D. B. (2004). Overview of steroidogenic enzymes in the pathway from cholesterol to active steroid hormones. Endocrine reviews, 25(6), 947–970. https://doi.org/10.1210/er.2003-0030

Pereira, A., Busch, A. S., Solares, F., Baier, I., Corvalan, C., & Mericq, V. (2021). Total and Central Adiposity Are Associated With Age at Gonadarche and Incidence of Precocious Gonadarche in Boys. The Journal of clinical endocrinology and metabolism, 106(5), 1352–1361. https://doi.org/10.1210/clinem/dgab064

Pinilla, L., Aguilar, E., Dieguez, C., Millar, R. P., & Tena-Sempere, M. (2012). Kisspeptins and reproduction: physiological roles and regulatory mechanisms. Physiological reviews, 92(3), 1235–1316. https://doi.org/10.1152/physrev.00037.2010

Plant T. M. (2015). Neuroendocrine control of the onset of puberty. Frontiers in neuroendocrinology, 38, 73–88. https://doi.org/10.1016/j.yfrne.2015.04.002

Qi, X., Zhang, M., Sun, M., Luo, D., Guan, Q., & Yu, C. (2022). Restoring Impaired Fertility Through Diet: Observations of Switching From High-Fat Diet During Puberty to Normal Diet in Adulthood Among Obese Male Mice. Frontiers in endocrinology, 13, 839034. https://doi.org/10.3389/fendo.2022.839034

Qiu, X., Dao, H., Wang, M., Heston, A., Garcia, K. M., Sangal, A., Dowling, A. R., Faulkner, L. D., Molitor, S. C., Elias, C. F., & Hill, J. W. (2015). Insulin and Leptin Signaling Interact in the Mouse Kiss1 Neuron during the Peripubertal Period. PloS one, 10(5), e0121974. https://doi.org/10.1371/journal.pone.0121974

Rabinowitz, J. D., & White, E. (2010). Autophagy and metabolism. Science (New York, N.Y.), 330(6009), 1344–1348. https://doi.org/10.1126/science.1193497

Rewitz, K. F., Rybczynski, R., Warren, J. T., & Gilbert, L. I. (2006). The Halloween genes code for cytochrome P450 enzymes mediating synthesis of the insect moulting hormone. Biochemical Society transactions, 34(Pt 6), 1256–1260. https://doi.org/10.1042/BST0341256

Rewitz, K. F., Rybczynski, R., Warren, J. T., & Gilbert, L. I. (2006). Identification, characterization and developmental expression of Halloween genes encoding P450 enzymes mediating ecdysone biosynthesis in the tobacco hornworm, Manduca sexta. Insect biochemistry and molecular biology, 36(3), 188–199. https://doi.org/10.1016/j.ibmb.2005.12.002

Rewitz, K. F., Yamanaka, N., & O'Connor, M. B. (2013). Developmental checkpoints and feedback circuits time insect maturation. Current topics in developmental biology, 103, 1–33. https://doi.org/10.1016/B978-0-12-385979-2.00001-0

Rewitz, K. F., Yamanaka, N., Gilbert, L. I., & O'Connor, M. B. (2009). The insect neuropeptide PTTH activates receptor tyrosine kinase torso to initiate metamorphosis. Science (New York, N.Y.), 326(5958), 1403–1405. https://doi.org/10.1126/science.1176450

Riddiford, L. M., Truman, J. W., Mirth, C. K., & Shen, Y. C. (2010). A role for juvenile hormone in the prepupal development of Drosophila melanogaster. Development (Cambridge, England), 137(7), 1117–1126. https://doi.org/10.1242/dev.037218

Roa, J., Navarro, V. M., & Tena-Sempere, M. (2011). Kisspeptins in reproductive biology: consensus knowledge and recent developments. Biology of reproduction, 85(4), 650–660. https://doi.org/10.1095/biolreprod.111.091538

Rom, O., Grajeda-Iglesias, C., Najjar, M., Abu-Saleh, N., Volkova, N., Dar, D. E., Hayek, T., & Aviram, M. (2017). Atherogenicity of amino acids in the lipid-laden macrophage model system in vitro and in atherosclerotic mice: a key role for triglyceride metabolism. The Journal of nutritional biochemistry, 45, 24–38. https://doi.org/10.1016/j.jnutbio.2017.02.023

Rosenfield, R. L., Lipton, R. B., & Drum, M. L. (2009). Thelarche, pubarche, and menarche attainment in children with normal and elevated body mass index. *Pediatrics*, *123*(1), 84–88. https://doi.org/10.1542/peds.2008-0146

Roux, M. J., & Supplisson, S. (2000). Neuronal and glial glycine transporters have different stoichiometries. Neuron, 25(2), 373–383. https://doi.org/10.1016/s0896-6273(00)80901-0

Sagers, R. D., & Gunsalus, I. C. (1961). Intermediatry metabolism of Diplococcus glycinophilus. I. Glycine cleavage and one-carbon interconversions. Journal of bacteriology, 81(4), 541–549. https://doi.org/10.1128/jb.81.4.541-549.1961

Salazar, G., Cullen, A., Huang, J., Zhao, Y., Serino, A., Hilenski, L., Patrushev, N., Forouzandeh, F., & Hwang, H. S. (2020). SQSTM1/p62 and PPARGC1A/PGC-1alpha at the interface of autophagy and vascular senescence. Autophagy, 16(6), 1092–1110. https://doi.org/10.1080/15548627.2019.1659612

Samavat, J., Natali, I., Degl'Innocenti, S., Filimberti, E., Cantini, G., Di Franco, A., Danza, G., Seghieri, G., Lucchese, M., Baldi, E., Forti, G., & Luconi, M. (2014). Acrosome reaction is impaired in spermatozoa of obese men: a preliminary study. Fertility and sterility, 102(5), 1274–1281.e2. https://doi.org/10.1016/j.fertnstert.2014.07.1248

Scacchi, P., Carbone, S., Szwarcfarb, B., Rondina, D., Wuttke, W., & Moguilevsky, J. A. (1998). Interactions between GABAergic and serotoninergic systems with excitatory amino acid neurotransmission in the hypothalamic control of gonadotropin secretion in prepubertal female rats. *Brain research. Developmental brain research*, *105*(1), 51–58. https://doi.org/10.1016/S0165-3806(97)00161-2

Schlomer, G. L., & Marceau, K. (2022). Father absence, age at menarche, and genetic confounding: A replication and extension using a polygenic score. Development and psychopathology, 34(1), 355–366. https://doi.org/10.1017/S0954579420000929

Setiawan, L., Pan, X., Woods, A. L., O'Connor, M. B., & Hariharan, I. K. (2018). The BMP2/4 ortholog Dpp can function as an inter-organ signal that regulates developmental timing. Life science alliance, 1(6), e201800216. https://doi.org/10.26508/lsa.201800216

Shah, R. D., Braffett, B. H., Tryggestad, J. B., Hughan, K. S., Dhaliwal, R., Nadeau, K. J., Levitt Katz, L. E., & Gidding, S. S. (2022). Cardiovascular risk factor progression in adolescents and young adults with youth-onset type 2 diabetes. Journal of diabetes and its complications, 36(3), 108123. https://doi.org/10.1016/j.jdiacomp.2021.108123

Shao, J., Wang, J., Wen, X., Xie, J., Huang, F., Guan, X., Hao, X., Duan, P., Chen, C., & Chen, H. (2023). Effects of aging and macrophages on mice stem Leydig cell proliferation and differentiation in vitro. Frontiers in endocrinology, 14, 1139281. https://doi.org/10.3389/fendo.2023.1139281

Shi, L., Jiang, Z., & Zhang, L. (2022). Childhood obesity and central precocious puberty. Frontiers in endocrinology, 13, 1056871. https://doi.org/10.3389/fendo.2022.1056871

Shimada-Niwa, Y., & Niwa, R. (2014). Serotonergic neurons respond to nutrients and regulate the timing of steroid hormone biosynthesis in *Drosophila*. Nature communications, 5, 5778. https://doi.org/10.1038/ncomms6778

Shimell, M., Pan, X., Martin, F. A., Ghosh, A. C., Leopold, P., O'Connor, M. B., & Romero, N. M. (2018). Prothoracicotropic hormone modulates environmental adaptive plasticity through the control of developmental timing. Development (Cambridge, England), 145(6), dev159699. https://doi.org/10.1242/dev.159699

Singh, R., Kaushik, S., Wang, Y., Xiang, Y., Novak, I., Komatsu, M., Tanaka, K., Cuervo, A. M., & Czaja, M. J. (2009). Autophagy regulates lipid metabolism. Nature, 458(7242), 1131–1135. https://doi.org/10.1038/nature07976

Singh, S. I., & Malhotra, C. I. (1964). Amino acid content of monkey brain. 3. Effects of reserpine on some amino acids of certain regions of monkey brain. Journal of neurochemistry, 11, 865–872. https://doi.org/10.1111/j.1471-4159.1964.tb06737.x

Singh, S. M., Gauthier, S., & Labrie, F. (2000). Androgen receptor antagonists (antiandrogens): structure-activity relationships. Current medicinal chemistry, 7(2), 211–247. https://doi.org/10.2174/0929867003375371

Soliman, A. T., Alaaraj, N., Noor Hamed, Alyafei, F., Ahmed, S., Shaat, M., Itani, M., Elalaily, R., & Soliman, N. (2022). Review Nutritional interventions during adolescence and their possible effects. Acta bio-medica: Atenei Parmensis, 93(1), e2022087. https://doi.org/10.23750/abm.v93i1.12789

Søreng, K., Neufeld, T. P., & Simonsen, A. (2018). Membrane Trafficking in Autophagy. International review of cell and molecular biology, 336, 1–92. https://doi.org/10.1016/bs.ircmb.2017.07.001

Soria-Gómez, E., Bellocchio, L., Reguero, L., Lepousez, G., Martin, C., Bendahmane, M., Ruehle, S., Remmers, F., Desprez, T., Matias, I., Wiesner, T., Cannich, A., Nissant, A., Wadleigh, A., Pape, H. C., Chiarlone, A. P., Quarta, C., Verrier, D., Vincent, P., Massa, F., … Marsicano, G. (2014). The endocannabinoid system controls food intake via olfactory processes. Nature neuroscience, 17(3), 407–415. https://doi.org/10.1038/nn.3647

Stanley, T., Misra, M. (2021). Delayed or Stalled Pubertal Development. In: Stanley, T., Misra, M. (eds) Endocrine Conditions in Pediatrics. Springer, Cham. https://doi.org/10.1007/978-3-030-52215-5_11

Stratford, T. R., & Wirtshafter, D. (2013). Lateral hypothalamic involvement in feeding elicited from the ventral pallidum. The European journal of neuroscience, 37(4), 648–653. https://doi.org/10.1111/ejn.12077

Summerville, J. B., Faust, J. F., Fan, E., Pendin, D., Daga, A., Formella, J., Stern, M., & McNew, J. A. (2016). The effects of ER morphology on synaptic structure and function in Drosophila melanogaster. *Journal of cell science*, *129*(8), 1635–1648. https://doi.org/10.1242/jcs.184929

Sun, Y., Huang, S., Wang, S., Guo, D., Ge, C., Xiao, H., Jie, W., Yang, Q., Teng, X., & Li, F. (2017). Large-scale identification of differentially expressed genes during pupa development reveals solute carrier gene is essential for pupal pigmentation in Chilo suppressalis. Journal of insect physiology, 98, 117–125. https://doi.org/10.1016/j.jinsphys.2016.12.007

Sun, Y., Zheng, Y., Wang, C., & Liu, Y. (2018). Glutathione depletion induces ferroptosis, autophagy, and premature cell senescence in retinal pigment epithelial cells. Cell death & disease, 9(7), 753. https://doi.org/10.1038/s41419-018-0794-4

Tanner J. M. (1981). Growth and maturation during adolescence. Nutrition reviews, 39(2), 43–55. https://doi.org/10.1111/j.1753-4887.1981.tb06734.x

Tarçin, G., Bayramoğlu, E., Güneş Kaya, D., Karakaş, H., Demirbaş, K. C., Turan, H., & Evliyaoğlu, O. (2024). The role of body composition and appetite-regulating hormones in idiopathic central precocious puberty and their changes during GnRH analog therapy. Journal of endocrinological investigation, 10.1007/s40618-024-02413-3. Advance online publication. https://doi.org/10.1007/s40618-024-02413-3

Tekirdag, K., & Cuervo, A. M. (2018). Chaperone-mediated autophagy and endosomal microautophagy: Joint by a chaperone. The Journal of biological chemistry, 293(15), 5414–5424. https://doi.org/10.1074/jbc.R117.818237

Terasawa, E., & Fernandez, D. L. (2001). Neurobiological mechanisms of the onset of puberty in primates. Endocrine reviews, 22(1), 111–151. https://doi.org/10.1210/edrv.22.1.0418

Texada, M. J., Malita, A., Christensen, C. F., Dall, K. B., Faergeman, N. J., Nagy, S., Halberg, K. A., & Rewitz, K. (2019). Autophagy-Mediated Cholesterol Trafficking Controls Steroid Production. Developmental cell, 48(5), 659–671.e4. https://doi.org/10.1016/j.devcel.2019.01.007

Tilbrook, A. J., & Clarke, I. J. (2001). Negative feedback regulation of the secretion and actions of gonadotropin-releasing hormone in males. Biology of reproduction, 64(3), 735–742. https://doi.org/10.1095/biolreprod64.3.735

Todde, V., Veenhuis, M., & van der Klei, I. J. (2009). Autophagy: principles and significance in health and disease. Biochimica et biophysica acta, 1792(1), 3–13. https://doi.org/10.1016/j.bbadis.2008.10.016

Toro, C. A., Aylwin, C. F., & Lomniczi, A. (2018). Hypothalamic epigenetics driving female puberty. Journal of neuroendocrinology, 30(7), e12589. https://doi.org/10.1111/jne.12589

Tracy, K., & Baehrecke, E. H. (2013). The role of autophagy in *Drosophila* metamorphosis. Current topics in developmental biology, 103, 101–125. https://doi.org/10.1016/B978-0-12-385979-2.00004-6

Tran, L. T., Park, S., Kim, S. K., Lee, J. S., Kim, K. W., & Kwon, O. (2022). Hypothalamic control of energy expenditure and thermogenesis. Experimental & molecular medicine, 54(4), 358–369. https://doi.org/10.1038/s12276-022-00741-z

Tsukada, M., & Ohsumi, Y. (1993). Isolation and characterization of autophagy-defective mutants of Saccharomyces cerevisiae. FEBS letters, 333(1-2), 169–174. https://doi.org/10.1016/0014-5793(93)80398-e

Turpin-Nolan, S. M., & Brüning, J. C. (2020). The role of ceramides in metabolic disorders: when size and localization matters. Nature reviews. Endocrinology, 16(4), 224–233. https://doi.org/10.1038/s41574-020-0320-5

Vainshtein, A., Grumati, P., Sandri, M., & Bonaldo, P. (2014). Skeletal muscle, autophagy, and physical activity: the ménage à trois of metabolic regulation in health and disease. Journal of molecular medicine (Berlin, Germany), 92(2), 127–137. https://doi.org/10.1007/s00109-013-1096-z

Varga, V. B., Schuller, D., Szikszai, F., Szinyákovics, J., Puska, G., Vellai, T., & Kovács, T. (2022). Autophagy is required for spermatogonial differentiation in the *Drosophila* testis. Biologia futura, 73(2), 187–204. https://doi.org/10.1007/s42977-022-00122-7

Vazquez, M. J., Toro, C. A., Castellano, J. M., Ruiz-Pino, F., Roa, J., Beiroa, D., Heras, V., Velasco, I., Dieguez, C., Pinilla, L., Gaytan, F., Nogueiras, R., Bosch, M. A., Rønnekleiv, O. K., Lomniczi, A., Ojeda, S. R., & Tena-Sempere, M. (2018). SIRT1 mediates obesity- and nutrient-dependent perturbation of pubertal timing by epigenetically controlling Kiss1 expression. Nature communications, 9(1), 4194. https://doi.org/10.1038/s41467-018-06459-9

Vellai, T., Bicsák, B., Tóth, M. L., Takács-Vellai, K., & Kovács, A. L. (2008). Regulation of cell growth by autophagy. Autophagy, 4(4), 507–509. https://doi.org/10.4161/auto.5670

Vij, N., Chandramani-Shivalingappa, P., Van Westphal, C., Hole, R., & Bodas, M. (2018). Cigarette smoke-induced autophagy impairment accelerates lung aging, COPD-emphysema exacerbations and pathogenesis. American journal of physiology. Cell physiology, 314(1), C73–C87. https://doi.org/10.1152/ajpcell.00110.2016

Vogeler, S., Carboni, S., Li, X., Ireland, J. H., Miller-Ezzy, P., & Joyce, A. (2021). Cloning and characterisation of NMDA receptors in the Pacific oyster, Crassostrea gigas (Thunberg, 1793) in relation to metamorphosis and catecholamine synthesis. Developmental biology, 469, 144–159. https://doi.org/10.1016/j.ydbio.2020.10.008

Vosberg, D. E., Syme, C., Parker, N., Richer, L., Pausova, Z., & Paus, T. (2021). Sex continuum in the brain and body during adolescence and psychological traits. Nature human behaviour, 5(2), 265–272. https://doi.org/10.1038/s41562-020-00968-8

Wang, L., Liu, S., Yang, W., Yu, H., Zhang, L., Ma, P., Wu, P., Li, X., Cho, K., Xue, S., & Jiang, B. (2017). Plasma Amino Acid Profile in Patients with Aortic Dissection. Scientific reports, 7, 40146. https://doi.org/10.1038/srep40146

Wang, M., Zeng, L., Su, P., Ma, L., Zhang, M., & Zhang, Y. Z. (2022). Autophagy: a multifaceted player in the fate of sperm. Human reproduction update, 28(2), 200–231. https://doi.org/10.1093/humupd/dmab043

Wang, S., Fang, J., Li, J., Wang, S., Su, P., Wan, Y., Tao, F., & Sun, Y. (2023). Identification of urine biomarkers associated with early puberty in children: An untargeted metabolomics analysis. Physiology & behavior, 270, 114305. https://doi.org/10.1016/j.physbeh.2023.114305

Wang, W., Wu, Z., Lin, G., Hu, S., Wang, B., Dai, Z., & Wu, G. (2014). Glycine stimulates protein synthesis and inhibits oxidative stress in pig small intestinal epithelial cells. Journal of Nutrition, 144(10), 1540–1548. https://doi.org/10.3945/jn.114.194001

Wang, Y., Jin, C., Li, H., Liang, X., Zhao, C., Wu, N., Yue, M., Zhao, L., Yu, H., Wang, Q., Ge, Y., Huo, M., Lv, X., Zhang, L., Zhao, G., & Gai, Z. (2024). Gut microbiota-metabolite interactions meditate the effect of dietary patterns on precocious puberty. iScience, 27(6), 109887. https://doi.org/10.1016/j.isci.2024.109887

Warren, J. T., Petryk, A., Marqués, G., Parvy, J. P., Shinoda, T., Itoyama, K., Kobayashi, J., Jarcho, M., Li, Y., O'Connor, M. B., Dauphin-Villemant, C., & Gilbert, L. I. (2004). Phantom encodes the 25-hydroxylase of Drosophila melanogaster and Bombyx mori: a P450 enzyme critical in ecdysone biosynthesis. Insect biochemistry and molecular biology, 34(9), 991–1010. https://doi.org/10.1016/j.ibmb.2004.06.009

Warren, J. T., Sakurai, S., Rountree, D. B., & Gilbert, L. I. (1988). Synthesis and secretion of ecdysteroids by the prothoracic glands of Manduca sexta. *Journal of Insect Physiology, 34*(5), 351-361. https://doi.org/10.1016/0022-1910(88)90061-3

Wasinski, F., Furigo, I. C., Teixeira, P. D. S., Ramos-Lobo, A. M., Peroni, C. N., Bartolini, P., List, E. O., Kopchick, J. J., & Donato, J., Jr (2020). Growth Hormone Receptor Deletion Reduces the Density of Axonal Projections from Hypothalamic Arcuate Nucleus Neurons. Neuroscience, 434, 136–147. https://doi.org/10.1016/j.neuroscience.2020.03.037

Wei, C., Davis, N., Honour, J., & Crowne, E. (2017). The investigation of children and adolescents with abnormalities of pubertal timing. Annals of clinical biochemistry, 54(1), 20–32. https://doi.org/10.1177/0004563216668378

Wojciechowska, K., Zie, W., Pietrzyk, A., & Lejman, M. (2024). A four-year-old girl with pathogenic variant in the NAA10 gene and precocious puberty - case report and literature review. Annals of agricultural and environmental medicine : AAEM, 31(2), 306–310. https://doi.org/10.26444/aaem/171758

Wu, G., Bazer, F. W., Dai, Z., Li, D., Wang, J., & Wu, Z. (2014). Amino acid nutrition in animals: protein synthesis and beyond. Annual review of animal biosciences, 2, 387–417. https://doi.org/10.1146/annurev-animal-022513-114113

Wu, J., Chernatynskaya, A., Pfaff, A., Kou, H., Cen, N., Ercal, N., & Shi, H. (2021). Extensive Thiol Profiling for Assessment of Intracellular Redox Status in Cultured Cells by HPLC-MS/MS. Antioxidants (Basel, Switzerland), 11(1), 24. https://doi.org/10.3390/antiox11010024

Xia, C., Zhang, X., Zhang, Y., Li, J., & Xing, H. (2021). Ammonia exposure causes the disruption of the solute carrier family gene network in pigs. Ecotoxicology and environmental safety, 210, 111870. https://doi.org/10.1016/j.ecoenv.2020.111870

Xie, H., Qian, T., Liu, L., Sun, R., Che, W., Zhao, M., Hou, X., Pan, H., Su, Y., Li, J., Dong, X., & Liu, P. (2024). Effect of progestin on thyroid function in female Wistar rats. Frontiers in endocrinology, 15, 1362774. https://doi.org/10.3389/fendo.2024.1362774

Yamanaka, N., Marqués, G., & O'Connor, M. B. (2015). Vesicle-Mediated Steroid Hormone Secretion in Drosophila melanogaster. *Cell*, *163*(4), 907–919. https://doi.org/10.1016/j.cell.2015.10.022

Yamanaka, N., Rewitz, K. F., & O'Connor, M. B. (2013). Ecdysone control of developmental transitions: lessons from Drosophila research. *Annual review of entomology*, *58*, 497–516. https://doi.org/10.1146/annurev-ento-120811-153608

Yang, C., Ran, Z., Liu, G., Hou, R., He, C., Liu, Q., Chen, Y., Liu, Y., Wang, X., Ling, C., Fang, F., & Li, X. (2021). Melatonin Administration Accelerates Puberty Onset in Mice by Promoting FSH Synthesis. Molecules (Basel, Switzerland), 26(5), 1474. https://doi.org/10.3390/molecules26051474

Yang, Z., & Klionsky, D. J. (2010). Mammalian autophagy: core molecular machinery and signaling regulation. Current opinion in cell biology, 22(2), 124–131. https://doi.org/10.1016/j.ceb.2009.11.014

Yin, J., Ren, W., Huang, X., Li, T., & Yin, Y. (2018). Protein restriction and cancer. Biochimica et biophysica acta. Reviews on cancer, 1869(2), 256–262. https://doi.org/10.1016/j.bbcan.2018.03.004

Yu, A., & Lau, A. Y. (2018). Glutamate and Glycine Binding to the NMDA Receptor. Structure (London, England: 1993), 26(7), 1035–1043.e2. https://doi.org/10.1016/j.str.2018.05.004

Yu, Y. M., Yang, R. D., Matthews, D. E., Wen, Z. M., Burke, J. F., Bier, D. M., & Young, V. R. (1985). Quantitative aspects of glycine and alanine nitrogen metabolism in postabsorptive young men: effects of level of nitrogen and dispensable amino acid intake. The Journal of nutrition, 115(3), 399–410. https://doi.org/10.1093/jn/115.3.399

Zhang, L., Li, S., Wang, H., Jia, X., Guo, B., Yang, Z., Fan, C., Zhao, H., Zhao, Z., Zhang, Z., & Yuan, L. (2024). The virtual staining method by quantitative phase imaging for label free lymphocytes based on self-supervised iteration cycle-consistent adversarial networks. *The Review of scientific instruments*, *95*(4), 045103. https://doi.org/10.1063/5.0159400

Zhang, Y., Jia, H., Jin, Y., Liu, N., Chen, J., Yang, Y., Dai, Z., Wang, C., Wu, G., & Wu, Z. (2020). Glycine attenuates LPS-induced apoptosis and inflammatory cell infiltration in mouse liver. Journal of Nutrition, 150(5), 1116–1125. https://doi.org/10.1093/jn/nxaa036

Zhang, Y., Proenca, R., Maffei, M., Barone, M., Leopold, L., & Friedman, J. M. (1994). Positional cloning of the mouse obese gene and its human homologue. Nature, 372(6505), 425–432. https://doi.org/10.1038/372425a0

Zhang, Z., Chen, T., & Ma, J. (2024). Beijing da xue xue bao. Yi xue ban = Journal of Peking University. Health sciences, 56(3), 418–423. https://doi.org/10.19723/j.issn.1671-167X.2024.03.007

Zhou, S., Zang, S., Hu, Y., Shen, Y., Li, H., Chen, W., Li, P., & Shen, Y. (2022). Transcriptome-scale spatial gene expression in rat arcuate nucleus during puberty. Cell & bioscience, 12(1), 8. https://doi.org/10.1186/s13578-022-00745-2

Zhuang, H., Wu, F., Wei, W., Dang, Y., Yang, B., Ma, X., Han, F., & Li, Y. (2019). Glycine decarboxylase induces autophagy and is downregulated by miRNA-30d-5p in hepatocellular carcinoma. Cell death & disease, 10(3), 192. https://doi.org/10.1038/s41419-019-1446-z

Annex 1

Mammalian puberty: a fly perspective

Juan Guirado, Juan Carranza-Valencia and Javier Morante 🄳

Instituto de Neurociencias, Consejo Superior de Investigaciones Científicas (CSIC) and Universidad Miguel Hernández (UMH), San Juan de Alicante, Spain

Mammalian puberty and *Drosophila* metamorphosis, despite their evolutionary distance, exhibit similar design principles and conservation of molecular components. In this Viewpoint, we review recent advances in this area and the similarities between both processes in terms of the signaling pathways and neuroendocrine circuits involved. We argue that the detection and uptake of peripheral fat by *Drosophila* prothoracic endocrine cells induces endomembrane remodeling and ribosomal maturation, leading to the acquisition of high biosynthetic and secretory capacity. The absence of this fat–neuroendocrine interorgan communication leads to giant, obese, non-pupating larvae. Importantly, human leptin is capable of signaling the pupariation process in *Drosophila*, and its expression prevents obesity and triggers maturation in mutants that do not pupate. This implies that insect metamorphosis can be used to address issues related to the biology of leptin and puberty.

Introduction

Puberty marks the transformation of the child into the adult. It constitutes a point of no return defined as the transitional period when sexual maturity is achieved along with important growth and behavioral changes [1,2]. When this change is initiated, upregulation of steroidogenesis leads to an irreversible juvenile-to-adult transition in humans. Insect metamorphosis is the developmental transition comparable to human

1

puberty, and despite more than 500 million years of evolutionary distance between insects and mammals, recent studies summarized in this Viewpoint have shown that the transition from juvenile to adult is well conserved in both and that it is governed by common molecular aspects ([3] and Fig. 1).

Endocrine control of mammalian puberty

In mammals, the reawakening of the hypothalamic–pituitary–gonadal (HPG) axis is what triggers pubertal maturation (Fig. 1). In response to incompletely defined nutrient, endocrine and environmental signals, neuroendocrine gonadotropin-releasing hormone (GnRH) hypothalamic neurons increase their firing properties [4,5], which stimulates the pituitary gland to release the gonadotropins luteinizing hormone and follicle-stimulating hormone. These hormones are then delivered via the circulatory system to promote the maturation of the gonads and the production of sex steroids, which signal back to the HPG axis.

GnRH neurons have the particularity of developing embryonically outside the brain, in the nasal placode, and they migrate to their final position in the hypothalamus before birth [6]. In addition, GnRH neurons during postnatal life recruit other populations—neuronal, glial (tanycytes and astrocytes), and endothelial—that connect with them to establish the 'GnRH neural network' [7–9]. This neural network fine-tunes GnRH production and secretion in time and space. Therefore, defects in the GnRH neurons themselves, or in the GnRH neural network, result in defective or delayed puberty [10]. Interestingly, the intercellular communication within the GnRH neural network is predominantly mediated by semaphorin signaling, which plays a fundamental role in the development of hypothalamic circuits but also in the control of GnRH release by circulating sex steroids [11]. Defective semaphorin signaling leads to hypogonadotropic
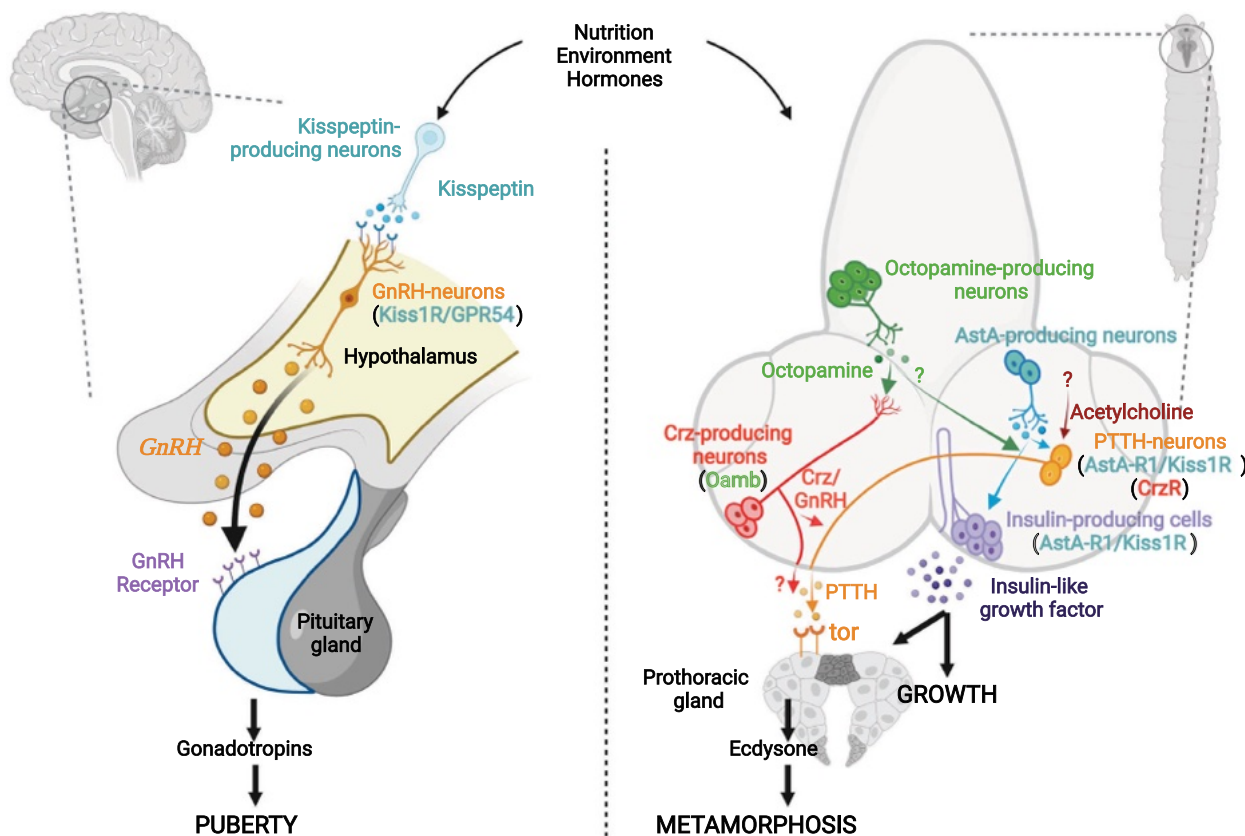
Fig. 1. Neuroendocrine circuits controlling puberty (left) and metamorphosis (right). Note that for simplicity, only one pathway in each *Drosophila* lobe is shown, although these neural circuits are duplicated in each lobe. We have also reversed the orientation of the *Drosophila* larval brain to facilitate comparison with the mammalian brain. AstA, allatostatin A; AstAR1, allatostatin A receptor 1; Crz, corazonin; CrzR, corazonin receptor; GnRH, gonadotropin-releasing hormone; Kiss1, kisspeptin 1; Kiss1R, kisspeptin 1 receptor; Oamb, octopamine receptor in mushroom bodies; PTTH, prothoracicotropic hormone; and tor, torso.

hypogonadism [12], defective neuroendocrine control of the adult ovarian cycle [13], and obesity [14].

The most potent upstream pubertal signal known to activate pulsatile firing of GnRH neurons is the neuropeptide kisspeptin, a product of the *Kiss1* gene, which activates the G protein–coupled membrane receptor Kiss1R (also known as GPR54) in GnRH neurons in the median eminence [15–18]. Mature kisspeptins in mammals are cleaved, and administration of decapeptide Kp10 (Kiss-10), the minimum active site, can elicit a robust increase in the circulating levels of GnRH [19]. Kisspeptin-positive neurons are widespread in the hypothalamus, mainly in the arcuate nucleus and in the rostral anteroventral periventricular area [20], with a third, less explored, population in the amygdala [21].

Kisspeptin neurons in the arcuate nucleus, named kisspeptin/neurokinin B/dynorphin (KNDy) neurons, also coexpress the tachykinin neurokinin B and the endogenous opioid peptide dynorphin [22,23]. Increased activity of the kisspeptin–Kiss1R signal in response to complex and ill-defined reciprocal positive and inhibitory signals mediated by KNDy neurons correlates with the GnRH pulse generator and the onset of puberty [24]. The kisspeptin neuron population in the anteroventral periventricular area is notably larger in female rodents and is involved in the preovulatory surge of gonadotropins [25]. Importantly, a lack of either kisspeptin or Kiss1R results in absent or delayed puberty onset in animals and hypogonadotropic hypogonadism in humans [26–28]. However, genetic ablation of kisspeptin or Kiss1R neurons using a diphtheria toxin fragment specifically in these cells leads to no change in the timing of the onset of puberty or attainment of fertility [29]. Interestingly, if kisspeptin neurons are ablated in adult mice, fertility is inhibited, suggesting that there is compensation during the formation of reproductive neural circuits that occurs early in development [30].

The onset of puberty is regulated by many permissive factors [31]. For example, in seasonal breeders the photoperiod signals the optimal time of year for the onset of puberty [32]. Among the different pubertal regulators, nutritional and metabolic cues have been shown to play a critical role in the central control of puberty, with numerous studies in rodents and humans indicating that a female's fat reserve must exceed a critical threshold to allow the onset of puberty [33] and thus signal the attainment of sufficient somatic growth to support pregnancy. In fact, the escalating prevalence of child obesity has been blamed for alterations of the age of onset of puberty [34], and malnutrition and intensive physical training can delay puberty [35,36].

In this regard, classical studies in mice [37] and humans [38,39] showed that a deficiency of leptin (a hormone secreted by fat cells) or its receptors (which signal the amount of energy stored in the body) leads to hyperphagia, early-onset obesity, and delayed or complete failure to initiate the pubertal transition. Despite these phenotypes and the fact that leptin modulates the expression of Kisspeptin in the hypothalamus [40], leptin receptors are low or null in Kisspeptin neurons and GnR neurons [20,41], which supports an indirect mode of action of leptin and other hormonal signals in the regulation of these neuronal populations via mechanisms that are poorly defined. For example, other populations that would play a fundamental role in these processes would be anorexigenic neurons expressing pro-opiomelanocortin and cocaine- and amphetamine-regulated transcript (POMC/CART neurons) and orexigenic neurons expressing neuropeptide Y and agouti-related peptide (NPY/AgRP neurons), which are activated in conditions of an excess and deficit of energy, respectively. NPY and AgRP have been shown to inhibit Kisspeptin neurons [42], whereas POMC neuropeptides (alpha-melanocyte stimulating hormone and CART) have been reported to modulate GnRH neurosecretory activity acting via melanocortin receptors (MC3R and MC4R) [43–45]. In a recent article, Lam et al. [46] reported that melanocortin signaling via MC3R also plays a fundamental role in the control of puberty in humans. Humans who carry loss-of-function mutations in MC3R showed delayed puberty accompanied by reductions in linear growth, lean mass and circulating levels of insulin-like growth factor I (IGF1), thus linking conserved nutritional cues to control of puberty [46]. Finally, an alternative to the canonical kisspeptin–HPG pathway involving *de novo* ceramide synthesis at the hypothalamic paraventricular nucleus and ovarian sympathetic innervation has recently been characterized as playing a fundamental role in obesity-induced precocious puberty in female rats [47].

While it is mainly lipid signaling molecules that seem to play a fundamental role in the onset of puberty, other master metabolic hypothalamic sensors, such as the mammalian target of rapamycin (mTOR), AMP-activated protein kinase (AMPK) and sirtuin 1 (SIRT1) [48], have also been linked to metabolic/nutritional status and pubertal timing.

For instance, AMPK (a highly conserved serine/threonine kinase that senses glucose and energy status) and SIRT1 (a nicotinamide adenine dinucleotide [NAD+]-dependent deacetylase) are activated in conditions of negative energy balance, and both operate in kisspeptin-positive neurons in the arcuate

hypothalamus to delay pubertal timing independently of body weight [49,50]. At least for SIRT1, pubertal timing mechanistically involves epigenetic repression of the puberty-activating gene *Kiss1* [50]. In contrast, mTOR (a second serine/threonine kinase, which detects amino acid availability) is activated in the inverse pattern and has the opposite behavior to those of AMPK and SIRT1, at the time of puberty [51]. Mechanistically, in mouse embryonic fibroblasts, activated AMPK can inhibit mTORC1 by directly phosphorylating the tumor suppressor tuberous sclerosis complex 2 (TSC2) and the critical mTOR complex 1 (mTORC1)-binding subunit, raptor [52]; in addition, glyceraldehyde 3-phosphate dehydrogenase (GAPDH), a glycolytic enzyme, has been shown to be a critical mediator of AMPK-driven SIRT1 activation [53]. Future research will determine the mode of action of these cellular sensors in Kiss1 cells or in other populations of the GnRH neural network in the control of puberty.

Integration of signals by PTTH neurons in the coordination of growth and metamorphosis

In the larval central brain of *Drosophila melanogaster*, a pair of prothoracicotropic hormone (PTTH)-releasing neurons located in each hemisphere has long been considered to be the primary promoting factor in the biosynthesis of the hormone ecdysone, the main steroid in insects. These neurons project and secrete PTTH, a neuropeptide initially identified in the silkworm *Bombyx mori* [54], into the prothoracic gland (PG), where they activate the Ras/Raf/ERK (extracellular-signal-regulated kinase) MAP (mitogen-activated protein) kinase pathway via its receptor tyrosine kinase, torso, to promote ecdysone production for regulating larval maturation [55]. *Ptth* gene transcription significantly increases 12 h before pupariation, and genetic ablation of PTTH neurons extends the third instar (L3) larval stage and delays the time to pupariation by 4 or 5 days, with a significant increase in adult body size [56]. A recent study in *Ptth*-null mutants showed only a modest delay of 1 day in the timing of metamorphosis [57], indicating that PTTH cannot be considered as the main promotor of ecdysone synthesis. The existence of one or more additional ecdysteroidogenic signals produced by the PTTH neurons could explain the difference in delay observed in response to PTTH loss compared with PTTH neuron ablation [58].

Recent studies have reported that the timing of PTTH secretion is controlled by different neuropeptides expressed in different larval cell populations (Fig. 1), including the *Drosophila* kisspeptin homolog allatostatin A (AstA) [59] and GnRH homolog corazonin [60], as well as the neurotransmitters acetylcholine and octopamine [61].

AstA is expressed in a pair of neurons located in the basolateral protocerebrum, and GRASP (green fluorescent protein [GFP] reconstitution across synaptic partners) analysis [62] detected a physical interaction between the axons of AstA neurons and the dendrites of PTTH neurons and insulin-producing cells [59]. AstA receptor 1 (AstAR1) is the insect homolog of mammalian Kiss1R, and its knockdown in PTTH neurons resulted in developmental delay and larger pupae—a phenotype similar to that of *Ptth*-null mutants [57,59].

A second neuropeptide, corazonin, is expressed in three pairs of neurons located in the dorsolateral and dorsomedial protocerebrum [63,64]. GRASP analysis on this cell population detected GFP expression in PTTH neurons and PG cells [60]. Interestingly, ultrastructural studies confirmed this communication and revealed bidirectional connectivity between corazonin and PTTH neurons [60]. In this case, knockdown of the corazonin receptor (CrzR), a member of the GnRH receptor superfamily on PTTH neurons, increased pupal body size without affecting pupariation timing [60].

Classical neurotransmitters that are widespread in the central larval nervous system are also involved in regulating the activity of PTTH neurons in *Drosophila*. In a recent report, Hao et al. [61] showed that among neurotransmitters, only acetylcholine and low doses of octopamine increased intracellular Ca^{2+} levels in PTTH neurons. Pharmacological treatment with cadmium chloride, a voltage-dependent Ca^{2+} channel antagonist, abolished octopamine-induced Ca^{2+} responses in the green fluorescent calcium sensor GCaMP6m (medium)-expressing PTTH cells [61], suggesting that low doses of octopamine might modulate the activity of PTTH cells via the G protein–coupled β3-octopamine receptors (Octβ3R). Octopamine-mediated signaling, likely occurring at the level of the subesophageal zone, has been shown to regulate corazonin neurons in systemic growth [60]. Genetic analysis performed only on acetylcholine receptors showed that depletion of the α1 and α3 subunits of nicotinic receptors, but not muscarinic receptors, reduced the Ca^{2+} responses of PTTH neurons to acetylcholine and also increased pupal body size without affecting pupariation timing [61]; this is a very similar phenotype to that obtained with the neuropeptide corazonin [60]. The lack of effect on pupariation time suggests that corazonin and acetylcholine neurons affect PTTH neurons to promote basal ecdysteroid biosynthesis, but not its peak. Monitoring of GCaMP6s (slow)

activity in PTTH neurons after corazonin neuron activation revealed a strong response only during the mid-L3 larval stage, but not later [60], which would support this hypothesis. In contrast, maximal AstA/AstAR1 activity has been observed toward the end of larval development [59], likely anticipating the rise in PTTH levels and the onset of metamorphosis.

Furthermore, extensive studies have shown that PTTH neurons are under the control of circadian rhythms in the blood-feeding hemipteran *Rhodnius prolixus* [65]. In *Drosophila*, pigment-dispersing factor (PDF)-producing clock neurons contact PTTH neurons, and PDF influences the transcriptional periodicity and attenuates the rise of *Ptth* transcription before pupariation [56] suggesting that circadian rhythms may control PTTH release in *Drosophila* as well. When larvae face tissue damage signals during their development, PTTH neurons and insulin-producing cells receive inputs from leucine-rich repeat–containing G protein–coupled receptor 3 (Lgr3)-positive neurons [66] to synchronize growth and maturation until the damage is resolved.

PG neurons as a neuroendocrine center in the coordination of growth and metamorphosis: a network of increasing complexity

As the major endocrine organ that dictates pupariation, the PG plays a central role in integrating multiple signals (Fig. 2) that inform the state of growth and maturation to ultimately control secretion from the organ and trigger the juvenile-to-adult transition. These cross talks include autocrine signals generated in the PG itself, which do not involve PTTH neuron activity [58,67,68], and brain-derived [64,69] and
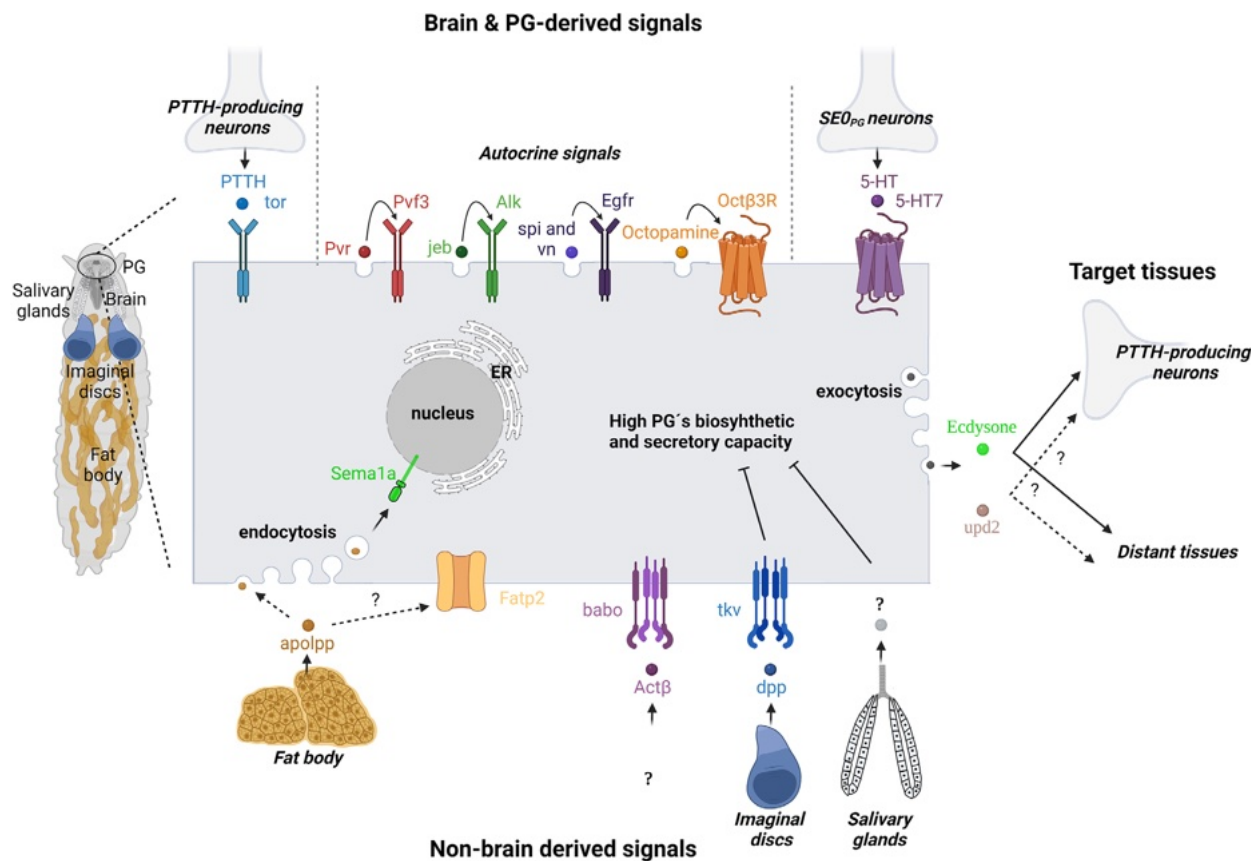
Fig. 2. Scheme of the integration of autocrine, brain- and non-brain-derived signals by the prothoracic gland for the coordination of growth and maturation in *Drosophila*. 5-HT, 5-hydroxytryptamine (serotonin); 5-HT7, 5-hydroxytryptamine (serotonin) receptor 7; Actβ, activin-β; Alk, anaplastic lymphoma kinase; apolpp, apolipophorin; babo, baboon; dpp, decapentaplegic; Ec, ecdysone; Egfr, epidermal growth factor receptor; ER, endoplasmic reticulum; Fatp2, fatty acid transport protein 2a; jeb, jelly belly; Octβ3R, octopamine β3 receptor; PTTH, prothoracicotropic hormone; Pvf3, PDGF- and VEGF-related factor 3; PG, prothoracic gland; Pvr, PDGF- and VEGF-receptor related; tkv, thickveins; Sema1a, semaphorin1a; spi, spitz; tor, torso; upd2, unpaired 2; and vn, vein.

non-brain-derived signals [70–73] from organs that convey nutritional status, environmental development and other unknown inputs that directly impact the PG.

Autocrine signals primarily include multiple receptor tyrosine kinases (anaplastic lymphoma kinase [Alk], PDGF- and VEGF-receptor related [Pvr], and epidermal growth factor receptor [EGFR]) that, together with PTTH/torso, seem to share the same signaling pathway to control pupation through Ras/ERK activation [58]. Why is there this redundancy of receptor tyrosine kinase signaling in the PG? Different explanations have been proposed: (a) to confer robustness and flexibility in response to changing developmental conditions, (b) to act synchronously or sequentially and achieve Ras/ERK activation that is strong enough to drive the massive PG secretion necessary for carrying out puparation or (c) to induce other unidentified downstream signaling pathways in addition to Ras/ERK signaling [58]. Although receptor tyrosine kinase activation is the predominant signaling in the PG, activation by monoaminergic autocrine signaling through the G protein–coupled octopamine-β3 receptor (Octβ3R) has also been reported to act upstream of insulin/insulin-like growth factor (IIS) ligand family and Ras/ERK signaling [68]. A second G protein–coupled receptor in the PG, 5-hydroxytryptamine receptor 7 (5-HT7), responds to food-related signals from a subset of stomatogastric serotoninergic (SE0$_{PG}$) neurons that directly innervate the PG [69]. In conditions of nutrient scarcity, the projections of SE0$_{PG}$ neurons are reduced [69], leading to decreased 5-HT signaling to PG cells and, as a result, reduced ecdysone release and delayed development, likely due to defective translation in those cells [74].

Multiple inputs from non-cerebral organs seem capable of influencing puparation through diffusible signals reaching the PG (Fig. 2). Unlike the signaling of tissue damage mediated by the positive regulation of insulin-like peptide 8 [66,75], under normal physiological conditions, decapentaplegic (Dpp), a ligand of the transforming growth factor-β (TGF-β) signaling pathway, is released from the imaginal disks to the hemolymph and its signaling via the thickveins (Tkv) receptor also negatively regulates the production of ecdysone [72]. Activin, another TGF-β ligand, the source of which is unknown, functions in this process in the PG antagonistically to Dpp signaling [71]. Although the mode of integration of these pathways is not well defined, the hypothesis predicts that Dpp signaling must be reduced in the PG to allow puparation to proceed. A recent study has shown that the salivary gland–derived peptide Sgsf is secreted into the hemolymph to regulate systemic growth via the IIS/target of rapamycin (TOR) signaling pathway without affecting metamorphic timing [73]. Interestingly, ablation of the salivary glands is necessary to control metamorphic timing, which also suggests the existence of one or more additional signals produced by salivary gland cells through mechanisms that are still unknown.

Despite this cross talk of multiple pathways converging on the PG, it remains to be clarified how these triggers of ecdysone biosynthesis affect cholesterol trafficking [76–78] and the transcription and chromatin remodeling of *Halloween* ecdysteroid biosynthetic genes [79,80] for timing ecdysone production in response to these stimulus-triggered signaling pathways. Although 20 ecdysteroidogenic transcription factors have been identified to date, we still do not fully understand their mechanism of action and whether it is direct or indirect, or their mode of interaction in the expression of *Halloween* genes. There is evidence that the transcription of *Halloween* genes is directly inhibited by epigenetic control, via the nuclear receptors methoprene-tolerant (Met) and germ cell–expressed (Gce) via Krüppel homolog 1 (Kr-h1) [81,82].

It is also unclear whether communication between the fat body, the larval fat and energetic reservoir, and the PG (either directly or indirectly via PTTH neurons) informs that adequate overall reserves of energy or specific nutrients/metabolites have been reached to meet the demands of subsequent reproduction and thus allow puparation. If this were so, it would mean that despite the evolutionary distance, the process of metamorphosis is governed by principles more similar to puberty than we might think. We also mostly do not know what cellular processes occur at the level of the PG once the larva has passed the critical weight, leading to the production and secretion of ecdysone [83].

We have recently described that inhibiting lipid transport from the fat body via knockdown of *apolipophorin* (*apolpp*), or in the PG via knockdown of *Fatty acid transport protein 2* (*Fatp2*), *Semaphorin1a* (*Sema1a*) and leptin-like *unpaired 2* (*upd2*), precludes the transition through the critical weight without measurable impairment in the IIS signaling pathway and results in larvae that never left the food and continued growing and gaining weight until death [70]; these effects are analogous to those of leptin/LepR loss in patients and mice. Silencing of cationic amino acid and sugar transporters had no effect. These results support a critical role of lipid signaling, transport, and sensing in the events leading to sexual maturation commitment. Validating our conclusion, expression of the human leptin transgene in the PG rescued both the

obese and non-pupating phenotypes of *upd2*-mutant and *Sema1a*-mutant animals, suggesting that a fat sensor mechanism similar to the leptin system in mammals may act in the larval PG to coordinate body weight and growth for pupariation. Supporting the involvement of lipids in sexual maturation, a recent study has shown that enhancing cholesterol signaling in PG cells, a substrate for ecdysone production, leads to increased body growth and premature pupariation [84].

Interestingly, *Sema1a^i* PGs are distinctly different from PGs with knockdown in the IIS/TOR pathway: we did not detect any alteration in the size or endoreplication of the *Sema1a^i* PG cells, a feature previously linked to ecdysone synthesis [85]. Neither IIS/TOR nor PTTH/torso/Ras activation corrected larval arrest and obesity caused by *Sema1a* depletion in PG cells [70]. Our finding that TOR activation cannot rescue *Sema1a* deficiency in the PG suggests either that nutrient sensing by TOR is upstream of Sema1a or that Sema1a-mediated events may provide competence for responding to TOR. We favor this second possibility.

Analysis of the metabolic status of *Drosophila* larvae using an optimized NMR profiling assay and other commercial assays in dissected tissues and whole animals [86] showed elevated levels of sugar and lipids accumulated during the extension of feeding behavior [70]. Together with this metabolic analysis, we used super-resolution imaging of the PG to determine that the high secretory competence of the PG requires endocytosis, endoplasmic reticulum remodeling and ribosomal maturation for the acquisition of the high biosynthetic and secretory capacity of the PG cells; all these processes are Sema1a-dependent. Interestingly, we found that nanobody-based retention of upd2::GFP in the nuclei of PG cells led to a non-pupating and massively obese phenotype that was indistinguishable from the phenotype resulting from the knockdown of *upd2* in PG cells [70]. In the brain and peripheral organs, fat body cells and imaginal disks respond to upd2 and ecdysone to initiate nutrient-independent growth, differentiation, and maturation [70,87–89].

Conclusions

Recent studies of mammalian puberty and insect metamorphosis have shown that, despite their evolutionary distance and physiological differences, these critical events exhibit similar design principles and conservation of the molecular components involved. A variety of environmental and internal cues (e.g., nutrition, photoperiod, temperature, and tissue damage) appear capable of influencing sexual maturation through the activation of neuroendocrine organs, culminating in steroid production and secretion. Among these signals, the communication between peripheral body fat levels and endocrine organs seems crucial and allows the assessment of nutrient availability and the growth status of internal organs, ensuring that maturation starts at the right time. This is extremely concerning given the current rampant prevalence of childhood obesity and its possible relationship with the increasing incidence of early puberty [34], which affects growth and final body size, and which is associated with a number of adult morbidities [90–92].

Holistic investigation through the combined use of model organisms is certainly necessary to identify upstream signals (lipids, amino acids, etc.) and their sensors in the brain, as well as how these signals are integrated in the control of metamorphosis and puberty.

Acknowledgements

Conflict of interest

The authors declare no conflict of interest.

Author contributions

JM, JG, and JC-V involved in writing—original draft; JM, JG, and JC-V contributed to review and editing; JM contributed to funding acquisition.

Data availability statement

Data sharing is not applicable to this article as no new data were created or analysed in this study.

References

1 Parent AS, Teilmann G, Juul A, Skakkebaek NE, Toppari J, Bourguignon JP. The timing of normal puberty and the age limits of sexual precocity: variations around the world, secular trends, and changes after migration. *Endocr Rev*. 2003;**24**:668–93.

2 Plant TM. Neuroendocrine control of the onset of puberty. *Front Neuroendocrinol*. 2015;**38**:73–88.

3 Pan X, O'Connor MB. Developmental maturation: Drosophila AstA signaling provides a kiss to grow up. *Curr Biol*. 2019;**29**:R161–4.

4 Herbison AE. Control of puberty onset and fertility by gonadotropin-releasing hormone neurons. *Nat Rev Endocrinol*. 2016;**12**:452–66.

5 Wang L, Guo W, Shen X, Yeo S, Long H, Wang Z, et al. Different dendritic domains of the GnRH neuron underlie the pulse and surge modes of GnRH secretion in female mice. *eLife*. 2020;**9**:e53945.

6 Casoni F, Malone SA, Belle M, Luzzati F, Collier F, Allet C, et al. Development of the neurons controlling fertility in humans: new insights from 3D imaging and transparent fetal brains. *Development*. 2016;**143**:3969–81.

7 Clasadonte J, Prevot V. The special relationship: glia–neuron interactions in the neuroendocrine hypothalamus. *Nat Rev Endocrinol*. 2018;**14**:25–44.

8 Pellegrino G, Martin M, Allet C, Lhomme T, Geller S, Franssen D, et al. GnRH neurons recruit astrocytes in infancy to facilitate network integration and sexual maturation. *Nat Neurosci*. 2021;**24**:1660–72.

9 Lopez-Rodriguez D, Franssen D, Bakker J, Lomniczi A, Parent A-S. Cellular and molecular features of EDC exposure: consequences for the GnRH network. *Nat Rev Endocrinol*. 2021;**17**:83–96.

10 Sykiotis GP, Pitteloud N, Seminara SB, Kaiser UB, Crowley WF Jr. Deciphering genetic disease in the genomic era: the model of GnRH deficiency. *Sci Transl Med*. 2010;**2**:32rv2.

11 Giacobini P. Shaping the reproductive system: role of Semaphorins in gonadotropin-releasing hormone development and function. *Neuroendocrinology*. 2015;**102**:200–15.

12 Cariboni A, André V, Chauvet S, Cassatella D, Davidson K, Caramello A, et al. Dysfunctional SEMA3E signaling underlies gonadotropin-releasing hormone neuron deficiency in Kallmann syndrome. *J Clin Invest*. 2015;**125**:2413–28.

13 Giacobini P, Parkash J, Campagne C, Messina A, Casoni F, Vanacker C, et al. Brain endothelial cells control fertility through ovarian-steroid-dependent release of semaphorin 3A. *PLoS Biol*. 2014;**12**:e1001808.

14 Van der Klaauw AA, Croizier S, Mendes de Oliveira E, Stadler LKJ, Park S, Kong Y, et al. Human Semaphorin 3 variants link melanocortin circuit development and energy balance. *Cell*. 2019;**176**:729–42.e18.

15 Kirilov M, Clarkson J, Liu X, Roa J, Campos P, Porteous R, et al. Dependence of fertility on kisspeptin-Gpr54 signaling at the GnRH neuron. *Nat Commun*. 2013;**4**:2492.

16 Sobrino V, Avendaño MS, Perdices-López C, Jimenez-Puyer M, Tena-Sempere M. Kisspeptins and the neuroendocrine control of reproduction: recent progress and new frontiers in kisspeptin research. *Front Neuroendocrinol*. 2022;**65**:100977.

17 Plant TM. The neurobiological mechanism underlying hypothalamic GnRH pulse generation: the role of kisspeptin neurons in the arcuate nucleus. *F1000Res*. 2019;**8**:F1000 faculty Rev-982.

18 Clarkson J, Han SY, Piet R, McLennan T, Kane GM, Ng J, et al. Definition of the hypothalamic GnRH pulse generator in mice. *Proc Natl Acad Sci USA*. 2017;**114**:E10216–23.

19 Messager S, Chatzidaki EE, Ma D, Hendrick AG, Zahn D, Dixon J, et al. Kisspeptin directly stimulates gonadotropin-releasing hormone release via G protein-coupled receptor 54. *Proc Natl Acad Sci USA*. 2005;**102**:1761–6.

20 Cravo RM, Margatho LO, Osborne-Lawrence S, Donato J Jr, Atkin S, Bookout AL, et al. Characterization of Kiss1 neurons using transgenic mouse models. *Neuroscience*. 2011;**173**:37–56.

21 Pineda R, Plaisier F, Millar RP, Ludwig M. Amygdala Kisspeptin neurons: putative mediators of olfactory control of the gonadotropic Axis. *Neuroendocrinology*. 2017;**104**:223–38.

22 Goodman RL, Lehman MN, Smith JT, Coolen LM, de Oliveira CV, Jafarzadehshirazi MR, et al. Kisspeptin neurons in the arcuate nucleus of the ewe express both dynorphin a and neurokinin B. *Endocrinology*. 2007;**148**:5752–60.

23 Moore AM, Coolen LM, Porter DT, Goodman RL, Lehman MN. KNDy cells revisited. *Endocrinology*. 2018;**159**:3219–34.

24 Nagae M, Uenoyama Y, Okamoto S, Tsuchida H, Ikegami K, Goto T, et al. Direct evidence that KNDy neurons maintain gonadotropin pulses and folliculogenesis as the GnRH pulse generator. *Proc Natl Acad Sci USA*. 2021;**118**:e2009156118.

25 Khan AR, Kauffman AS. The role of kisspeptin and RFamide-related peptide-3 neurones in the circadian-timed preovulatory luteinising hormone surge. *J Neuroendocrinol*. 2012;**24**:131–43.

26 de Roux N, Genin E, Carel J-C, Matsuda F, Chaussain J-L, Milgrom E. Hypogonadotropic hypogonadism due to loss of function of the KiSS1-derived peptide receptor GPR54. *Proc Natl Acad Sci USA*. 2003;**100**:10972–6.

27 Seminara SB, Messager S, Chatzidaki EE, Thresher RR, Acierno JS, Shagoury JK, et al. The GPR54 Gene as a regulator of puberty. *N Engl J Med*. 2003;**349**:1614–27.

28 d'Anglemont de Tassigny X, Fagg LA, Dixon JP, Day K, Leitch HG, Hendrick AG, et al. Hypogonadotropic hypogonadism in mice lacking a functional Kiss1 gene. *Proc Natl Acad Sci USA*. 2007;**104**:10714–9.

29 Mayer C, Boehm U. Female reproductive maturation in the absence of kisspeptin/GPR54 signaling. *Nat Neurosci.* 2011;**14**:704–10.

30 Kumar D, Boehm U. Genetic dissection of puberty in mice. *Exp Physiol.* 2013;**98**:1528–34.

31 Sisk CL, Foster DL. The neural basis of puberty and adolescence. *Nat Neurosci.* 2004;**7**:1040–7.

32 Chakradhar S. Animals on the verge: what different species can teach us about human puberty. *Nat Med.* 2018;**24**:114–7.

33 Frisch RE, Revelle R. Height and weight at menarche and a hypothesis of critical body weights and adolescent events. *Science.* 1970;**169**:397–9.

34 Reinehr T, Roth CL. Is there a causal relationship between obesity and puberty? *Lancet Child Adolesc Health.* 2019;**3**:44–54.

35 Sedlmeyer IL, Palmert MR. Delayed puberty: analysis of a large case series from an academic center. *J Clin Endocrinol Metabol.* 2002;**87**:1613–20.

36 Georgopoulos NA, Roupas ND, Theodoropoulou A, Tsekouras A, Vagenakis AG, Markou KB. The influence of intensive physical training on growth and pubertal development in athletes. *Ann N Y Acad Sci.* 2010;**1205**:39–44.

37 Zhang Y, Proenca R, Maffei M, Barone M, Leopold L, Friedman JM. Positional cloning of the mouse obese gene and its human homologue. *Nature.* 1994;**372**:425–32.

38 Clement K, Vaisse C, Lahlou N, Cabrol S, Pelloux V, Cassuto D, et al. A mutation in the human leptin receptor gene causes obesity and pituitary dysfunction. *Nature.* 1998;**392**:398–401.

39 Montague CT, Farooqi IS, Whitehead JP, Soos MA, Rau H, Wareham NJ, et al. Congenital leptin deficiency is associated with severe early-onset obesity in humans. *Nature.* 1997;**387**:903–8.

40 Navarro VM, Tena-Sempere M. Neuroendocrine control by kisspeptins: role in metabolic regulation of fertility. *Nat Rev Endocrinol.* 2012;**8**:40–53.

41 Louis GW, Greenwald-Yarnell M, Phillips R, Coolen LM, Lehman MN, Myers MG Jr. Molecular mapping of the neural pathways linking leptin to the neuroendocrine reproductive axis. *Endocrinology.* 2011;**152**:2302–10.

42 Padilla SL, Qiu J, Nestor CC, Zhang C, Smith AW, Whiddon BB, et al. AgRP to Kiss1 neuron signaling links nutritional state and fertility. *Proc Natl Acad Sci USA.* 2017;**114**:2413–8.

43 Manfredi-Lozano M, Roa J, Ruiz-Pino F, Piet R, Garcia-Galiano D, Pineda R, et al. Defining a novel leptin–melanocortin–kisspeptin pathway involved in the metabolic control of puberty. *Mol Metab.* 2016;**5**:844–57.

44 True C, Verma S, Grove KL, Smith MS. Cocaine- and amphetamine-regulated transcript is a potent stimulator

of GnRH and Kisspeptin cells and may contribute to negative energy balance-induced reproductive inhibition in females. *Endocrinology.* 2013;**154**:2821–32.

45 Manfredi-Lozano M, Roa J, Tena-Sempere M. Connecting metabolism and gonadal function: novel central neuropeptide pathways involved in the metabolic control of puberty and fertility. *Front Neuroendocrinol.* 2018;**48**:37–49.

46 Lam BYH, Williamson A, Finer S, Day FR, Tadross JA, Gonçalves Soares A, et al. MC3R links nutritional state to childhood growth and the timing of puberty. *Nature.* 2021;**599**:436–41.

47 Heras V, Castellano JM, Fernandois D, Velasco I, Rodríguez-Vazquez E, Roa J, et al. Central ceramide signaling mediates obesity-induced precocious puberty. *Cell Metab.* 2020;**32**:951–66.e8.

48 Wang Y-P, Lei Q-Y. Metabolite sensing and signaling in cell metabolism. *Signal Transduct Target Ther.* 2018;**3**:30.

49 Roa J, Barroso A, Ruiz-Pino F, Vázquez MJ, Seoane-Collazo P, Martínez-Sanchez N, et al. Metabolic regulation of female puberty via hypothalamic AMPK–kisspeptin signaling. *Proc Natl Acad Sci USA.* 2018;**115**:E10758–67.

50 Vazquez MJ, Toro CA, Castellano JM, Ruiz-Pino F, Roa J, Beiroa D, et al. SIRT1 mediates obesity- and nutrient-dependent perturbation of pubertal timing by epigenetically controlling Kiss1 expression. *Nat Commun.* 2018;**9**:4194.

51 Roa J, Garcia-Galiano D, Varela L, Sánchez-Garrido MA, Pineda R, Castellano JM, et al. The mammalian target of rapamycin as novel central regulator of puberty onset via modulation of hypothalamic Kiss1 system. *Endocrinology.* 2009;**150**:5016–26.

52 Gwinn DM, Shackelford DB, Egan DF, Mihaylova MM, Mery A, Vasquez DS, et al. AMPK phosphorylation of raptor mediates a metabolic checkpoint. *Mol Cell.* 2008;**30**:214–26.

53 Chang C, Su H, Zhang D, Wang Y, Shen Q, Liu B, et al. AMPK-dependent phosphorylation of GAPDH triggers Sirt1 activation and is necessary for autophagy upon glucose starvation. *Mol Cell.* 2015;**60**:930–40.

54 Kawakami A, Kataoka H, Oka T, Mizoguchi A, Kimura-Kawakami M, Adachi T, et al. Molecular cloning of the Bombyx mori prothoracicotropic hormone. *Science.* 1990;**247**:1333–5.

55 Rewitz KF, Yamanaka N, Gilbert LI, O'Connor MB. The insect neuropeptide PTTH activates receptor tyrosine kinase torso to initiate metamorphosis. *Science.* 2009;**326**:1403–5.

56 McBrayer Z, Ono H, Shimell M, Parvy JP, Beckstead RB, Warren JT, et al. Prothoracicotropic hormone regulates developmental timing and body size in Drosophila. *Dev Cell.* 2007;**13**:857–71.

57 Shimell M, Pan X, Martin FA, Ghosh AC, Leopold P, O'Connor MB, et al. Prothoracicotropic hormone

modulates environmental adaptive plasticity through the control of developmental timing. *Development*. 2018;**145**:dev159699.

58 Pan X, O'Connor MB. Coordination among multiple receptor tyrosine kinase signals controls Drosophila developmental timing and body size. *Cell Rep*. 2021;**36**:109644.

59 Deveci D, Martin FA, Leopold P, Romero NM. AstA signaling functions as an evolutionary conserved mechanism timing juvenile to adult transition. *Curr Biol*. 2019;**29**:813–22.e4.

60 Imura E, Shimada-Niwa Y, Nishimura T, Huckesfeld S, Schlegel P, Ohhara Y, et al. The Corazonin-PTTH neuronal Axis controls systemic body growth by regulating basal Ecdysteroid biosynthesis in *Drosophila melanogaster*. *Curr Biol*. 2020;**30**:2156–65.e5.

61 Hao S, Gestrich JY, Zhang X, Xu M, Wang X, Liu L, et al. Neurotransmitters affect larval development by regulating the activity of prothoracicotropic hormone-releasing neurons in *Drosophila melanogaster*. *Front Neurosci*. 2021;**15**:653858.

62 Feinberg EH, Vanhoven MK, Bendesky A, Wang G, Fetter RD, Shen K, et al. GFP reconstitution across synaptic partners (GRASP) defines cell contacts and synapses in living nervous systems. *Neuron*. 2008;**57**:353–63.

63 Choi YJ, Lee G, Hall JC, Park JH. Comparative analysis of Corazonin-encoding genes (Crz's) in Drosophila species and functional insights into Crz-expressing neurons. *J Comp Neurol*. 2005;**482**:372–85.

64 Hückesfeld S, Schlegel P, Miroschnikow A, Schoofs A, Zinke I, Haubrich AN, et al. Unveiling the sensory and interneuronal pathways of the neuroendocrine connectome in Drosophila. *Elife*. 2021;**10**:e65745.

65 Steel CG, Vafopoulou X. Circadian orchestration of developmental hormones in the insect, *Rhodnius prolixus*. *Comp Biochem Physiol A Mol Integr Physiol*. 2006;**144**:351–64.

66 Vallejo DM, Juarez-Carreño S, Bolivar J, Morante J, Dominguez M. A brain circuit that synchronizes growth and maturation revealed through Dilp8 binding to Lgr3. *Science*. 2015;**350**:aac6767.

67 Cruz J, Martín D, Franch-Marro X. Egfr signaling is a major regulator of ecdysone biosynthesis in the drosophila prothoracic gland. *Curr Biol*. 2020;**30**:1547–54.e4.

68 Ohhara Y, Shimada-Niwa Y, Niwa R, Kayashima Y, Hayashi Y, Akagi K, et al. Autocrine regulation of ecdysone synthesis by beta3-octopamine receptor in the prothoracic gland is essential for drosophila metamorphosis. *Proc Natl Acad Sci USA*. 2015;**112**:1452–7.

69 Shimada-Niwa Y, Niwa R. Serotonergic neurons respond to nutrients and regulate the timing of steroid hormone biosynthesis in Drosophila. *Nat Commun*. 2014;**5**:5778.

70 Juarez-Carreño S, Vallejo DM, Carranza-Valencia J, Palomino-Schätzlein M, Ramon-Cañellas P, Santoro R, et al. Body-fat sensor triggers ribosome maturation in the steroidogenic gland to initiate sexual maturation in Drosophila. *Cell Rep*. 2021;**37**:109830.

71 Gibbens YY, Warren JT, Gilbert LI, O'Connor MB. Neuroendocrine regulation of Drosophila metamorphosis requires TGFbeta/activin signaling. *Development*. 2011;**138**:2693–703.

72 Setiawan L, Pan X, Woods AL, O'Connor MB, Hariharan IK. The BMP2/4 ortholog Dpp can function as an inter-organ signal that regulates developmental timing. *Life Sci Alliance*. 2018;**1**:e201800216.

73 Li Z, Qian W, Song W, Zhao T, Yang Y, Wang W, et al. A salivary gland-secreted peptide regulates insect systemic growth. *Cell Rep*. 2022;**38**:110397.

74 Deliu LP, Jadir D, Ghosh A, Grewal SS. Serotonergic neuron ribosomes regulate the neuroendocrine control of Drosophila development. *bioRxiv*. 2021. https://doi.org/10.1101/2021.06.10.447971

75 Garelli A, Gontijo AM, Miguela V, Caparros E, Dominguez M. Imaginal discs secrete insulin-like peptide 8 to mediate plasticity of growth and maturation. *Science*. 2012;**336**:579–82.

76 Texada MJ, Malita A, Christensen CF, Dall KB, Faergeman NJ, Nagy S, et al. Autophagy-mediated cholesterol trafficking controls steroid production. *Dev Cell*. 2019;**48**:659–71.e4.

77 Pan X, Neufeld TP, O'Connor MB. A tissue- and temporal-specific autophagic switch controls drosophila pre-metamorphic nutritional checkpoints. *Curr Biol*. 2019;**29**:2840–51.e4.

78 Danielsen ET, Moeller ME, Yamanaka N, Ou Q, Laursen JM, Soenderholm C, et al. A Drosophila genome-wide screen identifies regulators of steroid hormone production and developmental timing. *Dev Cell*. 2016;**37**:558–70.

79 Kamiyama T, Niwa R. Transcriptional regulators of Ecdysteroid biosynthetic enzymes and their roles in insect development. *Front Physiol*. 2022;**13**:823418.

80 Drelon C, Rogers MF, Belalcazar HM, Secombe J. The histone demethylase KDM5 controls developmental timing in drosophila by promoting prothoracic gland endocycles. *Development*. 2019;**146**:dev182568.

81 Liu S, Li K, Gao Y, Liu X, Chen W, Ge W, et al. Antagonistic actions of juvenile hormone and 20-hydroxyecdysone within the ring gland determine developmental transitions in Drosophila. *Proc Natl Acad Sci USA*. 2018;**115**:139–44.

82 Zhang T, Song W, Li Z, Qian W, Wei L, Yang Y, et al. Krüppel homolog 1 represses insect ecdysone biosynthesis by directly inhibiting the transcription of steroidogenic enzymes. *Proc Natl Acad Sci USA*. 2018;**115**:3960–5.

83 Pan X, Connacher RP, O'Connor MB. Control of the insect metamorphic transition by ecdysteroid production and secretion. *Curr Opin Insect Sci*. 2021;**43**:11–20.

84 Texada MJ, Lassen M, Pedersen LH, Koyama T, Malita A, Rewitz K. Insulin signaling couples growth and early maturation to cholesterol intake in Drosophila. *Curr Biol*. 2022;**32**:1548–62.e6.

85 Ohhara Y, Kobayashi S, Yamanaka N. Nutrient-dependent endocycling in steroidogenic tissue dictates timing of metamorphosis in *Drosophila melanogaster*. *PLoS Genet*. 2017;**13**:e1006583.

86 Palomino-Schätzlein M, Carranza-Valencia J, Guirado J, Juarez-Carreño S, Morante J. A toolbox to study metabolic status of *Drosophila melanogaster* larvae. *STAR Protoc*. 2022;**3**:101195.

87 Christensen CF, Koyama T, Nagy S, Danielsen ET, Texada MJ, Halberg KA, et al. Ecdysone-dependent feedback regulation of prothoracicotropic hormone controls the timing of developmental maturation. *Development*. 2020;**147**:dev188110.

88 Okamoto N, Viswanatha R, Bittar R, Li Z, Haga-Yamanaka S, Perrimon N, et al. A membrane transporter is required for steroid hormone uptake in Drosophila. *Dev Cell*. 2018;**47**:294–305.e7.

89 Okamoto N, Yamanaka N. Steroid hormone entry into the brain requires a membrane transporter in Drosophila. *Curr Biol*. 2020;**30**:359–66.e3.

90 Cheng TS, Day FR, Lakshman R, Ong KK. Association of puberty timing with type 2 diabetes: a systematic review and meta-analysis. *PLoS Med*. 2020;**17**:e1003017.

91 Day FR, Thompson DJ, Helgason H, Chasman DI, Finucane H, Sulem P, et al. Genomic analyses identify hundreds of variants associated with age at menarche and support a role for puberty timing in cancer risk. *Nat Genet*. 2017;**49**:834–41.

92 Day FR, Elks CE, Murray A, Ong KK, Perry JRB. Puberty timing associated with diabetes, cardiovascular disease and also diverse health outcomes in men and women: the UKbiobank study. *Sci Rep*. 2015;**5**:11208.

10. Acknowledgments

A quienes siempre han estado ahí y a quienes ya no, aunque siempre supieron que yo si…

Se hace tan necesario como placentero poder agradecer, finalmente, al laboratorio que me ha acogido a mí y a mis inquietudes científicas durante esta etapa tan dura como gratificante. Sin duda, este trabajo no hubiera sido posible sin la ayuda de quien se sitúa al mando de la que ha sido mi pequeña factoría de ciencia durante los últimos 6 años, Javier. Muchas horas de discusión científica, muchas dudas resueltas a base de boli y papel en el despacho y, por supuesto, muchas dudas que van más allá de la ciencia y en las que he buscado casi más que un científico, un mentor, un guía que me facilitase de alguna manera la comprensión de esta larga carrera que elegimos los que nos empeñamos en hacer crecer el conocimiento científico. Sin duda, debo extender este agradecimiento a María Domínguez, que ha facilitado en muchas ocasiones tanto mi situación como la del propio laboratorio, por algo le asignamos la categoría de "la madre" todos los que trabajamos directa o indirectamente con ella. También me apetece extender este agradecimiento a todos los componentes tanto de mi laboratorio como del laboratorio "hermanado", aunque al fin y al cabo lo mejor que tenemos entre "moscólogos" es que solemos hacer bastante piña. Dicho esto, y empezando por mi propio laboratorio, tengo que agradecer la ayuda de Pol Ramón, de quien soy sucesor si queremos verlo así y con el que me he sentido siempre muy acompañado. Del poco tiempo que tuve la suerte de coincidir contigo, sin duda me llevo algo valioso. Sergio, ¿qué se puede decir de este chico sin que se le quede pequeño? Sin duda algo que me llevo de esta etapa tanto en el plano académico como fuera de él, un auténtico grande. Como siempre dices: "¡Gracias guapo!". Siguiendo con mi laboratorio, el equipo actual, con Juan Ramón y la nueva incorporación, mamá Marta. Así nombrada por la auténtica mosca del laboratorio, Mónica, "el extractor", que ha dado tanto ruido como buen ambiente y charla en las tardes, a veces demasiado largas, en el laboratorio. Parada obligada en Luis, "el veterano del laboratorio" un hombre con una actitud envidiable, de los de "quiero ser así de mayor". Por acabar con este círculo cercano de personas relevantes para mi durante esta etapa, tengo que mencionar algunos "fichajes" importantes del laboratorio de María. Ernesto, desde compañero de laboratorio hasta casi un hermano. Las personas nos unimos y nos separamos, pero la parte buena siempre es más fácil de recordar, un abrazo grande para ti y gracias, por supuesto. Dani, siempre viene bien un Dani vayas a donde vayas. Lucía, también una persona de las que hay que tener en el laboratorio. Por supuesto, recorriendo las personas de este laboratorio tenemos que detenernos en Bob (Rrrob para mí). Un amigo de verdad que me llevo de alicante, hemos viajado, construido, hablado y debatido sobre prácticamente cualquier cosa que exista (o que pudiera remotamente existir). Sin duda Roberto y Selene sois dos personas que me llevo en mi maleta emocional para siempre.

Sin salir de los laboratorios de mosca aún, hay que pararse en el de Ana Carmena, en su laboratorio he tenido la suerte de encontrar a dos personas que han aportado mucho a mi etapa por allí: Sandra y Maribel. Sandra sabe siempre cómo y cuándo y si te ve dudando antes de que preguntes ya te ha echado una mano, "easy going" sería una buena descripción breve para ti, gracias. Por supuesto, hablar de Sandra implica inmediatamente acordarse de Alex. Que tío tan peculiar, que buen rollo y con qué facilidad somos capaces de convertir un rato cualquiera en un festival del humor y darle un parón a la seriedad para dejar que la cabeza se relaje, muchas gracias por eso de verdad. Por otro lado, Maribel, la experiencia, la revolución y al mismo tiempo la buena aura. Mujer andaluza, mujer de bien, ¡y más si es de Malaguita! Por último, entre los "Fly-Labs", Juan Antonio Alcañiz, no solo es una mente clara y con un razonamiento científico exquisito, sino que además alberga en su laboratorio a tres fichajes estrella: Manuel, el de "¿un dulsesito después de un *da filipito*?" se Sevilla sí, pero muy buen chaval también. Chema, la cordura y la tranquilidad de este chico es envidiable sin duda, ¡tenemos alguna inmersión pendiente eh! Y finalmente Rubén, hace poco que te tocó a ti defender tu tesis y ya tienes prácticamente encaminado tu futuro, me alegro muchísimo por ti, y por la fiesta que como de costumbre habrá que pegarse para celebrarlo.

Salimos de los "Fly-Labs". Pancho, uno de los mejores contactos que tener en Alicante. No solo es un tío de 10 sino que además he tenido la suerte de poder contar contigo tanto para discusión científica, como para simplemente hablar de la vida. Para salir a por un par de "chelas" y acabar a las 4 de la mañana conociendo los antros y "huevones" de la noche alicantina. De ti me llevo un amigo sin duda, ¡gracias! Aprovecho para dar el agradecimiento general al grupo que poco a poco ha ido creciendo y con el que tantas celebraciones y tardes de cervezas y playa hemos pasado; Emily, Enrico, Luwei, Heleni, Giovani y Martina, Sofía y Sebastián et al., ¡Este último requiere parada también! Muchas gracias, Sebastián, las veces que hemos coincidido siempre he sacado algo bueno y se agradece en mucho. Quedan rutas pendientes con las motos para "que cates una moto de verdad". Por supuesto quiero acordarme del "otro Roberto" hemos vivido muchas horas tanto de charla, como de ciencia e incluso de sparring. ¡Gracias por todo Roberto! Otro imprescindible en este apartado fuera de los "Fly-Labs" es Antonio Caler, sin su ayuda probablemente varias figuras de la tesis se hubieran quedado en una idea, muchas gracias por todas esas horas, que algunas ni te tocaban y ahí estaba el tío.

Hamida y Fran (y por supuesto el resto de camaradas que no se me olvida ni "el chino" ni "el trucha" ni "el Unai", por vosotros va también). Probablemente sin saberlo, habéis contribuido mucho a que este trabajo sea posible, es difícil explicar lo bien que sienta veros en el parque con ganas de una cerveza después de 14 horas de laboratorio. Me habéis acogido como uno más en ese pequeño oasis de tranquilidad que para mí ha sido ese parque de las pierdas. Sin duda, muchas gracias.

Por último, y precisamente para darle su espacio, quiero agradecer muy fuerte a los tres pilares imprescindibles de mi vida: Mi familia y mi pareja y mis amigos de toda la vida.

A mi familia, dedicaros este trabajo, no por lo que aquí ponga sino por lo que significa. Significa que he tenido unos valores de los que creo que puedo estar bastante orgulloso. Significa que he tenido una infancia y una educación envidiables. He aprendido tanto de vosotros que se me hace muy complicado escribir aquí en varias frases algo que os haga justicia. Creo que lo sabéis. Creo que mi madre sabe lo necesaria que ha sido siempre para mí. Cuánto me alegro de que te vaya bien, de verte feliz, de verte siendo tú. Te quiero mucho, madre. A quien hoy día te acompaña, Antonio, tengo que darle las gracias por haberte traído a ti y a nosotros parte de esta paz desprende. Es evidente que no puede salir un guiso bien si no cuentas con un fondo medio bueno. Me refiero ahora a quien dio la vida por mantener la familia de mi madre a flote, mis abuelos. A la abuela Carmen nunca tuve el placer de conocerla, pero apostaría casi algún órgano a que fue una auténtica mujer de bien. Al abuelo si lo conocí, Andrés, probablemente una de las personas más transparentes y buenas (en el sentido más amplio del término) que he conocido en mi vida. Tuve la suerte de acompañarlo en sus últimos días, los disfruté, los cantamos, nos los bebimos con una pajita pequeña con canal sur de fondo. Sigue descansando abuelo, por aquí lo tenemos medio controlado, te quiero mucho. Estar aquí hoy escribiendo esto significa que he llegado, que casi lo he conseguido, y ahí tiene mucho que decir mi padre. Siendo un punto de referencia siempre para mí, desde como sujetar la linterna en las noches de "tiro al gorrión" en Cáceres, hasta cómo dar forma a ideas complejas de las que podemos pasar horas y horas hablando sin tener en cuenta que los relojes, a lo suyo, siguen dando vueltas en un acto casi de ignorancia. Muchas veces mi norte, la manera coherente de salir de situaciones complicadas tanto laboral como personalmente, lo pragmático. Te quiero mucho, padre. Dicho esto, tengo que hacer una parada obligatoria en quienes te han visto crecer. Un abrazo enorme de agradecimiento y cariño a los abuelos "Conchi" y Juan (El primer Dr. Carranza de la saga). Lo que yo entiendo por una familia unida y del propio concepto de familia, reside mucho en lo que vosotros me habéis dejado ver en cada cena de navidad, comida

familiar, cada espeto en la playa, un millón de gracias. Os quiero abuelos. Por supuesto, todos esos momentos son únicos por quienes lo hacen así. Independientemente de que la comida sea "de los Carranza" o "de los Valencia" siempre han sido sinónimo de echar un buen rato. Por ello, infinitas gracias a tíos, tías, primos, primas, parejas de primos y de primas y parejas de tíos y tías.

Para terminar de hablar de la familia, es imprescindible dar las gracias a mi hermanita, la "sista". Que alegría que todo lo que hemos batallado se haya convertido en una relación tan sólida. Muchas gracias por tus consejos, tus ratos tratando de escuchar mis turras incluso aunque te vengan largas, el saber estar en situaciones en las que la ciencia, para bien o para mal, copaba completamente la conversación, tu hombro... Ahí has estado y confío en que seguirás por aquí. Te quiero mucho, hermana.

La familia que elegimos. Mis amigos de siempre, los del instituto, los del skatepark, los de antes, durante y después de la universidad. Por suerte sois muchos y sois enormes. Sin duda una raíz fuerte a la que agarrarme cuando las cosas se ponen o muy mal o muy bien. Y si no, nos las tomamos también. Se os quiere, nos quedan muchos planes que hacer y celebrar, hace dos días nos sorprendimos como adolescentes celebrando cosas de adultos, ¡algunos del grupo empiezan a ser incluso papás! Quería mencionar especialmente a Jorge, muchas gracias por esas charlas interminables, los ratos de guitarras, prácticamente todo lo que está escrito en esta tesis ya lo has escuchado tu entre cañas. Muchas gracias Antonio por tu buen rollo incansable y tus ratos de "campeo". A Juampi, por esas visitas express a Alicante que me han dado la vida más de un finde. Y por supuesto a todos los del grupo de "Mesitas" (con Gabri, Paco, Sebas, Indi, Tolo, etc) y al grupo de las "paellaitas" (con Jorge Vera dando forma a los arroces, Bono trayendo una mochila de buen rollo y Luis deleitándonos con su "cante hondo", entre otras cosas). Esos ratitos valen mil.

Apartado imprescindible para agradecer a mis compañeros desde que entré en Rabanales, tanto en ese campus como en el maravilloso crucero de final de carrera, ¡hemos vivido más de lo que puedo yo contar sin ponernos a los tres en un compromiso! Un millón de gracias, Juanito y Emilio.

Chrysa, debería dedicar otro volumen de esta tesis para poder agradecértelo. El "Flow" de mi proyecto no sería el mismo sin ti, pero probablemente el de mi vida a día de hoy tampoco, muchas gracias.